IMPERIAL COLLEGE OF SCIENCE,
TECHNOLOGY
AND MEDICINE

University of London

IDENTIFICATION OF THE DYNAMIC CHARACTERISTICS OF STRUCTURAL JOINTS

by

Ali Salehzadeh Nobari

A thesis submitted to the University of London for
the degree of Doctor of Philosophy and for the
Diploma of Imperial College

Dynamics Section
Department of Mechanical Engineering
Imperial College of Science, Technology and Medicine
London SW7, U.K.

December 199 1

ABSTRACT

With the advent of delicate and high speed structures like guided missiles, aircraft and rotating machines, researchers have been discovering the importance of joint effects on the structural dynamic response. In order to be able to analyse joint effects and to incorporate them in calculations, it is necessary first to identify the joint dynamic characteristics.

There are several different methods for identifying a joint's dynamic characteristics but almost all of them are restrictated to some particular applications and cannot easily be generalized This thesis seeks to develop a uniform approach to the identification of linear dynamic parameters of joints.

It is shown in this thesis that although most of the existing model updating techniques are applicable to the joint identification problem, these subjects, i.e model updating and joint identification, constitute two completely different problems from a computational point of view and the joint identification problem is more complicated in this respect. Also, it has been argued that joint identification and model updating problems cannot effectively be solved simultaneously and within one problem.

Thus, the computational aspects of identification problem in general, and joint identification problem in particular, have been discussed thoroughly and the methods of dealing with these complications have been investigated.

Having classified the different joint identification methods and divided them into FRF-based and modal-based techniques, the performance of different joint identification methods has been investigated and their advantages and drawbacks have been discussed. Furthermore, a new modal-based identification method has been developed for which a similar assessment is shown to prove its efficiency.

It has been found that almost all joint identification methods are sensitive to measurement noise and the reason for this sensitivity and ways of coping with it are investigated.

The ultimate goal of this thesis is to provide the best approach to the joint identification problem for each particular case and to enable the analyst to identify the best possible

linear mathematical model for a joint which can subsequently be incorporated into an F.E. model of a structure.

ACKNOWLEDGEMENTS

I am very grateful to my supervisor, Mr. D.A. Robb, for his guidance and unstinting encouragement during the course of this project. Also, I would like to express my deep gratitude to Prof. D.J. Ewins for his valuable instructions and for his interest in this work.

My thanks are also due to the members of the Dynamics section, both past and present, especially to Dr. W.M. To, Dr. R.M. Lin, Dr. H. Mehdigoli and Mr. R. Yen for their helpful advice and discussions.

The author is deeply grateful to his family, especially to his parents, without their support and encouragement, the work might never have culminated in this thesis.

Finally, the author is indebted to the ministry of education of Islamic Republic of Iran and to the Overseas Research Student (ORS) Award Scheme for providing the financial support.

NOMENCLATURE

A	-	A substructure's symbol
	-	Analytical structure symbol
B	-	B substructure's symbol
C	-	Assembled structure's symbol
A-C		Analytically coupled structure's symbol
$[E]$	-	Noise induced error matrix in Chapters. 4 & 9
		Contribution of higher neglected terms in expansion equation (7.10)
$[K]_e$	-	Elemental stiffness matrix
$[M]_e$	-	Elemental mass matrix
$[D]_J$	-	joint damping matrix
α	-	Relative error of coefficient matrix of a LS problem (chapter 4)
β	-	Relative error of solution vector of a LS problem (chapter 4)
β_i		ith modification factor of damping matrix (chapter 8)
r		Residual vector of a LS problem (chapter 4)
	-	Mode index
$\{X\}$	-	Vector of unknowns
$[M]_0$	-	Mass matrix of analytical model with modelling error
$[K]_0$	-	Stiffness matrix of analytical model with modelling error
$[\Delta M]_i$	-	Error in mass matrix of element i
$[\Delta K]_i$	-	Error in stiffness matrix of element i
$\{\phi\}^o$	-	Eigenvector of analytical model with mass & stiffness error
λ^o	-	Eigenvalue of analytical model with mass & stiffness error
k_{ij}	-	Element ij of stiffness matrix
m_{ij}	-	Element ij of mass matrix
m	-	Number of modes involved in calculations (chapter 8)
L	-	Number of coords involved in calculations (chapter 8)
n	-	Number of elements of mass & stiffness matrices being corrected (chapter 8)
q		Number of rigid body modes
		Number of mass related unknowns after imposing symmetry &

	connectivity conditionds (chapter 6)
$[R_M]$	Rigid body modes residual
$[R_K]$	higher modes residual
s_m^λ	Element of sensitivity matrix representing $\partial\lambda/\partial m$
s_k^λ	Element of sensitivity man-ix representing $\partial\lambda/\partial k$
s_m^ϕ	Element of sensitivity matrix representing $\partial\phi/\partial m$
s_k^ϕ	Element of sensitivity man-ix representing $\partial\phi/\partial k$
e_1	Error multiplier for eigenvalues
e_2	Error multiplier for eigenvectors
D	Dummy structure
$[H]^{ss}$	Slave coordinates receptances
$[H]^{si}$	Transfer receptances between slave and interface coordinates
$[H]^{ii}$	Inter-face coordinatess receptances
$\{f\}$	Force vec tor
$\{\hat{f}\}$	Vector of the interface forces
$\{\tilde{f}\}$	Vector of the slave or applied forces
[I]	Unity matrix
E	Index for correction structure (chapter 6)
	Young's modulus
x	Physical generalized coordinates
	symbol of real structure.
$\{\phi_{xr}\}$	*rth* mode modal vector of real structure
$\{\phi_{ar}\}$	*rth* mode modal vector of analytical structure
λ_{xr}	rth eigenvalue of real structure
ω_{ak}^2	k*th* kept eigenvalue of analytical model
$\omega_{ae}^2=\lambda_{ae}$	*eth* eliminated eigenvalue of analytical model
k	Number of kept modes and index for kept modes
e	Number of eliminated higher modes and index for eliminated higher modes.
n	Number of coordinates.
P	Number of stiffness related unknowns after imposing symmetry and connectivity conditions
	Principal coordinate
	Number of constraint equations (chapter 4)
p_1	number of stiffness related unknowns after imposing symmetry and connectivity conditions and considering localized error(s) or macro-elements

q_1	-	number of mass related unknowns after imposing symmetry and connectivity conditions and considering localized error(s) or macro-elements
[K]	-	Stiffness matrix
[M]	-	Mass matrix
n_i	-	Total number of interface coordinates
n_e	-	Number of coordinates which should be corrected in chapter 6
“a	-	Number of analytical model’s coordinates used in transformation equation (6.2), equal to the number of measured coordinates of real structure
n_{as}	-	Number of coordinates of analytical model which are assumed that have been modelledcorrectly (chapter 6)
	-	Number of slave coordinates of substructure A (chapter 10).
m_x	-	Number of measured modes of real structure (chapter 6)
m_b	-	Number of measured modes of substructure B (chapter 10)
[ΔK]	-	Analytical and experimental model stiffness difference matrix, $[K_x]$-$[K_a]$, error matrix
[ΔM]	-	Analytical and experimental models mass difference matrix
[ΔD]	-	Analytical and experimental models damping difference matrix
[ΔZ]	-	Analytical and experimental models impedance difference matrix
$[K_a]$	-	Stiffness matrix of analytical model
	-	Stiffness matrix of substructure A
$[K_x]$	-	Stiffness matrix of real structure
$\{\Delta\phi\}$	-	Eigenvector difference vector
$\{\Delta\lambda\}$	-	Eigenvalue difference vector
[S]	-	Sensitivity matrix
	-	The square coefficient matrix of a normal equation derived from an over-determined set of equations
$[S]_R$	-	Real part of sensitivity matrix
$[S]_I$	-	Imaginary part of sensitivity matrix
$[H_a]$	-	Receptance matrix of analytical model
	-	Receptance matrix of substructure A
$[H_x]$	-	Measured receptance matrix of real structure
L_e	-	Length of base element

L_{jx}	-	Length of joint in real structure
L_{jt}	-	Length of joint in analytical structure or trial joint
a	-	Index for analytical model
	-	Index for substructure A
ρ	-	Mass density
	-	Typical variable (chapter 8)
α_{im}	-	i*th* mass modification factor in regular updating practice
α_{ik}	-	ith stiffness modification factor in regular updating practice
α_i	-	*ith* modification factor in equations (3.8.1) and (3.8.2)
$\|\| \Delta\phi \|\|_0$	-	Norm of initial (before any updating) difference between eigenvectors
$\|\| \Delta\lambda \|\|_0$	-	Norm of initial (before any updating) difference between eigenvalues
$\|\| \Delta\phi \|\|_R$	-	Norm of residual (after updating) difference between eigenvectors
$\|\| Ah \|\|$,	-	Norm of residual (after updating) difference between eigenvalues
$[\Delta X]$	-	The matrix which contains the unknown mass and stiffness modifications which are necessary to update the analytical model
$[C_1(\omega_i)]$	-	Coefficient matrix of algebraic version of matrix equation (4.1) at frequency ω_i before separation of variables
$[L(\omega_i)]$	-	Matrix on the r.h.s of the matrix equation (4.1)
$\{L(\omega_i)\}$	-	Vector on the r.h.s of the algebraic version of matrix equation (4.1)
$[C(\omega_i)]$	-	As for $[C_1(\omega_i)]$ after separation of variables
c_{ij}	-	ij element of viscous damping matrix
[P]	-	The coefficient matrix of the final set of algebraic equations obtained by combining equations of different frequencies
k_{j0}	-	Initial value for stiffness element k_j in Fig. 4.3
ΔZ_1	-	Variation in particle 1 impedance due to variation in stiffness element k_j
$\{\Delta V\}_r$	-	Variation in *rth* right singular vector
$\{V\}_r$	-	*rth* right singular vector
$\{U\}_r$	-	*rth* left singular vector
$\{{}_R\phi\}_r$	-	*rth* right eigenvector
$\{{}_l\phi\}_r$	-	*rth* left eigenvector

$[\Delta Z]_j$	Modification to joint impedance matrix
n_f	Number of frequency points used for averaging in LS solution
d	Number of interfacing stations Dummy structure index (Chapters 2,9 and 10)
n_{ir}	Number of interface coordinates involved in interfacing station r
$[K]_t$	Trial joint stiffness matrix
$[M]_t$	Trial joint mass matrix
ω_r	*rth* natural frequency of test structures Rad/Sec
$[\bar{K}]_j$	Mean stiffness matrix of joint calculated by neglecting joint mass in identification calculations
$[Z]_j$	Joint impedance matrix
$[H]_c$	Receptance matrix of assembled structure
$[H]_j$	Joint receptance matrix
s	Slave coordinates Index for coordinates which are modelled correctly (chapter 6)
i	Interface coordinates Index for coordinates which should be updated
$[K]_j$	joint stiffness matrix
$[M]_j$	Joint mass matrix
$[R_{dr}]$	Resudual effect of higher neglected modes of substructures
$[R_{dr}^*]$	Residual effect of higher neglected modes of substructures without any joint at interface
ω	Circular frequency Rad/Sec
λ_{cr}	*rth* eigenvalue of assembled structure
f	Frequency Hz
θ_r	The angle between rth left & right eigenvectors
LS	Least squares
$\|\|_p$	p norm of a matrix and/or vector
K	Condition number of a matrix
σ_i	*ith* singular value
σ	Standard deviation
E(X)	Statistical expected value
$E(X^2)$	Mean square value
I I	Absolute value
^	Slave coordinates' superscript

	-	Interface coordinates superscript
$[\ ]'$	-	Pseudo-inverse of a matrix
$[\ ]^H$	-	Conjugate transpose of a matrix
$[\ ]^T$	-	Transpose of a matrix
$O(\ )$	-	Order of magnitude

LIST OF FIGURES

LIST OF TABLES

TABLE OF CONTENTS

CHAPTER 1

INTRODUCTION

1.1 THE JOINT IDENTIFICATION PROBLEM

With the advent of delicate and high speed structures like guided missiles, aircraft and rotating machinery, researchers have been discovering the increasingly important role of structural stiffness in structural design. This important role can be due to a variety of system design considerations. For example, considering the case of guided missiles, the airframe stiffness has a significant effect on the characteristics such as airframe aeroelastic coupling with guidance and control systems, structural dynamic loads and the response induced by flight enviroment ,.....etc. An other example is in the field of machine tool design where the stiffness of the structure plays a crucial role in the precision of the metal forming process.

Experience has shown [1,2] that many of the joints commonly employed in structures to serve design requirements can result in substantial and often unpredictable reductions in the stiffness of the primary structure. In the absence of reliable analysis methods for estimating joint effects on structural stiffness, a common practice is to rely on experimental data for definition of the joint properties. The shortcoming of this approach, however, is that data obtained for a particular joint design on a given structure often cannot be extrapolated with any confidence to a different structure design or even, in many cases, to a different location on the same structure.

Ewins, Silva and Maleci [2] pointed out the deteriorating effects of neglecting the joint in a coupling analysis of a helicopter structure.

The significant effect of the joint on a structure's stiffness and, the consequent dynamic behaviour on the one hand, and the need to identify joint characteristics and incorporate

Note that although equations (3.3) and (3.4) look similar, there are two significant differences between them, namely: equation (3.3) is approximate while equation (3.4) is exact and the first matrix in r.h.s. of equation (3.4) is [H,] while it is $[H_a]$ for equation (3.3).

Now, if a complete coordinate set is used, the updating analysis using equation (3.4) does not require any iteration and there should be no limit for the II $[H_a]$ - [H,] II but, since it is practically impossible to achieve a complete measured coordinate set, in order to be able to perform $[H_x]([\Delta Z])[H_a]$ in (3.4), Lin proposes to fill the unmeasured FRFs in H_x with their analytically-derived counterparts. This assumption, plus the application of an incomplete coordinate set, makes iteration necessary in application of Lin's method. Also, if $\| [H_a] -$ [H,] $\|$ is greater than a certain limit, then the above-mentioned assumption, i.e using the analytical FRF to fill H_x, will not be valid and the calculations will not converge. Thus, Lin's method is one which originally is derived from a direct approach but which, due to practical limitations, has to adopt certain assumptions which imply a need for iteration and a limit on the extent of the differences which can be determined.

Apart from differences in formulation, all updating methods share certain shortcomings. The most important of these comes from the fact that the experimental data are always incomplete and, compared with the analytical model, comprise a very small amount of information. To get around the computational difficulties associated with this incompleteness, different methods use different assumptions and techniques but, due to the nature of the problem (expecting a large amount of information from a relatively small amount of available experimental information), the results of all methods suffer from this problem in one way or another. For example, some methods like EMM use expansion or condensation techniques to resolve the incompleteness problem, which spreads the error in the analytical model all over the matrices, On the other hand, some other methods like the modal or FRF perturbation-based methods or Lin's method do not use expansion or condensation techniques but, due to other assumptions, their abilities are limited to a certain amount of difference between two consistent models of structure.

3.3 JOINT IDENTIFICATION METHODS

3.3.1 GENERAL CONSIDERATIONS

All the classifications and methods introduced in section 3.2 are completely applicable to joint identification methods as well. The only, but very important, difference between the two cases is a difference in the way of applying the methods, as will be discussed

shortly. In addition to the methods of section 3.2, there is another family of direct methods which are especially useful for joint identification purposes. These methods are refered to here as “Decoupling Methods”, DM.

The essential difference in the application of updating methods for joint identification is that in this case we can assume that the only source of error (causing the difference between consistent models of structure) is the joint and this not only makes the incompleteness problem discussed in section 3.2 less serious but also reduces the number of unknowns significantly, compared with the true updating case.

It should be noted that, in using any of the updating method for joint identification, it is necessary to consider the joint explicitly in an analytical model. This can be done by considering extra elements at the joint location in the FE model to represent the joint.

To validate an assumption of localized error, one has to make sure that there is no source of error apart from that in the joint and there are two ways of doing this as, follows:

(i) - by updating the analytical models of the substructures which constitute the assembled structure one by one beforehand, so that one can assume the only remaining source(s) of error in assembled structure is(are) due to the joint(s); or

(ii) - by using experimental models for the substructures which constitute the assembled structure in order to generate an analytical model involved in the analysis.

Option (ii) means that instead of comparing the analytical model of the structure with its experimental counterpart, one can use the experimental models of, say, two substructures of the assembled structure and then, assuming a model for joint, couple the two substructures through that joint. Then, one can compare the generated structure- which is called the “analytically-coupled structure”- with the real structure.

To avoid the coupling of substructures -which is inevitable in case of option (ii)- the so-called “decoupling method” has been developed [10,11] (see also chapters 9 & 10), as discussed next

3.3.2 DECOUPLING METHOD

In this approach, instead of using the difference(s) between the consistent models of the assembled structure (which makes coupling necessary, in case of option (ii) of previous section) to identify the joint, the joint model is extracted by decoupling the assembled structure so as to expose its constitutent substructures, which include the joint. Then, having the individual substructure models, one can identify the joint model. Since the substructure models are used directly in this method, there is no need for coupling or for prescribing a model for the joint, Categories similar to those in section 3.2 can be defined for decoupling methods as well, i.e. the FRF decoupling method and modal decoupling method.

Dealing with the decoupling method, two points should be noted as follows:

(a) - usually, the decoupling method is used for the identification of a single typical joint between two substructures but the method developed in chapters 9 & 10 can easily be generalised to identify **n** joints of an assembled structure simultaneously. This generalisation requires an experimental model of each of the substructures involved in the assembled structure;

(b) - the decoupling method is sensitive to noise (chapter 9). This means that it can be potentially advantageous to use analytical models of substructures (instead of their experimental models) along with experimental data from the assembled structure in a decoupling process. This substitution will eliminate from the decoupling process the noise typical of experimental models. It should be noted, though, that using FE models of substructures again introduces the possibility of mis-modeled regions which will affect the results of the identified joint.

It is convenient at this stage to restate the major differences between model updating and joint identification methods.

(a) - In joint identification, the joint is the only unknown element and this fact reduces the number of unknowns significantly compared with the number of unknowns in a model updating problem.

(b) - Using certain identification techniques, there is no problem due to incompleteness involved in joint identification

3.4 IS JOINT IDENTIFICATION A SPECIAL CASE OF MODEL UPDATING?

The main purpose of posing the above question is to establish the possible redundancy of developing joint identification methods distinct from those used for model updating.

Considering the discussions in sections 3.2 and 3.3, an answer to the above-mentioned question is proposed:

" strictly, one can consider joint identification as a special case of model updating but this does not imply that joint identification can be considered as ***part*** *of a model updating procedure since this is not a well-conditioned process itself and adding the joint(s) as further unknown(s) will worsen the situation, as will be shown later. Thus, although similar mathematical techniques can broadly be used to tackle both model updating and joint identification problems, the considerations which are necessary for each case are quite* ***different*** *and one cannot solve both problems in one solution process so they should be dealt with separately."*

To explain this statement, we consider the three following questions.

(i) - Considering joints as extra elements in an FE model of a structure, and as mis-modeled elements along with other mis-modeled elements, is it possible to identify the joint in an updating process?;

(ii) - Is it possible to spot the location of the joint in an FE model?;

(iii) - Can we update an FE model ignoring the joints altogether?.

As will be shown below, questions (ii) and (iii) are natural extensions of question (i).

The answer to question (i) is that, theoretically, it **is** possible to identify a joint as a part of a model updating problem but, computationally and practically, it may result in some difficulties. These difficulties arise from the nature of the joint, which is a complicated element, and of the updating problem, and are as follows:

(a) - since the number of joints in an assembled structure is usually large, adding the joints to an FE model as extra unknowns can increase the size of the model

dramatically which, in turn, will cause poorer condition for the updating computations and will increase computation time significantly [29];

(b) - considering the joint(s) in an FE model requires a prescribed model for each joint which must be accurate: this can be quite difficult to achieve in practice;

(c) - considering the fact that some of the joints in an assembled structure can be very stiff in some directions, inclusion of the joint identification task in an updating process can make the calculations very ill-conditioned. For example, if, in the limit, one of the joints is rigid in one direction, then the updating problem will become singular. It should be noted that in the updating case, even for direct methods, there is a limit to the difference between the models of the structure which can be accommodated, and this might well be exceeded in the case of certain types of joint.

Generally speaking, treating joint identification as a part of model updating may simply result in adding more difficulties to a problem which is not very well-conditioned to begin with. Thus, it is not recommended to seek to undertake a joint identification exercise at the same time as a general model updating process. Rather, it is possible to use updating methods for direct joint identification since, in this case, the number of unknowns is much smaller and the incompleteness problem is less severe. Note that even in this case there is a high risk of ill-conditioned calculations. For example, using the FRF-based direct method for joint identification, one has (see chapter 5) :

$$[H]_a^{ss} - [H]_x^{ss} = [H]_x^{si}([\Delta Z])[H]_a^{is} \qquad (3.5)$$

where equation (3.5) has been derived from equation (3.4) with notations "s" and "i" designating slave and interface coordinates, respectively. Now, if the joint is stiff in some direction(s), then the columns of $[H]_x^{si}$ related to that direction(s), say rotation, will be linearly dependent (or near linearly dependent) which will make the calculations ill-conditioned or even rank-deficient.

Considering the answer to the first question, the 2nd and 3rd questions follow naturally. The second question arises because one can ask “is it not possible to spot the location of significant joints (i.e. those joints in an assembled structure which are reasonably flexible) and then to consider only these in the FE model of the assembled structure?“. Of course, by doing this one will be able to avoid the additional ill-conditioning of the

problem signalled above by not introducing stiff joints into the FE model and by not increasing the number of unknowns.

The nature of the third question is different from the second one and it raises the possibility of ignoring the existence of the joint(s) in a structure altogether. This question will be irrelevant if the objective of joint identification is something apart from updating a model but, for the time being, we confine ourselves here to the common objective of model updating.

In order to demonstrate the problems associated with identifying a joint as a part of model updating, and to be able to answer the 2nd and 3rd questions above, the case studies described in the next section have been undertaken.

3.5 CASE STUDIES

The first set of case studies is aimed at the answering the first question posed in section 3.4, i.e.

" considering joints as extra elements in an FE model of a structure, and as mis-modeled elements along with other mis-modeled elements, is it possible to identify the joint(s) in an updating process?"

The following points will be explored during this set of case studies,

(a) - what problems may be introduced by considering joint identification as a part of an updating process?; and

(b) - how can updating methods be used for direct joint identification?

The test structure used for this set of case studies is the beam shown in Fig. 3.1.

In all case studies of this series, structure X, which simulates the "real" structure, is a 6-element FE model of a simply-supported beam where element 4 is designated as the joint element. The base element of X has the geometrical and mechanical properties shown in Fig. 3.2.

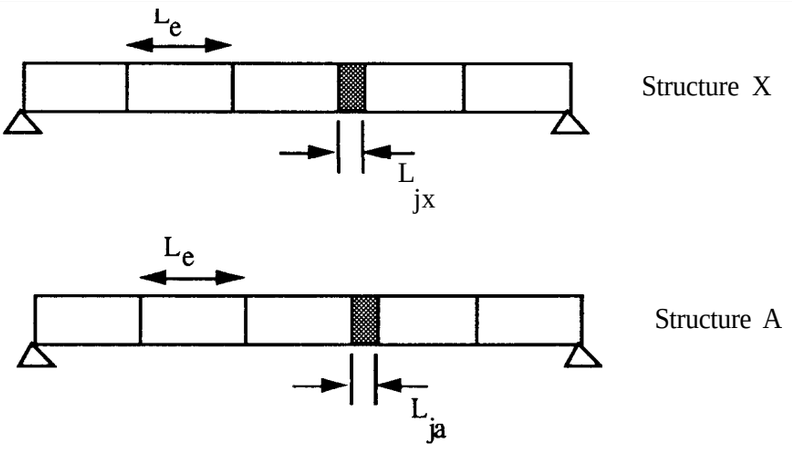

Fig. 3.1 Model of real structure X & analytical model A

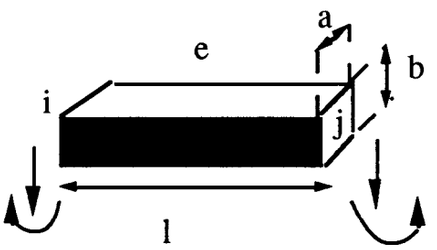

l_e=.3 [m], b_e=.012 [m], a_e=.05 [m]

ρ = 7547 [kg/m^3] , E= 207E9 [N/m^2]

Fig. 3.2 The geometrical and mechanical properties of base element

The joint element in this "real" structure has the following properties:

$$L_{jx} = 5\%\ L_e,\ E_{jx} = 10\%\ E_e,\ \rho_{jx} = 0 \qquad (3.5)$$

Thus, the joint model is a short element which is more flexible than it would be if it were composed of the beam material.

Structure A, which simulates the analytical model of the real structure, is a 6-element FE model of a simply supported beam with element 4 again acting as a joint. The geometrical and mechanical properties of base element of model A are exactly the same as those of X and are shown in Fig. 2. The joint element in structure A has the following properties for the different case studies in this series as follows:

$L_{ja} = 20\%\ L_{jx} = 1\%\ L_e$ $E_{ja} = E_{jx}$ $\rho_{ja} = o$ (3.6.1)

$L_{ja} = 60\%\ L_{jx} = 3\%\ L_e$ $E_{ja} = E_{jx}$ $\rho_{ja} = 0$ (3.6.2)

$L_{ja} = 200\%\ L_{jx} = 10\%\ L_e$ $E_{ja} = E_{jx}$ $\rho_{ja} = 0$ (3.6.3)

$L_{ja} = 300\%\ L_{jx} = 15\%\ L_e$ $E_{ja} = E_{jx}$ $\rho_{ja} = 0$ (3.6.4)

$L_{ja} = 2000\%\ L_{jx} = 100\%\ L_e$ $E_{ja} = E_{jx}$ $\rho_{ja} = 0$ (3.6.5)

Thus, in all cases the joint model of structure A has the same material flexibility (Young's modulus) as structure X: both joint models in X and A are massless, and the only difference between the two models comes from the difference between the length of the joint models in X and A.

Now, using the inverse **eigen-sensitivity** analysis method [24] we will try to update model A to match model X for the different cases in equations (3.6.1) to (3.6.5). Note that in all the case studies only slave coordinates or off-joint coordinates have been considered in $\{\Delta\phi\}$.

Fig. 3.3 shows the variation of II $\Delta\phi\|_0$ and II $\Delta\lambda\|_0$ as a function of variation of (L_{ja}/L_{jx}). As is evident from Fig. 3.3, both II $\Delta\phi\|_0$ and II Ah $\|_0$ increase as the joint model in structure A becomes shorter or longer relative to joint model in X.

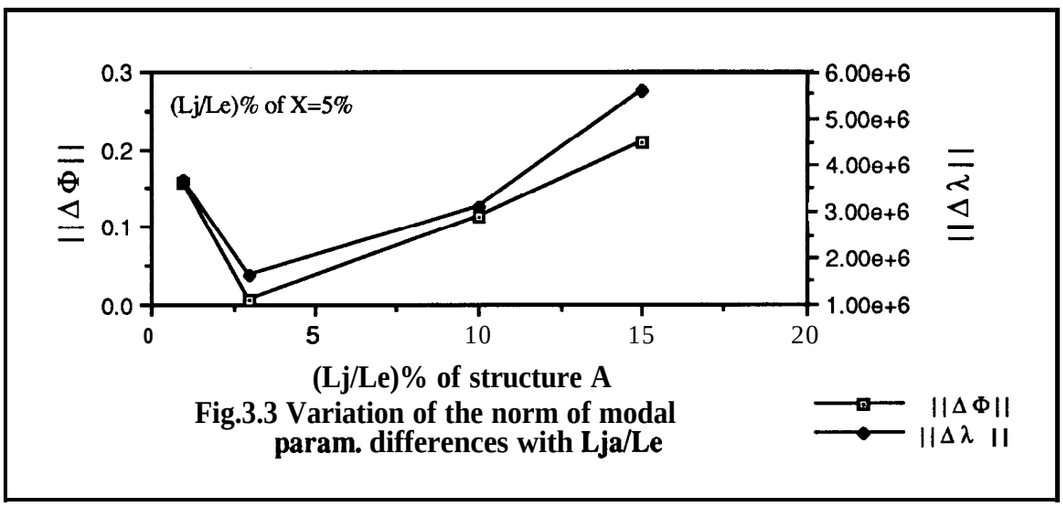

Fig.3.3 Variation of the norm of modal param. differences with Lja/Le

Fig. 3.3 also reveals that the rate of variation of II $\Delta\phi\|_0$ and II $\Delta\lambda\|_0$ is higher for a shorter joint than for a longer one, compared with L_{jx}. Table 3.1 shows the results of updating attempts for different cases in (3.6.1) to (3.6.5).

$(L_{ja}/L_{jx})\%$	$(\|\|\Delta\phi\|\|_{min}/\|\|\Delta\phi\|\|_0)\%$	$(\|\|\Delta\lambda\|\|_{min}/\|\|\Delta\lambda\|\|_0)\%$
20	1600	3e7
60	24	15
200	34	15
300	38	15
2000	50	30

Table 3.1 The results of attempts made to update structure A to structure X for cases (3.6.1) to (3.6.5).

As is evident from Table 3.1, calculations diverge for cases where the joint length in model A is less than about 20% of the true joint length. For all other cases, although $\|\Delta\phi\|$ and $\|Ah\|$ reduce, absolute convergence is not achieved and there are always some residual values for $\|\Delta\phi\|$, and $\|Ah\|_R$. These residuals increase as the (L_{ja}/L_{jx}) ratio increases.

The reasons for the divergence in the case of $(L_{ja}/L_{jx}) \leqq 20\%$, and for the presence of residuals in other cases, can be explained as follows. Fig. 3.4 shows the stiffness modification factors for structure A achieved after the first run for the case of equation (3.6.1).

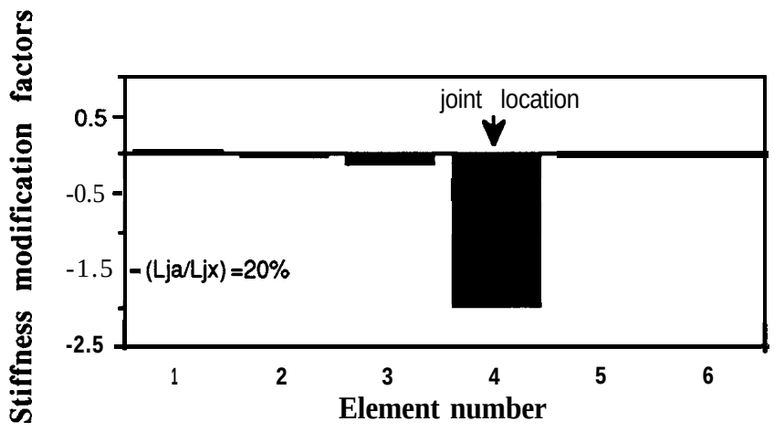

Fig. 3.4 Results with (Lj/Le)% equals to 1 and 5 for structures A & X, respectively, 1st run

It is evident from Fig. 3.4 that the results of the fiit run correctly spot the mis-modeled element, i.e. the joint element, and also indicate that the flexibility of this element should be increased. The modification factor for the joint element is about -1.9, which makes the stiffness matrix negative-definite and causes divergence of calculations in this case.

Different techniques (like introducing the mass modification factors to the analysis or dividing the modification factors by an amount so as to prevent the negative definiteness of stiffness matrix) have been tried to see if it is possible to reduce II $\Delta\phi$ II$_0$ and II $\Delta\lambda$ II$_0$ for this case, but all attempts failed in this respect.

To explain the existence of II $\Delta\phi$ II, and II Ah II, in the cases (3.6.2) to (3.6.5), consider the following elemental mass and stiffness matrices for a simple beam element:

$$[K_e] = (EI/L_e^3)\begin{bmatrix} 12 & 6L & -12 & 6L \\ & 4L^2 & -6L & 2L^2 \\ & & 12 & -6L \\ & & & 4L^2 \end{bmatrix} \qquad (3.7.1)$$

$$[M_e] = (\rho AL_e/420)\begin{bmatrix} 156 & 22L & 54 & -13L \\ & 4L^2 & 13L & -3L^2 \\ & & 156 & -22L \\ & & & 4L^2 \end{bmatrix} \qquad (3.7.2)$$

It can be seen from (3.7.1) and (3.7.2) that all the stiffness matrix elements are linearly proportional to E and, also, that all the mass matrix elements are linearly proportional to p. On the other hand, for both mass and stiffness matrices, the elements related to different degrees of freedom present in [K]^e and [M]^e are themselves quite different functions of L_e, the length of the element. For example, translational elements in the stiffness and mass matrices are proportional to $(1/L_e^3)$ and L_e, respectively, while rotational elements in these matrices are proportional to $(1/L_e)$ and L_e^3, respectively. This means that changing E and ρ does **not affect the** proportionality ratio between different degrees of freedom but changing L_e will affect it.

On the other hand, almost all the updating methods are based on elemental modification factors α_{ik} and α_{im}, for $[K]_i^e$ and $[M]_i^e$ and modifying elemental mass and stiffness matrices of an element by multiplying them with α_{ik} and α_{im} just modifies E_{ei} and ρ_{ei} but not L_{ei}. Thus, if the differences between elemental mass and stiffness matrices of the real structure and its analytical model are caused by length differences or simply, if the proportionality between elements of the mass and stiffness matrices of the real joint, related to different degrees of freedom, is not similar to that assumed in analytical model base element, it will not be possible to make II $\Delta\phi$ II, and II $\Delta\lambda$ II, zero just by adjusting E and p of the mis-modeled analytical elements, as has been proposed in [7].

It should be noted that a joint is a very complicated mechanical or structural element and that it can easily deviate from the analytical pattern which is assumed when modelling the joint as a simple FE element.

To deal with this problem, one has to consider a separate modification factor for each group of degrees of freedom involved in the joint model (degrees of freedom involved in interfacing). For example, to model the joint in Fig.3.1, one has to consider three modification factors for the stiffness matrix, α_1 to α_3, and three modification factors for the mass matrix, α_4 to α_6. The details are:

$$[K]_j = \begin{bmatrix} a_1 & a2 & -a_1 & 2 \\ & 2a_3 & -a_2 & 3 \\ & & a_1 & a2 \\ & & & 2a_3 \end{bmatrix}$$

leading to

$$[K]_j = \alpha_1 \begin{bmatrix} a_1 & 0 & -a_1 & 0 \\ & 0 & 0 & 0 \\ & & a^1 & 0 \\ & & & 0 \end{bmatrix} + \alpha_2 \begin{bmatrix} 0 & a_2 & 0 & a2 \\ & & -a_2 & \\ & & 0 & -a_2 \\ & & & 0 \end{bmatrix} + \tilde{\alpha}_3 \begin{bmatrix} & & & \\ & & & a_3 \\ & & 0 & 0 \\ & 2a_3 & 0 & 2a_3 \end{bmatrix} \qquad (3.8.1)$$

and similarly,

$$[M]_j = \alpha_4 \begin{bmatrix} 156a_4 & 0 & 54a_4 & 0 \\ & 0 & 0 & 0 \\ & & 156a_4 & 0 \\ & & & 0 \end{bmatrix} + \alpha_5 \begin{bmatrix} 0 & 22a_5 & 0 & -13a_5 \\ & 0 & 13a_5 & 0 \\ & & 0 & -22a_5 \\ & & & 0 \end{bmatrix} + \alpha_6 \begin{bmatrix} 0 & 0 & 0 & 0 \\ & 4a_6 & 0 & -3a_6 \\ & & 0 & 0 \\ & & & 4a_6 \end{bmatrix} \qquad (3.8.2)$$

It should be noted that using modification factors α_1 to α_6 in equations (3.8.1) and (3.8.2) in an updating process, will seriously affect the condition of the updating calculations. This effect has been examined in the following case study.

Considering two models A and X in Fig. 3.1 for this case study, the mis-modeled element in A, i.e. element 4, has the same length as element 4 of structure X but its Young's modulus and density are reduced by 50% compared with the mechanical properties of the pertinent element in X. This means that elements of the mass and stiffness matrices of the mis-modeled element are equal to 50% of those belonging to element 4 of structure X. The mass and stiffness matrices of element 4 in models A and X are then as follows:

* Note that defining $[K]_j$ & $[M]_j$ as in equations (3.8.1) & (3.8.2) may cause inconsistency in calculated mechanical & physical properties. Another way of defining $[\Delta K]_j$ & $[\Delta M]_j$ is as follow:

$$[\Delta K]_j = \frac{\partial K_e}{\partial L}\Delta L + \frac{\partial K_e}{\partial E}\Delta E + \frac{\partial K_e}{\partial \rho}\Delta \rho$$

$$[M_4]_x = \begin{bmatrix} .504 & .02 & .17 & -.012 \\ & .0011 & .0126 & -.00087 \\ & & .504 & -.021 \\ & & & .0011 \end{bmatrix} \quad (3.9.1)$$

$$[K_4]_x = \begin{bmatrix} 644000 & 96600 & -644000 & 96600 \\ & & 644000 & -96600 \\ & 19320 & -96600 & 19320 \end{bmatrix} \quad (3.9.2)$$

and* ,

$$[M_4]_a = \begin{bmatrix} .252 & .01 & .087 & -.006 \\ & & .252 & -.01 \\ & .00058 & .006 & -.00058 \end{bmatrix} \quad (3.9.3)$$

$$[K_4]_a = \begin{bmatrix} 322000 & 48300 & -322000 & 48300 \\ & 9660 & -48300 & 4830 \\ & & 322000 & -48300 \\ & & & 9660 \end{bmatrix} \quad (3.9.4)$$

The updating task has been undertaken using two different approaches. In the first approach the regular updating technique, i.e. using one modification factor for each one of the mass and stiffness matrices of all elements involved in the model, has been adopted. hence, for this case there are 6x2=12 modification factors involved in the calculation.

In the second approach, the modification factors in equations (3.8.1) and (3.8.2) have been used and only for the mis-modeled element. This means that for this case there are 6 modification factors, α_1 to α_6. For both cases modes 1 to 5 have been used in the calculation and, thus, the dimensions of the sensitivity matrices for two cases are 20x12 and 20x6, respectively.

Table 3.2 shows the biggest and smallest singular values and condition number of the sensitivity matrix as well as the number of iterations necessary to achieve the solution.

* A 12 digit accuracy computer is used in calculations

results for first run	σ_1	σ_n	$\kappa(S)=\sigma_1/\sigma_n$	No. of iteration
first approach	1.74	.002	870	3
second approach	12.26	6.4E-5	2E5	3

Table 3.2. Results for two approaches to update model A to model X

It is evident from Table 3.2 that in the case of the second approach, even though the number of unknowns is as half that of the first approach, the condition number of the sensitivity matrix is much higher than that in the first approach.

The reason for the poorer condition in the case of the second approach can be explained by exploring the elements of sensitivity matrices for the two cases. Table 3.3 shows the typical eigenvalues related elements of the sensitivity matrix for three modes, for two cases.

	α_{1m}	α_{2m}	α_{3m}	α_{4m}	α_{5m}	α_{6m}
$\partial\lambda_1 / \partial\alpha_i$	-.03	-.17	-.3	-.3	-.17	-.03
$\partial\lambda_2 / \partial\alpha_i$	-.1	-.3	-.1	-.1	-.3	-.1
$\partial\lambda_3 / \partial\alpha_i$	-.17	-.17	-.17	-.17	-.17	-.17

Table 3.3.1. Typical sensitivity matrix elements for the first approach

	α_{1k}	α_{2k}	α_{3k}	α_{4k}	α_{5k}	α_{6k}
$\partial\lambda_1 / \partial\alpha_i$	.029	.167	.3	.3	.167	.03
$\partial\lambda_2 / \partial\alpha_i$	.098	.3	.098	.1	.3	.1
$\partial\lambda_3 / \partial\alpha_i$	.167	.166	.167	.17	.17	.17

Table 3.3.2. Typical sensitivity matrix elements for the first approach

	α_1	α_2	α_3	α_4	α_5	α_6
$\partial\lambda_1 / \partial\alpha_i$	.53	-1	.94	-.18	-.012	-.00026
$\partial\lambda_2 / \partial\alpha_i$	1.4	-2.34	1.05	-.065	-.0062	.0008
$\partial\lambda_3 / \partial\alpha_i$	.4	-.51	.29	-.1	-.033	-.0064

Table 3.3.3. Typical sensitivity matrix elements for the second approach

Comparing Tables 3.3.1 and 3.3.2 with 3.3.3, it is evident that, for the first two of these, the elements of the sensitivity matrix related to mass and stiffness variations are of the same order of magnitude but, for the Table 3.3.2 this is not the case and, especially, the elements related to cross and rotary inertia have markedly smaller orders of magnitude than the other elements.

It should be noted that the following matrices have been used in calculating the sensitivity matrix for the case of the second approach :

$$[\Delta K]_4 = \alpha_1 \begin{bmatrix} 322000 & 0 & -322000 & 0 \\ & 0 & 0 & 0 \\ & & 322000 & 0 \\ & & & 0 \end{bmatrix} + \alpha_2 \begin{bmatrix} 0 & & & \\ 48300 & 0 & 48300 & \\ 0 & -48300 & 0 & \\ & 0 & -48300 & + \\ & & 0 & 1 \end{bmatrix}$$

$$\alpha_3 \begin{bmatrix} 0 & 0 & 0 & 0 \\ & 9660 & 0 & 4830 \\ & & 0 & 0 \\ & & & 9660 \end{bmatrix} \qquad (3.10.1)$$

and,

$$[\Delta M]_4 = \alpha_4 \begin{bmatrix} .252 & 0 & .087 & 0 \\ & 0 & 0 & 0 \\ & & .252 & 0 \\ & & & 0 \end{bmatrix} + \alpha_5 \begin{bmatrix} 0 & .01 & 0 & -.006 \\ & 0 & .006 & 0 \\ & & 0 & -.01 \\ & & & 0 \end{bmatrix} + \alpha_6 \begin{bmatrix} 0 & 0 & 0 & 0 \\ & .00058 & 0 & -.00044 \\ & & 0 & 0 \\ & & & .00058 \end{bmatrix}$$

(3.10.2)

and the sensitivity matrices corresponding to two approaches are balanced* using similar techniques.

Takingthevery small values of elements of coefficient matrices of α_5 and α_6 in equation (3.10.2) into consideration, the reason for the small order of magnitude of the elements of the sensitivity matrix related to cross and rotary inertia becomes clear.

Examining Tables 3.3.1 and 3.3.2 reveals that in the case of the first approach, i.e. regular updating, the stiffness-related sensitivity elements for eigenvalues are positive for all modes and those related to mass are negative. This means that, as expected, increasing elements stiffness or decreasing their mass will increase the natural frequencies of

* Balancing is a technique which is used to reduce the large differences in order of magnitude of elements of a matrix. For more explanation see Chapter 4.

structure. On the other hand, Table 3.3.3 shows that in the case of second approach the cross stiffness-related elements of the sensitivity matrix behave in a reverse manner, i.e. increasing cross stiffness will **decrease** natural frequencies of all modes. Also, for the second mode, rotary inertia-related element acts in a reverse way. This observation shows that updating the stiffness matrix of an element as a whole, as is a common practice in model updating, the positive sensitivity of eigenvalues relative to translational and rotational stiffness variation will compensate for negative sensitivity of eigenvalues relative to cross stiffness and thus the outcome will always be positive sensitivity of eigenvalues relative to stiffness variations.

Thus, trying to identify the joints of the structure during a model updating process, one is faced with (at least) the following problems :

(i) - the number of modification factors for the joint elements is significantly larger than for other elements. This will affect the condition of the matrices involved in calculations and will tend to make them ill-conditioned [29];

(ii) - there is a high risk of divergence when a soft joint has been modelled by a stiff joint, as in the case of relation (3.6.1).

If, on the other hand, one of the updating methods is going to be used for the direct joint identification application, then the number of modification factors should be defined according to equations (3.8.1) and (3.8.2) which, in this case, results in a manageable number of unknowns because it is much smaller compared with the updating application.

From this point on, a second set of case studies will be considered in which the 2nd and 3rd questions posed in section 3.4 will be addressed. These questions are:

(a) - is it possible to spot the location of joints in an analytical model of the structure and, if so, can we decide which of the joints are rigid enough to be ignored?;

and

(b) - is it possible to update the analytical model of a structure ignoring its joints altogether?.

The test structures for this series of case studies are shown in Fig. 3.5.

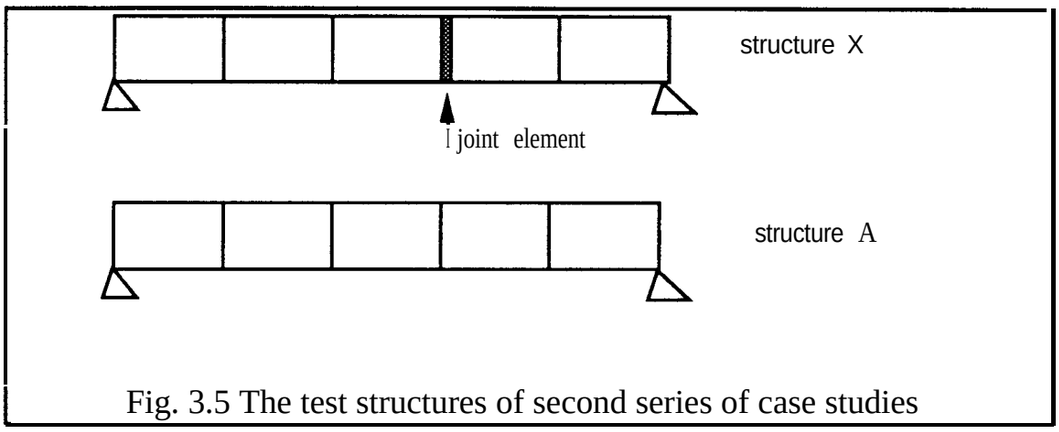

Fig. 3.5 The test structures of second series of case studies

Structure X, which simulates the real structure, is exactly the same as structure X in Fig.3.1 with its 4th element acting as a massless joint. The elemental mechanical and geometrical properties are identical to those in Fig. 3.2. Structure A, which simulates the analytical model of structure X, is similar to that structure except that it does not contain the joint element, i.e. A has only 5 elements. The analysis is based on an attempt to update model A to match model X, using the inverse eigen-sensitivity analysis method, and to examine the effect of various different parameters on the analysis. It should be noted, again, that only slave or off-joint coordinates have been included in $\{\Delta\phi\}$.

The following parameters have been considered in the case studies:

$$E_j = 10\%\ E_e \quad , L_j = 0.1\%\ L_e \quad , Lj = 1\%\ L_e \quad , L_j = 10\%\ L_e$$
$$Lj = 100\%\ L_e \tag{3.11}$$

$$Lj = 5\%\ L_e \quad , E_j = .01\%\ E_e \ , E_j = .1\%\ E_e \quad , E_j = 1\%\ E_e \quad , E_j = 10\%\ E_e , \ E_j = 100\%\ E_e \tag{3.12}$$

Each of the cases in equations (3.11) and (3.12) has been considered both with and without mass modification factors included in the analysis.

Tables 3.4 and 3.5 and Figs. 3.6 and 3.7 show the results of the analysis of cases (3.10) and (3.11) when only the stiffness modification factors are involved in the analysis.

Examining Figs. 3.6 and 3.7 reveals that, as the joint becomes stiffer, the modification factors become smaller and location of the joint becomes more accurate. On the other hand, if the joint flexibility goes beyond a certain limit, the location ability of modification factors is badly reduced.

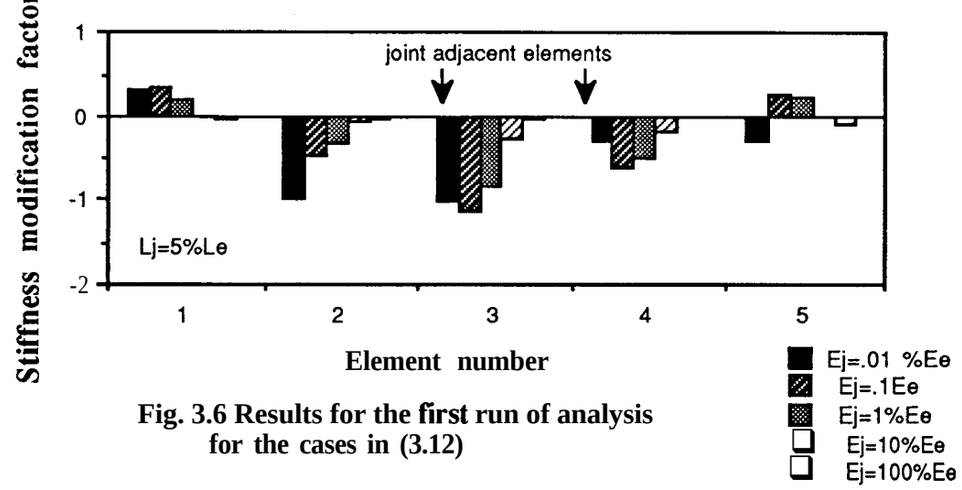

Fig. 3.6 Results for the first run of analysis for the cases in (3.12)

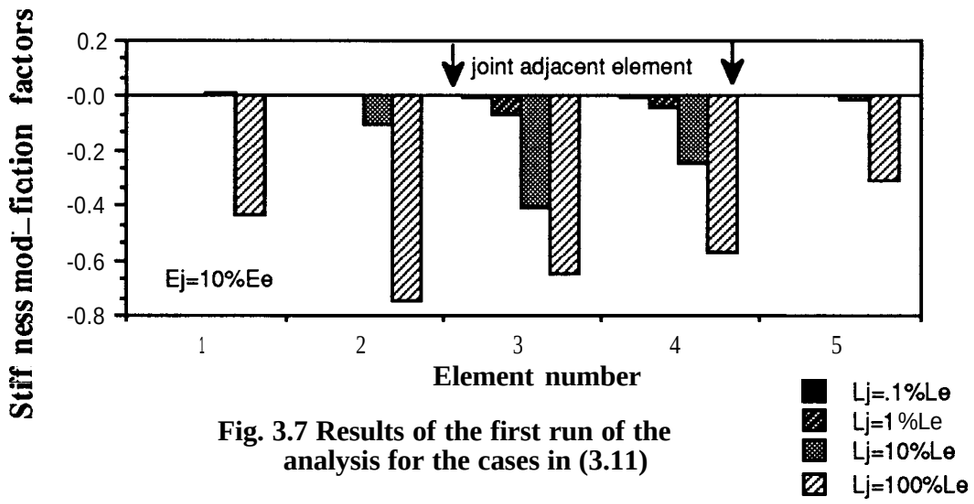

Fig. 3.7 Results of the first run of the analysis for the cases in (3.11)

Lj = 5% Le	$\|\|\Delta\phi\|\|_{min}/\|\|\Delta\phi\|\|_0$	$\|\|\Delta\lambda\|\|_{min}/\|\|\Delta\lambda\|\|_0$	$\|\|\Delta\phi\|\|_0$	$\|\|\Delta\lambda\|\|_0$
Ej=.Ol%Ee	211%	40%	.998	2.24e7
Ej=. 1 %Ee	82.6	53%	.646	1.32e7
Ej=l %Ee	63%	42%	.561	8.37e6
Ej=10%Ee	71%	5%	.22	4.96e6
Ej=100%Ee	97%	26%	.084	2.74e6

Table 3.4 Results for the cases in (3.12),mass modification factors not involved

Ej=lO% Ee	$\|\Delta\phi\|_{min}/\|\Delta\phi\|_0$	$\|\Delta\lambda\|_{min}/\|\Delta\lambda\|_0$	$\|\Delta\phi\|_0$	$\|\Delta\lambda\|_0$
Lj=.l% Le	78.9%	10.5%	.007	135596
Lj=l% Le	78%	9%	.0615	1.27e6
Li=lO% Le	63%	6%	.32	8.1e6
Li=100% Le I	104%	24%	1.252	2.26e7

Table 3.5 Results for the cases in (3.1 1), mass modification factors not involved

It is evident from Tables 3.4 and 3.5 that $\|\Delta\phi\|_0$ and $\|\Delta\lambda\|_0$ become smaller as the joint becomes stiffer but this is not the case for $\|\Delta\phi\|_{min}/\|\Delta\phi\|_0$ and $\|\Delta\lambda\|_{min}/\|\Delta\lambda\|_0$, and there is an optimum flexibility which yields minimum $\|\Delta\phi\|_{min}/\|\Delta\phi\|_0$ and $\|\Delta\lambda\|_{min}/\|\Delta\lambda\|_0$. Also, Tables 3.4 and 3.5 reveal that if the joint flexibility exceeds a certain limit, the updating attempt will fail. It should be noted that although $\|\Delta\phi\|_{min}/\|\Delta\phi\|_0$ and $\|\Delta\lambda\|_{min}/\|\Delta\lambda\|_0$ increase with joint stiffness, nevertheless, since for very stiff joints (stiff in a certain direction sense) $\|\Delta\phi\|_0$ and $\|\Delta\lambda\|_0$ become very small, one can ignore their effects (in the direction(s) in which the joint is stiff).

Further examination of Figs. 3.6 and 3.7 reveals the interesting fact that for the range of moderately flexible joints for which it is possible to spot their location on the analytical model accurately (according to Figs. 3.6 and 3.7), it is also possible to see their relative flexibility by comparing their modification factors. Thus, the stiffer the joint is (in certain direction(s)), the smaller become the stiffness modification factors (for those direction(s)). As a result of the joint's complicated nature, it is quite possible that a joint is stiff in some directions and flexible in others and, thus, in order to be able to distinguish between the rigidity of the joint in different directions involved in interfacing, it is necessary that for different directions one has to define separate modification factors for the joint adjacent elements, similar to those in equations (3.8.1) and (3.8.2).

Another point, deduced from Tables 3.4 and 3.5, is that the reduction in $\|\Delta\lambda\|_0$ is much greater than the reduction of $\|\Delta\phi\|_0$ and $\|\Delta\lambda\|_R$ is much smaller than $\|\Delta\phi\|_R$. So, it seems that eigenvectors are much more sensitive to the presence of a joint than are the eigenvalues.

Tables 3.6 and 3.7 and Figs. 3.8 to 3.11 show the results of the analysis for cases in (3.11) and (3.12). this time with mass modification factors also involved in analysis.

It is seen from Figs. 3.8 to 3.11 that by introducing mass modification factors into the analysis, the joint location performance of the modification factors has become very poor.

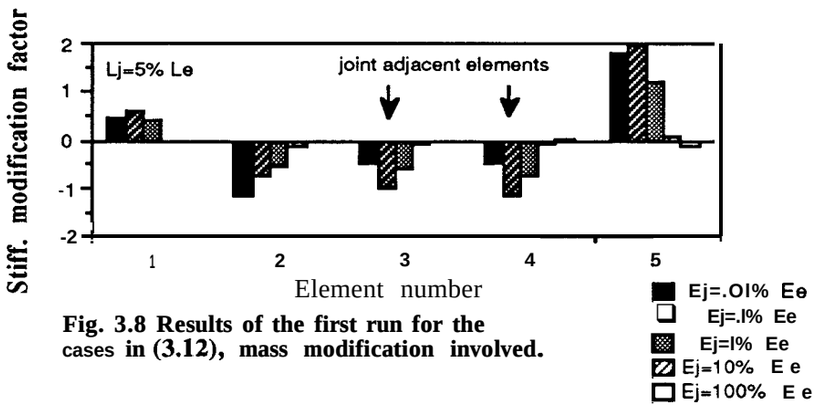

Fig. 3.8 Results of the first run for the cases in (3.12), mass modification involved.

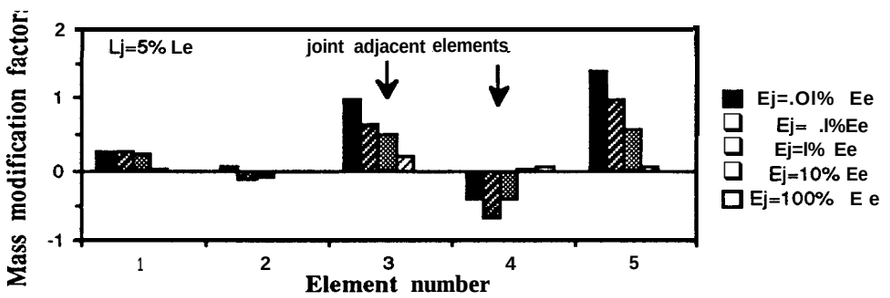

Fig. 3.9 Results of first run for the cases in (3.12).

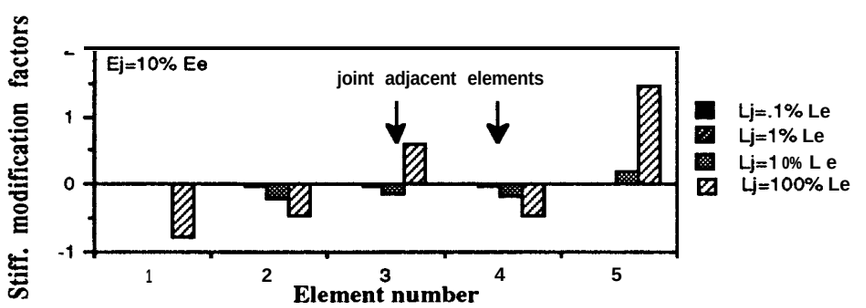

Fig. 3.10 Results of the first run for the cases in (3.11), mass modification involved

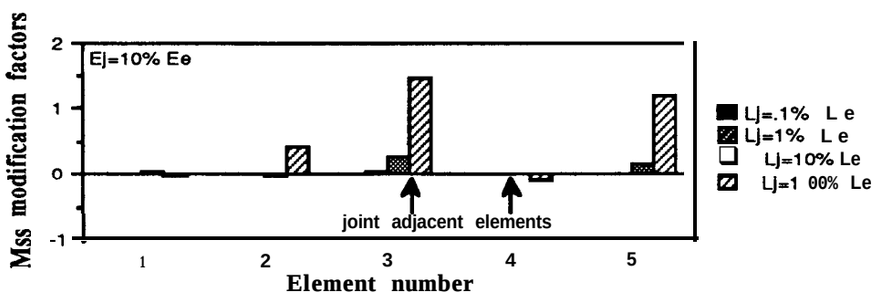

Fig. 3.11 Results of the first run for the cases in (3.11).

Examining Tables 3.6 and 3.7 reveals that, generally speaking, introduction of the mass modification factors into the analysis has reduced $\|\Delta\phi\|_R$ and $\|\Delta\lambda\|_R$ and, in some cases, this reduction is significant.

L_j = 5% Le	$\|\Delta\phi\|_{min}/\|\Delta\phi\|_0$	$\|\Delta\lambda\|_{min}/\|\Delta\lambda\|_0$	$\|\Delta\phi\|_0$	$\|\Delta\lambda\|_0$
Ej=.01%Ee	183%	12%	.998	2.24e7
Ej=.1%Ee	284%	169%	.646	1.28e7
Ej=1%Ee	57%	11%	.561	8.37e6
Ej=10%Ee	58%	5.6%	.22	4.96e6
Ej=100%Ee	68%	20%	.084	2.72e6

Table 3.6 Results for the cases in (3.12), mass modification factors involved

Ej=lO% Ee	$\|\Delta\phi\|_{min}/\|\Delta\phi\|_0$	$\|\Delta\lambda\|_{min}/\|\Delta\lambda\|_0$	$\|\Delta\phi\|_0$	$\|\Delta\lambda\|_0$
Lj=.l% Le	69.5%	11.5%	.007	135596
Lj=l% Le	67.5%	10.6%	.0615	1.27e6
Lj=lO% Le	48%	3%	.32	8.1e6
Lj=100% Le	89%	24%	1.252	2.26e7

Table 3.7 Results for the cases in (3.1 1), mass modification factors are involved in calculations.

The reason for a reduction in $\|\Delta\phi\|_R$ and $\|\Delta\lambda\|_R$ is that by letting mass become involved in the analysis, more parameters are available for adjustment to make the two models A and X closer.

On the other hand, the same effect is responsible for the worsening of the joint location spotting capability because part of the flexibility which is required to update model A is produced by mass modifications and the distribution of this mass modification is quite different from the distribution of stiffness modification factors. (Stiffness modification affects lower modes more significantly while mass modification affects higher modes more significantly.)

In order to see if attribution of mass to joint makes any difference in the above-mentioned deduction, the case of L_j=5% L_e and E_j=10% E_e has been repeated, this time with $\rho_j = \rho_e$ and both with and without mass modification factors being involved. The results of this case study confii the above-mentioned deductions, i.e. introducing mass modification factors into the analysis reduces $\|\Delta\phi\|_R$ and $\|\Delta\lambda\|_R$ and damages the location capability. The interesting fact is that even for this case, where the joint mass is not zero, one is able

to spot the joint location and to assess its relative flexibility using only stiffness modification factors in the analysis.

3.6 CONCLUDING REMARKS

From what has been reported so far, the answer to the question posed in section 3.4 :

"is joint identification a special case of model updating?"

is as follows:

"Similar mathematical techniques can be used for both problems but the nature of the two problems is different and due to this different nature the two problems cannot be tackled simultaneously in an updating process, at once, Thus they are two separate problems" .

The following conclusions can also be deduced,

(a) - Adding joint identification to a model updating problem increases the number of unknowns dramatically and affects the condition of the calculations. In some cases, if the joint model has not been selected carefully, the calculation diverges.

(b) - Considering only stiffness modification factors, it seems that for joints with moderate flexibility it is possible to spot joint locations in an analytical model and to assess their relative flexibility. In order to be able to assess the relative flexibility of a joint in the different directions which are involved in interfacing, one has to introduce separate modification factors for each direction and this, again, will increase the number of unknowns.

(c) - Very stiff joints can be ignored in an updating analysis. The question here is how can we recognize a "stiff" joint? As has been shown, a stiff joint has two characteristics which are, first, the stiffness modification factors of the joint adjacent elements would be very small and, second, $\|\Delta\phi\|_R$ and $\|\Delta\lambda\|_R$ are very small. Since, even without any joint-related problems, there are many mis-modeled regions in an analytical model, in order to be able to use either of the above-mentioned criteria one has to go through the updating process first and then, after updating mis-modeled regions, one can decide on the degree of rigidity of the joint(s).

(d) - For a wide range of moderately flexible joints, it is not possible to update the analytical model ignoring the joint.

(e) - It seems that the only practical approach to the updating problem for complex structures is to update separate substructures without any joints (or with obviously rigid joints) and then to assemble them together, making sure that the only sources of difference between the analytical model and the real structure come from the joints. Naturally, the next step will be to identify the joints and to incorporate them into the analytical model.

CHAPTER 4

COMPUTATIONAL ASPECTS OF THE GENERAL SYSTEM IDENTIFICATION PROBLEM

4.1 PRELIMINARIES:

The objective of structural identification is to determine the physical properties such as mass, stiffness and damping of a structure, or a part of a structure, using a set of given (often measured) information. The information which is used to identify the structure's dynamic characteristics is either in a modal parameters format or in a response model format. Identification techniques have been broadly categorized in chapter 1 into direct* and adaptive techniques. In a direct identification approach, the information set is related only to the structure under identification and calculations will result in a mass and stiffness and damping matrix attributed to the structure. In an adaptive approach, on the other hand, the data are related to an assumed analytical model of the structure and to the structure itself and, using the difference between two models and a cause-and-effect principle to formulate a governing equation, the difference between the characteristics of the real structure and the assumed analytical model will be calculated. The adaptive identification technique, or as it is usually called "model updating technique**" , is more popular as it is expected to provide more information than the direct technique can (due to the fact that more information is available).

Mathematically, the identification problem falls into the category of inverse problems. Basically, a direct problem is shaped physically first and is then tackled mathematically while an inverse problem is shaped mathematically first and then the solution to it may or may not gain any physical meaning. Generally speaking, having a set of properties (information) about a structure, there can be no physically meaningful system (existence

* Not to be confused with direct model updating technique, explained in chapter 3.
** As mentioned in chapter 1, model updating is an application of adaptive identification technique.

question), a unique system (uniqueness question) or many systems having these properties [30]. The existence and uniqueness problems are mainly dependent on the amount of the data which is available for identification.

From the above definition of direct and inverse problems, it is clear that, for example, coupling is a direct problem while the model updating is an inverse problem and some problems like structural modification analysis can be considered in either category, depending on the definition of the problem.

Since, the physical properties of the structure are known in a direct problem, using Newton's second law, the governing equation of the problem will be of the "differential equation" type. Depending on the type of mathematical model used for the structure, i.e. continuous or discrete, the governing differential equations of a direct problem can be partial or ordinary, respectively. On the other hand, the nature of the governing equation of an inverse problem is algebraic and this is why the theories of linear (or even non-linear) algebra and matrix computations are at the heart of identification analysis.

In what follows, some essential theories related to the computational aspects of the identification problem in general, and the joint identification problem in particular, will be presented. It should be noted that unless otherwise stated, by the "general identification problem" we mean model updating which, as explained above, is an adaptive identification technique.

4.2 THE ESSENCE OF A LEAST-SQUARES (LS) FORMULATION IN AN IDENTIFICATION ANALYSIS

The governing equation of an identification problem is usually formulated in a matrix equation format. (The exception is the inverse eigen-sensitivity technique where the governing equation is in the form of a set of linear algebraic equations). The governing equation can generally be considered as follows:

$$[\,A\,]_{a \times n_i}\,[\,\Delta X\,]_{n_i \times n_i}\,[\,B\,]_{n_i \times b} = [\,L\,]_{a \times b} \qquad (4.1)$$

where the matrices [A], [B] and [L] are known and elements of matrix [AX] contain the unknown modifications which are necessary to update the mass and stiffness matrices of the analytical model to those of the real structure.

All the matrices in equation (4.1) are either frequency- or eigenparameter-dependent. The data required to construct [A], [B] and [L] can be acquired in 3 different ways as follows:

(a) - from a pure theoretical analysis;

(b) - from a hybrid analysis. In this case part of the data comes from theoretical analysis and the other part from experimental analysis; and

(c) - from a pure experimental analysis.

The first case, is of no interest to us here and will not be discussed. Further, there are two problems associated with cases (b) and (c), namely:

1 - incompleteness of experimental data; and

2 - measurement noise in the experimental data.

The effect of the two above problems on the matrix equation (4.1) will be discussed in the following sections.

4.2.1 EFFECTS OF INCOMPLETENESS OF EXPERIMENTAL DATA ON EQUATION (4.1).

Experimental data always suffer from spatial and modal incompleteness. "Incompleteness" means that we are able to measure only a limited number of coordinates and modes of a real structure which has an infinite number of coordinates and modes. The questions of existence and uniqueness posed in section 4.1 are closely connected with incompleteness of the experimental data.

The incompleteness of these data has two important effects on a general identification problem, as follows:

(a) - if the identification method being used is a direct* one (as explained in chapter 3), then data incompleteness will introduce an approximation to equation (4.1) which is due to incompatibility between the dimensions of the experimental and analytical data and will lead to an iterative solution of equation (4.1). Also,

* By "direct" we mean direct model updating method and not direct identification method explained in section 4.1

(b) - due to the large number of unknowns in matrix [X] and, again, a smaller amount of data, i.e. $a < n_i$ in equation (4.1), there is no unique solution for equation (4.1). The non-uniqueness of the solution is quite expected as it is impossible to extract a large amount of information, uniquely, from a relatively small amount of data.

As will be shown in later chapters, using proper identification techniques, the first problem in (a) may be avoided for the joint identification problem but, for a general identification problem, **it is computationally impossible to solve equation (4.1) without approximation,** (unless of course, using a direct updating method, the amount of data is equivalent to amount of unknowns).

Considering the second problem, in (b), i.e. the non-uniqueness problem, the amount of data can be magnified by constructing equation (4.1) for each individual frequency or mode and combining them Having done this, the amount of data will be magnified by the number of measured frequencies (or modes) while the number of unknowns remains constant.

Since the elements of matrix [AX] in equation (4.1) are frequency-dependent (from here on we will only use the term frequency-dependent but every conclusion is true also for the case of a modal parameter-dependent [AX]), then in order to be able to combine equations from different frequencies, it is necessary first to transform the matrix equation (4.1) to a set of algebraic equations and, second, to separate the mass, stiffness and damping parameters in $[\Delta X]$. For the first step, one has:

$$[\ C_1(\omega_i)\ ]_{(axb)x(\ n_i x(n_i+1)/2)}\ \{\ \Delta X(\omega_i)\ \}_{n_i x(n_i+1)/2} = \{\ L(\omega_i)\ \}_{(axb)x1} \qquad (4.2)$$

where matrix $[\ C_1(\omega_i)\ ]$ is generated from [A] and [B] at frequency ω_i. Note that the symmetry of matrix $[\Delta X]$ has been already taken into account in equation (4.2).

For the second step, i.e. separating mass, stiffness and damping parameters, considering the following equation for each element Δx_{ij} of $[\Delta X]$:

$$\Delta x_{lj} = \Delta k_{lj} - \omega_i^2 \Delta m_{lj} + (\omega_i \Delta c_{lj})\, i \qquad (4.3)$$

equation (4.2) can be rewritten as:

$$[\ C(\omega_i)\ ]_{(axb)x(3n_jx(n_j+1)/2)} \left\{ \begin{matrix} \{\Delta K\} \\ \{\Delta M\} \\ \{\Delta D\} \end{matrix} \right\}_{3n_jx(n_j+1)/2} = \{\ L(\omega_i)\ \}_{(axb)x1} \qquad (4.4)$$

Combining equation (4.4) for different frequencies leads to the following over-determined set of algebraic equations:

$$[\ P\ ]_{(n_fxaxb)x(3n_jx(n_j+1)/2)} \left\{ \begin{matrix} \{\Delta K\} \\ \{\Delta M\} \\ \{\Delta D\} \end{matrix} \right\}_{3n_jx(n_j+1)/2} = \{\ q\ \}_{(axb)x1} \qquad (4.5)$$

where n_f is the number of frequency points used in the calculation. The over-determined set of equations in (4.5) can be efficiently solved by a least-squares technique. Although it is possible to construct equation (4.5) as a square system, for the following reasons, this equation must always be overdetermined in a general identification problem (even when noise-free data are considered, as here):

(a) - a square coefficient matrix has a high risk of being ill-conditioned or even rank-deficient due to modelling and/or computational reasons. For example, considering the inverse eigen-sensitivity identification method, the sensitivity matrix (i.e. [P] in equation (4.5)) can be ill-conditioned due to the existence of linearly dependent rows related to eigenvectors. The rows are linearly dependent due to improper modelling of the analytical system, whereby some coordinates may be redundant. Computational reasons for ill-conditioning of matrix [P] will be discussed in more detail later in this chapter and

(b) - inconsistency in the data. The matter of inconsistency in data requires more detailed explanation which will be given in following section.

4.2.1.1 THE SOURCE OF INCONSISTENCY IN NOISE-FREE DATA

Taking symmetry into consideration, a general undamped n degree-of-freedom system has a maximum of n(n+l) mass and stiffness elements which could be identified and, theoretically, there are n(n+l) modal parameters of the system which can be used for identification. For example, considering a three degree-of-freedom system in Fig.4.1, there are 12 mass and stiffness elements which must be identified and the number of

known modal parameters equals to 12 as well. Thus, having a complete modal model, one will be able to construct the physical system model uniquely.

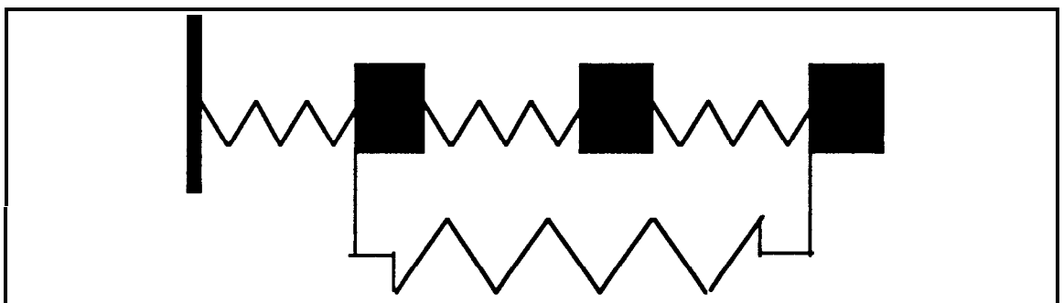

Fig. 4.1 Three degrees of freedom system

Now let us consider the case where only part of the modal data is available, say, 9 parameters out of the total of 12. Since we have incomplete data, it is not possible to identify the true physical system directly. So, the analyst chooses to use an adaptive identification method, such as the inverse eigen-sensitivity method. If the analyst has a priori knowledge about the connectivity properties of the real system in Fig.4.1, then by imposing connectivity constraints onto the analytical model, the number of unknowns, i.e. mass and stiffness differences between two models, can be reduced to 7. The question here is "can we identify the real system using only 7 items of known modal data?" and if the answer is yes, then what would be the role of the 2 extra modal data items available. To answer this question, having assumed that the inverse eigen-sensitivity method is to be used for identification, consider the governing equation for the above problem as:

$$\begin{Bmatrix} \{\Delta\phi\} \\ \{\Delta\lambda\} \end{Bmatrix}_{9x1} = \begin{bmatrix} s_{11} \cdots s17 \\ \cdots \\ \cdots \\ s71 \cdots s77 \\ \hline s_{81} \cdots s_{87} \\ s_{91} \cdots s_{97} \end{bmatrix} \begin{Bmatrix} \{\Delta K\} \\ \{\Delta M\} \end{Bmatrix}_{7x1} \qquad (4.6)$$

Assuming that the 7x7 square matrix partitioned in [S] is not rank-deficient, then it can be shown that it is always possible to express the 8th and 9th rows of [S] as linear combinations of the other rows, as follows:

$$(s_{81},.,.,.,s_{87}) = \alpha_1(s_{11},.,.,.,s_{17}) + \alpha_2(s_{21},.,.,.,s_{27}) + \ldots + \alpha_7(s_{71},.,.,.,s_{77}) \quad (4.7)$$

or

$$\{s_8\}_{7x1} = [\,S\,]^{T}_{7x7}\,\{\alpha\}_{7x1} \tag{4.8}$$

Since the matrix [S] in equation (4.8) is assumed not to be singular, one can always calculate the coefficients vector {a}. Equation (4.8) means that introduction of connectivity constraints will make the sensitivity of the modal parameters linearly dependent so that only the number of sensitivity elements equal to the number of unknowns are independent.

It should be noted that the same conclusion will be true for the l.h.s of equation (4.6) related to the 8th and 9th rows, i.e. the differences in modal parameters related to the 8th row will be a linear combination of { A$} and {Δλ} related to rows 1 to 7. This can easily be proved as follows:

pre-multiplying both sides of equation (4.8) by $\begin{Bmatrix}\{\Delta K\}\\ \{\Delta M\}\end{Bmatrix}^{T}$, one obtains:

$$\begin{Bmatrix}\{\Delta K\}\\ \{\Delta M\}\end{Bmatrix}^{T}\{s_8\}_{7x1} = \begin{Bmatrix}\{\Delta K\}\\ \{\Delta M\}\end{Bmatrix}^{T}[\,S\,]^{T}_{7x7}\,\{\alpha\}_{7x1} \tag{4.9}$$

Substituting for $\begin{Bmatrix}\{\Delta K\}\\ \{\Delta M\}\end{Bmatrix}^{T}[\,S\,]^{T}_{7x7}$ from equation (4.6) in equation (4.9) yields:

$$\begin{Bmatrix}\{\Delta K\}\\ \{\Delta M\}\end{Bmatrix}^{T}_{1x7}\{s_8\}_{7x1} = \begin{Bmatrix}\{\Delta \phi\}\\ \{\Delta \lambda\}\end{Bmatrix}^{T}_{1x7}\{\alpha\}_{7x1} \tag{4.10}$$

or

$$(\{\Delta\phi\} \text{ or } \{\Delta\lambda\})_{\text{related to 8th row}} = \begin{Bmatrix}\{\Delta \phi\}\\ \{\Delta \lambda\}\end{Bmatrix}^{T}_{1x7}\{\alpha\}_{7x1} \tag{4.11}$$

So, generally speaking, having a priori knowledge about a system's connectivity and an incomplete set of data, one is able to identify the physical system **uniquely and exactly** without using redundant data, i.e. the square system of equations in (4.5) is adequate.

Now consider the more realistic case where the analyst has no or little a priori knowledge about the connectivity of the system but assumes a prescribed connectivity pattern for it,

Fig.4.2. (note that in practice the analyst has no alternative but to keep a sort of connectivity which has been assumed in forming the analytical model, otherwise the number of unknowns will increase dramatically)

Fig.4.2 The analytical model considered for system in figure 4.1

Assuming again that 9 modal data items out of 12 are available, although here the number of unknowns is 6 for the analytical model in Fig. 4.2, all the available modal data must be used to identify the unknowns in equation (4.6). The reason why all the modal data must be used here is that, although according to equations (4.7) and (4.8) the 7th, 8th and 9th rows of [S] can be expressed as combinations of the other 6 rows, equation (4.11) is not true for this case, i.e. the $\{\Delta\phi\}$ or {Ah} related to rows>6 cannot be expressed as a linear combination of those related to other rows, as the effect of the missing spring in the analytical model is not reflected in [S] (but is reflected in $\Delta\phi_8$ or $\Delta\lambda_8$). Thus, due to the lack of information about the system's connectivity, the system of equations in (4.6) is inconsistent and in order to find the closest system to the real one (in a least-squares sense) one must use all the information available. For this case, using all available data, one will identify a **unique, but inexact,** model for the physical system.

In addition to the above-mentioned reason for inconsistency, i.e. lack of information about connectivity, approximation(s) made in deriving equation (4.5) will be another cause of inconsistency. The approximation in equation (4.5), as explained in chapter 3 and section 4.2.1, is either due to the nature of the identification method, i.e. perturbation-based method, or due to incompleteness of data, but in any event is inevitable. Now, the vector {q} on the r.h.s of equation (4.5) which represents the differences between either modal parameters or FRFs of the real and analytical systems is exact while the elements of [P] are approximate and thus, even if the analyst has a complete knowledge of the connectivity of the real system, the set of over-determined equations in (4.5) is inconsistent.

So, generally speaking, the source of inconsistency in equation (4.5) is an insufficiency and incompleteness of the data, and since this is inevitable in practice, in order to obtain

the best results in a least-squares sense, one has to use as many as equations as possible. Note that sometimes adding extra equations to an over-determined set of equations increases the error level in the results. This can be either due to significant noise effect in equations added to the original set for with-noise case, or due to.invalidity of the first order perturbation approximation for perturbation-based identification techniques (see section 7.6.2.1)

4.2.2 EFFECT ON EQUATION (4.1) OF MEASUREMENT NOISE IN EXPERIMENTAL DATA

There is a special class of identification problem where only a part of a structure, e.g. a joint, needs to be identified. For this class of problem, it is possible to solve equation (4.1) uniquely at each individual frequency point, using certain identification methods. This possibility depends, again, on the number of unknowns and available data and since the amount of data which is desired is usually small in this case, the incomplete measured data may be sufficient to provide the desired information.
Although it is computationally possible to solve equation (4.1) uniquely in such a cases, it is still necessary to construct the over-determined set of equations in (4.5) in order to reduce the measurement noise effect in the calculations.

4.2.2.1 NOISE AVERAGING PROPERTY OF LS FORMULATION.

If a random nature is assumed for the measurement noise, then its mean value will tend to zero. Although the nature of measurement errors is complicated, and is not restricted to random noise, the main contribution to measurement error is due to random noise, neglecting the systematic errors* .

As mentioned above, the mean value of a random noise signal is supposed to be zero, but this is true if and only if one takes an infinite number of samples of the signal which, in turn, means an infinite number of measurements. In a real case, where only a finite number of measurements are available, the effect of noise is expected to be reduced by using as many equations in the calculations as possible.

It is important to note that if the error effect dominates any of the matrices [A], [B] or [L] in equation (4.1), for each individual frequency, then using a LS solution may not make

* It should be noted that in any case LS has no improving effect over systematic errors.

any improvement effect on the result. To clarify this matter, consider the following example.

4.2.2.2 SENSITIVE NATURE OF AN IDENTIFICATION PROBLEM

EXAMPLE 1

In some identification techniques, such as the decoupling method, the matrix [A] in equation (4.1) is composed of some submatrices as follows:

$$[A] = [I - B^{+}[A_1 - H_c]C^{+}] \tag{4.12}$$

The submatrices in equation (4.12) are frequency-dependent and will be defined in chapter 9*. Equations (4.13) and (4.14) define the matrices $[A_1 - H_c]$ and $B^{+}[A_1 - H_c]C^{+}$, respectively at f = 100 Hz. Equation (4.15) shows the matrix $B^{+}[A_1 - H_c]C^{+}$ again, this time with 5% random noise, proportional to H_c, added to $[H_c]$ (A_1, B^{+} and C^{+} are unchanged). Comparing equations (4.14) with (4.15), it is evident that the effect of added noise has dominated the matrix $B^{+}[A_1 - H_c]C^{+}$ and, consequently, matrix [A].

$$[A_1 - H_c] = \begin{bmatrix} -8.3337\text{E-}6 & 4.1\ 1\text{E-}6 & 1.57\text{E-}6 & -3.17\text{E-}6 & 1.60\text{E-}6 \\ & -2.028\text{E-}6 & -7.738\text{E-}7 & 1.607\text{E-}6 & -8.115\text{E-}7 \\ & & -2.9\text{E-}7 & 7.91\text{E-}7 & -3.87\text{E-}7 \\ & & & 2.85\text{E-}6 & -\ 1.047\text{E-}6 \\ & & & & 3.61\text{E-}7 \end{bmatrix} \tag{4.13}$$

$$B^{+}[A_1 - H_c]C^{+} = \begin{bmatrix} & -1891 & 16248 & -2611 & \\ & & -47988 & -7947 & \\ -23853 & -12299 & 10049 & 4700 & I \end{bmatrix} \tag{4.14}$$

* Note that there is no connection between [B] and [C] in equation (4.12) and those in equations (4.1) and (4.4)

$$B^{+}[A_1 - H_c]C^{+} = \begin{vmatrix} 124138 & -34989 & 42061 & 12543 \\ -34549 & 1464 & 11858 & -3398 \\ 4288 & 19790 & -132616 & -29537 \\ 5667 & -1805 & -26099 & 181 \end{vmatrix} \quad (4.15)$$

Having defined [E] as the error matrix to be added to $[H_c]$ and $\|[E]\| << \|[H_c]\|$, one has:

$$B^{+}[A_1 - H_c + E]C^{+} = B^{+}[A_1 - H_c]C^{+} + B^{+}[E]C^{+} \quad (4.16)$$

The dominant error effect in equation (4.15) means that ;

$$\|B^{+}[E]C^{+}\| \geq \| B^{+}[A_1 - H_c]C^{+}\| \quad (4.17)$$

in equation (4.16). Physically, the quantity on the r.h.s of inequality (4.17) represents the effect of the joint on the structure's behaviour and, thus, inequality (4.17) means that joint effect is so insignificant that the noise effect dominates. The same explanation applies to the general identification or updating problems. For example, in the case of model updating, the effect of some mass or stiffness parameters of a structure may be so insignificant on the response of the structure, within a specific frequency range, that their effect can be easily become dominated by noise.

It is convinient here to demonstrate the sensitive nature of the identification problem through a simple example as follow.

EXAMPLE 2

Consider the two degrees of freedom system in Fig. 4.3

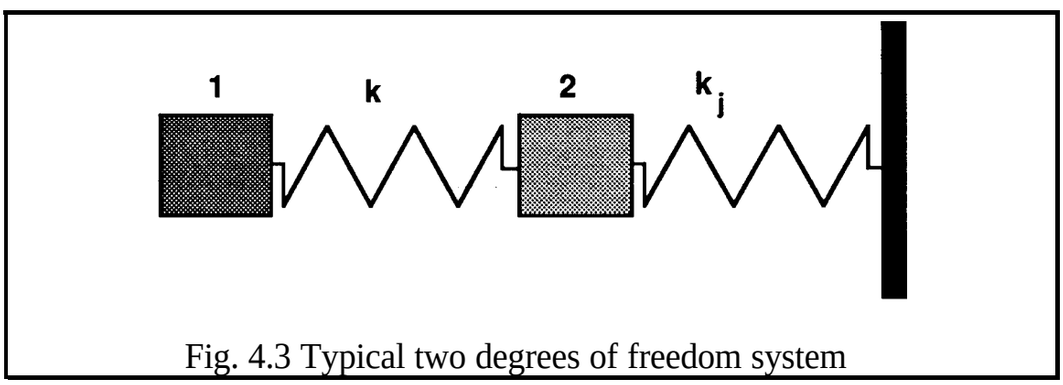

Fig. 4.3 Typical two degrees of freedom system

Both particles in Fig. 4.3 have identical mass, m, and the spring, K_j, can be considered either as a joint, in a joint identification analysis, or a typical component of the structure, in a general identification problem. It is desired to examine the significance of K_j's variation on the impedance of particle 1, z_1, and to examine the effect of this significance on the sensitivity of the process of identification of K_j, to noise.

For the impedance of particle 1, one can write:

$$\frac{dz_1}{dK_j} = \frac{K}{(-m\omega^2 + K + K_j)^2} \tag{4.18}$$

It is evident from equation (4.18) that stiffer K_j is, the less significant its effect on the z_1 becomes. To demonstrate the effect of this insignificance of K_j on the identification process, the variation of z_1 due to finite variations in K_j can be formulated as:

$$AZ, = \frac{K^2\, AK.}{[(K-m\omega^2) + K_{j0}]\,\Delta K_j + [(K-m\omega^2) + K_{j0}]^2} \tag{4.19}$$

and

$$\frac{d(\Delta Z_1)}{d(\Delta K_j)} \frac{K^2}{[\Delta K_j + (K-m\omega^2) + K_{j0}]^2} \tag{4.20}$$

where K_{j0} is the initial value of K_j and ΔK_j shows its finite variation. The following information can be deduced from equations (4.19) and (4.20):

$$\Delta K_j \text{ ----> } 0 \text{ ==> } \Delta Z_1\text{---->0} \text{ and } \frac{d(\Delta Z_1)}{d(\Delta K_j)} \text{-----> } \frac{K^2}{[(K-m\omega^2) + K_{j0}]^2}$$

$$\Delta K_j \text{ ----> } +\infty \text{ ==> } A\text{+---> } \frac{K^2}{[(K-m\omega^2) + K_{j0}]} \text{ and } \frac{d(\Delta Z_1)}{d(\Delta K_j)} \text{----->+0}$$

$$\Delta K_j \text{ ----> } -\infty \text{ ==> } \Delta Z_1\text{----> } \frac{K^2}{[(K-m\omega^2) + K_{j0}]} \text{ and } \frac{d(\Delta Z_1)}{d(\Delta K_j)} \text{----->+0}$$

$$\Delta K_j \text{ ----> } -[(K-m\omega^2) + K_{j0}] \text{ ==> } \Delta Z_1\text{----> } +\infty \text{ and } \frac{d(\Delta Z_1)}{d(\Delta K_j)} \text{----->+}\infty \tag{4.21}$$

For a very flexible joint (relative to the impedances of the substructures at the interface coordinates), one has:

$$K_{j0} << (K-m\omega^2) \text{ ==> } \frac{d(\Delta Z_1)}{d(\Delta K_j)}\Big|_{\Delta K_j=0} = \frac{K^2}{(K-m\omega^2)^2} >= 1$$

and

$$\Delta Z_1|_{\Delta K_j \to +\infty} \longrightarrow \frac{K^2}{(K-m\omega^2)} \tag{4.22}$$

For a very stiff joint :

$$K_{j0} >> (K-m\omega^2) \quad ==> \quad \frac{d(\Delta Z_1)}{d(\Delta K_j)}|_{\Delta K_j=0} >= 0 \text{ and } \Delta Z_1|_{\Delta K_j \to +\infty} \to 0 \tag{4.23}$$

Using these data, the variation of AZ, relative to ΔK_j, for high and low frequency ranges and for flexible and stiff K_{j0}, is shown in Fig. 4.4. As is evident from this figure, the asymptotic value of AZ as well as $\frac{d(\Delta Z)}{d(\Delta K_j)}|_{\Delta K_j=0}$ are very small for a very stiff joint. Note that both parameters are frequency-dependent but, for stiff joints, both of them are small to a reasonably high frequency range (as will be shown with a numerical example).

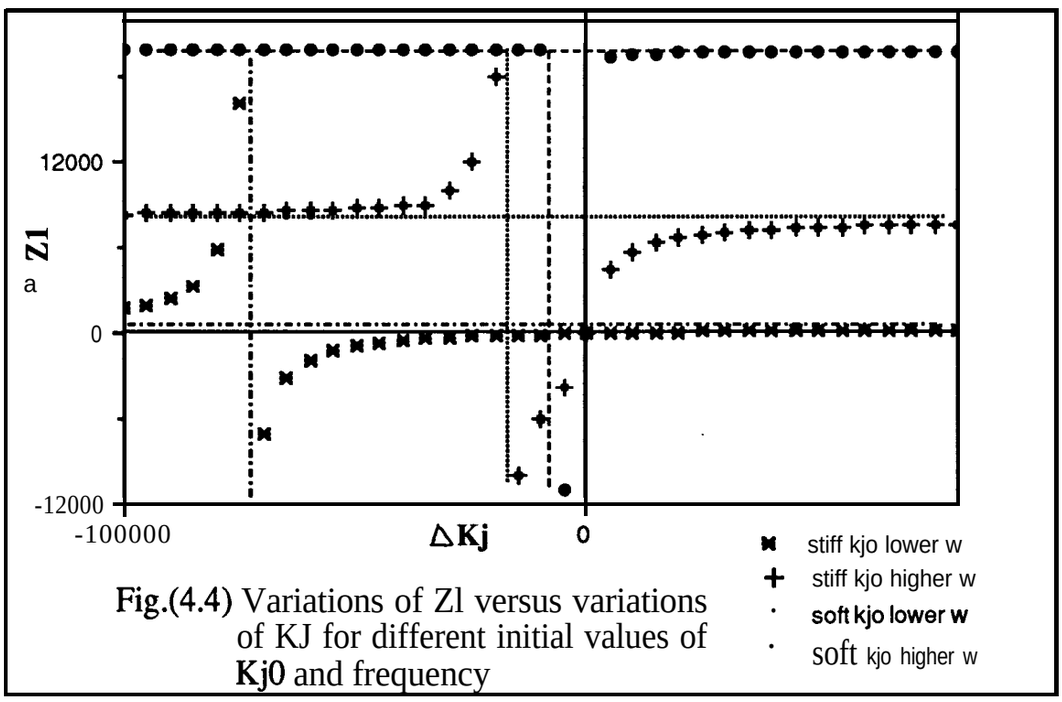

Fig.(4.4) Variations of Zl versus variations of KJ for different initial values of Kj0 and frequency

These small values for the slope at $\Delta K_j=0$ and for a limiting value of ΔZ_1 as $\Delta K_j \to \infty$ reveal that very small changes in ΔZ_1 will result in very large changes in ΔK_j and vice-versa, i.e., very large variations in ΔK_j may cause negligible changes in AZ.

As K_{j0} decreases or as frequency increases (effect of the inertia term), the situation becomes better. For flexible joints, for example, where the slope at $\Delta K_j=0$ is almost 1, any small changes in AZ will cause changes in ΔK_j of the same order of magnitude.

The following numerical example will demonstrate the effect of joint flexibility on sensitivity to error. Considering Fig. 4.3, let

$K=662{,}400$ N/m $m=0.55$ kg $K_{j0}=662{,}4000$ N/m (4.24)

For the above-mentioned values for joint properties at frequency $f=300$ Hz one has:

$$Z_1=(K-m\omega^2)-K^2(K_{j0}+K-m\omega^2)^{-1} = -1372057 \text{ N/m}$$

and the asymptotic value of $\Delta Z_1=$ 56662 N/m (4.25)

Taking $+5\%$ of Z_1 in equation (4.25) as error yields,

$+5\% Z_1=$ AZ,= -68603 N/m

Using equation (4.19) one has:

ΔK_j = -2425833 N/m (4.26)

This value represents a 37% variation from the true joint's stiffness value. If one now uses -5% Z_1 error, one has:

$\Delta K_j = 26786048$ N/m (4.27)

which is an error of about 400% in the joint's stiffness. Using data similar to those in equation (22) but here taking K_{j0} = 198720, i.e. a more flexible joint relative to the previous one, yields,

AZ,= 332827.9 N/m
$Z_1=$ 282546 N/m
5% $Z_1=$ 14127 N/m

$\Delta K_j=$ 202 N/m (4.28)

which is about 0.1% error in joint stiffness and for AZ, = -5% Z_1 the error becomes

ΔK_j = -201 N/m (4.29)

which is again 0.1% error in joint stiffness. Equal absolute values for ΔK_j were expected in this case, considering Fig. 4.4 for the case of the flexible joint.

It is worth mentioning that in the first case, i.e. a relatively stiff joint, if AZ, becomes equal to 82257, which is equal to 6% Z_1, then ΔK_j will be infinity and if AZ exceeds this value very slightly, ΔK_j will be very large negative value. Also, Fig. 4.4 reveals that for a stiff joint, ΔK_j is positive over a very narrow band of AZ variations, but otherwise is always negative.

It will be shown in later chapters, related to analysis of the performance of different identification techniques, that almost all identification techniques, either joint identification or general identification, are sensitive to noise in the above mentioned respect and that the noise effect may dominate the matrices involved in calculations for each individual frequency. In such cases, where the noise effect is dominant at each individual frequency, questions concerning the condition number of [A] or application of the S.V.D technique to invert it or using LS technique to reduce the noise effect, are irrelevant These concepts are only useful when the noise acts as a perturbation and does not dominate the matrix.

Using data from different frequencies, the only way to reduce the noise effect on the matrix [A] in equation (4.12) is to average the error at source, i.e. [AI - H,], before multiplying this matrix with matrices B^+ and C^+, which process magnifies the error. For the case of [A] in equation (4.12), due to the pattern of equation (4.12), it is not possible to put [AI - H_c] from different frequencies together (before multiplying it with B^+ and C^+) and, thus, application of a least-squares technique in this case is not associated with any error averaging advantage. As will be discussed in chapter 9, the dominant error effect is an inherent issue and depends on the nature of the identificatin problem and for these cases the error effect can only be reduced using special techniques.

An important conclusion deduced from example 1 is that governing equations like (4.1) (in which matrices [A] and [B] are simple matrices, i.e. not composed from other frequency dependent submatrices as in equation (4.12)), are the most suitable ones for LS formulation from an error averaging point of view.

4.3 COMPUTATIONAL ASPECTS OF THE LS PROBLEM

As was discussed in section 4.2, the least-squares formulation is an essential part of any identification problem, due to the incompleteness of data and/or noise effects. In this section, theorems related to the solution of a LS problem and the effect of noise on it will be discussed.

It is convenient, first, to consider the perturbation bounds for the solution of the least-squares problem. This matter has been discussed thoroughly by Lawson and Hanson in [29] and we shall only present the principal conclusions here.

4.3.1 PERTURBATION BOUNDS FOR THE SOLUTION OF LS PROBLEM

Consider equation (4.5) as:

$$[P]_{m\times n}\{\{X_1\}\}_{n\times 1} = \{q\}_{m\times 1} \tag{4.5}$$

where $$\{X_1\} = \begin{Bmatrix}\{\Delta K\}\\ \{\Delta M\}\\ \{\Delta D\}\end{Bmatrix}$$

For convenience in stating results in term of relative perturbations we define the following relative parameters:

$$\alpha = \frac{\|E\|}{\|P\|}$$

$$\beta = \frac{\|dq\|}{\|q\|}$$

$$\gamma = \frac{\|q\|}{\|P\|\,\|X_1\|} \le \frac{\|q\|}{\|PX_1\|} \tag{4.30}$$

$$\rho = \frac{\|r\|}{\|P\|\,\|X_1\|} \le \frac{\|r\|}{\|PX_1\|} \qquad (r=q-PX_1) \tag{4.31}$$

$$\kappa = \|P\|\,\|P^{+}\| = \text{condition number}([P]) \tag{4.32}$$

$$\hat{\kappa} = \frac{\kappa}{1-\kappa.\alpha} = \frac{\| P \| \| P^{+} \|}{1 - \| E \| \| P \|} \tag{4.33}$$

THEOREM 1

Let Xl be the minimum-length solution to the least-squares problem PXl=q with residual vector r=q-PX_1. Assume $\|E\|\|P^{+}\| \leq 1$ and Rank &Rank(P), and let $X_1=X_1+dX_1$ be the minimum length solution to the least-squares problem

$$\tilde{P}(X_1+dX_1) = (P + E)(X_1 + dX_1) = q + dq$$

Then

$$\text{Rank}(\tilde{P})=\text{Rank}(P) \tag{4.34}$$

and

$$\frac{\| dX_1 \|}{\| X_1 \|} \leq \hat{\kappa}\,\alpha + \hat{\kappa}\,\gamma\,\beta + \kappa\,\hat{\kappa}\,\rho\,\alpha + \kappa\,\alpha$$

$$\leq \hat{\kappa}\,[(2 + \kappa\,\rho)\,\alpha + \gamma\,\beta] \tag{4.35}$$

THEOREM 2

Assume $m>n=k$ = Rank(P) and $\| E \| \| P^{+} \| < 1$. Then

$$\frac{\| dX_1 \|}{\| X_1 \|} \leq \hat{\kappa}\,[(1 + \kappa\,\rho)\,\alpha + \gamma\,\beta] \tag{4.36}$$

Equation (4.36) indicates that the upper bound of the relative error for solution of the LS problem is proportional to the relative errors in [P] and {q} as well as the condition number of [P] and the relative norm of the residual. Thus, reducing a, β and K may improve the results.

4.3.2 IMPOSING CONSTRAINTS ON THE LS PROBLEM AND REDUCING THE NUMBER OF UNKNOWNS

The subject of imposing constraints on the LS problem and/or reducing the number of unknowns has important practical applications. A set of constraints can be imposed on the solution of a LS problem by changing equation (4.5) to following equation [29]:

$$\begin{bmatrix} [A] \\ [F] \end{bmatrix} \{X\} = \begin{Bmatrix} \{B\} \\ \{D\} \end{Bmatrix} \tag{4.37}$$

where [F] is a pxn matrix, {D} is a p dimensional vector and [F] {X}= {D} expresses the set of desired constraints. For example, suppose one requires that the solution vector {X} should be close to a known vector $\{\zeta\}$. Setting [F]=[I] and $\{D\}=\{\zeta\}$ in equation (4.37) expresses this requirement.

Constraints can be imposed on equations (4.5) using one of the following methods:

(a) - imposing constraints as a preference by adding rows to equation (4.5) as is shown in equation (4.37). In this case the constraints will be satisfied as close as possible (in a least-squares sense). The order of [P] in this case is $(m+p)x(n)$; or

(b) - imposing constraints explicitly by modifying [P] and deleting an appropriate number of unknowns in $\{X_1\}$. In this case [P] will be $mx(n-p)$.

Generally speaking, deleting some of the unknowns in any LS problem increases the residual norm $\|r\|$ (note that this does not necessarily means worse results) and at the same time reduces the condition number of [P], according to the following theorem [29]

THEOREM 3

Let [P] be an mxn matrix. Let k be an integer, $1 \leq k \leq n$. Let [B] be the mx(n-1) matrix resulting from the deletion of column k from [P]. Then the ordered singular values of [B] σ_{ib} interlace with those of [P], σ_{ip}, as follows:

case 1 $m \geq n$

$$\sigma_{1p} > \sigma_{1b} > \sigma_{2p} > \sigma_{2b} > \ldots\ldots\ldots\ldots\ldots\ldots\ldots\ldots > \sigma_{(n-1)b} > \sigma_{np} > 0 \qquad (4.38)$$

case 2 $m < n$

$$\sigma_{1p} > \sigma_{1b} > \sigma_{2p} > \sigma_{2b} > \ldots\ldots\ldots\ldots\ldots\ldots\ldots\ldots > \sigma_{mp} > \sigma_{mb} > 0 \qquad (4.39)$$

Thus, considering the definition of condition number, it is clear that cond([B]) $\leq$ cond([P]).

So, using method (b) above, one decreases, or at least does not increase, the condition number of coefficient matrix [A] at the expense of increasing, or at least not decreasing, the norm of the residual vector $\{r\}$.

4.3.3 PERTURBATION THEOREM FOR SINGULAR VALUES OF A MATRIX

THEOREM **4**

Let [B], [P] and [E] be mxn matrices with [B]-[P]=[E]. Denote their respective singular values by β_i, α_i, and ε_i, i=1,....., k; k=*min*(m,n), each set labled in nonincreasing order. Then

$$|\beta_i - \alpha_i| \leq \varepsilon_i = \|E\| \qquad i=1,\ldots,k \qquad (4.40)$$

According to equation (4.40), if the noise added to a matrix has a small norm, i.e. it is a perturbation, then provided the original matrix is not ill-conditioned, the singular values of original matrix can be considered unchanged.

4.3.4 SOLUTION TECHNIQUES FOR A LS PROBLEM.

The solution to the LS problem in equation (4.5) can be generally presented as:

$$\{X_1\} = [P]^{+}_{nxm} \{q\}_{mx1} \qquad m>n \qquad (4.41)$$

where $\{X_1\}$ is the minimum second norm solution to the LS problem and $[P]^{+}_{nxm}$ is the pseudo- or generalized inverse of the rectangular matrix [P].[29,32,33,34]. The main difference between these different methods of solving equation (4.5) lies in the method used to calculate $[P]^{+}_{nxm}$.

The two popular techniques for calculation of $[P]^{+}_{nxm}$ are as follows:

1 - application of the normal equation; and

2 - application of the S.V.D technique

4.3.4.1 APPLICATION OF NORMAL EQUATION

Premultiplying both sides of equation (4.5) with $[P]^T$, it can be rewritten as:

$$[P]^{T}_{nxm}[P]_{mxn}\{X_1\} = [P]^{T}_{nxm}\{q\}_{mx1} \qquad (4.42)$$

The nxn square system of equation (4.42) is called the system of normal equations for the linear least-squares problem. If [P] is a full-rank matrix, i.e. its columns are linearly independent, then $[P]^T[P]$ is nonsingular and the solution $\{X_l\}$ can be written in the form:

$$\{X_1\} = ([P]^T[P])^{-1}[P]^T\{q\} \tag{4.43}$$

Where the matrix

$$[P]^+_{nxm} = ([P]^T[P])^{-1}[P]^T \tag{4.44}$$

is the pseudo-inverse of [P]. Although the normal equation method is simple and easy to implement, it has a computational drawback which is due to squaring of matrix [P] in equation (4.42). Due to premultiplication of [P] with $[P]^T$, the condition number of matrix $[P]^T[P]$ can be much greater than that of the original matrix, [P]. The relationship between the condition numbers of $[P]^T[P]$ and [P] is as follows:

$$\kappa([P]^T[P]) = \text{II}\,([P]^T[P])\,\text{Ii}\,\text{II}\,([P]^T[P])^{-1}\,\text{ll} \leq \|[P]^T\|\,\|[P]\|\,\|[P]^{-T}\|\,\|[P]^{-1}\| = \kappa^2([P]) \tag{4.45}$$

or if a second norm is used to define condition number of $[P]^T[P]$ as $\kappa([P]^T[P]) = \sigma_1/\sigma_n$, then one obtains:

$$[P]^T[P] = (V\,\Sigma_p\,U^H)\,(U\,\Sigma_p\,V^H) = V\,\Sigma_p^2\,V^H \Rightarrow \kappa([P]^T[P]) = \sigma_1/\sigma_n = (\sigma_1^p/\sigma_n^p)^2 = \kappa^2([P]) \tag{4.46}$$

Thus, the condition number of matrix $[P]^T[P]$ can be as large as the square of that of [P] and this may cause serious computational errors in subsequent calculations.

4.3.4.2 APPLICATION OF S.V.D TECHNIQUE TO CALCULATE THE PSEUDO-INVERSE

Application of the S.V.D technique to calculate $[P]^+$ in equation (4.41) does not have the increased condition number problem which the normal equation has. Furthermore, the S.V.D technique has the advantage of calculating the singular values of [P] and this enables the analyst to assess the condition of this matrix and, if it is poor, to use appropriate techniques to improve the results [31].

The S.V.D technique has two disadvantages which are (i) the lengthy calculations and (ii) the large dimensions which are involved in it. For example, if the matrix [P] is generated using n_f frequency points, as in equation (4.5), then for a=10 and b=10 and n_f=100 the dimension of matrix [P] will be $10000 \times (3n_i(n_i+1)/2)$. Usually, a and b and n_f are much larger than the above values, and thus, the dimension of matrix [P] will be very large. The large dimension of [P] not only increases computation time but also reduces the accuracy of the calculations.

On the other hand, the normal equation technique is not faced with the dimension problem, as matrix $[P]^T[P]$ can be generated using equation (4.4) at each individual frequency, as follows:

$$[P]^T[P] = \sum_{i=1}^{n_f} [C^T(\omega_i)\, C(\omega_i)] \qquad (4.47)$$

Thus, using the normal equation technique, one avoids the memory size and time consumption problems but the method will be useful if and only if the condition of matrix [P] is not high and a computer with sufficient floating point accuracy is being used.

So, it is now clear that the condition of matrix [P] is a crucial issue and in subsequent sections, the computational causes of ill-conditioning of matrix [P], and consequently $[P]^T[P]$, will be discussed and the methods to cope with these causes will be presented.

4.4 ILL-CONDITIONING PROBLEM OF A LS FORMULATION

It was mentioned earlier in section 4.2.1 that poor modelling of the analytical model used in an adaptive identification approach is one reason for the ill-condition (or even rank deficiency) of matrix [P], in equation (4.5). In this section, the computational factors which may result in an ill-conditioned [P] are discussed.

Refering back to section 4.2.1, formulation of the LS problem in equation (4.5), from matrix equation in (4. 1), requires two following steps:

1 - transforming matrix equation (4.1) to an set of algebraic equations in equation (4.2); and then

2 - separating mass, stiffness and damping parameters in {X} and generating equation (4.4) at each frequency point.

Each of the above steps introduces certain computational difficulties to the solution of a LS problem, and these will be discussed below.

4.4.1 ILL-CONDITIONING ARISING FROM TRANSFORMING A MATRIX EQUATION TO A SET OF LINEAR ALGEBRAIC EQUATIONS.

Consider equations (4.1) and (4.2).

$$[\,A\,]_{axn_i}\,[\,\Delta X\,]_{n_i xn_i}\,[\,B\,]_{n_i xb} = [\,L\,]_{axb} \tag{4.1}$$

$$[\,C_1(\omega_i)\,]_{(axb)x(3n_i x(n_i+1)/2)}\,\{\,\Delta X(\omega_i)\,\}_{n_i x(n_i+1)/2} = \{\,L(\omega_i)\,\}_{(axb)x1} \tag{4.2}$$

Each element c_{1pq} related to Δx_{ij} can be calculated from the following equation (assuming symmetry):

$$c_1((t-1)xa+g,(i-1)x(n_i-i/2)+j) = a(t,i)\ x\ b(j,g) + a(t,j)\ x\ b(i,g)$$
$$i,j = 1.\ldots\ldots ni \text{ and } j>i \qquad t = 1..... a \quad \text{and } g = 1..... b \tag{4.48}$$

If i=j then

$$c((t-1)xa+g,(i-1)x(n_i-i/2)+j) = a(t,i)\ x\ b(j,g) \tag{4.49}$$

Examining equation (4.48) reveals that the summation on the right hand side of this equation may lead to a poorly conditioned matrix, [Cl], because the summation on the r.h.s may generate elements with large differences in order of magnitude and sometimes can lead to a sparse matrix. Also, in cases where noise is present, the summation on the r.h.s of equation (4.48) may cause the noise effect in some elements to be larger than the correct value itself.

4.4.2 ILL-CONDITIONING ARISING FROM SEPARATION OF VARIABLES IN ALGEBRAIC EQUATION (4.2)

Having transformed equation (4.1) to a set of algebraic equations for each frequency ω, and having imposed a symmetry constraint on $[\Delta K],[\Delta M]$, one obtains:

$$[C(\omega)]_{(axb)x(n_i(n_i+1))}\left\{\begin{matrix}\{K\}\\ \{M\}\end{matrix}\right\}_{(n_i(n_i+1))x1} = \{L(\omega)\}_{(axb)x1} \tag{4.4}$$

where the matrix $[C(\omega)]$ is partitioned as follows:

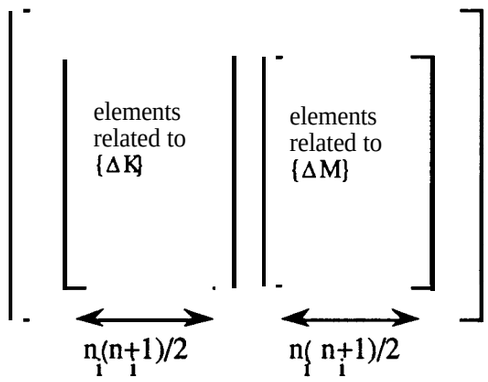

(4.50)

Each element c_{pq} related to Akij can be calculated from equations (4.48) and (4.49) and elements of c_{pq} related to mass are exactly equal to those related to stiffness multiplied by $-\omega^2$.

The matrix [C(o)] in the l.h.s of equation (4.4) has been generated from the r.h.s of equation (4.1), i.e.

$$[A]\,[\Delta X]\,[B] \text{ leading to } [C(\omega)]\begin{Bmatrix}\{\Delta K\}\\ \\ \{\Delta M\}\end{Bmatrix} \tag{4.51}$$

Now, two cases are possible for the relative dimensions of matrices [A], [B] and [X], i.e. either $axb < n_i(n_i+1)$ which means an under-determined set of equations in (4.4) and happens in the case of a general identification problem (model updating), or $axb > n_i(n_i+1)$ which usually happens in the case of the joint identification problem. For the first case, i.e. $axb < n_i(n_i+1)$, it is obvious that equation (4.4) is rank deficient. In what follows it will be shown that even for the second case, i.e. $axb > n_i(n_i+1)$, equation (4.4) is still rank deficient.

Let $axb > n_i(n_i+1)$ and

$$[T(\omega)]_{axb} = [A][\Delta X][B] \tag{4.52}$$

Considering the maximum possible rank of the constituent matrices of [T] in equation (4.52), and the following inequality:

$$\text{rank } ([A].[B]) \leq \min (\text{rank}([A] \text{ or } [B])$$

it becomes clear that matrix [T] is rank-deficient and its maximum rank cannot exceed (ni). This rank-deficiency means that there are only ni rows (or columns) of [T] which are independent of each other and these constitute $(n_i)^2$ independent linear equations in [C(o)] in equation (4.4). On the other hand, the number of unknowns in equation (4.4) is ni(ni+l), which is greater than maximum possible number of independent equations in equation (4.4). It should be noted that in cases where any one of the constituent matrices of matrix [T] in equation (4.52) is rank deficient, the rank of matrix [T] will decrease and so will the number of independent equations in equation (4.4).

Let us now to demonstrate how using a LS formulation as mentioned in section 4.2.1 can improve the rank deficiency problem of individual equations like (4.4). Using the normal equation technique in equations (4.42) and (4.47) to solve the least-squares problem defined in equation (4.5), one obtains the following equation:

$$\left[[C(\omega_1)]^T[C(\omega_1)]+[C(\omega_2)]^T[C(\omega_2)]+....+[C(\omega_{nf})]^T[C(\omega_{nf})]\right]\begin{Bmatrix}\{\Delta K\}\\ \{\Delta M\}\\ \{\Delta D\}\end{Bmatrix} =$$

$$\left[[C(\omega_1)]^T\{L(\omega_1)\}+[C(\omega_2)]^T\{L(\omega_2)+....+[C(\omega_{nf})]^T\{L(\omega_{nf})\}\right] \quad (4.53)$$

or

$$[P]^T[P]\begin{Bmatrix}\{\Delta K\}\\ \{\Delta M\}\\ \{\Delta D\}\end{Bmatrix} = [P]^T\{q\} \quad (4.30)$$

Examining equation (4.53) shows that although each of the matrices added together in the l.h.s of this equation is itself rank deficient, one expects that, adding them together, the resultant matrix will be of full rank. It should be noted that there is no mathematical proof to support this expectation but, combining sufficient equations, nf, the coefficient matrix on the l.h.s of equation (4.53) turns out to be well-conditioned (with further considerations which will be explained shortly). In order to be able to decide how large

nf must be, the simplest way is to check the rank of the coefficient matrix on the l.h.s of equation (4.53) each time after adding a new set of equations like (4.4) to it.

In addition to the "increasing number of unknowns" problem caused by the separation of parameters, there is another problem associated with separating mass, stiffness and damping parameters in {AK}. In order to explain this problem, we return to equations (4.4) and (4.50). Considering the nature of matrix [C(o)], which is explained in equation (4.50), the columns of $[C(\omega_i)]$ related to M for each frequency ω_i are exactly equal to the columns related to K multiplied by $-\omega_i^2$ and, if a viscous damping model is in use, the columns related to D are exactly similar to those related to K multiplied by $i\omega_i$. The difference in order of magnitude caused by multiplying mass-related elements by $-\omega_i^2$, especially at higher frequencies, makes matrix $[C(\omega_i)]$ ill-conditioned at each individual frequency and also makes the resultant set of equations in equation (4.5), and consequently in equation (4.42), ill-conditioned. This ill-condition has a significant effect on results and should be dealt with through balancing of the matrix [P] in equation (4.5).

4.4.3 BALANCING TECHNIQUES AND REDUCTION OF THE NUMBER OF THE UNKNOWN PARAMETERS

It was shown in section 4.4.2 that separation of the parameters in {AK} leads to an ill-conditioned [P] due mainly to the increased number of unknowns (rank deficient $[C(\omega_i)]$ in equation (4.4)) and to the difference in the order of magnitude of the elements related to different parameters. In this section we will show that both the above causes of ill-conditioning can be dealt with by balancing [P] through a reference analytical model.

Generally speaking, a typical model updating problem does not require any balancing, as the above-mentioned difference of order of magnitude between elements of [P] do not exist in this case. The matrix [P] in a model updating analysis is automatically balanced, because of the following model used for $[\Delta K], [\Delta M]$ and [AD].

$$[\Delta K] = \sum_{e=1}^{n} \alpha_{ke} [K]_e$$

and

$$[\Delta M] = \sum_{e=1}^{n} \alpha_{me} [M]_e \qquad (4.54)$$

where n is the number of elements and $[M]_e$ and $[K]_e$ are the elemental matrices used to generate the analytical counterpart of the real structure.

Using equation (4.54) to generate matrix $[C(\omega_i)]$ from [A][AX][B] will automatically balance matrices $[C(\omega_i)]$ and [P] because the order of magnitude of $[M]_e$ is very small compared with that of $[K]_e$ and, thus, multiplying it with ω_i^2 will not cause an ill-conditioning problem.

For joint identification applications, where one may not have an FE-generated analytical model available, one of the following techniques can be used for balancing matrix **[P]**:

(a) - balancing can be performed by multiplying the columns of [P] related to mass and damping by suitable scaling factors to make these columns' order of magnitude comparable with that of columns related to stiffness.

The scaling of mass- and damping-related columns must be performed on the final coefficient matrix [P] in equation (4.5) and one cannot balance matrices at each individual frequency unless a similar scaling factor is used for all frequencies.

Although improving the condition of [P] significantly, the method of balancing described above sometimes still yields a large condition number of **[P],** especially when identification is carried out over a wide frequency range. Also, finding a proper scaling factor is analyst-dependent and sometimes difficult;

(b) - a more efficient way of balancing the matrix **[P],** inspired by equation **(4.54),** is to choose a prescribed model for [AK],[AM] and [AD] as a reference joint model and, then, to consider [AK],[AM] as follows (damping is ignored from here on as it is straightforward to extend any result to the damped case):

$$[\Delta K]_j = \sum_{d=1}^{m_i} \alpha_{kd} [\Delta K]_{re}^d$$

and

$$[\Delta M]_j = \sum_{d=1}^{m_i} \alpha_{md} [\Delta M]_{re}^d \qquad (4.55)$$

where m_i is the number of interface stations in joint identification applications where each interface station consists of a set of interface coordinates. Note that always

$$m_i < n_i \tag{4.56}$$

Each matrix $[M]^d_{re}$ (or $[K]^d_{re}$) in equation (4.55) is an $n_i x n_i$ matrix with non-zero elements in locations related to constituent interface coordinates of interface station d, and n_i is the number of total interface coordinates.

As noted earlier, using an adaptive identification technique, one requires an analytical model* for comparison with the real structure. In the case of joint identification, in order to be able to generate the analytical model, one has to consider a trial joint model.

Principally, the quality of a reference joint model is dictated by the model assumed for the trial joint (i.e. features like number of interface coordinates at each interface station or connectivity assumed between different interface coordinates) but quantitatively the trial joint model and the reference joint model can be completely different.

Using equation (4.55) in generating matrix [C(o)] from matrix [A][AX][B] will automatically balance matrices [C(o)] and [P] because the order of magnitude of $[M]^d_{re}$ is very small compared with $[K]^d_{re}$ and thus multiplying it with ω_i^2 will not cause an ill-condition problem.

Apart from the automatic balancing feature associated with technique using equation (4.55), another advantage of this balancing is that in this case the number of unknowns is reduced to $2m_i$, i.e. α_{mr}, α_{kr} r =1,2,.....mi, (or 3mi in the case of viscous damping where one extra coefficient must be considered for damping) and thus there will be no problem of rank deficiency associated with matrix [C(o)] in equation (4.4) if the following inequality is satisfied:

$$3m_i \leq n_i^2 \tag{4.57}$$

Considering (4.56), it is clear that inequality (4.57) is always satisfied. In order to clarify further the matter of unknown reduction property of reference model, consider the following example. Fig. 4.5 shows the "real" structure for this example and, as is

* Note that the analytical model can be entirely generated by F.E. method or can be generated from composing experimental data acquired from structure itself and a prescribed model assumed for the unknown part of structure, e.g. a joint. The analytical model generated using the latter technique is called by author: "the analytically coupled structure". (see chapter 3)

evident from this figure, there is one interfacing station with 4 interfacing coordinates in it** , i.e. $m_i=1$ and $n_i=4$.

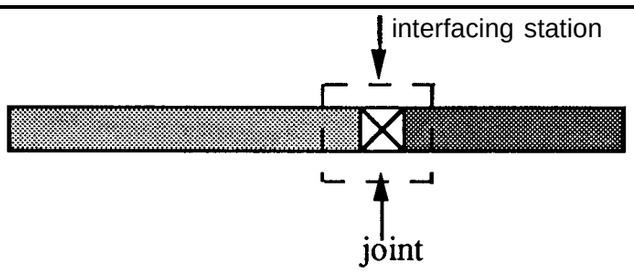

Fig. 4.5 The example structure with one interfacing station comprising of 4 interface coordinates

Now, considering the reference model in equation (4.55) for the joint in Fig. 4.5, the number of unknowns in equation (4.4) is reduced from 30, in the general case, to 3, i.e. three unknowns a,, α_k and α_c, while the number of independent equations available in equation (4.4) is 16.

The model adopted for modifications $[\Delta K]_j$ and $[\Delta M]_j$ to the trial joint model in equation (4.55) is exactly similar to the mass and stiffness modification models which are used in model updating practice. In spite of all the advantages associated with taking modification factors as in equation (4.55) (stated above), it is not applicable to joint identification problem directly and must be modified. The reason for this impracticality has been explained in chapter 3 and, briefly, is due to the fact that assigning only one modification factor for the whole set of degrees of freedom involved in an interface station d in $[M]^d_{re}$ (or $[K]^d_{re}$) only reflects the need to change the density (or Young's modules) of the reference joint model at that station and does not take into account the essence of any variation of the geometrical characteristics of the reference joint. Keeping the geometrical features of the reference joint model unchanged means that the geometrical characteristics assumed for the reference joint model are a correct representation of the geometrical characteristics of the real joint, which is not true.

Considering a beam element model for the joint in Fig. 4.5, in order to give necessary flexibility to parameters α in equation (4.55) to change the geometry (in this case length)

** It is relatively easy to decide about the number of interfacing stations but it is not so easy to decide about the proper number of interfacing coordinates within each interfacing station. As a general rule, the number of interface coordinates in each interfacing station is equal to the minimum number of coordinates required to couple substructures across that interfacing station.

of reference joint model, as well as E and p, (at least) the following model must be adopted for mass and stiffness modifications:

$$[\Delta K]_j = \alpha_1 \begin{bmatrix} a_1 & 0 & -a_1 & 0 \\ & 0 & 0 & 0 \\ & & a_1 & 0 \\ & & & 0 \end{bmatrix} + \alpha_2 \begin{bmatrix} 0 & a_2 & 0 & a_2 \\ & 0 & -a_2 & 0 \\ & & 0 & -a_2 \\ & & & 0 \end{bmatrix} + \alpha_3 \begin{bmatrix} 2a_3 & 0 & a_3 & \\ & 0 & 0 & \\ 0 & 0 & 0 & 2a_3 \end{bmatrix}$$

and similarly,

$$[\Delta M]_j = \alpha_4 \begin{bmatrix} 156a_4 & 0 & 54a_4 & 0 \\ & 0 & 0 & 0 \\ & & 156a_4 & 0 \\ & & & 0 \end{bmatrix} + \alpha_5 \begin{bmatrix} 0 & 22a_5 & 0 & -13a_5 \\ & 0 & 13a_5 & 0 \\ & & 0 & -22a_5 \\ & & & 0 \end{bmatrix} + \alpha_6 \begin{bmatrix} 0 & 0 & 0 & 0 \\ & 4a_6 & 0 & -3a_6 \\ & & 0 & 0 \\ & & & 4a_6 \end{bmatrix} \tag{4.58}$$

Equation (4.58) means that there will be 6 modification factors (9 if viscous damping is involved) at each interfacing station, for reference joints with a beam element model (i.e. with 4 degrees of freedom involved in interfacing) and, thus, the necessary (but not sufficient) condition for a full rank matrix [C(U)] in equation (4.4) is:

$$9m_i \leq n_i^2 \tag{4.59}$$

In the general case where nid interface coordinates are involved at each interfacing station d, the number of modification factors at each station depends on the connectivity model between the different interfacing degrees of freedom;

(c) - in real engineering applications there are cases where it is very difficult, if not impossible, to assign any prescribed model to a real joint, and consequently to trial and reference joints. In such cases, the reference model described by equation (4.58) is not applicable and a completely general pattern must be considered for the reference (and trial) joint models. For example, considering the joint in Fig. 4.5 as a joint with 4 degrees of freedom, i.e. four interface coordinates, and without considering any pattern for the joint mass and stiffness matrices, apart from symmetry, the reference model is:

$$[\Delta K]_j = \begin{bmatrix} \alpha_1 a_1 & \alpha_2 a_2 & \alpha_3 a_3 & \alpha_4 \\ & \alpha_5 a_5 & \alpha_6 a_6 & \alpha_7 \\ & & \alpha_8 a_8 & \alpha_9 a_9 \\ & & & \alpha_{10} a_{10} \end{bmatrix}$$

$$[\Delta M]_j = \begin{bmatrix} \alpha_{11} a_{11} & \alpha_{12} a_{12} & \alpha_{13} a_{13} & \alpha_{14} a_{14} \\ & \alpha_{15} a_{15} & \alpha_{16} a_{16} & \alpha_{17} a_{17} \\ & & \alpha_{18} a_{18} & \alpha_{19} a_{19} \\ & & & \alpha_{20} a_{20} \end{bmatrix} \qquad (4.60)$$

As equation (4.59) indicates, using the general balancing approach for a joint with 4 degrees of freedom, there will be 10 modification factors α_i for each of the mass and stiffness (and damping if it is viscous) parameters at each interfacing station, each of which must be calculated. It is clear from equation (4.60) that a general reference joint model in this equation balances the matrix [P] but does not reduce the number of unknowns.

In the general case where nid interface coordinates are involved at each interfacing station d,the number of modification factors at each station is equal to $n_{id}(n_{id}+1)/2$ for each of the mass or stiffness or damping parameters and thus the full rank condition for equation (4.4) will be:

$$3m_i n_{id}(n_{id}+1)/2 \leq n_i^2$$

Note that: $n_i = m_i n_{id}$

To demonstrate how balancing can affect the condition of matrix [P], Table 4.1 shows the condition number of matrix $[P]^T[P]$, in equation (4.47), for a typical joint identification calculation, using different balancing techniques. Note that in all cases the number of unknowns is the same.

	No balancing	Simple scaling balancing in ta)	Balancing using ref. joint model in (4.58)
$\kappa([p]^T[P])$	7E22	9E8	4E8

Table 4.1 Condition number of matrix $[P]^T[P]$ using different balancing methods

4.5 A DISCUSSION OF THE CONCEPT OF ILL-CONDITIONING AND SENSITIVITY OF A MATRIX

The question which will be addressed in this section is: "is the condition number of a matrix a necessary and sufficient criterion for determining its sensitivity to small perturbation?". The answer to the question, as it will be shown shortly, is "condition number is not a sufficient (defined below) condition and is not necessary. In other words, there may be cases where the condition number is reasonably low but the matrix is very sensitive to perturbations".

Consider the set of equations in (4.5) as a general algebraic equation:

$$[P]_{m\times n}\{\{X_1\}\}_{n\times 1} = \{q\}_{m\times 1} \tag{4.5}$$

The upper bound for errors in solution of matrix equation (4.9, induced by errors added to the coefficient matrix [P], is given in equation (4.36) and is:

$$\frac{\| dX_1 \|}{\| X_1 \|} \leq \hat{\kappa}[(1 + \kappa\, p)\, a + \gamma\, \beta] \tag{4.36}$$

where parameters in equation (4.36) have been defined in section 4.3.1. According to equation (4.36), the condition number of matrix [P], κ, is an upper bound for errors and having large values for this upper bound does not necessarily means that error value is high. So, condition number is not a sufficient criterion, i.e. if the condition number of a matrix is large it does not necessarily imply that the matrix is ill-conditioned but, in most cases that condition number of a matrix is large enough, there is a substancial chance of that matrix being sensitive. So, here we make a distinction between matrix sensitivity and ill-conditioned, i.e. a matrix is ill-conditioned whenever its condition number is high but not every ill-conditioned matrix is sensitive to perturbations.

In what follows, we will demonstrate the non-necessity of condition number for sensitivity assessment of a matrix and, having comprehensively discussed the various aspects of sensitivity of a matrix, we will present a sufficient (but not necessary) condition for a matrix to be ill-conditioned.

Let us first demonstrate the non-necessity of condition number, as a sensitivity assessment criterion, through an example.

Consider the receptance matrix, [H], of a structure in expression (4.61). Expressions (4.62) and (4.63) show the inverse of [H] before and after adding 5% random noise, proportional to elements of [Hj, to it, respectively.

$$[H] = \begin{bmatrix} 6.157E\text{-}8 & 1.156E\text{-}7 & -6.63E\text{-}9 & -5.418E\text{-}8 & -2.4E\text{-}8 \\ & 1.58E\text{-}8 & -3.639E\text{-}9 & -2.568E\text{-}8 & -1.14E\text{-}8 \\ & & -3.757E\text{-}8 & 1.676E\text{-}8 & 7.45E\text{-}9 \\ & & & -1.677E\text{-}7 & 1.2E\text{-}8 \\ & & & & -3.36E\text{-}8 \end{bmatrix} \quad (4.61)$$

$$[H]^{-1} = \begin{bmatrix} -1.4E6 & 9.1E6 & -1.29E6 & -1.08E6 & -2.44E6 \\ & -7.34E6 & -2.19E6 & -2.1E6 & -4.7E6 \\ & & -2.717E7 & -2.18E6 & -4.9E6 \\ & & & -5.24E6 & -680700 \\ & & & & -2.6887 \end{bmatrix} \quad (4.62)$$

$$[H]^{-1} = \begin{bmatrix} -1.07E8 & -1.7E8 & -3E9 & -3.1E8 & -9.58E7 \\ -9.72E7 & 1.23E23 & 1.07E24 & 1.2E23 & 1E23 \\ -1.15E9 & 4.8E23 & -1.4E24 & -6.2E22 & 2.7E24 \\ -1.17E8 & 6.4E22 & 1.8E22 & 1.12E22 & 2.8E23 \\ -5E8 & 3.3E23 & 5.18E24 & 5.5E23 & -6.9E23 \end{bmatrix} \quad (4.63)$$

Comparing expressions (4.62) and (4.63) reveals the high sensitivity of matrix [H] to perturbation. On the other hand, the condition number of [H] is equal to 6. Now, the question is: "what is the underlying factor which makes matrix [H] in equation (4.61) sensitive to noise?". To answer this question, let us first consider just what is meant by the sensitivity of a matrix.

Consider a general complex matrix [A] and its singular value decomposition as:

$$[A]_{mxn} = [U]_{mxm}\,[\Sigma]_{mxn}\,[V]^{H}_{nxn} \quad (4.64)$$

where [U] and [V] are unitary matrices and their columns are the left and right singular vectors of [A] respectively. Mathematically, [V] and [U] are eigen-matrices of $[A]^{H}[A]$ and [A] $[A]^{H}$, respectively.

The diagonal matrix $[\Sigma]$ contains the singular values σ_i of matrix [A] so that, if rank [A] is r ≦ min(m,n), the matrix $[\Sigma]$ will only have r non-zero diagonal elements. Equation (4.64) can be rewritten as:

$$[A]^{r}_{mxn} = \{u\}_1\{v\}^H_1\sigma_1 + \ldots\ldots\ldots + \{u\}_r\{v\}^H_r\sigma_r \qquad (4.65)$$

Although the inverse of a rank-deficient matrix does not exist, one can define the pseudo-inverse of the matrix, for this case [32,33,34]. Using the pseudo-inverse of a matrix, the minimum 2 norm least-squares solution of [A] {x}={ b} can be calculated. The pseudo-inverse is defined as:

$$[A]^{+}_{nxm} = \{v\}_1\{u\}^H_1.1/\sigma_1 + \ldots\ldots\ldots + \{v\}_r\{u\}^H_r.1/\sigma_r \qquad (4.66)$$

It can be shown [33] that the smallest singular value of [A] is the 2-norm distance of [A] to the set of all rank-deficient matrices. This means that if $[A]_k$ is a member of the set of matrices with its rank k ≦ r = rank [A], then:

$$\min \text{II } [A] - [A]_k \text{ II} = \text{II } [A] - [A], 1 \text{ II} = \sigma_r \qquad (4.67)$$

Matrix [A] of equation (4.64) is called sensitive if, after adding a small amount of noise to it, some or all of its singular parameters, i.e. singular vectors and singular values in equations (4.65) and (4.66), change dramatically.

Note that in the case of equation (4.65), in spite of major changes in some of the singular parameters, the elements of the matrix itself show only very small variations (as small noise has been added to matrix) but, for $[A]^{-1}$ in equation (4.64), changes in singular parameters of [A] are associated with dramatic variations in $[A]^{-1}$ itself.

The Taylor series expansions of σ_r and $\{v\}_r$, the rth singular value and right singular vector of matrix [A], in terms of variable e_i are:

$$\sigma_r = \sigma_{r0} + \sum_{i=1}^{n} \frac{\partial \sigma_r}{\partial e_i} \Delta e_i + \ldots\ldots\ldots \qquad (4.68)$$

$$\{v\}_r = \{v\}_{r0} + \sum_{i=1}^{n} \frac{\partial \{v\}_r}{\partial e_i} \Delta e_i + \ldots. \qquad (4.69)$$

where in a first-order approximation the higher-order terms are neglected. For this case

$$\Delta\sigma_r = \sum_{i=1}^{n} \frac{\partial \sigma_r}{\partial e_i} \Delta e_i \qquad (4.70)$$

$$\Delta\{v\}_r = \sum_{i=1}^{n} \frac{\partial \{v\}_r}{\partial e_i} \Delta e_i \qquad (4.7\ 1)$$

Equations (4.70) and (4.71) indicate that variation of singular parameters depends on both the magnitude of error and sensitivity of singular parameters themselves. Since, as mentioned earlier in this section, $\{v\}$ and $\{u\}$ are right and left modal vectors of $[A]^H[A]$ and $[A][A]^H$, respectively, study of the following section is necessary, in order to be able to investigate singular parameters' sensitivity to perturbation.[28,35]

4.5.1 SENSITIVITY OF MODAL PARAMETERS OF A MATRIX TO SMALL PERTURBATIONS.

This problem has been efficiently explained in [28] (and [35]) which can be summerized as follows:

Suppose λ_r is a simple eigenvalue of a real matrix [B] and $\{{}_l\phi\}_r$ and $\{{}_R\phi\}_r$ are the corresponding left-hand and right-hand eigenvectors . Then as [AB] tends to the null matrix, [B+AB] has an eigenvalue $\lambda_r + \Delta\lambda_r$ in accordance with the stationary property of eigenvalues (Rayleigh principle), or by using first-order eigenvalue sensitivity, such that the change of the rth eigenvalue can be calculated from:

$$\Delta\lambda_r = \frac{\{{}_l\phi\}_r^T [\Delta B] \{{}_R\phi\}_r}{\{{}_l\phi\}_r^T \{{}_R\phi\}_r} \qquad (4.72)$$

From equation (4.72), the absolute value of $\Delta\lambda_r$ can be expressed as:

$$|\Delta\lambda_r| \le \frac{\|\{{}_l\phi\}_r^T\| \, \|[\Delta B]\| \, \|\{{}_R\phi\}_r\|}{|\{{}_l\phi\}_r^T \{{}_R\phi\}_r|} \qquad (4.73)$$

and $|\{{}_l\phi\}_r^T \{{}_R\phi\}_r|$ is the cosine of the angle θ_r between the left and right-hand eigenvectors. When $\cos\theta_r$ is very small, the corresponding eigenvalue is very sensitive to perturbations in the elements of [B]. Wilkinson [35] suggested that $|\{{}_l\phi\}_r^T \{{}_R\phi\}_r|$ is a condition number for a nonrepeated eigenvalue. When the matrix [B] is symmetric and

θ_r=0, since $\{_I\phi\}_r^T\{_R\phi\}_r$ is normalized to unity, the condition number for a nonrepeated eigenvalue is dependent on the norm of modification matrix [AB].
For a general matrix with distinct eigenvalues, the eigenvector $\{_R\phi'\}_r$ of [B+AB] corresponding to $\{_R\phi\}_r$ is such that ($\|[\Delta B]\| \rightarrow 0$)

$$\{_R\phi'\}_r - \{_R\phi\}_r = \sum_{\substack{s=1 \\ s\neq r}}^{N} \frac{\{_R\phi\}_s \{_I\phi\}_s^T [\Delta B] \{_R\phi\}_s}{\{_I\phi\}_s^T \{_R\phi\}_s (\lambda_r - \lambda_s)} = \sum_{\substack{s=1 \\ s\neq r}}^{N} \frac{\{_R\phi\}_s \{_I\phi\}_s^T [\Delta B] \{_R\phi\}_s}{\cos\theta_r (\lambda_r - \lambda_s)} \quad (4.74)$$

Again, it can be seen that the quantity $\cos\theta_r$ is important, however, the sensitivity of the eigenvector is also dependent on the proximity of λ_r to the other eigenvalues. From equation (4.74), the smallest value $(\lambda_r - \lambda_s)$, indicating the separation of eigenvalue λ_r from its neighbours, is usually defined as a condition number for the corresponding eigenvector $\{_R\phi\}_r$.

Denoting [AB] in equations (4.73) and (4.74) as perturbation to matrix $[A]^H[A]^*$, let us now consider the sensitivity of singular values of matrix [A], rewriting equation (4.73) as:

$$|\Delta\sigma_r| \leq \frac{\|\{v\}_r^T\| \, \|[\Delta B]\| \, \|\{v\}_r\|}{|\{v\}_r^T \{v\}_r|} \quad (4.75)$$

Since $|\{v\}_r^T\{v\}_r\| = 1$ then, according to equation (4.75), $|\Delta\sigma_r|$ can only be large if $\|[\Delta B]\|$ is large. In this case since;

$$\sigma_1 = \|[A]\|_2 \text{ and assuming that } \|[\Delta B]\| << \|[A]\|_2 \implies \|[\Delta B]\| << \sigma_1 \quad (4.76)$$

$|\Delta\sigma_r|$ may be relatively large for smaller singular values and, thus, the smallest singular value is the likeliest one to be affected most. As a matter of fact, the sensitivity of the smallest singular value of a matrix, just explained, is measured by the condition number of the matrix, i.e. if the smallest singular value of a matrix is very small comparing to the norm of the matrix (or its biggest singular values), it is very likely that a relatively moderate $\|[\Delta B]\|$ will affect σ_n dramatically. On the other hand, if σ_n is not very small relative to σ_1, then, according to inequality (4.76), σ_n will not be affected too much.

---

* Note that in this case [B] $\doteq [A]^H[A]$, then $\{_R\phi\} \doteq \{v\}$ and $\{_I\phi\}$ $\{v\}$ for singular parameter applications

It is convenient now to examine the possibility of having sensitive right and left singular vectors. Actually, the possibility of having sensitive singular vectors is usually dismissed in a routine sensitivity analysis and the author found it to be a quite an important matter.

Consider equation (4.74) as* :

$$\{\Delta v\}_r = \sum_{s=1}^{N} \sum_{s\neq r} \frac{\{v\}_s \{v\}_s^T [\Delta B]\{v\}}{\{v\}_s^T \{v\}_s (\sigma_r - \sigma_s)} \qquad (4.77)$$

From equation (4.77) it is clear that a singular vector whose pertinent singular value is close to a neighbouring singular value is a sensitive singular vector. Sensitive singular vectors can lead to a sensitive matrix and, as a matter of fact, the reason that matrix [H] in equation (4.61) is sensitive to noise, in spite of having a small condition number, is that its singular values are very close to each other. To demonstrate how close the singular values of [H] are, Table 4.2 shows the values with and without noise effect.

	σ_1 X 1E-7		σ_2 X 1E-7		σ_3 x 1E-8		σ_4 X 1E-8		σ_5 x 1E-8	
	- noise	+noise	- noise	+noise	- noise	+noise	- noise	+noise	- noise	+noise
σ_i	1.816	1.789	1.710	1.715	7.848	7.700	4.330	4.302	2.911	2.854
σ_i/σ_{i+1}	1.06	1.04	2.18	2.22	1.81	1.79	1.487	1.5		

Table 4.2 Singular values of matrix [H]

As is evident from Table 4.2, the 1st and 2nd singular values are very close to each other and, also, the 4th and 5th singular values are relatively close. Figs 4.4 to 4.8 show the singular vectors of matrix [H] before and after adding 5% noise.

Examining Figs. 4.4 through 4.8, it is evident that variation in 1st and 2nd singular vectors, which have very close singular values, is much greater than corresponding variations in other singular vectors.

* Same argument applies to $\{Au\}_r$ with $[B] \triangleq [A][A]^H$

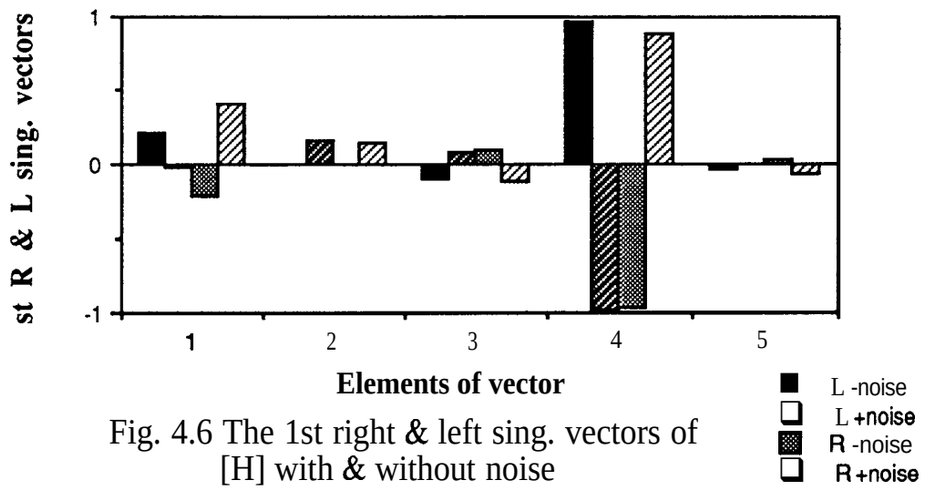

Fig. 4.6 The 1st right & left sing. vectors of [H] with & without noise

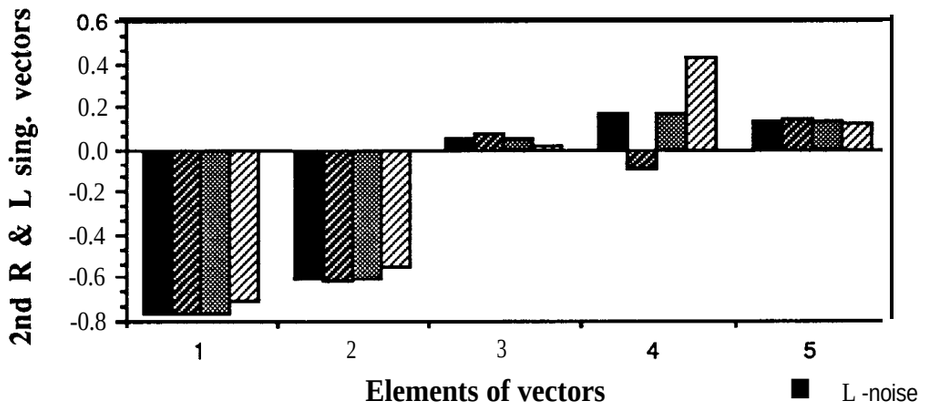

Fig. 4.7 The 2nd right & left sing. vectors of [H] with & without noise

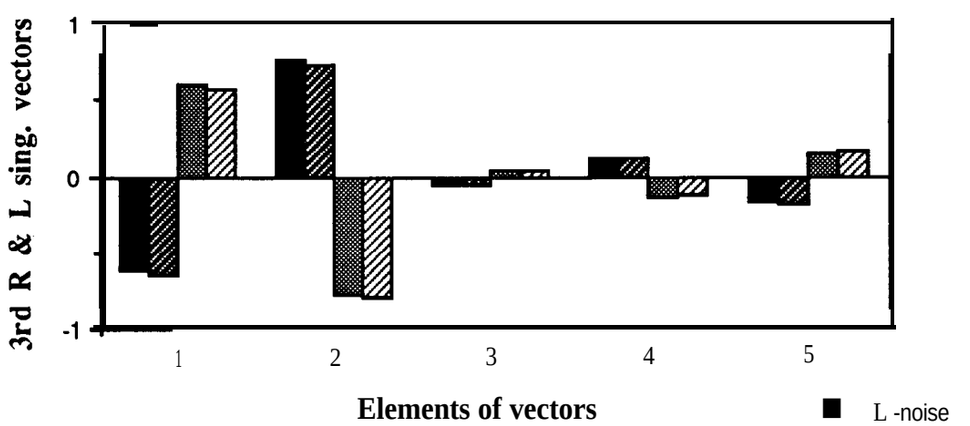

Fig. 4.8 The 3rd right & left sing. vectors of [H] with & without noise.

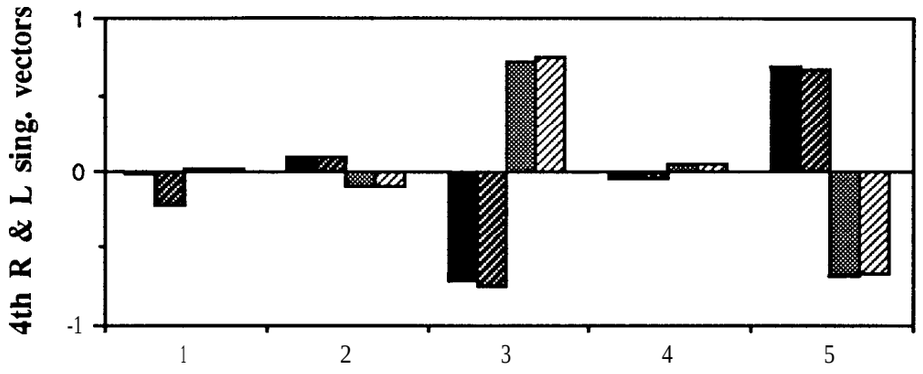

Fig. 4.9 The 4th right & left sing. vectors of [H] with & without noise

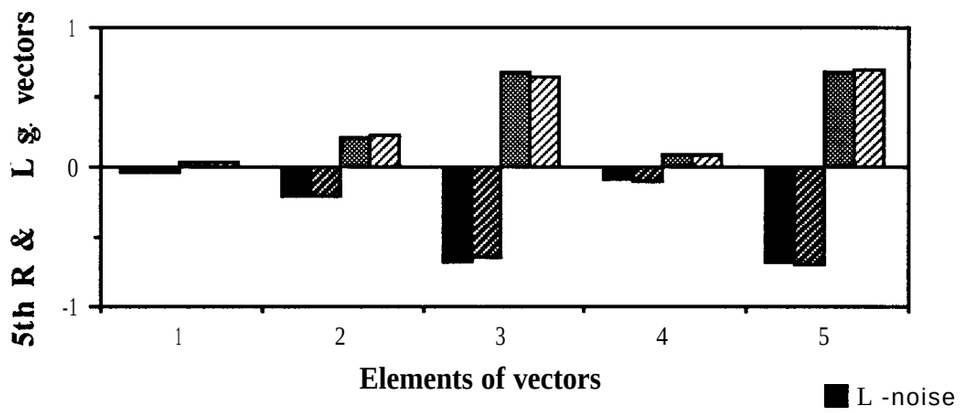

Fig. 4.10 The 5th right & left sing. vectors of [H] with & without noise

4.6 CONCLUDING REMARKS

Some formulation and computational aspects of the general identification problem have been discussed in this chapter. It seems that the nature of the identification problem is generally ill-posed mainly due to the small amount of available information. The identification problem may also be ill-conditioned which can be due to poor modelling of the analytical model and/or ill-condition of the matrices which are used to construct the governing equations and are related to the real structure. Also, it has been argued that the solution procedure itself can be responsible for poor conditioning of the calculations and, in this case, using as much data as possible and a proper balancing technique, that the condition of calculations can be improved.

In order to reduce the number of unknowns in an identification problem, it is a common practice to preserve the connectivity pattern of the analytical model as additional constraints. It has been shown that, by preserving connectivity pattern, one may identify the closest possible analytical model to the real structure, in a least-squares sense, but it is not possible to identify the real structure exactly (unless one knows the real connectivity pattern of the real structure).

It has also been shown that, even for a noise-free data case, a least-squares formulation is a necessary part of any identification problem, due to the inevitable incompleteness of the data being used

Assuming that the condition of a particular identification calculation is acceptable, most identification methods (in fact almost all of them) are still very sensitive to measurement noise. It has been argued here that the sensitive nature of identification calculations is inherent and this matter will therefore need to be further discussed in the chapters related to each particular identification technique.

Having discussed the concept of ill-conditioning of a matrix, it has been shown that the closer the singular values of a matrix are to each other, the more sensitive becomes the matrix and this is true regardless of the condition number of the matrix.(Note that the theory essentially holds for matrices with distinct eigenvalues and thus singular values)

CHAPTER (5)

APPLICATION OF AN FRF-BASED DIRECT METHOD TO THE JOINT IDENTIFICATION PROBLEM.

5.1 INTRODUCTION

In the present chapter, the performance of an FRF-based direct identification procedure, for dealing with the joint identification problem will be examined. Generally speaking, FRF- based methods are usually preferred to modal-based methods, due to the advantages associated with them, including;

relative ease in handling the damping problem;

simplicity of FRF-based coupling techniques, especially, when a joint is present;(see chapter 2)

in the case of a pure experimental analysis, there is no need for modal analysis when using an FRF-based identification method;

having measured FRFs for a limited frequency range, the effect of out-of-range modes is already reflected in the measured data; and

usually, the amount of information measured in the frequency domain is large and this provides the flexibility of selecting proper data points for an identification analysis.

As mentioned in chapter 3, the FRF-based direct method was originally developed by Lin* [27] for model updating applications and locating non-linearities in structures and here the method will be modified to make it suitable for joint identification applications.

* The same technique is used in [13] & [14] for joint identification

5.2 GENERAL FORMULATION

5.2.1 FORMULATION OF THE FRF-BASED DIRECT METHOD

Consider the following mathematical identity,[27]:

$$[[A]+[B]]^{-1} = [A]^{-1} - [[A]+[B]]^{-1}[B][A]^{-1} \quad (5.1)$$

where [A] and [B] are general matrices satisfying the condition that both [A] and [A+B] are nonsingular.

Designating suffices a and x to the analytical and experimental models of the structure, respectively, and assuming that [A] and [A+B] in equation (5.1) are the impedances of the analytical and experimental models of structure, respectively, one has:

$$[Z_x(\omega)]^{-1} = [Z_a(\omega)]^{-1} - [Z_x(\omega)]^{-1}[Z_x(\omega) - Z_a(\omega)][Z_a(\omega)]^{-1} \quad (5.2)$$

or, from (5.2)

$$[H_a(\omega)] - [H_x(\omega)] = [H_x(\omega)][\Delta Z(\omega)][H_a(\omega)] \quad \mathbf{(5.3)}$$

where $[\Delta Z(\omega)]$ is the impedance error matrix defined as

$$[\Delta Z(\omega)] = [Z_x(\omega)] - [Z_a(\omega)].$$

Although equation (5.3) is quite general, due to incompatibility between dimensions of [H,(o)] and [AZ(o)] caused by coordinate incompleteness of measured data, it is difficult to use equation (5.3) for general identification and model updating problems (see chapter 3). On the other hand, if one can localize the error between the two models, then the dimension of [AZ(o)] can be reduced and the "incompatibility of dimensions" problem, stated above, does not exsist. Thus, from an implementation point of view, equation (5.3) is very suitable for joint identification applications as the source of the error between two models is localized to the interfaces.

5.2.2 MODIFYING EQUATION (5.3) TO MAKE IT SUITABLE FOR JOINT IDENTIFICATION APPLICATIONS

Assuming that a real structure consists of a number of substructures and, furthermore, that the difference between two models A and X, [AZ], is concentrated at the interfaces between the substructures, equation (5.3) can be rewritten as follows:

$$\begin{bmatrix} [\Delta H]^{ss} & [\Delta H]^{si} \\ [\Delta H]^{is} & [\Delta H]^{ii} \end{bmatrix} = \begin{bmatrix} [H]_x^{ss} & [H]_x^{si} \\ [H]_x^{is} & [H]_x^{ii} \end{bmatrix} \begin{bmatrix} [0] & [0] \\ [0] & [\Delta Z] \end{bmatrix} \begin{bmatrix} [H]_a^{ss} & [H]_a^{si} \\ [H]_a^{is} & [H]_a^{ii} \end{bmatrix} \qquad (5.4)$$

Equation (5.4) can be resolved into 4 sub-matrix equations from which the following is selected as the most suitable for joint identification:

$$[\Delta H(\omega)]^{ss} = [H(\omega)]_x^{si} [\Delta Z(\omega)][H(\omega)]_a^{is} \qquad (5.5)$$

In the following section, the reason for choosing equation (5.5) out of the 4 possible equations derivable from (5.4), and the practical difficulties associated with equation (5.5), are discussed.

5.3 DIFFICULTIES ASSOCIATED WITH USING EQUATION (5.5)

Refering back to the equation (5.4), the four equations deducible from this equation are:

$$[\Delta H(\omega)]^{ss} = [H(\omega)]_x^{si} [\Delta Z(\omega)][H(\omega)]_a^{is} \qquad (a)$$

$$[\Delta H(\omega)]^{si} = [H(\omega)]_x^{si} [\Delta Z(\omega)] [H(\omega)]_a^{ii} \qquad (b)$$

$$[\Delta H(\omega)]^{is} = [H(\omega)]_x^{ii} [\Delta Z(\omega)][H(\omega)]_a^{is} \qquad (c)$$

$$[\Delta H(\omega)]^{ii} = [H(\omega)]_x^{ii} [\Delta Z(\omega)][H(\omega)]_a^{ii} \qquad (d) \qquad (5.6)$$

Of these, (c) and (d) are not suitable due to the presence of $[H(\omega)]_x^{ii}$ on the r.h.s of the equations which, in most cases, is very difficult to measure. Having defined n_s and n_i as the numbers of slave and interface coordinates, respectively, the reason for choosing equation (a) in (5.6) is that by transforming this equation to a set of algebraic equations, one obtains $n_s x n_s$ equations for each frequency, while the corresponding number of equations achievable from (b) equals to $n_s x n_i$. Now, while the number of interface

coordinates, n_i, is constant, one can increase the number of slave coordinates as much as possible and, having $n_s > n_i$, equation (a) always yields a larger number of algebraic equations.

On the other hand, as discussed in chapter 4, the maximum number of independent equations at each frequency point is constant and equal to $n_i x n_i$, regardless of the number of equations achievable from equation (5.5). Thus, it seems that for the noise-free case, equation (5.6.a), or (5.5), does not have any advantage over equation (5.6.b) (because the numbers of independent equations are identical in the two cases). However, if measurement noise is present in the calculations, the algebraic equations achievable either from (5.5) or from (5.6.b) become inconsistent and it is better to use equation (5.5) in this case as it provides more equations (and thus more information).

The question which may arise here is "what is lost by using only one possible equation, out of the 4 available in equation (5.6)?". The answer to this question is that, qualitatively, there is no difference between the 4 equations in (5.6) and, indeed, the effects of the joints are reflected on the l.h.s of each of them but, quantitatively, the effects of joints may be reflected more significantly in one than the others. From this point of view, it is case-dependent and difficult to decide which equation is superior.

Having chosen equation (5.5) for joint identification, there are 2 problems associated with using this equation, as follows:

(a) - the elements of matrix $[H(\omega)]_x^{si}$ on the r.h.s of equation (5.5) are difficult, if not impossible, to measure; and

(b) - if the joint is stiff in some directions, then the columns (or rows) of $[H(\omega)]_x^{si}$ related to those directions will be linearly dependent, or almost linearly dependent, which deteriorates the results.

5.4 SOLUTION TECHNIQUES FOR EQUATION (5.5) AND THE EFFECT OF VARIOUS PARAMETERS ON RESULTS

As equation (5.5) is frequency-dependent, it can be solved by one of two different techniques, as follows:

solution technique 1- solving matrix equation (5.5) at each individual frequency over the frequency range of interest; or

solution technique 2- transforming equation (5.5) into a set of algebraic equations and then combining the equations from different frequencies together and solving them simultaneously as a "least-squares" problem. In this case, equation (5.5) becomes:

$$[P]\begin{Bmatrix}\{\Delta K\}\\ \{\Delta M\}\\ \{AD\}\end{Bmatrix} = \{q\} \qquad (5.7)$$

As is evident from equation (5.7), [AZ] has been decomposed to its constituent variables and [ΔK],[ΔM],[ΔD] are explicitly present in the governing equation (5.7).

If the first technique is used for solving equation (5.5), then in order to be able to have meaningful inversions of $[H]^{si}$ and $[H]^{is}$, the following inequality must be satisfied:

$$n_s \geq ni \qquad (5.8)$$

As explained in section (5.3), the bigger n_s is, the more accurate becomes the result, in cases where noise is involved in the data.

If the second technique is applied, it is not necessary to satisfy (5.8) provided that sufficient frequency points are used in setting up equation (5.7). It should be noted that, again, the bigger n_s is, the more accurate becomes the result.

One other important issue in the identification procedure based on equation (5.5) is the method used for setting up the analytical model. In practice, depending on the type of approach, there are 2 ways of constructing an analytical model, as follows:

(a) - if the analysis is based on the application of purely experimental data, i.e. if no FE model is used, then the analytical model can be set up by coupling the constituent substructures of the real structure through a trial joint model, using their experimental FRFs (model A-C);

(b) - if a hybrid approach is used, some of the data related to model X are derived from experiment and the rest related to the analytical model are generated using the finite element models of the substructures, again coupled to each other through a trial joint model using the spatial model of substructures and the trial joint

In the case of using approach (a), there is a coupling process necessary to set up the model A-C.

The trial joint model, which is used to set up the analytical model, can be considered to be either damped or undamped*. If a damped trial model is used for the joint, then it is necessary to use a prescribed damping model for the trial joint. Since joint elements show different damping mechanisms for different frequency ranges (usually hysteretic damping is dominant at lower to moderate frequencies and viscous damping is more appropriate at higher frequencies), the prescribed damping model can be a combination of both hysteretic and viscous damping and, at least theoretically, the result will show which damping mechanism is dominant within a particular frequency range.

It should be noted that the configurational model of the trial joint is dictated by the interface coordinates of the real structure.

5.5 CASE STUDIES

To study the performance of the solution based on equation (5.5) and to examine its sensitivity to measurement noise, a series of case studies have been undertaken.

The test structures for all case studies are shown in Fig. 5.1

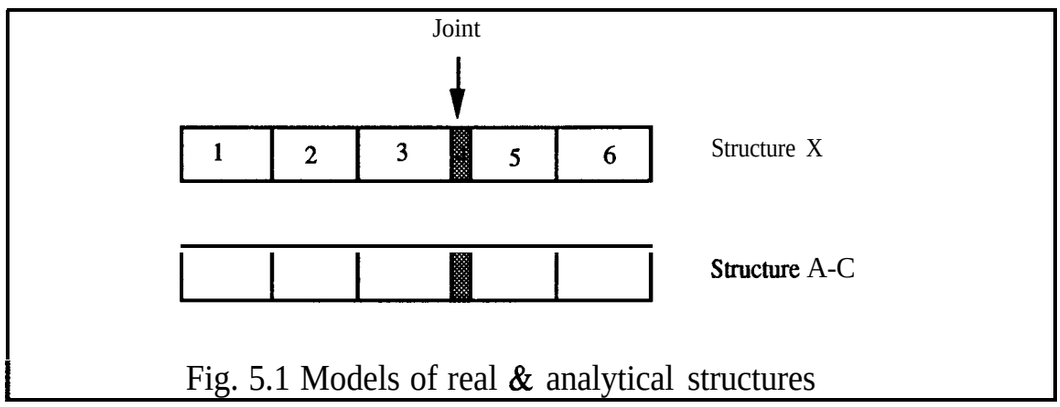

Fig. 5.1 Models of real & analytical structures

Structure X, which simulates the real (i.e. experimental) structure, is a 6-element FE model of a free-free beam where element 4 is designated as the joint element. In order to be able to simulate practice as closely as possible, only translational slave coordinates are

* Note that since equation (5.5) is based on a **direct** identification **approach,** at least for the present application (i.e. joint identification), there is no limitation on the MSDU

considered in the calculations and, thus, the numbers of slave coordinates, n_s, and of interface coordinates, n_i, for all case studies are equal to 5 and 4, respectively.

The base element of structure X has the geometrical and mechanical properties shown in Fig.3.2.

The joint element of the real structure has the following properties:

$$L_{jx} = 100\%\, L_e \quad , \quad E_{jx} = 1000\%\, E_e , \quad \rho_{jx} = 10\%\, \rho_e \tag{5.10}$$

Thus, the joint element is 10 times stiffer and 10 times lighter than the base element.

The specification in equation (5.10) yields the following mass and stiffness matrices for the real joint (i.e. experimental) model:

$$[M]_{jx} = \begin{bmatrix} .05 & .0021 & .01746 & -.00126 \\ & .00011 & .00126 & -.000087 \\ & & .05 & -.0021 \\ & & & .00011 \end{bmatrix}$$

$$[K]_{jx} = \begin{bmatrix} 6440000 & 966000 & -6440000 & 966000 \\ & 193200 & -966000 & 96600 \\ & & 6440000 & -966000 \\ & & & 193200 \end{bmatrix} \tag{5.11}$$

Structure A-C, which simulates the analytical model of the structure, is also a 6-element FE model of a free-free beam with element 4 again representing the joint. The geometrical and mechanical properties of the base element of model A-C are exactly the same as those of X (shown in Fig. 3.2.), except for element 4 which represents the trial joint. Since the process of coupling may induce more errors into the calculations, so, in all the case studies, we will simulate approach (a) of section 5.4, i.e. model A-C is set up by coupling substructures through a trial joint, using substructures' FRFs.

5.5.1 CASE STUDIES USING SOLUTION TECHNIQUE 1

In this series of case studies, equation (5.5) will be solved as a matrix equation and at each individual frequency.

CASE STUDY 1

Fig. 5.2 shows typical results for the joint identified using equation (5.5). The trial joint for this case study (and subsequent case studies unless otherwise stated) has the following specifications:

$$L_{jt} = L_{jx} \quad , \quad E_{jt} = 50\%\, E_{jx} \quad , \quad \rho_{jt} = 50\%\, \rho_{jx} \tag{5.12}$$

which yields the following mass and stiffness matrices

$$[M]_j^t = \begin{bmatrix} .025 & .00105 & .00873 & -.00063 \\ & .000055 & .00063 & -.0000435 \\ & & .025 & -.00105 \\ & & & .000055 \end{bmatrix}$$

$$[K]_j^t = \begin{bmatrix} -3220000 & 483000 & -3220000 & 483000 \\ & 96600 & -483000 & 48300 \\ & & 3220000 & -483000 \\ & & & 96600 \end{bmatrix} \tag{5.13}$$

As Fig. 5.2 shows, the results are satisfactory over whole range of frequency of interest.

To examine the performance of equation (5.5) in the presence of measurement noise, "5% random noise"* has been added to both real and imaginary parts of all FRFs involved in the calculations.

* The n% random noise effect has been simulated using random number generator command RND as follows

$e_{ij} = (n/100)x(RND)x(H_{ij})x((-1)^{(INT(RND)x10)})$

where RND generates random numbers between 0 and 1 and INT command is used to take integer part of a real number. e_{ij} is the error added to H_{ij}. Note that e_{ij} is calculated separatly for real and imaginary parts of H_{ij} and also its sign is choosen randomly

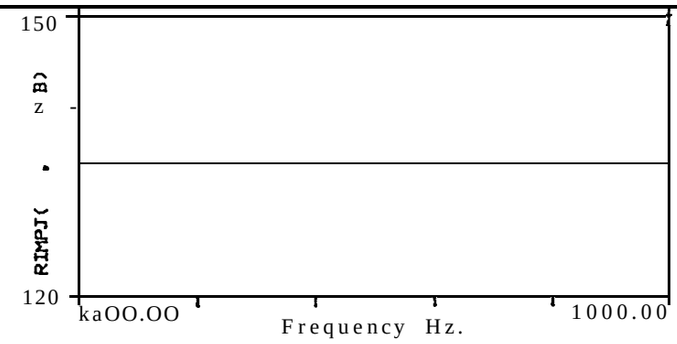

Fig. 5.2 Typical result of identified joint impedance using solution technique 1

Typical results of the analysis, with noise, are shown in Fig 5.3 . Examining Fig 5.3, it is evident that the results are very poor and thus this method is very sensitive to noise.

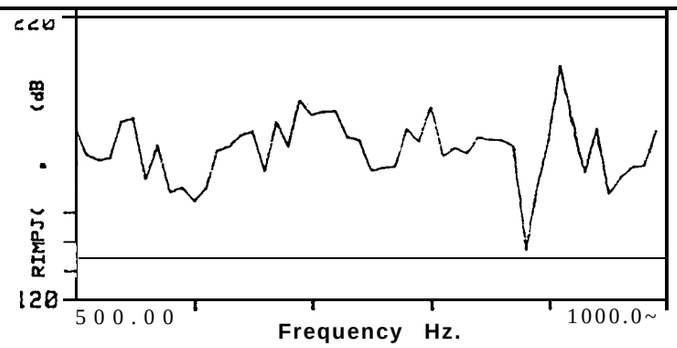

Fig. 5.3 Typical result of identified joint impedance with 5% noise and using solution technique 1. correct value

As discussed in section 4.2.2.2, the reason for this high sensitivity to noise lies in the nature of the identification problem and is not a computational issue. For example, having defined [E] as the noise effect matrix, equation (5.3) can be rewritten :(for the sake of simplicity, it has been assumed that matrices [H,] and $[H_a]$ on the r.h.s of equation (5.3) are not affected by noise) as:

$$[H_x]^{-1}[H_a - H_x + E][H_a]^{-1} = [AZ] \quad \Rightarrow [H_x]^{-1}[\Delta H][H_a]^{-1} + [H_x]^{-1}[E][H_a]^{-1} = [AZ]$$

The first term on the l.h.s of the above equation yields the correct value for [AZ] and, physically, this term contains the receptance difference matrix, [AH], resulting from the effect of mass and stiffness errors between models X and A. Now, if the effect of large variations in some of the mass and/or stiffness elements of the structure is insignificant

on its response, then small changes in [AH] due to noise in [H,] will cause very marked changes, in the identified [AZ] which, in this case, the effect of second term on the r.h.s of above equation has dominated the effect of the first term.

So, for joint identification applications, if the joint in the real structure is stiff enough (even if in some directions), very large variations in joint stiffness will cause insignificant changes in structural response, so that 1000% variation in joint stiffness may cause only a 1% variation in the eigenvalues. This means that, when solving the inverse problem, very small variations in system response may cause very remarkable changes in identified joint parameters. The nature of this type of inherent sensitivity to noise will be further examined in chapter 9.

Thus, generally speaking, the FRF-based method based on equation (5.5) is not as efficient using solution technique 1. In what follows the application of solution technique 2 to the joint identification problem will be examined.

5.5.2 CASE STUDIES USING SOLUTION TECHNIQUE 2

In this section we shall examine the application of solution technique 2, i.e. transforming equation (5.5) to a set of linear algebraic equations by separating joint mass and stiffness parameters in [AZ] and then, combining the set of equations relating to different frequencies together, solving the resulting over-determined set of algebraic equations using a least-squares method.

Having assumed a random distribution for the measurement noise, its effect on each equation will be averaged out by adding the equations for different frequencies together and, thus, a reduced sensitivity to noise is expected. (Note that as explained in chapter 4, **random** noise effects can theoretically be eliminated completely if one can add an **infinite** number of independent equations together.)

5.5.2.1 COMPUTATIONAL ASPECTS OF SOLUTION TECHNIQUE 2

As mentioned before, using solution technique 2, the following two steps are necessary:

(a) - transforming matrix equation (5.5) into a set of algebraic equations at each frequency o.; and

(b) - separating the mass and stiffness (and damping) parameters in [AZ]

Computational problems caused by the above steps have been discussed in chapter 4 (see section 4.4).

Considering matrix [AZ(o)] as:

$$[AZ(o)] = [AK] - [\Delta M]\omega^2 + i\,[AD] \tag{5.14}$$

equation (5.5) can be transformed into a set of algebraic equations for each frequency ω, and having imposed a symmetry constraint on [AK],[AM] and [AD], one obtains:

$$[C(\omega)]_{(n_s x n_s) x 3/2(n_i(n_i+1))} \begin{Bmatrix} \{\Delta K\} \\ \{\Delta M\} \\ \{AD\}) \end{Bmatrix}_{3/2(n_i(n_i+1))x1} = \{L(\omega)\}_{(n_s x n_s) x 1} \tag{5.15}$$

where the matrix [C(o)] is partitioned as follows:

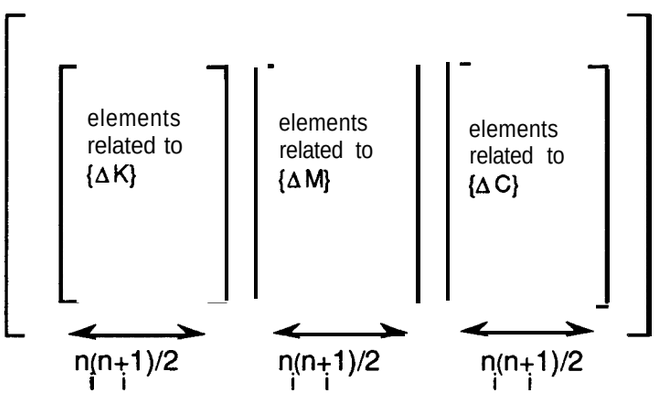

(5.16)

Each element c_{pq} related to Δk_{ij} can be calculated from the following equation (assuming symmetry):

$$c((t-1)xn_s+g\,,\,(i-1)x(n_i-i/2)+j) = h_x(t,i) \times h_a(j,g) + h_x(t,j) \times h_a(i,g)$$

$$i,j = 1 \ldots\ldots n_i \text{ and } j>i \qquad t,\ g = 1 \ldots\ldots\ldots\ldots n_s \tag{5.17}$$

If i=j then

$$c((t-1)xn_s+g\,,\,(i-1)x(n_i-i/2)+j) = h_x(t,i) \times h_a(j,g) \tag{5.18}$$

Having combined equations (5.15) for each of nf frequency points together, let us set up the final over-determined set of equations as follows:

$$[P]_{(n_s x n_s x n_f)x3/2(n_i(n_i+1))} \left\{ \begin{matrix} \{\Delta K\} \\ \{\Delta M\} \\ \{\Delta D\} \end{matrix} \right\}_{3/2(n_i(n_i+1))x1} = \{q\}_{(n_s x n_s x n_f)x1} \qquad (5.19)$$

Using the normal equation technique (explained in section 4.3) to solve the least-squares problem defined in equation (5.19), one obtains the following determined set of equations:

$$[S] \left\{ \begin{matrix} \{\Delta K\} \\ \{\Delta M\} \\ \{\Delta D\} \end{matrix} \right\} = \{Q\} \qquad (5.20)$$

The number of the unknowns in equation (5.20) depends on the type of the model which is assumed for the joint, as described in section 4.4.3.

Here, one of the following models will be used for the joint:

joint model 1- in which a "beam element type" joint model is used. The number of unknowns for this case is equal to 6 (3 unknowns for mass and 3 unknowns for stiffness, see equation (4.58)).

joint model 2- general joint model which does not assume any relationship between the degrees of freedom involved in interfacing. The number of unknowns for this case is equal to 20 (see equation (4.60)).

5.5.2.2 EFFECT OF NATURAL FREQUENCIES OF TEST STRUCTURES ON CALCULATIONS

It is convenient at this stage to examine the effect of the natural frequencies of models X and A-C on the calculations. As explained in sec. 4.4, if any of the matrices involved in the r.h.s of equation (5.5), i.e. $[H]_x^{si}$, and $[H]_a^{is}$, are ill-conditioned, then according to following inequality:

$$\kappa([A].[B]) \leq \min(\kappa([A] \text{ or } [B])) \quad (5.21)$$

the coefficient matrix [C(o)] in equation (5.15) will be ill-conditioned, leading to an ill-conditioned matrix [P] in equation (5.19). Now, at natural frequencies of the real structure model X and the analytical model A-C, the matrices $[H]_x^{si}$ and $[H]_a^{is}$, respectively become ill-conditioned and this will affect the result of solving equation (5.19) using a least-squares technique.

CASE STUDY 2

To illustrate the above-mentioned problem, equation (5.19) has been solved using the normal equation technique leading to equation (5.20), for the, (a)-500 - 1000 Hz, (b)-405-981 Hz and (c)-549-981 Hz frequency ranges and with 100 Hz, 144 Hz and 72 Hz frequency increment steps, respectively.

Considering the natural frequencies of structures X and A-C within the 400-1000 Hz frequency range shown in Table 5.1, it is clear that 2 out of the 4 frequency points used in the joint identification in case (b) coincide with natural frequencies of the structure X.

Also, for case (c), 2 out of the 6 frequency points coincide with natural frequencies of structure X, but, for this case the frequency points within the following band are excluded from the calculations:

$$\omega_r - 60 \text{ (rad/s)} < \omega_i < \omega_r + 60 \text{ (rad/s)}$$

which leaves 4 non-coincident frequency points in the calculations.

Natural Freqs	f_8 Hz	f_9 Hz	f_{10} Hz
Structure x	549	693	981
Structure A	546	688	974

Table 5.1. Natural frequencies of test structures in the range of interest.

Table 5.2 shows the errors in typical parameters of identified joint parameters for the different cases.

Examining Table 5.2 the following conclusions can be drawn from this case study:

(a) - using frequencies close to or equal to the natural frequencies of the structures involved in calculations deteriorates the results;

(b) - error values for mass parameters are larger than those for stiffness and this is especially true for rotary inertia.

		Trans K Error%	Cross K Error %	Rotary K Error %	Trans M Error %	Cross M Error %	Rotary M Error %
Case a	1 point close to resonance.	2.2	1.9	0.5	1.6	2.8	13.7
Case b	2 points coincide	1200	1300	1500	6700	22700	60000
Case c	no close or coincid.points	.01	.022	.017	.013	.02	.04

Table 5.2 Typical error percentages in identified joint parameters for three cases.(a), (b) and (c)

5.5.2.3 SENSITIVITY ANALYSIS

In this section, the effect of measurement noise on the results will be examined. Measurement noise has been simulated by introducing 5% random error, proportional to the receptances of the test structures. The test structures and real and trial joint models are similar to those in Figs. 5.1 and 5.2 and expressions (5.10), (5.11), (5.12) and (5.13).

Before starting to discuss the case studies, it is convenient at this stage to explain the technique which has been used to solve equation (5.20). Consider equation (5.20) again:

$$[S]\begin{Bmatrix}\{\Delta K\}\\ \\ \{\Delta M\}\end{Bmatrix} = \{Q\} \qquad (5.20)$$

where, for the sake of simplicity, damping has been neglected.

Partitioning matrix [S] in (5.20) one obtains:

$$\begin{bmatrix}[S_{11}] & [S_{12}]\\ \\ [S_{21}] & [S_{22}]\end{bmatrix}\begin{Bmatrix}\{\Delta K\}\\ \\ \{\Delta M\}\end{Bmatrix} = \begin{Bmatrix}\{Q_1\}\\ \\ \{Q_2\}\end{Bmatrix} \qquad (5.22)$$

After some matrix manipulation, the unknown vectors $\{\Delta M\}$ and $\{\Delta K\}$ can be calculated from following equations:

$$([S_{22}] - [S_{21}][S_{11}]^{-1}[S_{12}])\{\Delta M\} = \{Q_2\} - [S_{21}][S_{11}]^{-1}\{Q_1\} \quad (5.23)$$

and

$$\{\Delta K\} = [S_{11}]^{-1}(\{Q_1\} - [S_{12}]\{\Delta M\}) \quad (5.24)$$

So, the vector $\{Q_2\} - [S_{21}][S_{11}]^{-1}\{Q_1\}$ on the r.h.s of equation (5.23) can be shown as the contribution of joint mass to difference matrix [AH].

Note that solving equations (5.23) and (5.24) offers no advantage over solving equation (5.20) directly, i.e. direct inversion of [S], but, as will be shown shortly, partitioning the matrix [S] and solving equations (5.23) and (5.24) will make it easier to find an explanation for the high sensitivity of equation (5.20) to noise and to fiid ways of coping with this high sensitivity.

CASE STUDY 3

In this case study, equations (5.23) and (5.24) have been solved within the frequency range of 100-1000 Hz and with 5 Hz frequency increment steps. The results of this analysis are shown in expressions (5.25), (5.26).

$$[M]_j = \begin{bmatrix} -.0062(5000\%) & .0125 & .0047 \\ & .036 & -.0212 \\ -.36(614\%) & .021(890\%) & -.123 \quad -.0063 \end{bmatrix}$$

$$[K]_j = \begin{bmatrix} -2.12E7(2300\%) & -3E6(210\%) & 2.12E7 & -3E6 \\ & -571611(200\%) & 3E6 & -285805 \\ & & -2.12E7 & 3E6 \\ & & & -571611 \end{bmatrix} \quad (5.25)$$

$$[\bar{K}]_j = \begin{bmatrix} 5.265E6(18\%) & 783703(19\%) & -5.265E6 & 783703 \\ & 157812(18\%) & -783703 & 78906 \\ & & 5.265E6 & -783703 \\ & & & 157812 \end{bmatrix} \quad (5.26)$$

As expression (5.25) indicates, the results of solving equations (5.23) and (5.24) are very poor. On the other hand, the joint mean stiffness matrix $[K]_j$ in expression (5.26) is satisfactory. The mean stiffness matrix in expression (5.26) has been calculated from equation (5.24) by ignoring the mass in the calculations, using following equation:

$$\{\Delta K\}_j = [S_{11}]^{-1}\{Q_1\} \qquad (5.27)$$

The better results for calculations without mass indicate the very small effect of the joint mass in the calculations (at least in some directions*) which can easily become polluted by measurement noise.

Having scanned the 100-1000 Hz frequency range, the above results, i.e. significantly better results for $[K]_j$ compared to $[K]_j$ and the deteriorating effects of joint mass on the results when noise is present, are confirmed.

It should be noted that for all case studies the largest error in the results is always associated with rotary inertia and this implies the insignificant effect of this parameter on the structure's response.

5.5.2.4 EFFECT OF FREQUENCY ELIMINATION BAND WIDTH

It was shown in case study 2 that avoidance of the natural frequencies of the test structures can significantly improve the results for the noise-free case. In this section, the effects of the natural frequencies, and the effect of eliminating them from the calculations, on the results will be investigated for the with-noise case.

CASE STUDY 4

In this case study, the analysis within the 500-1000 Hz range will be repeated for 5 cases. In the first case there is no frequency elimination and for the rest of the cases the bandwidths of elimination around resonance frequency ω_r are as follows:

$$\omega_r - 10\ (d/s) < \omega_i < \omega_r + 10\ (rad/s) \qquad (a)$$

---

* As will be shown in later chapters, the structure's response is insensitive to variations in joint rotary

ω_r - **20** (rad/s) < ω_i c ω_r + **20** (rad/s) (b)

ω_r - **30** (rad/s) < ω_i < ω_r + 30 (rad/s) (c)

ω_r - 60 (rad/s) < ω_i < ω_r + 60 (rad/s) (d)

Fig. 5.4 shows the variation of a typical element, say k(l,l), of stiffness and mean stiffness matrices versus frequency elimination bandwidth.

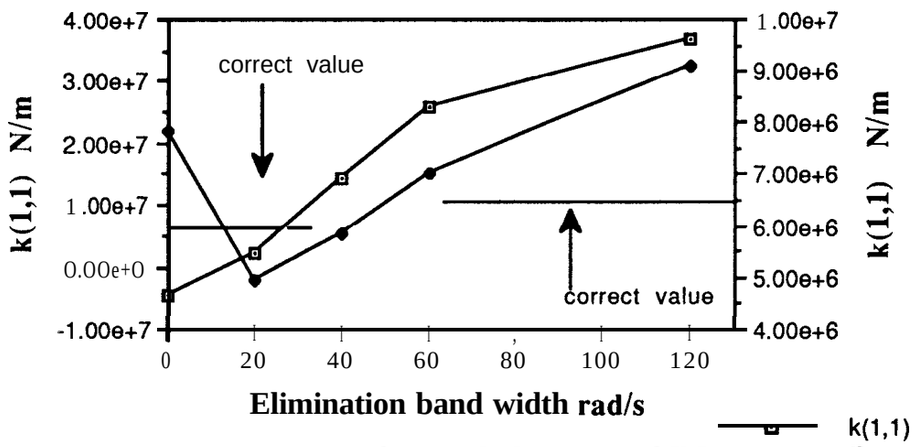

Fig. 5.4 Variation of typical elements of [k] & [k] with elimination band width

Examining Fig. 5.4 reveals that for low to moderate elimination bandwidths, say up to 40 **rad/s,** frequency elimination improves the results for both $[K]_j$ and $[\bar{K}]_j$ and increasing the elimination bandwidth beyond a certain limit, i.e. excluding all resonances and high level responses from calculations, will reduce the level of responses of structures involved in the calculation and thus the effect of structures in the calculations will be similar to very stiff structures with high-frequency resonances and this will result in over-estimation of stiffness values (as figure 5.4 indicates).

Considering Fig. 5.4 and the above deductions, it seems that it is possible to have a reasonably accurate estimation for stiffness (and damping if it is hysteretic). This can be achieved by repeating the calculations within the different frequency ranges and, for each frequency range, with different elimination bandwidth and then calculating a mean of the (mean stiffness matrix), using statistical techniques.

5.5.2.5 EFFECT OF INCREASING FREQUENCY RANGE OF -ANALYSIS

CASE STUDY 5

The main purpose of performing this case study is to examine the effect of a higher frequency range on the results and to find out why, in spite of increasing frequency range and consequently increased mass effect, the results for the mass and stiffness matrices of the joint are still poor.

The test structures and real and trial joint models are similar to those in previous case studies and are shown in Figs. 5.1 and 5.2 and expressions (5. 10), (5.1 1), (5.12) and (5.13). The noise effect is again simulated by a 5% random noise added to the receptances of the test structures.

Calculations have been performed for the two frequency ranges of 500-1040 Hz and 1500-2040 Hz with 90 Hz frequency increments in both cases. Table 5.3 shows the order of magnitude of typical elements of the coefficient matrices involved in equations (5.20), (5.23) and (5.24) for with- and without- noise cases. Note that frequency ranges and increments have been chosen in such a way that no resonance frequency coincidence occurs in either case.

	Typical v. without noise		Typical error %	
	500-1040	1500-2040	500-1040	1500-2040
[S] of equation (20)	O(E-10)	O(E-13)	O(5)	O(600)
$[S_{22}] - [S_{21}] [S_{11}]^{-1} [S_{12}]$	O(E-16)	O(E-17)	O(50)	O(70)
$\{Q_1\}$	O(E-11)	O(E-13)	O(25)	O(500)
$\{Q_2\} - [S_{21}] [S_{11}]^{-1}\{Q_1\}$	O(E-17)	O(E-16)	O(800)	O(800)

Table 5.3. Typical values related to coefficient matrices in equations (5.20), (5.23) and (5.24)

It is evident from typical without-noise values in Table 5.3 that by increasing the frequency range, the mass effect in calculations reflected in vector $\{Q_2\}-[S_{21}][S_{11}]^{-1}\{Q_1\}$ has been increased (note that vector {Q} in the r.h.s of equation (5.20) has been generated from vector $\{\Delta H\}$ on the l.h.s of equation (5.5)).

On the other hand, a higher frequency range has reduced the order of magnitude of the elements of the coefficient matrices. In other words. increasing the freauencv range of

analysis will reduce the norm of the coefficient matrices involved in calculations. This small order of magnitude can make (real value/noise effect) ratio very small which in turn causes poor results.

The above-mentioned observation yields this result that "increasing the frequency range of the calculations does not yield better results, although it increases the mass effect in the calculation".

Table 5.3 also reveals the very large value of error in vector $\{Q_2\}-[S_{21}][S_{11}]^{-1}\{Q_1\}$ for the with-noise case. As this vector represents the contribution of joint mass to difference matrix [AH], this large error indicates the insignificance of joint mass contribution to $[\Delta H]$.

5.6 CONCLUSIONS AND REMARKS.

From what has been presented in this chapter, the following conclusions can be drawn:

(a) - there are two drawbacks associated with using the FRF-based direct method for joint identification, namely:

(i)- it is necessary to measure transfer FRFs between the interface and slave coordinates, and this may be difficult, if not impossible, in practice; and

(ii)- to set up the analytical model, or the analytically-coupled structural model, a coupling process is necessary which may induce extra errors to the identified joint;

(b) - using the individual frequency points solution technique, i.e. technique 1 in sec. 5.4, equation (5.5) yields satisfactory results for cases without noise. If noise is introduced into the calculations, equation (5.5) fails to give sensible results;

(c) - transforming matrix equation (5.5) to a set of algebraic equations, and using a least-squares technique, one should be careful about the rank and condition of the over-determined set of algebraic equations. Unless sufficient frequency points are used, the coefficient matrix in equation (5.19) will be ill-conditioned;

(d) - for the with-noise case, the mean stiffness matrix is a reasonable approximation to the real stiffness matrix. The satisfactory result for the mean stiffness matrix

means that the effect of mass in the calculations is insignificant and thus can easily be affected by noise and this, in turn, will affect the stiffness matrix (see equations 5.23 and 5.24 and Table 5.3);

(e) - the accuracy of the mean stiffness matrix as well as the mass and stiffness matrices depends significantly on the frequency elimination bandwidth used in the calculations;

(f) - to have a sensible approximation to the stiffness (and damping) matrix of a joint for the with-noise case, the best way is to perform calculations within the different frequency ranges and, for each range, with a different elimination bandwidth. Having calculated mean stiffness matrices for each case, and using statistical techniques, one can calculate a mean of the (mean stiffness matrix).

CHAPTER 6

A NEW MODAL-BASED DIRECT IDENTIFICATION METHOD FOR JOINT IDENTIFICATION & MODEL UPDATING

6.1 INTRODUCTION

6.1.1 THE NEED FOR A NEW JOINT IDENTIFICATION AND MODEL UPDATING METHOD

Model updating and joint identification methods have been categorized in chapters 1 and 3. As discussed in these chapters, due to certain similarities between the mathematical techniques used in joint identification and model updating (chapter 3), one can use almost the same classification for both fields. The usefulness of the classification of joint identification methods is due to the fact that, following this classification, one can identify the areas which have not yet been fully discussed or explored.

The classification proposed in chapter 1 is shown in more detail in Fig. 6.1, where it can be seen that the various techniques used for formulating the relationship between cause (i.e. the mis-modeled elements or joint(s)) and effect (the differences between two consistent models of the structure) are broadly divided into two groups: perturbation- (or sensitivity)-based and direct methods. As mentioned in chapter 3, a sort of n^{th} order approximation has been used in the former group to formulate the cause and effect relationship while in the latter group no approximation is involved in the formulation. It should be noted that the classification in Fig.6.1 is based on the mathematical basis of the derivation only: no computational considerations are involved at this stage.

Examination of Fig.6.1 reveals that there are at least two areas which have not yet been investigated, i.e. spatial-based and modal-based direct methods. Thus, it is necessary to

study these areas and to explore their performance. In the present chapter the modal-based method will be studied.

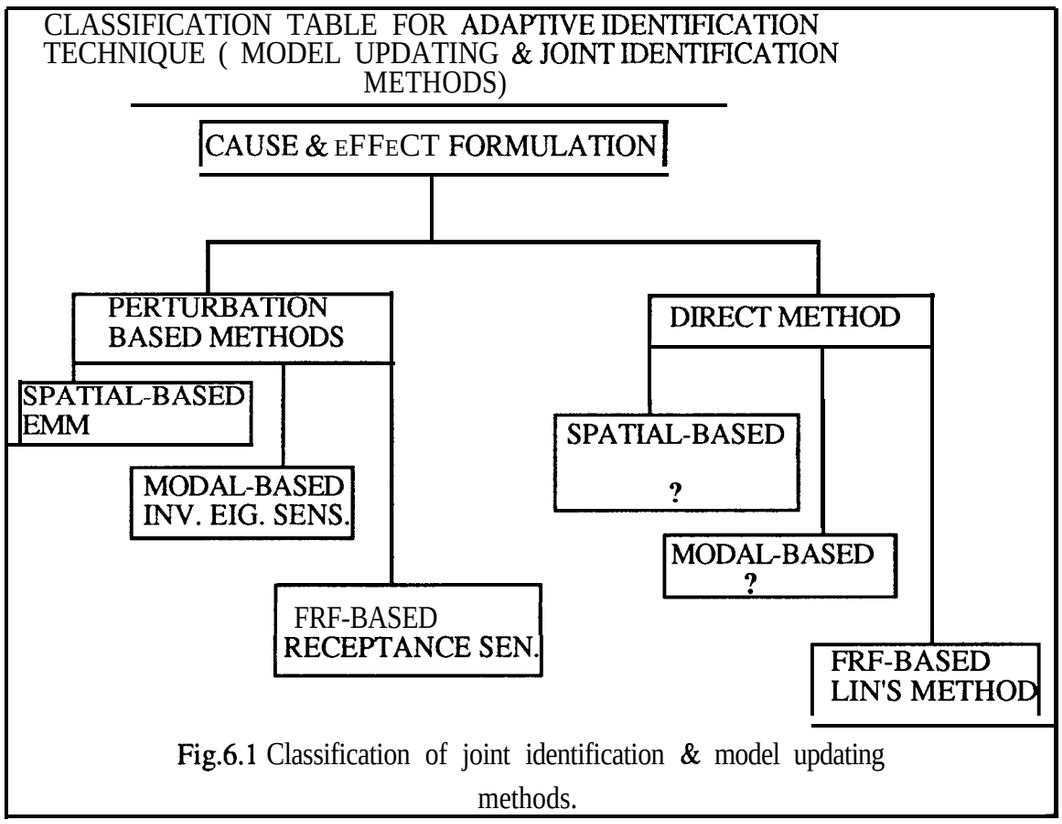

Fig.6.1 Classification of joint identification & model updating methods.

The modal-based direct method, as the author calls the new method, is described below and will be seen to be a natural extension of the component mode synthesis method [17,19,20]. Using the same concept as for component mode synthesis and solving the inverse problem, one should be able to identify unknown (or mis-modeled) elements. Formulation of the method is based on the free interface component mode synthesis method and, in what follows, the general formulation of the method which is applicable to model updating and structural modification will be presented first followed by application of the method to the joint identification problem.

6.2 GENERAL FORMULATION OF MODAL-BASED DIRECT METHOD APPLICABLE TO MODEL UPDATING

We shall use the following definitions:

X = exact (i.e. experimental and updated analytical, FE) model of a structure which exhibits the dynamic properties observed in test;

A = original (i.e. before updating) analytical model;

E = structural modification(s) added to model A to update it to model X

Considering complete coordinate interfacing between A and E, the equation of motion for model A can be written as:

$$[M]\{\ddot{x}_a\} + [K]\{x_a\} = \{\tilde{f}\} \tag{6.1}$$

where $\{\tilde{f}\}$ contains the reaction forces at the interface coordinates.

Considering the coordinate transformation from physical coordinates to principal coordinates $\{p_a\}$, and separating the n_a modes into kept (k) and eliminated (e) categories, one has:

$$\{x_a\} = [\phi_a]\{p_a\} = [\phi_{ak} | \phi_{ae}] \begin{Bmatrix} \{p_{ak}\} \\ \{p_{ae}\} \end{Bmatrix} \tag{6.2}$$

Using (6.2) and taking advantage of the orthogonality relationships between the eigenvectors and the mass and stiffness matrices, equation (6.1) can be rewritten as follows:

$$\{\ddot{p}_{ak}\} + [\omega_{ak}^2]\{p_{ak}\} = [\phi_{ak}]^T\{\tilde{f}\} \tag{6.3}$$

$$\{\ddot{p}_{ae}\} + [\omega_{ae}^2]\{p_{ae}\} = [\phi_{ae}]^T\{\tilde{f}\} \tag{6.4}$$

Assuming that the smallest ω_{ae} is much larger than the maximum frequency which is of interest, i.e. $\omega_{ae} >> \omega_{\text{max of investigation}}$, the inertia effects of higher modes will become much smaller than their contribution to the flexibility of the structure and, thus, one can ignore the inertia term in equation (6.4) so that this equation can be written as:

$$[\omega_{ae}^2]\{p_{ae}\} \cong [\phi_{ae}]^T\{\tilde{f}\} \tag{6.5}$$

A = original (i.e. before updating) analytical model;

E = structural modification(s) added to model A to update it to model X

Considering complete coordinate interfacing between A and E, the equation of motion for model A can be written as:

$$[M]\{\ddot{x}_a\} + [K]\{x_a\} = \{\tilde{f}\} \tag{6.1}$$

where $\{\tilde{f}\}$ contains the reaction forces at the interface coordinates.

Considering the coordinate transformation from physical coordinates to principal coordinates $\{p_a\}$, and separating the n_a modes into kept (k) and eliminated (e) categories, one has:

$$\{x_a\} = [\phi_a]\{p_a\} = [\phi_{ak} \mid \phi_{ae}] \begin{Bmatrix} \{p_{ak}\} \\ \{p_{ae}\} \end{Bmatrix} \tag{6.2}$$

Using (6.2) and taking advantage of the orthogonality relationships between the eigenvectors and the mass and stiffness matrices, equation (6.1) can be rewritten as follows:

$$\{\ddot{p}_{ak}\} + [\omega_{ak}^2]\{p_{ak}\} = [\phi_{ak}]^T\{\tilde{f}\} \tag{6.3}$$

$$\{\ddot{p}_{ae}\} + [\omega_{ae}^2]\{p_{ae}\} = [\phi_{ae}]^T\{\tilde{f}\} \tag{6.4}$$

Assuming that the smallest ω_{ae} is much larger than the maximum frequency which is of interest, i.e. $\omega_{ae} >> \omega_{\text{max of investigation}}$, the inertia effects of higher modes will become much smaller than their contribution to the flexibility of the structure and, thus, one can ignore the inertia term in equation (6.4) so that this equation can be written as:

$$[\omega_{ae}^2]\{p_{ae}\} \cong [\phi_{ae}]^T\{\tilde{f}\} \tag{6.5}$$

Equation (6.5) reflects the fist-order (static) approximation to the contribution of the higher eliminated modes to the flexibility of the structure [36] (usually referred to as the "residual" effect)

The response model of structure E can now be expressed as

$$[Z_E]\{x_a\} = -\{\tilde{f}\} \tag{6.6}$$

noting that the compatibility and equilibrium conditions have already been imposed on the response model of E in equation (6.6).

Using equation (6.2), equation (6.6) can be written as:

$$-\{f\} = [Z_E]\,[\,\phi_{ak} \mid \phi_{ae}\,]\begin{Bmatrix}\{p_{ak}\}\\ \{p_{ae}\}\end{Bmatrix} \tag{6.7}$$

Calculating $\{p_{ae}\}$ from equation (6.5) and substituting it into equation (6.7), one obtains:

$$-[\,I + [Z_E][\phi_{ae}][\omega_{ae}^2]^{-1}[\phi_{ae}]^T\,]\{\tilde{f}_i\} = [Z_E][\phi_{ak}]\{P_{ak}\} \tag{6.8}$$

The term $[\phi_{ae}][\omega_{ae}^2]^{-1}[\phi_{ae}]^T$ on the l.h.s of equation (6.8) represents the contribution of the higher modes to the flexibility matrix and can be calculated as follows:

$$[K_a]^{-1} = [\phi_{ak}][\omega_{ak}^2]^{-1}[\phi_{ak}]^T + [\phi_{ae}][\omega_{ae}^2]^{-1}[\phi_{ae}]^T \tag{6.9}$$

leading to
$$[\phi_{ae}][\omega_{ae}^2]^{-1}[\phi_{ae}]^T = [K_a]^{-1} - [\phi_{ak}][\omega_{ak}^2]^{-1}[\phi_{ak}]^T = [R_a] \tag{6.10}$$

Designating $[R_a]$ to the l.h.s of equation (6.10) reflects the fact that, as mentioned before, the term $[\phi_{ae}][\omega_{ae}^2]^{-1}[\phi_{ae}]^T$ represents the residual flexibility due to the higher modes which, in the case of purely experimental applications, can be determined from the measured FRFs of structure A.

Substituting for $[\phi_{ae}][\omega_{ae}^2]^{-1}[\phi_{ae}]^T$ from equation (6.10) in equation(6.8) yields:

$$\{\tilde{f}\} = -[\,I + [Z_E][R_a]\,]^{-1}[Z_E][\phi_{ak}]\{p_{ak}\} \tag{6.11}$$

Substituting $\{\tilde{f}\}$ from equation (6.11) into equation (6.3), and after some algebraic manipulation, one has:

$$-\lambda_{xr}\{p_{xr}\} + [[\omega_{ak}^2] + [\phi_{ak}]^T CH, + R_a]^{-1}[\phi_{ak}]]\{p_{xr}\}=0 \qquad (6.12)$$

where in equations (6.11) and (6.12) $[Z_E]$ and $[H_E]$ are structure E impedance and receptance matrices, respectively.

Equation (6.12) is the main formula for this part of the analysis. Theoretically, having measured the modal parameters of a real structure X, and having calculated the modal parameters of analytical model A, one should be able to calculate $[H_E]$ or $[Z_E]$ from equation (6.12), yielding the mass and stiffness correction matrices necessary to update the FE model A. It should be noted that $[H_E]$ in equation (6.12) is frequency-dependent and that solving equation (6.12) using the r^{th} mode's modal parameters yields $[H_E]$ at $\omega^2 = \lambda_{xr}$, i.e. at the resonant frequency of the updated structure. So, equation (6.12) is not a standard eigenvalue problem in its present form.

6.2.1 SOLUTION PROCEDURE FOR EQUATION (6.12) HAVING COMPLETE COORDINATES MEASURED

The solution procedure will be as follows.

Assume that n_x and m_x are the numbers of measured coordinates and modes of model X, respectively. Also, that na and k are the numbers of coordinates and kept modal parameters of model A, respectively. The vector {p,} for mode r can be calculated using the measured modal vector of mode r and the transformation in equation (6.2), as follows:

$$\{\phi_{xr}\}_{n_x x 1} = [\phi_{ak}]_{n_x x k}\{p_{xr}\}_{kx1} \qquad \text{where } r=1, 2, \ldots\ldots m_x \text{ and } n_x \geq k \qquad (6.13)$$

Having calculated $\{p_{xr}\}_{kx1}$ for mode r and put it in equation (6.12), one has:

$$[[\phi_{ak}]^T [H_E + R_a]^{-1}[\phi_{ak}]]\{p_{xr}\} = \lambda_{xr}\{p_{xr}\} - [\omega_{ak}^2]\{p_{xr}\} \qquad (6.14)$$

or, letting [HE + R_a]$^{-1}$ = [A],

$$[\,[\phi_{ak}]^{T}_{kxn_a}\,[A]_{n_axn_a}\,[\phi_{ak}]_{n_axk}\,]\{p_{xr}\}_{kx1} = \lambda_{xr}\{p_{xr}\} - [\omega^2_{ak}]\{p_{xr}\} \qquad (6.15)$$

Transforming matrix equation (6.15) into a set of algebraic equations with elements a_{ij} of [A] as unknowns gives k equations with $n_a(n_a+1)/2$ unknowns (assuming a symmetric [A]). In the case where a complete set of coordinates and modes of model A are involved in the analysis, the total number of equations will be $k=n_a$ and thus the number of equations will be less than that of unknowns. To prevent the construction of an under-determined set of equations, it is possible to combine k $(=n_a)$ equations like (6.15) for each mode r together and thus to increase the number of equations. To be able to do this, since $[H_E]$ is frequency-dependent, one has to write equation (6.14) as follows (note that for the case of complete modes and coordinates $[R_a] = 0$):

$$[\,[\phi_{ak}]^{T}_{kxn_a}\,[[K]_E - \lambda_{xr}[M]_E]_{n_axn_a}\,[\phi_{ak}]_{n_axk}\,]\,\{p_{xr}\}_{kx1} = \lambda_{xr}\{p_{xr}\} - [\omega^2_{ak}]\,\{p_{xr}\} \qquad (6.16)$$

or

$$[C(\lambda_{xr})]_{n_axn_a(n_a+1)} \begin{Bmatrix} \{K_E\} \\ \{M_E\} \end{Bmatrix}_{n_a(n_a+1)x1} = \{L(\lambda_{xr})\}_{n_ax1} \qquad (6.17)$$

where equation (6.17) is the algebraic version of equation (6.16) with $\begin{Bmatrix} \{K_E\} \\ \{M_E\} \end{Bmatrix}$ as the vector of unknowns. Now, it is possible to put up to n_a sets of equations like (6.17) together (one for each mode) and in doing this one will have up to n_a^2 equations (depending upon how many modes are used). On the other hand, separation of the mass and stiffness variables in equation (6.16) increases the number of unknowns to $n_a(n_a+1)$. Thus, although the number of equations has been increased, the set of equations is still under-determined. This means that this method is not applicable to cases where structure E has a general form and some restriction must be imposed on the mis-modelled coordinates to reduce the number of unknowns.

One restriction which can be imposed on E is preservation of the connectivity of the analytical model. This restriction is not only convenient but is necessary, too. Having imposed a connectivity restriction, the numbers of unknowns for $[K]_E$ and $[M]_E$ are assumed to be equal to p and q, respectively. Thus the necessary and sufficient condition for equation (6.17) to be solved uniquely, for the case of complete measured modes and coordinates, is:

$$p+q \leq n_a x\, n_a \qquad (6.18)$$

which is not difficult to satisfy.

6.2.2 SOLUTION PROCEDURE OF EQUATION (6.12) BASED ON INCOMPLETE MEASURED COORDINATES & MODES

6.2.2.1 SOLUTION PROCEDURE 1, APPROXIMATE SOLUTION

In this section, we will try to deduce the necessary and sufficient conditions under which the method can be used for updating applications in the case of incomplete measured modes and coordinates.

The first step in dealing with the case of data incompleteness is to modify equation (6.14). Assuming that

$$\| [R_a] \| << \| [H_E] \| \tag{6.19}$$

one can ignore $[R_a]$ in equation (6.14), thus reducing it to equation (6.16), i.e.

$$[[\phi_{ak}]^T_{kxn_a} [[K]_E - \lambda_{xr} [M]_E]_{n_a x n_a} [\phi_{ak}]_{n_a x k} 1 \{p_{xr}\}_{kx1} = \lambda_{xr} \{p_{xr}\} - [\omega^2_{ak}] \{p_{xr}\} \tag{6.20}$$

To see the effect of ignoring $[R_a]$, expand [H, + R_a]$^{-1}$ as:

$$\begin{aligned} [H_E + R_a]^{-1} &\cong [Z]_E - [Z]_E [R_a] [Z]_E \\ &= [K] - [M] \lambda_{xr} - [[K] - [M] \lambda_{xr}][R_a][[K]-[M] \lambda_{xr}] \\ &= [[K]-[K][R_a][K]] - [[M]-[K][R_a][M]-[M][R_a][K]]\lambda_{xr} - [M][R_a][M]\lambda^2_{xr} \end{aligned} \tag{6.21}$$

Note that in order to save space the index E for [M] and [K] has been omitted in equation (6.21).

As is evident from equation (6.21), modification terms to [M] and [K] in this equation can be neglected, using the lower measured modes (i.e. smaller λ_{xr}) and as many modes of the analytical model as possible (i.e. very small $\|[R_a]\|$).

Generating equation (6.20) for each measured mode, transforming the results into a set of algebraic equations like equation (6.17) and combining them and then solving them

simultaneously will produce a solution for unknown vector $\begin{Bmatrix} \{K_E\} \\ \{M_E\} \end{Bmatrix}$. For this case the inequality (6.18) has the following form:

$$p+q \leq m_x x\ k \tag{6.22}$$

On the other hand, according to equation (6.13), the following inequality must also be satisfied:

$$k \leq n_x \tag{6.23}$$

Thus, combining (6.22) and (6.23), the single inequality which must be satisfied is (along with (6.23)).

$$p+q \leq m_x x\ n_x \tag{6.24}$$

Since relatively few modes and coordinates can be measured in practice (compared with an FE model), inequality (6.24) can constitute a serious restriction on the application of the method. In such cases, where inequality (6.24) cannot be satisfied, there are two ways of dealing with this shortcoming, as follows:

(a) - to decrease p and q by assuming specific locations for the error(s) (or by considering macro-elements). In this case, the number of erroneous degrees of freedom, i.e. the number of degrees of freedom of the hypothetical structure E, is n_e and equation (6.2) can be written as:

$$\begin{Bmatrix} \{x_{as}\} \\ \{x_{ai}\} \end{Bmatrix} = [\phi_a]\{p_a\} = \begin{bmatrix} [\phi_{aks}]\ [\phi_{aes}] \\ [\phi_{aki}]\ [\phi_{aei}] \end{bmatrix} \begin{Bmatrix} \{p_{ak}\} \\ \{p_{ae}\} \end{Bmatrix} \tag{6.25}$$

The coordinates of structure A have been divided into those which should be modified shown with index "i" and with the total number of n_e, and those which are assumed to be modelled correctly, shown with index "s" and a total number of n_s. In this case, equations (6.1), (6.3) and (6.4) can be written as:

$$[M]\begin{Bmatrix} \{\ddot{x}_{as}\} \\ \{\ddot{x}_{ai}\} \end{Bmatrix} + [K]\begin{Bmatrix} \{x_{as}\} \\ \{x_{ai}\} \end{Bmatrix} = \begin{Bmatrix} \{0\} \\ \{\tilde{f}_i\} \end{Bmatrix} \tag{6.26}$$

$$\{\ddot{p}_{ak}\} + [\omega_{ak}^2]\{p_{ak}\} = [\phi_{aki}]^T\{\tilde{f}_i\} \quad (6.27)$$

$$\{\ddot{p}_{ae}\} + [\omega_{ae}^2]\{p_{ae}\} = [\phi_{aei}]^T\{\tilde{f}_i\} \quad (6.28)$$

Following the same method as for a case with complete coordinates, equations (6.11) and (6.12) can be rewritten as :

$$\{\tilde{f}_i\} = -[I + [Z_E][R_{ai}]]^{-1}[Z_E][\phi_{aki}]\{p_{ak}\} \quad (6.29)$$

and

$$-\lambda_{xr}\{p_{xr}\}_{kx1} + [[\omega_{ak}^2] + [\phi_{aki}]_{kxne}^T [H_E + R_{ai}]_{nexne}^{-1} [\phi_{aki}]_{nexk}]\{p_{xr}\} = 0 \quad (6.30)$$

where $[R_{ai}]$ in equations (6.29), and (6.30) is defined as follows:

$$[R_{ai}] = [\phi_{aei}][\omega_{ae}^2]^{-1}[\phi_{aei}]^T = [K_{ai}]^{-1} - [\phi_{aki}][\omega_{ak}^2]^{-1}[\phi_{aki}]^T \quad (6.31)$$

This means that only the coordinates which are modified are involved in the calculation of $[R_{ai}]$.

Assuming, again, that $\|[R_{ai}]\| << \|[H_E]\|$, equation (6.30) reduces to:

$$-\lambda_{xr}\{p_{xr}\}_{kx1} + [[\omega_{ak}^2] + [\phi_{aki}]_{kxne}^T [[K]_E - \lambda_{xr}[M]_E]_{nexne}[\phi_{aki}]_{nexk}]\{p_{xr}\} = 0 \quad (6.32)$$

For this case, as before, the solution procedure starts by calculating $\{p_{xr}\}_{kx1}$ from equation (6.25) as follows:

$$\{\phi_{xrs}\}_{n_{xs}x1} = [\phi_{aks}]_{n_{xs}xk}\{p_{xr}\}_{kx1} \quad \text{where } r=1, 2, \ldots\ldots m_x \quad (6.33)$$

Note that although $\{\phi_{xri}\}$ and $[\phi_{aki}]$ could be used in equation (6.33) to calculate $\{P_{xr}\}$, by using the correctly modeled coordinates' modal parameters in $\{\phi_{xrs}\}$ and $[\phi_{aks}]$, one has the advantage that it is usually easier to measure certain correctly modeled coordinates than those coordinates which are assumed to be wrongly modelled (for example, coordinates across a joint). The inequalities which must be satisfied in this case are

$$k \leq n_{xs}$$

$p_1 + q_1 \leq m_x \times k$

(b) - **to increase n_x in inequality (6.24) and thereby k.** This can be done by compensating for incompleteness of the measured coordinates by filling the unmeasured coordinates of the measured eigenvectors with their analytical counterparts. Although, for the time being, there is no justification for the correctness of this compensation, experience shows [27] that if the errors in the FE model are not large, then this compensation converges using iteration.

Another more logical way of increasing n_x is to expand the measured eigenvectors to the unmeasured coordinates using the FE model mass and stiffness matrices as interpolation and extrapolation matrices [37,38]. It should be noted that the analytical modal parameters are unique in the sense that they minimize the potential function (or Rayleigh quotient) of the model that we have assumed for the structure and so what we get from the expansion of experimental modal parameters is just an interpolation and does not have any functional properties.

6.2.2.2 THE ROLE OF $[R_a]$ IN THE CALCULATION AND ITS EFFECT ON RESULTS

In cases where incomplete modes are involved in the transformation (6.2), which is inevitable in practice due to the incompleteness of the measured coordinates, the matrix $[R_a]$ must be introduced into the calculations. This matrix, whose norm, $\|[R_a]\|$, depends on the number of kept modes of the analytical model (k), represents the effect of higher modes on the flexibility of the analytical model.

On the one hand, neglecting $[R_a]$ means that what we introduce to equation (6.12) as the "analytical model" is stiffer than the real analytical model as defined by its mass and stiffness matrices. This will result in a more flexible modifying structure E (as is also evident from equation (6.12)). On the other hand, incorporating $[R_a]$ in the calculations will cause a problem in efforts to impose the connectivity (which is necessary to reduce the number of unknowns). It should be noted that using a simplifying assumption in equation (6.21), one has a problem in imposing connectivity as matrices [K]-[K][R][K] and [M[R][K]+[K][R][M] do not have any connectivity pattern.

Now, the smaller $\|[R_a]\|$ is, the more valid become both approximate equations (6.20) and (6.32). Thus, in order to be able to apply the method in the case of incomplete modes and

coordinates while preserving connectivity, one has to increase the number of kept modes of the analytical model, (k), as much as possible.

The other point which can improve the accuracy of the results is the proper selection of experimental modes in the l.h.s of equation (6.13). If one assumes that the difference between the real structure and the analytical model is not very large, then one can represent the lower modes of the real structure as a linear combination of a relatively large number of the lower analytical modes with high accuracy. For example, assume that there are 10 measured modes for the real structure and 15 kept analytical modes. In this case, using equation (6.13), the first mode of the real structure can be represented with high accuracy as a linear combination of the first 15 analytical modes and, as the mode number of the real structure on the l.h.s of (6.13) increases, the accuracy of this approximation (in equation (6.13)) decreases. Thus, it is recommended to use as few measured modes as possible in equation (6.13).

6.2.2.3 SOLUTION PROCEDURE 2, EXACT SOLUTION

In this section, we shall modify equation (6.12) in order to be able to solve it without any approximation on $[R_a]$ and we shall discuss the shortcomings of this approach.

After some matrix manipulations, equation (6.12) can be rewritten as:

$$[\phi_{ak}]^{T}_{kxn_a} [Z_E] \left[[\phi_{ak}]_{n_a xk} - [R_a] [\phi_{ak}]^{T+}_{n_a xk} [\Delta\lambda] \right] \{p_{xr}\} = [\phi_{ak}]^{T}_{kxn_a} [\phi_{ak}]^{T+}_{n_a xk} [\Delta\lambda] \{p_{xr}\} \quad \textbf{(6.34)}$$

where

$$[\Delta\lambda] = [\lambda_{xr}] - [\omega^2_{ak}] \quad \textbf{(6.35)}$$

Note that $[\lambda_{xr}]$ is a diagonal matrix. Equation (6.34), which holds for each mode r of structure X, has the advantage that $[Z_E]$ is explicit in it and thus no approximation is involved in solving this equation.

The major problem in dealing with equation (6.34) is that, in order to be able to calculate $[\phi_{ak}]^{T+}_{kxn_a}$, one has to satisfy the following inequality for each mode of X:

$$k \geq n_a \quad \textbf{(6.36)}$$

Inequality (6.36) cannot be satisfied (considering inequality (6.24)) unless either a complete set of modes are used or one of the methods described in sec. 6.2.2.1 is used to reduce n_a or to increase n_x and thereby to increase k. Assuming specific locations for the error(s), as in section 6.2.2.1, equation (6.34) can be written as:

$$[\phi_{aki}]^T_{kxn_e} [Z_E] \left[[\phi_{aki}]_{n_e xk} - [R_{ai}] [\phi_{aki}]^{T+}_{n_e xk} [\Delta\lambda] \right] \{p_{xr}\} = [\phi_{aki}]^T_{kxn_e} [\phi_{aki}]^{T+}_{n_e xk} [\Delta\lambda] \{p_{xr}\} \quad (6.37)$$

Now, since $n_e << n_a$, it is easy to satisfy both (6.36) and (6.23)

So, it is clear from the above discussion that **equation** (6.34) **is not suitable for model updating applications** while it does seem promising for joint identification.

6.3 RELATIONSHIP OF THE NEW METHOD TO THE EIGENDYNAMIC CONSTRAINT METHOD.

Although the method introduced in section 6.2 was originally derived from a component mode synthesis analysis, it is now clear that it can also be derived from eigendynamic constraint theory [28,39,40,41]. In this context, and in contrast to conventional eigendynamic constraint methodology, it should be noted that the advantage of the new method is that it can be applied in cases of spatially-incomplete modal data.

The eigendynamic constraint method is essentially based on the following formula:

$$[[K+\Delta K] - \lambda_{xr}[M + \Delta M]] \{\phi_{xr}\} = 0$$

leading to

$$[[\Delta K] - \lambda_{xr}[\Delta M]] \{\phi_{xr}\} = \lambda_{xr}[M]\{\phi_{xr}\} - [K]\{\phi_{xr}\} \quad (6.38)$$

The main problem with applying equation (6.38) is the inevitable inconsistency between the number of measured coordinates in $\{\phi_{xr}\}$ and the dimension of the mass and stiffness matrices of the analytical model. To resolve this problem, equation (6.38) will be transformed to equation (6.12) as follows:

pre-multiplying equation (6.38) by $[\phi_a]^T_{kxna}$ and post-multiplying it by $[\phi_a]_{naxk}$ $[\phi_a]^+_{kxna}$, one obtains:

$$[\phi_a]^T_{kxna}[[\Delta K] - \lambda_{xr}[\Delta M]][\phi_a]_{naxk}[\phi_a]^+_{kxna}\{\phi_{xr}\}_{nx1} =$$
$$\lambda_{xr}[\phi_a]^T_{kxna}[M][\phi_a]_{naxk}[\phi_a]^+_{kxna}\{\phi_{xr}\}_{nx1} - [\phi_a]^T_{kxna}[K][\phi_a]_{naxk}[\phi_a]^+_{kxna}\{\phi_{xr}\}_{nx1}$$

leading to

$$[\phi_a]^T_{kxna}[[\Delta K] - \lambda_{xr}[\Delta M]][\phi_a]_{naxk}[\phi_a]^+_{kxna}\{\phi_{xr}\}_{nx1} =$$
$$\lambda_{xr}[\phi_a]^+_{kxna}\{\phi_{xr}\} - \lambda_a[\phi_a]^+_{kxna}\{\phi_{xr}\}_{nx1} \quad (6.39)$$

Now, assuming that the complete set of coordinates have been measured, the following relation holds (see equation (6.13)):

$$\{\phi_{xr}\}_{nax1} = [\phi_a]_{naxk}\{p_{xr}\}_{kx1}$$

or

$$\{p_{xr}\}_{kx1} = [\phi_a]^+_{kxna}\{\phi_{xr}\}_{nax1} \quad (6.40)$$

where the vector $\{\phi_{xr}\}_{nax1}$ has been transformed to a sub-space of the analytical model's principal space, using equation (6.40) (or, simply, the vector $\{\phi_{xr}\}_{nax1}$ has been expressed as a linear combination of k eigenvectors of the analytical model).

Combining equations (6.39) and (6.40) yields:

$$[\phi_a]^T_{kxna}[[\Delta K] - \lambda_{xr}[\Delta M]][\phi_a]_{naxk}\{p_{xr}\}_{kx1} = \lambda_{xr}\{P_{xr}\}_{kx1} - \lambda_a\{p_{xr}\}_{kx1} \quad (6.41)$$

Now, provided that $\{P_{xr}\}_{kx1}$ can be calculated from (6.40), equation (6.41) yields k equations for each measured mode. Combining these together, there will be $m_x xk$ equations available.

Noting that equation (6.40) can be rewritten as:

$$\{\phi_{xr}\}_{n_x x 1} = [\phi_a]_{n_x x k} \{p_{xr}\}_{k x 1}$$

or

$$\{p_{xr}\}_{k x 1} = [\phi_a]^{+}_{k x n x} \{\phi_{xr}\}_{n_x x 1} \qquad n_x \geq k \tag{6.42}$$

equation (6.42) has been derived from (6.40) simply by eliminating the unmeasured coordinates from $\{\phi_{xr}\}$ and $[\phi_a]$.

Equation (6.41) is similar to equation (6.12) except for the presence (or absence) of $[R_a]$.

16.41 APPLICATION OF PROPOSED METHOD TO THE JOINT IDENTIFICATION PROBLEM

Equations (6.32) and (6.37) could be used for joint identification purposes. For this particular application, the erroneous coordinates are known to be those across the joint and thus the inequality of equation (6.24) can easily be satisfied. This method is especially useful when several joints in an assembled structure are to be identified.

The identification procedure will start with the explicit consideration of the joint(s) in the FE model of the assembled structure and then continue using any of equations (6.32) or (6.37). This approach has three problems associated with it, as follows:

(a) - the proper and accurate modelling of a joint is very important and sometimes very difficult. If the joint has not been modelled properly, the identified joint will not be correct ;

(b) - the mis-modeled substructures which constitute the assembled structure will affect the characteristics of the identified joint;

(c) - sometimes, the FE model of a structure is very difficult and expensive to construct. Thus, in this case, if only identification of the joint(s) is (are) desired, it may not be worthwhile developing such an FE model.

The second and third problems listed above can be avoided by using experimental models of the substructures, assembling them through a hypothetical trial joint model and then calculating the modal parameters of this analytically-coupled structure, A-C, using them

along with the modal parameters of the assembled structure in equation (6.32) (or (6.37)). This approach still has the disadvantage of requiring consideration of a prescribed model for each joint and, besides, one has to couple experimental models of substructures which itself is difficult and introduces some error to the problem.

In what follows, the computational aspects of the method will be discussed and its performance and sensitivity to noise will be examined through a series of case studies.

6.5 CASE STUDIES

The main objective of this section is to examine the performance of the proposed modal-based direct identification method. The section has been divided into two parts, as follows:

part 1- application of the method to the joint identification problem, based on equations (6.37) or (6.32); and

part 2- application of the method to the model updating problem, based on equation (6.20)

It may seem that the application of equation (6.32) to joint identification is redundant, when it is possible to solve the problem more accurately using equation (6.37). However, if equation (6.32) turns out to have the same degree of efficiency as equation (6.37), then using (6.32) is, at least, associated with advantage that the higher modes' residual matrix $[R_a]$ is not required in this equation. This is a great advantage, especially when purely experimental data are used to generate structure A-C.

PART 1 CASE STUDIES RELATED TO THE JOINT IDENTIFICATION PROBLEM

6.5.1 COMPUTATIONAL ASPECTS

Solving either equation (6.32) or equation (6.37) requires certain computational considerations which will be discussed in this section.

To clarify the concepts and conclusions which will be discussed through this and the following sections, each conclusion will be illustrated with a numerical case study. It should be noted that in all these case studies, in order to simulate real practice as closely

as possible, only the translational slave coordinates of the real structure will be used in the calculations. It should also be noted that, unless stated otherwise, deductions and conclusions which will be discussed throughout the part 1 apply both to equation (6.32) and to equation (6.37).

6.5.1.1 TEST STRUCTURES AND JOINT MODELS

The test structures which are used in all case studies of this part are shown in Fig. 6.2. Structure X, which simulates the real structure, is an 16-element clamped-clamped beam with element 9 designated as the joint element.

As mentioned in section 6.4, the analytical model (i.e. structure A-C), is generated by coupling the constituent substructures of the assembly through a trial joint model. Since, as mentioned before, only the translational slave coordinates of the A-C and X structures are used in calculations, there are 13 coordinates in the eigenvectors of structures A-C and X in the transformation equation (6.33). Also, unless stated otherwise, the modes of the A-C structure used in the calculations will be the first 7 modes. So, the transformation matrix in equation (6.33) is a 13x7 matrix.

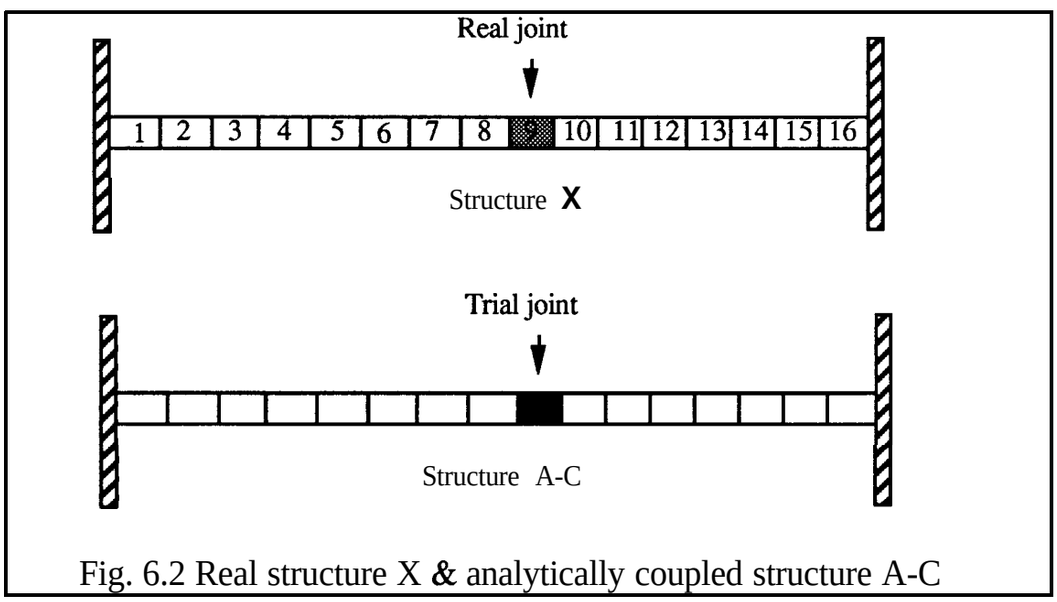

Fig. 6.2 Real structure X & analytically coupled structure A-C

The base element used in developing the FE models of the various structures has the geometrical and mechanical properties shown in Fig.3.2.

The joint element of the real structure has the following properties:

$$L_{jx} = 800/3\%\ L_e\ ,\ E_{jx} = 500\%\ E_e\ ,\quad \rho_{jx} = 10\%\ \rho_e \qquad (6.43)$$

and is thus 5 times stiffer and 10 times lighter than the base element.

The specifications in equation (6.43) yield the following mass and stiffness matrices for the real joint model:

$$[M]_{jx} = \begin{bmatrix} .00011 & .00126 & -.000087 \\ & .05 & -.0021 \\ .05 & .0021 & .01746 \end{bmatrix}$$

$$[K]_{jx} = \begin{bmatrix} 3220000 & 483000 & -3220000 & 483000 \\ & 96600 & -483000 & 48300 \\ & & 3220000 & -483000 \\ & & & 96600 \end{bmatrix} \qquad (6.44)$$

The configurational model of the trial joint is dictated by the interfacing configuration of the real structure and the trial joint specification will be given for each case study.

6.5.1.2 THE EFFECT OF THE NUMBER OF MODES INVOLVED IN CALCULATIONS ON THE RESULTS.

In order to be able to solve equation (6.37) (or (6.32)), it is necessary to transform it into a set of algebraic equations. Having done this, the resultant set of algebraic equations has the following form for each eigenvalue, λ_{xr}:

$$[C]_{kx1/2(n_i(n_i+1))} \left\{ \Delta Z_j(\lambda_{xr}) \right\}_{1/2(n_i(n_i+1))x1} = \{L(\lambda_{xr})\}_{kx1} \qquad (6.45)$$

where k is the number of kept modes of structure A-C and n_i is the total number of interface coordinates. It should be noted that the symmetry of the joint impedance matrix has already been taken into account in equation (6.45).

Although it seems that equation (6.45) can be solved for each individual eigenvalue of structure X, due to ill-conditioning of coefficient matrix [C] and due to the fact that the coordinates involved in the calculations are incomplete, in order to obtain reasonable results a minimum number of modes is usually required to make up the condition of

matrix [C] and to reflect sufficiently the effect of the joint in the equation. The reasons for the ill-conditioning of matrix [C] have been explained in chapter 4 and the number of modes required to achieve an acceptable condition number depends mainly on the degree of ill-condition of matrix [C] which, in turn, depends on the number of unknowns in the vector $\{\Delta Z_j(\lambda_{xr})\}$ of equation (6.45).

Separating the variables in equation (6.45), one obtains:

$$[C(\lambda_{xr})]_{kxn_u} \begin{Bmatrix} \{\Delta K_j\} \\ \{\Delta M_j\} \end{Bmatrix}_{n_u} = \{L(\lambda_{xr})\}_{kx1} \qquad (6.46)$$

The number of unknowns in equation (6.46) depends on the model which is considered for the $[\Delta K_j]$ and $[\Delta M_j]$, as explained in section 4.4.3. In the case studies below the following model is used for $[\Delta K_j]$ and $[\Delta M_j]$:

> beam element model. In this model a "beam element type" joint model is used, as defined in equation (4.58). The number of modification factors, α_i, for this case is 6, three for mass and three for stiffness.

So, if the real joint can be considered as a beam element, i.e. with 4 degrees of freedom involved in interfacing and having the same connectivity properties as a beam element, then there will be 6 modification factors at the interfacing station in Fig. 6.1 (or 9 if damping is involved) and a necessary condition (but not sufficient) for a full rank matrix $[C(\lambda_{xr})]$ in equation (6.46) is:

$$k \geq 9 \qquad (6.47)$$

For our present applications where.there is only one interfacing station and no damping is considered, inequality (6.47) becomes:

$$k \geq 6 \qquad (6.48)$$

As is evident from (6.48), it is easy to satisfy this inequality but , as mentioned before, the condition of matrix [C] is not the only problem and due to incompleteness of the coordinates involved in the calculations one still needs to use several modes in order to achieve reasonable results (as will be shown below).

On the other hand, there is a limitation to the number of modes of a real structure which can be used in the calculations. This limitation arises from the approximation made in the derivation of equation (6.37). According to this approximation, the effect of the higher neglected modes in the calculation can be approximated by a residual matrix [R] and the higher the mode number, r, involved in the calculation, the less valid becomes this approximation (see equation (6.28)). So, the best way of deciding whether the number of modes considered in the calculation is adequate is to check the condition number of the final coefficient matrix [S] in equation (6.49) and to check the results to see if they are reasonable for each particular application.

Having calculated equation (6.46) for each mode of structure X, by combining the equations of m_x modes together using the standard approach as explained in section 4.3.4.1, the following algebraic equation is obtained:

$$[S]\begin{Bmatrix}\{\Delta K\}\\ \{\Delta M\}\\ \{AD\}\end{Bmatrix} = \{Q\} \qquad (6.49)$$

CASE STUDY 1.

To demonstrate the above concepts, the following case study has been undertaken. The test structures for this case study are shown in Fig. 6.2 and according to this figure there are 13 translational slave coordinates which are used in the calculation. Also, the total number of modes for structure A-C is 30 from which 7 are used in the calculation as "kept" modes.

The trial joint model has the following specifications:

$$L_{jt} = (800/3)\%\ L_e\ ,\ E_{jt} = (250)\%\ E_e\ ,\quad \rho_{jt} = 8\%\ \rho_e \qquad (6.50)$$

Thus, the trial joint model has the same length as the real joint but with 50% and 20% error in stiffness and mass matrices, respectively.

Having used one mode of structure X in the calculation and using equation (6.37), Table 6.1 shows the first six singular values of matrix [S] in equation (6.49),

	σ_1	σ_2	σ_3	σ_4	σ_5	σ_6
σ of [S]	9.1E11	7E9	3E8	1E6	2.8E-8	4E-15

Table 6.1 Singular values of matrix [S] using one mode in the calculation

As seen from Table 6.1, the rank of matrix [S] is equal to 4 which is the rank of matrix $[\Delta Z_j]$ in equation (6.45).

Table 6.2 shows the variation of the condition number of matrix [S] with number of modes.

m_x	1	2	3	4	5	6
κ of [S]	2.2E26	1E10	4.2E8	2.1E7	1E7	3E5

Table 6.2 Variation of condition number of matrix [S] with number of modes involved in the calculations

As Table 6.2 indicates, adding a 2nd mode to the calculations causes the condition number to drop dramatically. This drop at 2 modes is due to the fact that the rank of equation (6.49) for each mode is 4 (as Table 6.1 shows) and, thus, having 6 unknowns in this equation, i e. a 6x6 matrix, equations of **at least** two modes should be combined to make up the condition of matrix [S].

It is worth mentioning here that although inequality (6.48) is satisfied by using only one mode in the calculation, according to Tables 6.3 and 6.4, matrix [C] of equation (6.46) is rank-deficient using only one mode (which means that inequality (6.48) is a necessary but insufficient condition).

Based on the results of this case study, it is recommended that one should increase the number of modes until the condition number of matrix [S] is acceptable and a dramatic drop in condition number is evident but no further as increase in the number of modes beyond this limit will reduce the accuracy of the results.

6.5.2 ITERATIVE SOLUTION OF EQUATIONS (6.32) & (6.37)

Experience shows that although joint mass and stiffness matrices identified using equation (6.49) are good, the level of residual errors in these matrices are still high. In this section the reason for this unsatisfactory result is discussed and it is shown how an iterative solution procedure can improve the results.

Equation (6.25) (or 6.2) can be written in a compact form as:

$$\{\phi_{xr}\} = [\phi_{ak}]\{p_{xrk}\} + [\phi_{ae}]\{p_{xre}\} \qquad (6.5\ 1)$$

As explained in section 6.2.1, having used a complete modal model and coordinates, the vectors $\{p_{xrk}\}$ and $\{p_{xre}\}$ can be calculated from equation (6.51) for each mode of structure X. Substituting the calculated $\{p_{xrk}\}$ in equation (6.37), and solving it, one will obtain the desired joint mass and stiffness matrices. In the case of incomplete data in respect of modes and coordinates, however, there are two problems which affect the results, and these are:

(a) - the calculated vector $\{p_{xrk}\}$ is approximate, due to the neglected effects of the higher modes in equation (6.51); and

(b) - some part of the information relating to the joint effect in the calculation is missed, due to the incomplete set of the coordinates.

The problem in (b) can be dealt with using significant* modes in calculations.

The first problem in (a) can be explained as follows. Dividing the modes of the A-C structure into 'kept' and 'eliminated' modes, and using only the kept modes in the calculation, has two separate effects on the computation. The first appears either in equation (6.37) when the effect of the higher eliminated modes is approximated by a constant residual matrix [R], or in equation (6.32) where the effect of higher modes is neglected altogether.

The second effect appears in equation (6.51). As mentioned above, due to the neglected contribution of the higher modes, the vector $\{p_{xrk}\}$, whose elements are the participation factors of each kept mode of the A-C structure in expansion of $\{\phi_{xr}\}$ in equation (6.51), is approximate. Now, as structures X and A-C become closer to each other, the effect of the higher modes becomes smaller and, thus, $\{p_{xrk}\}$ becomes more accurate. For example, consider the case where X and A-C are exactly the same and r equals 1, i.e. the first mode of the real structure is expanded in terms of the modes of the A-C structure. In this case, only the participation factor of first mode of the A-C structure, i.e the first element of $\{p_{xrk}\}$, is non zero and equals to 1.

The above argument suggests that an iterative solution to equation (6.37) (or 6.32) can potentially be useful. A suitable iterative solution procedure is shown in Fig. 6.3

* A mode is a significant mode if it is markedly affected by the joint presence.

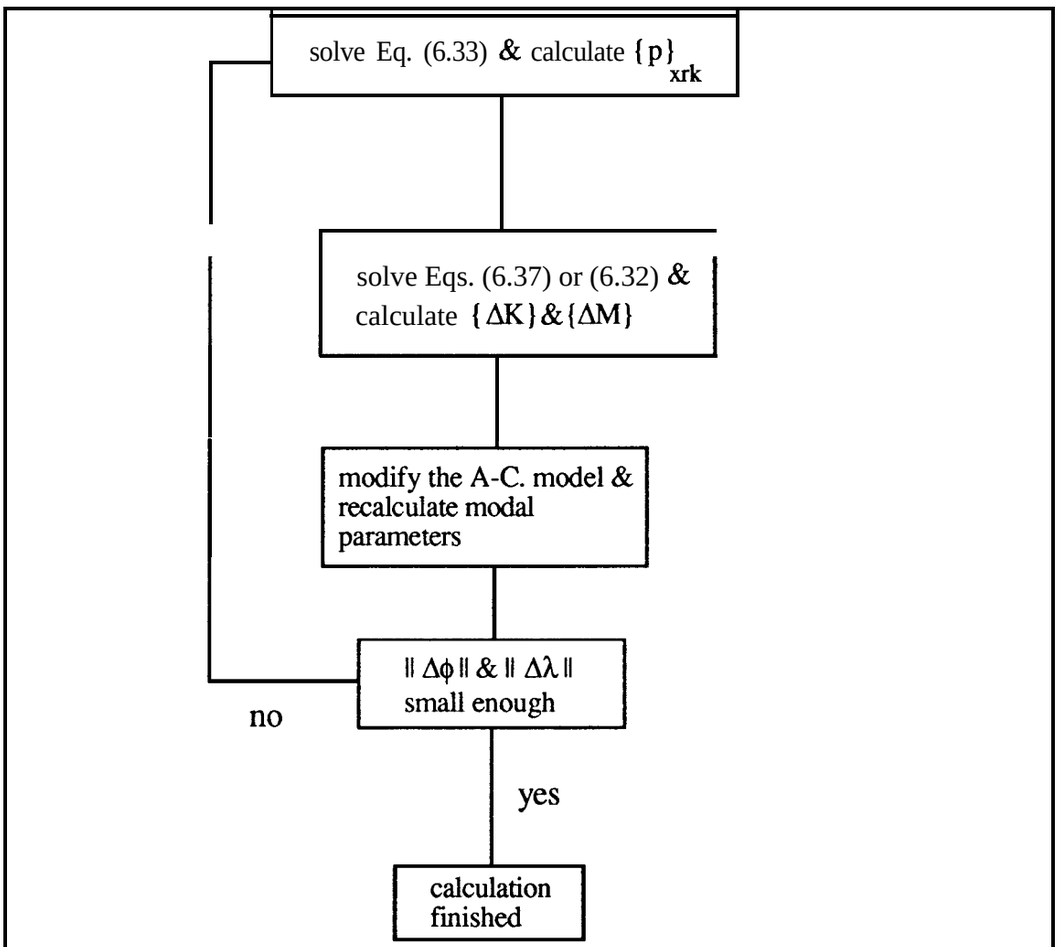

Fig. 6.3 The flow chart for iterative solution of equations (6.37) &(6.32)

The philosophy behind the iterative procedure in Fig. 6.3 is simply that since, at each iteration, structures X and A-C become closer, so the vector $\{p_{xrk}\}$ calculated after each iteration is more accurate than that for the previous iteration, thereby yielding better results.

To show the performance of the iterative method, the following case study has been undertaken.

CASE STUDY 2

In this case study, the effect of iteration on the results will be investigated.

The variation of the condition number of [S] of equation (6.49) can be seen in Table 6.2 and according to this table application of 5 or 6 modes in the calculation will be sufficien. Thus, 5 modes of structure X will be used in the calculations here.

Using equations (6.32) and (6.37), Figs. 6.4 and 6.5 show the variation of $\|\Delta\phi\|$ and $\|\Delta\lambda\|$ with iteration number, respectively.

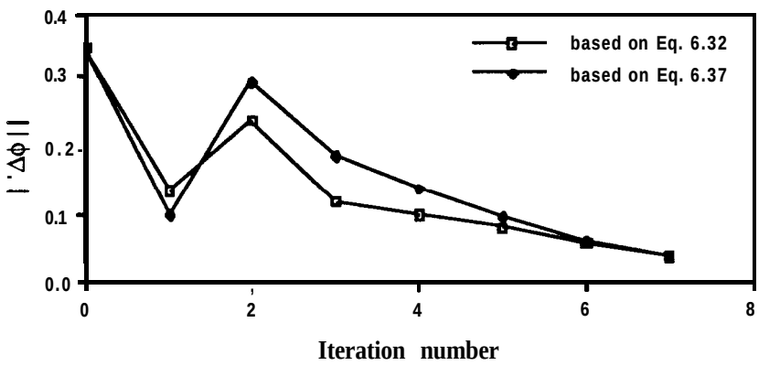

Fig. 6.4 Variation of norm of difference of eigenvectors with iteration, using equations (6.37) & (6.32)

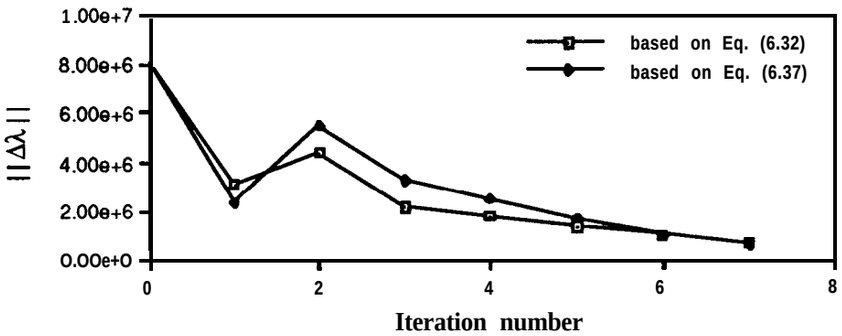

Fig. 6.5 Variation of norm of difference of eigenvalues with iteration, using equations (6.32) & (6.37)

Table 6.3 shows the residual errors in a typical joint parameter identified using equations (6.32) and (6.37).

	k_{11} Error %	k_{12} Error %	k_{22} Error %	m_{11} Error %	m_{12} Error %	m_{22} Error %
Eq. 6.32	0.62	0.58	0.6	0.8	0.94	11
Eq. 6.37	0.6	0.4	0.4	0.4	0.5	0.9

Table 6.3 Residual errors in typical joint parameters for with-residual-effect & without-residual-effect cases, respectively.

Examining Table 6.3, it is evident that, although the results achieved from equation (6.37) are slightly better than those achieved from (6.32), there is no remarkable difference between the two sets of results, except for rotary inertia. The similar results for equations (6.32) and (6.37) show the insignificant effect of the higher modes' residual matrix $[R_a]$ on the results in this case. The greater effect of $[R_a]$ on rotary inertia is due to the fact that the effect of the latter parameter on the structure's response is so insignificant that any approximation (or noise) will affect the identified inertia values dramatically.

Trying to implement the iterative procedure in some case studies, the author came across the problem of a non-positive-definite mass matrix. The reason for this was that, due to a poorly identified joint mass matrix, attempts to update the trial mass matrix can result in a non-positive-definite mass matrix. The way of dealing with this problem is to ignore the mass in the calculations and to update the stiffness matrix only and to carry on the iteration. The mass matrix should then be identified after each iteration and provided that it does not lead to a non-positive-definite mass matrix, one can take it back to the calculations, i.e. to update the mass matrix after each iteration.

6.5.2.1 GUIDE-LINES FOR ITERATIVE SOLUTION IMPLEMENTATION

It was shown in case study 1 that in order to achieve a reasonable condition number for matrix [S] it is necessary to use a certain number of modes in the calculations. On the other hand, using the higher modes in the calculations will introduce more approximations and may spoil the result. Experience shows that for large values of $\|\Delta K\|$ and $\|\Delta M\|$, where it is difficult to converge to a solution, one can achieve better results by using the following procedure.

The vector $\{p_{xrk}\}$, calculated from equation (6.51) for a small number of the lower modes of structure X, is usually accurate. The only problem with using a small number of the lower modes in the calculation is rank deficiency of matrix [S]. Now, if one neglects [AM] in the calculations, then the number of unknowns will be cut by half. The smaller number of unknowns means that a smaller number of modes is required to make

up the rank of the matrix [S]. It should be noted that, using the lower modes in the calculation, neglecting the joint mass effect (which is very small) will not have any detrimental effect on the accuracy of the results.

So, for the first or second iterations, it is recommended to neglect the mass in the calculations and to update only the stiffness matrix and then, having reduced $\|\Delta K\|$, one can take the mass back to the calculations and iterate again.

The other practical consideration is that, in order to calculate the vector $\{p_{xrk}\}$ from equation (6.33)(or 6.51) as accurately as possible, it is necessary that in expanding the r^{th} mode of the structure X in equation (6.33), the r^{th} mode of the structure A-C must be included in the basis of the transformation matrix, $[\phi_{ak}]$, on the r.h.s of equation (6.33).

6.5.3 CONDITION NUMBERS OF AN EIGENVALUE & EIGENVECTOR AND THEIR APPLICATION AS CRITERIA FOR MODE SELECTION

As discussed in section 6.52, an important factor for the iteration procedure in Fig. 6.3 to converge to a solution, is the accuracy of vector $\{p_{xrk}\}$, calculated from equation (6.33). It was argued in section 6.5.2 that the closer the eigenvectors of two structures are to each other, i.e. the smaller are $\|\Delta\phi\|$ and $\|\Delta\lambda\|$ and the more accurate becomes the expansion.

Since, in solving either equation (6.37) or equation (6.32), the analyst has some flexibility in selecting which modes he wishes to use in the calculations, and if one can identify the modes with the smallest $\| \Delta\phi \|$ and $\| Ah \|$ and use them, then there will be a greater chance of achieving convergence. On the other hand, if the larger $\| \Delta\phi \|$ and $\| Ah \|$ are due to a larger effect of the errors (in the trial joint) on a particular mode, then by eliminating that mode from the calculations one may lose valuable information. So, in order to be able to decide whether a mode with large $\| \Delta\phi \|$ and $\| Ah \|$ should be eliminated or not, one must enquire whether these large norms are due to large $\| AK \|$ and $\| AM \|$ or whether the mode is a sensitive one, i.e. large $\|\Delta\phi\|$ and $\|\Delta\lambda\|$ for small $\| AK \|$ and $\| AM \|$.

In what follows, a criterion will be developed to allow the analyst to select the best modes, in the above sense, in calculations using the condition numbers of the eigenvalue and eigenvector.

It was shown in section 4.5.1 that variations in the eigenvalues and eigenvectors of a general matrix [A], due to small perturbation [AA] in [A], can be found from the following equations:

$$\Delta\lambda_r \cong \frac{\{{}_l\phi\}_r^T[\Delta A]\{{}_R\phi\}_r}{\{{}_l\phi\}_r^T\{{}_R\phi\}_r} \tag{6.52}$$

From equation (6.52), the absolute value of $\Delta\lambda_r$ is expressed as:

$$|\Delta\lambda_r| \leq \frac{\|\{{}_l\phi\}_r^T\|\,\|[\Delta A]\|\,\|\{{}_R\phi\}_r\|}{|\{{}_l\phi\}_r^T\{{}_R\phi\}_r|} \tag{6.53}$$

and

$$\{{}_R\phi'\}_r - \{{}_R\phi\}_r \cong \sum_{s=1\ s\neq r}^{N} \frac{\{{}_R\phi\}_s\{{}_l\phi\}_s^T[\Delta A]\{{}_R\phi\}_s}{\{{}_l\phi\}_s^T\{{}_R\phi\}_s(\lambda_r-\lambda_s)} = \sum_{s=1\ s\neq r}^{N} \frac{\{{}_R\phi\}_s\{{}_l\phi\}_s^T[\Delta A]\{{}_R\phi\}_s}{\cos\theta_r(\lambda_r-\lambda_s)} \tag{6.54}$$

where $\{{}_R\phi\}_r$ and $\{{}_l\phi\}_r$ are the right and left eigenvectors of [A] and $|\{{}_l\phi\}_r^T\{{}_R\phi\}_r|$ is the cosine of the angle θ_r between the left and right-hand eigenvectors. From equation (6.53) it is evident that when $\cos\theta_r$ is very small, the corresponding eigenvalue is very sensitive to perturbations in the elements of [A]. As mentioned in section 4.5.1, Wilkinson [35] suggested that $|\{{}_l\phi\}_r^T\{{}_R\phi\}_r|$ is a condition number for nonrepeated eigenvalues.

It can be seen from equation (6.54) that the quantity $\cos\theta_r$ is again important. However, the sensitivity of the eigenvector is also dependent on the proximity of λ_r to the other eigenvalues. From equation (6.54), the smallest value of $(\lambda_r-\lambda_s)$, indicating the separation of the eigenvalue from its neighbours, is usually defined as a condition number for the corresponding eigenvector $\{{}_R\phi\}_r$.

So, using $\cos\theta_r$ and $(\lambda_r-\lambda_s)$ as criteria, the analyst can decide whether a mode associated with a large $\|\Delta\phi\|$ should be eliminated from the calculations or not, i.e. if the large $\|\Delta\phi\|$ is associated with large $(\cos\theta_r(\lambda_r-\lambda_s))^{-1}$ then that mode should be eliminated.

6.6 SENSITIVITY ANALYSIS.

Experiments suggest [42] that measurement noise will typically induce up to 1% errors in eigenvalues and 10% errors in eigenvectors. The sensitivity of the present method to measurement noise has been examined by carrying out a further series of case studies. After spending some time trying different methods, the following error adding mechanism has been adopted:

$$\lambda_r = \lambda_r \pm (1/r) \times (e_1/100) \times \lambda_r \times RND$$

$$\phi_r = \phi_r \pm (e_2/100) \times \phi_r \times RND \qquad (6.55)$$

where, in equation (6.55), e_1 and e_2 are error multipliers and are equal to 1 and 5, respectively. Also, the RND function generates random numbers between 0 and 1, i.e. $0<RND<1$. Note that the sign of the noise induced errors in equation (6.55) is also determined randomly.

CASE STUDY 3

Case study 2 has been repeated here with noise added in equation (6.55), introduced to the modal models of both structures X and A-C.

Figs. 6.6 and 6.7 show the variation of $\|\Delta\phi\|$ and $\|\Delta\lambda\|$ with iteration number using equations (6.32) and (6.37).

The results in Figs. 6.6 and 6.7 were obtained using 7 modes of structure X in the calculations and, further, the joint mass has been ignored through all iterations and this is due to the problem that the mass results are so poor that considering them in the calculations will result in a non-positive-definite mass matrix.

Figs. 6.6 and 6.7 indicate that, by using only stiffness in the iteration, the $\|\Delta\phi\|$ and $\|\Delta\lambda\|$ values cannot be reduced beyond a certain limit and reasonably good results may be achieved after the 1st run of the calculations. It is also clear from Figs. 6.6 and 6.7 that results obtained from equation (6.32), i.e. ignoring residual effects, are better than those obtained from (6.37). There are two reasons for the better results achieved using equation (6.32), namely:

(a) - the effect of error on the higher modes' residual matrix $[R_a]$. Examining this matrix for the with- and without- noise cases it is realized that the error effect on $[R_a]$ is not dramatic ; and

(b) - as explained in section 4.2.2.2, since the coefficient matrices on the l.h.s of equation (6.32) are simple matrices, i.e. are not composed of other submatrices, this equation has a better error averaging performance using a least-squares technique.

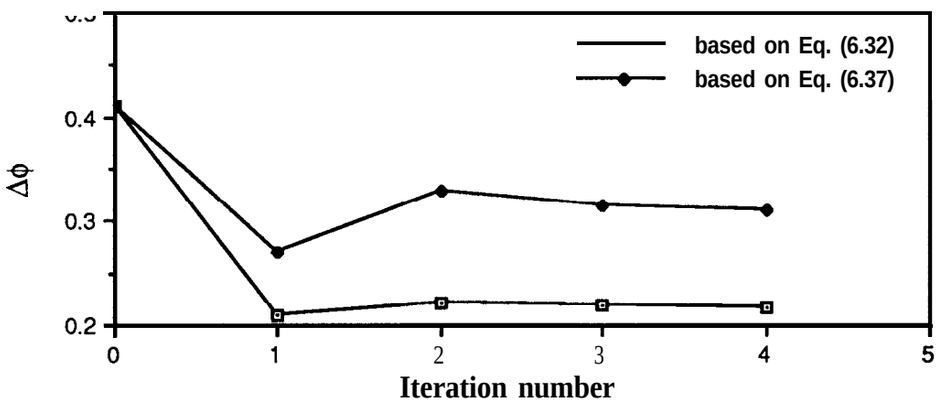

Fig. 6.6 Variation of norm of difference of eigenvectors with iteration, noise added.

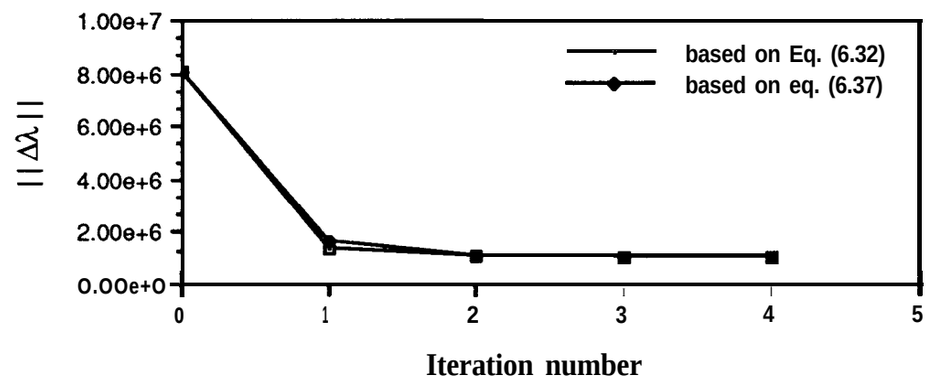

Fig. 6.7 Variation of norm of difference of eigenvalues with iteration, noise added.

Expression (6.56) shows the identified mass and stiffness matrices after the 3rd iteration.

$$[M_7]_j = \begin{bmatrix} .0412(18\%) & .00208(2\%) & .0142 & -.0012 \\ & -.00039(400\%) & .OO\,124 & .00029 \\ & & .0412 & -.00209 \\ & & & -.00039 \end{bmatrix}$$

$$[K_7]_j = \begin{bmatrix} 1.9E6(41\%) & 302685(35\%) & -1.9E6 & 302685 \\ & 69743(35\%) & -302685 & 3487\,1 \\ & & 1.9E6 & -302685 \\ & & & 69743 \end{bmatrix} \qquad (6.56)$$

and

$$\bar{[K_7]}_j = \begin{bmatrix} 2.12E6(26\%) & 344464(27\%) & -2.12E6 & 344464 \\ & 80875(16\%) & -344464 & 40437 \\ & & 2.12E6 & -344464 \\ & & & 80875 \end{bmatrix} \qquad (6.57)$$

Examining the results in expressions (6.56) and (6.57) shows that the mean stiffness matrix in expression (6.57) is much more accurate than that in expression (6.56). Also, examining the mass matrix in expression (6.56) indicates that the only element of that matrix which is very poor is the rotary inertia term, and this is responsible for the non-positive-definiteness of the mass matrix. Otherwise, the results for other elements are reasonably good. This great effect of noise on the rotary inertia, once again (see chapters 5 to 10) proves that this element's effect on the structure's response is insignificant and, thus, is detrimental when noise is present (see chapter 4). It should be noted that an attempt was made to prevent the mass matrix from becoming non-positive definite by scaling it but still no further improvement is achieved.

It is worth mentioning that case study 3 has been repeated for the case where no noise is present in the modal parameters of structure A-C. This was done to examine the performance of the method when using a hybrid technique, i.e. part of the data from the FE model and part from experiment.

The result of this case study shows no improvement over the results in equations (6.56) and (6.57) (as was expected).

PART 2 CASE STUDIES RELATED TO MODEL UPDATING

CASE STUDY 4

6.7 TEST STRUCTURES DESCRIPTION

Fig 6.8 shows the test structures used in the case studies related to model updating.

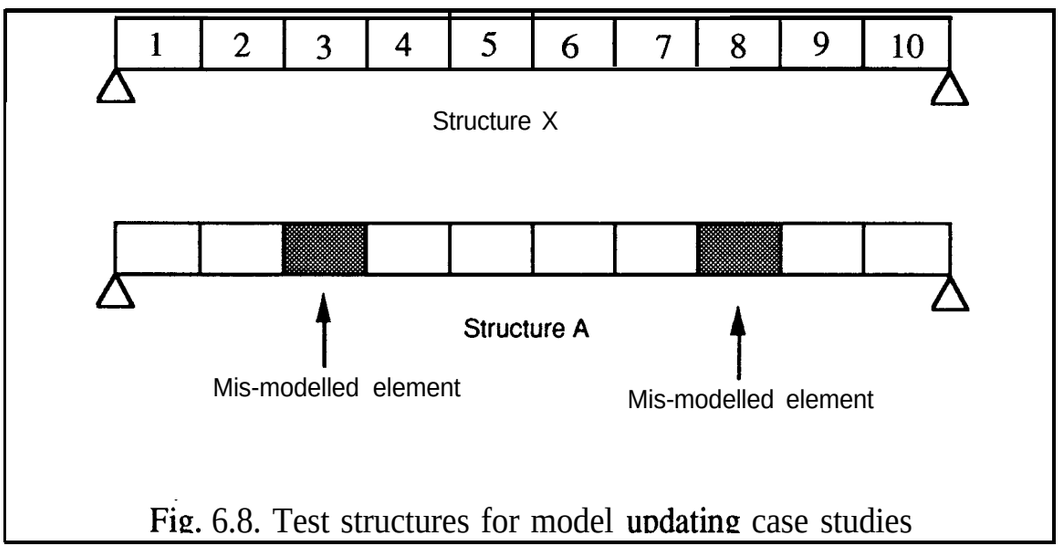

Fig. 6.8. Test structures for model updating case studies

Structure X, which simulates the real structure, is a lo-element FE model of a simply-supported beam. Structure A, which simulates analytical model of structure X, is also a lo-element simply-supported beam model but with 100% error in the stiffness matrices of elements 3 and 8.

The first 6 modes of structure X and the first 9 modes (out of 20) of model A are used in the calculations. These start by calculating {p,} for mode r of structure X from equation (6.13), i.e.

$$\{\phi_{xr}\}_{n_x x 1} = [\,\phi_{ak}\,]_{n_x x k}\,\{p_{xr}\}_{k x 1} \qquad (6.13)$$

where n_x=9 in equation (6.13) (note that only translational slave coordinates of X are used in calculations) and k=9. The next step is to set up equation (6.20) for mode r and transform it to a set of linear algebraic equations similar to (6.46). The coefficient matrix of this set of equations is a 9x10 matrix (under-determined), for each mode r. Combining a set of equations for the first 6 modes of structure X, the order of coefficient matrix of the final set of equations will be 54x10.

Fig. 6.9 shows the stiffness modification factors calculated in the first run of calculation.

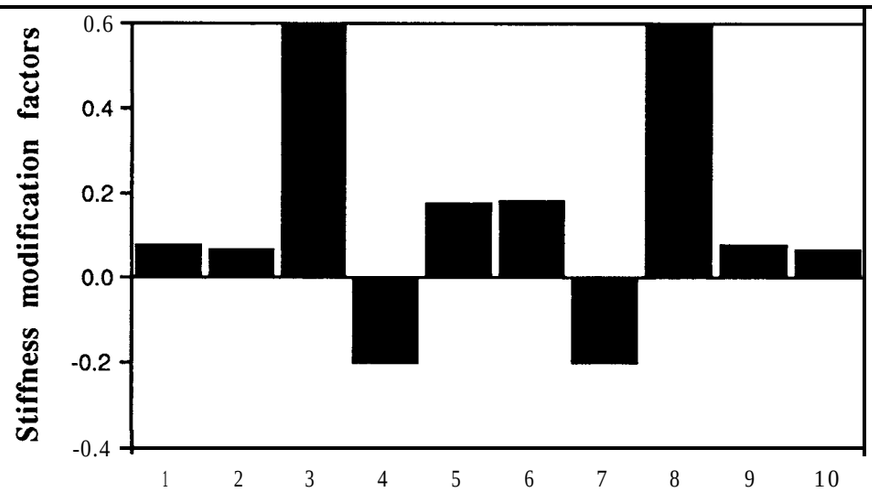

Fig. 6.9 stiffness modification factors after first run

As is evident from Fig. 6.9, the results of this first run have correctly located the mis-modeled elements.

Fig. 6.10 shows the variation of $\|\Delta\phi\|$ and $\|\Delta\lambda\|$ with iteration number. It is evident from Fig. 6.10 that complete convergence is achieved after 6 iterations and significant reductions in $\|\Delta\phi\|$ and $\|\Delta\lambda\|$ are obtained after 4 iterations.

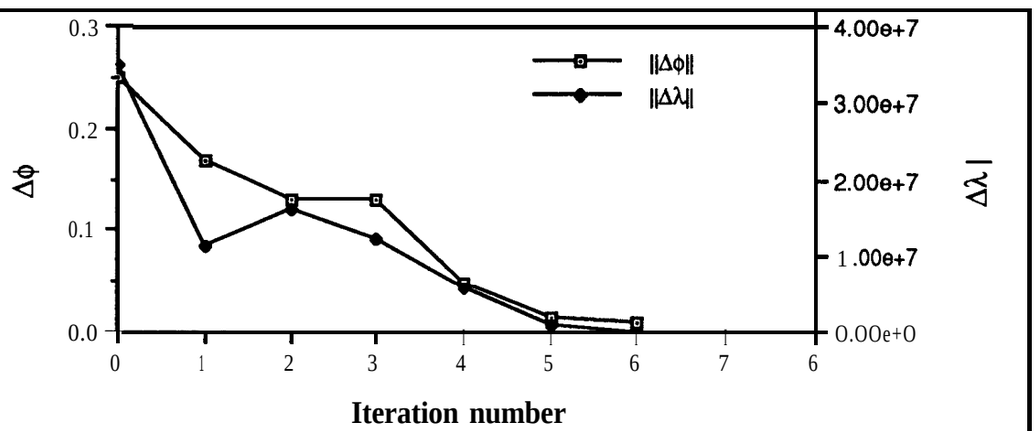

Fig. 6.10 Variation of norm of difference of modal parameters with iteration

6.7.1 COMPARISON OF THE MODAL-BASED DIRECT METHOD WITH THE INVERSE EIGEN-SENSITIVITY METHOD

The performance of the proposed technique for model updating has been examined in case study 4 and seems to be promising. Since both the proposed method and IEM are modal-based, it is convenient to compare their relative advantages and disadvantages.

A modal-based direct updating technique has the following advantages over IEM:

(a) - since the differences of modal parameters are not directly involved in formulation, no correlation analysis is necessary to identify related modes of the real structure and analytical model. The only requirement in the proposed method is that, using mode r of the structure X on the l.h.s of transformation (6.13), the relevant mode of analytical model must be present in matrix $[\phi_{ak}]$ on the r.h.s of the equation. The fulfilment of this requirement does not need such detailed correlation analysis; and

(b) - the modal-based direct method does not require the effect of higher modes to be included in formulation.

The only advantage of the IEM over the modal-based direct method introduced here is that the former method can be implemented using only eigenvalues in the calculation, (provided a sufficient number of these have been measured).

6.7.2 SENSITIVITY ANALYSIS

CASE STUDY 5

Case study 4 has been repeated for case 5, this time with the error mechanism in equation (6.56) applied to the modal parameters.

The modification factors obtained after first run are shown in Fig 6.11

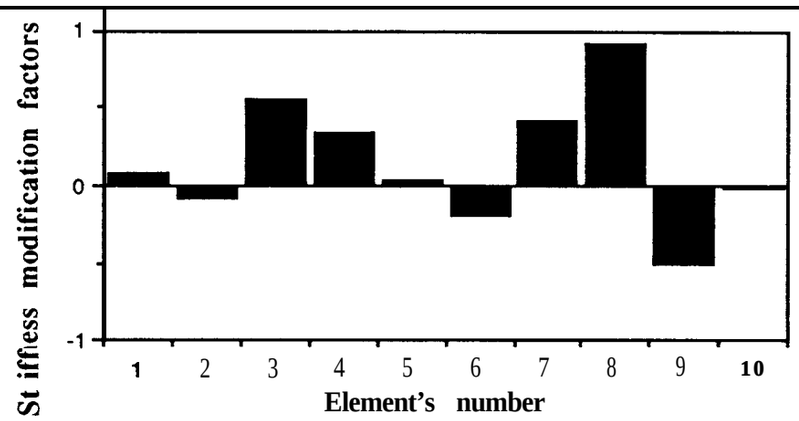

Fig. 6.11 Stiffness modification factors, error added to modal parameters

, As is evident from Fig. 6.11, having added errors to the modal parameters, it is still possible to spot the mis-modeled elements with a reasonable degree of certainity. Fig. 6.12 demonstrates the variation of $\|\Delta\phi\|$ and $\|\Delta\lambda\|$ with iteration number.

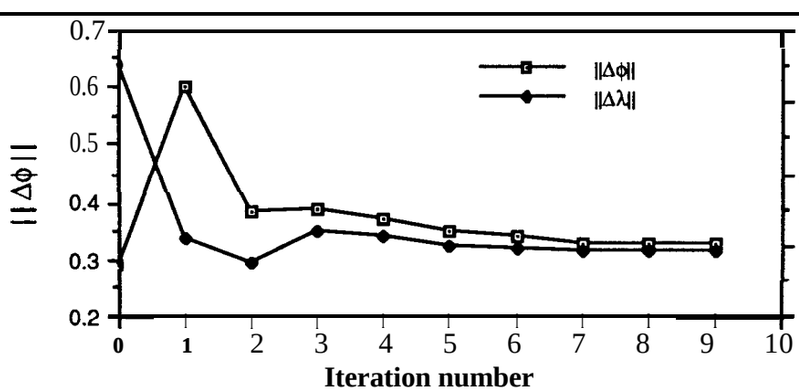

Fig. 6.12 Variation of the norm of difference of modal parameters with iteration, error added

It is clear from Fig.6.12 that a reasonably good reduction in $\|\Delta\lambda\|$ is achieved after 1 run of the calculations but no improvement is obtained on $\|\Delta\phi\|$.

In an attempt to improve the results in Fig. 6.12, the calculation was repeated, this time considering only the modification factors with local maximum values. Examining Fig. 6.11, it is evident that modification factors related to elements 3 and 8 are local maxima of modification factors, considering absolute values of modification factors. So, forcing

modification factors other than those related to elements 3 and 8 to be zero, Fig. 6.13 shows the variation of modal parameters with iteration number.

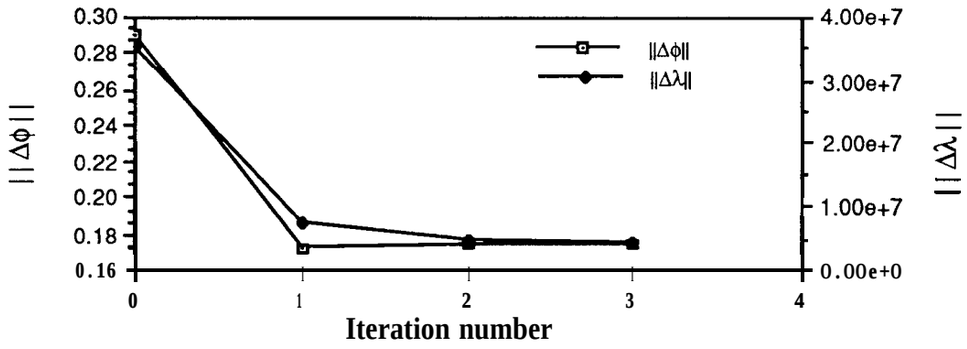

Fig. 6.13 Variation of the norm of difference of modal parameters with iteration, error added

Results in Fig.6.13 demonstrate a marked improvement over those in Fig.6.12.

6.8 CONCLUSIONS & REMARKS

A new modal-based direct method has been proposed for joint identification and model updating. The performance of the proposed method when applied to joint identification and model updating problems has been investigated both with and without measurement noise included.

An important conclusion, deduced from case studies 2 through 5, is that although the proposed identification (and updating) technique is a direct modal-based technique, one has to use an iterative technique to achieve satisfactory results because of data incompleteness, as all other identification techniques. Also, for the same reason, i.e. incompleteness, there is a limitation to II AK II and II AM II for the calculations to converge to a solution. Experience shows that the calculations converge for error levels as much as 100% in mass and stiffness.

In the case of model updating, the similarity and advantages of the proposed method with the eigendynamic constraint method and inverse eigen-sensitivity method has been discussed.

The new method developed for joint identification has the advantage that for structure X only the measurement of slave coordinates is required in the identification process. Also, it is possible to identify a joint using only one measured mode of the assembled structure.

The method could be generalized to a damped case but, since complex eigenvector extraction from measured data is generally associated with large errors, the application of any modal-based method is not recommended for damped systems and the best method to be used in such a case is one of the FRF-based methods described in (chapters 5 & 9).

It has been shown that iterative application of equations (6.32) and (6.37) to the joint identification problem, and equation (6.20) to the model updating problem, yields good results. Also, guidelines have been given for practical implementation of iteration and for proper selection of the A-C structure's modes involved in the calculation. According to these guidelines, sensitive modes can be identified, and distinguished from significant modes, and excluded from the calculations

When noise is present in the calculations, the identified mass matrix is most affected by the noise and since using few lower modes, the mass effect on the calculation is fairly insignificant, it is recommended that the mass be ignored in the calculations. Also, it has been shown that, for the model updating case, using only local maxima of modification factors yields satisfactory results.

For the joint model and test structures used in part 1 of the case studies in this chapter, i.e. beam element type joint at approximately the middle of a clamped-clamped beam, the effect of rotary inertia of the joint on the structure's response is very insignificant and, thus, noise can dominate its effect. This is responsible for a poor identified mass matrix in general and a very poor identified rotary inertia in particular. As is shown in chapter 5, and for test structures with different boundary conditions, the rotary inertia of a joint has the same insignificant and, when noise is present, detrimental effect on the results.

CHAPTER 7

APPLICATION OF FRF-BASED PERTURBATION ANALYSIS TO THE JOINT IDENTIFICATION PROBLEM.

7.1 INTRODUCTION

The application of an FRF-based direct method to the joint identification problem has been discussed in chapter 5. It was mentioned in that chapter that one of the drawbacks of an FRF-based direct method is that it requires transfer FRFs between interface and slave coordinates, and these may be difficult to measure in practice.

The FRF-based **perturbation** analysis which will be presented in this chapter is not faced with the above problem in that it is not necessary to measure transfer FRFs. Also, since the technique is FRF-based, it has all the advantages associated with FRF-based techniques mentioned in section 5.1, such as a large amount of data available which provides the flexibility of selecting proper data points or, relative ease in handling the damping problem.

On the other hand, as discussed in chapter 3 and will be shown here, since the technique is perturbation-based, thus a number of iterations are necessary to achieve a solution and, for the same reason, there is a limitation to the amount of error between the structure and its analytical model which can be identified using this type of technique.

In this chapter the performance of an FRF-based perturbation analysis to deal with the joint identification problem will be examined. If this method turns out to be efficient (at least comparable to the associated FRF-based direct technique), then it will be more convenient to use the perturbation method from the above problem point of view.

7.2 GENERAL FORMULATION OF AN FRF-BASED PERTURBATION TECHNIQUE

In this section the FRF-based perturbation method will be formulated first in a general manner (as in reference [25]) and then a version of the method suitable for joint identification will be derived.

Designating suffices A and X to the analytical and experimental models of the structure, respectively, one has:

$$[H_X(\omega)]=[Z_A(\omega)+\Delta Z(\omega)]^{-1} \tag{7.1}$$

Expanding equation (7.1) using the binomial expansion yields:

$$[H_X(\omega)]= [H_A(\omega)] - [H_A(\omega)][\Delta Z(\omega)][H_A(\omega)] + \ldots\ldots\ldots\ldots\ldots \tag{7.2}$$

Assuming that $\|[\Delta Z(\omega)]\| << \|[Z_A(\omega)]\|$ and ignoring orders of [AZ] higher than one, equation (7.2) can be approximated to:

$$[H_A(\omega)] - [H_X(\omega)] \cong [H_A(\omega)] [\Delta Z(\omega)] [H_A(\omega)]$$

$$\text{or..}\ [\Delta H(\omega)] \cong [H_A(\omega)] [\Delta Z(\omega)] [H_A(\omega)] \tag{7.3}$$

The matrix equation (7.3) is the general governing equation of FRF-based perturbation analysis.

7.3 MODIFYING EQUATION (7.3) TO MAKE IT SUITABLE FOR JOINT IDENTIFICATION APPLICATIONS

Assuming that a real structure consists of some substructures and, furthermore, that the difference [AZ] between two models A and X is concentrated at the interfaces of the substructures (a reasonable assumption for joint identification problem), equation (7.3) can be rewritten as follows:

$$\begin{bmatrix} [\Delta H]^{ss} & [\Delta H]^{si} \\ [\Delta H]^{is} & [\Delta H]^{ii} \end{bmatrix} \cong \begin{bmatrix} [H]_A^{ss} & [H]_A^{si} \\ [H]_A^{is} & [H]_A^{ii} \end{bmatrix} \begin{bmatrix} [0] & [0] \\ [0] & [\Delta Z] \end{bmatrix} \begin{bmatrix} [H]_A^{ss} & [H]_A^{si} \\ [H]_A^{is} & [H]_A^{ii} \end{bmatrix} \tag{7.4}$$

where suffices "s" and "i" relate to slave and interface coordinates, respectively.

Equation (7.4) can be resolved into 4 sub-matrix equations from which the following is selected as the most suitable one for joint identification:

$$[\Delta H(\omega)]^{ss} \cong [H(\omega)]_A^{si}[\Delta Z(\omega)][H(\omega)]_A^{is} \qquad (7.5)$$

The reasons for choosing equation (7.5) out of the 4 possible equations deducible from (7.4), and the consequences of ignoring the other 3 equations, have been thoroughly discussed in section 5.3. Briefly, the obvious advantage of equation (7.5) is that only FRFs relating to the slave coordinates are involved in the difference matrix $[\Delta H]^{ss}$, on the l.h.s of equation (7.5), and this is a great advantage from the measurement point of view.

Note that if we rewrite the earlier equation (5.5), i.e. the basic formula for FRF-based direct joint identification technique, we obtain:

$$[\Delta H(\omega)]^{ss} = [H(\omega)]_X^{si}\,[\Delta Z(\omega)][H(\omega)]_A^{is} \qquad (7.6)$$

The advantage of the current method's equation (7.5) over equation (7.6), as mentioned in the introduction, is that, using the former equation, one does not have to measure transfer FRFs $[H(\omega)]_X^{si}$, but instead to generate $[H(\omega)]_A^{si}$, which seems to be more practical and an easier task.

Trying to set up model A-C, i.e. generating the analytical model using only experimental data in the analysis, a coupling process is necessary as explained in section 5.4. Since equation (7.5) is a perturbation-based technique, a number of iterations will be necessary in order to achieve a solution. After each iteration, the trial joint model must be updated and model A must be generated again which means that a coupling process will be required after each iteration. Requiring a series of repeated couplings is a drawback of the FRF-based perturbation technique using only experimental data, as it may induce more errors to the results and make the calculations time-consuming.

On the other hand, if the analytical model is setup by using FE models of the constituent substructures of the structure X, one is not faced with above problem but there is the possibility of having mis-modeled FE models of constituent substructures.

The other details concerning the generation of the model A-C, such as the damping model and the configurational model of trial joint, have already been discussed in section 5.4.

7.4 CONVERGENCE BOUND FOR EQUATION (7.5)

Since equation (7.3) is a first-order approximation to equation (7. 1), it will be valid only up to a certain value of $\|[\Delta Z(\omega)]\|$. In other words, writing equation (7.2) as:

$$[H_x(\omega)] = [H_A(\omega)] - [H_A(\omega)][\Delta Z(\omega)][H_A(\omega)] + [H_A(\omega)][\Delta Z(\omega)][H_A(\omega)][\Delta Z(\omega)][H_A(\omega)] \quad (7.7)$$

then, in order to have equation (7.3) converge to a solution, it is necessary to satisfy the following inequality:

$$\| \sum_{r=2}^{\infty} \text{rth order element of equation (7.7)} \| < \|[H_a][\Delta Z][H_a]\| \quad (7.8)$$

From chapter 5, the directly-formulated version of equation (7.3) is:

$$[H_A(\omega)] - [H_x(\omega)] = [H_x(\omega)][\Delta Z(\omega)][H_A(\omega)] \quad (7.9)$$

Now, comparing equations (7.9) and (7.3), the difference between the matrices [AH(o)] on the l.h.s of the two equations, a difference which is due to the elimination of the higher order elements in (7.7), can be deduced as:

$$[E(o)] = \text{contribution of higher order elements in the r.h.s of equation (7.7)} = [\Delta H(\omega)][\Delta Z(\omega)][H(\omega)]_A] \quad (7.10)$$

Using equation (7.10), inequality (7.8), which is necessary and sufficient condition for equation (7.3) to converge to a solution, can be written as:

$$\| [\Delta H(\omega)][\Delta Z(\omega)][[H(\omega)]_A] \| < \| [H(\omega)]_A)][\Delta Z(\omega)][H(\omega)]_A] \| \quad (7.11)$$

Examining inequality (7.1 1), it is evident that if $\|[\Delta H(\omega)]\|$ becomes large, then there will be a high risk of inequality (7.11) not being satisfied and, thus, that the calculations based on equation (7.3) will diverge. So, natural frequencies of the structure X, at which $\|[\Delta H(\omega)]\|$ becomes large, are potentially high-risk points. The same argument applies to natural frequencies of the analytical model, i.e. at the natural frequencies of A, $\|[\Delta H(\omega)]\|$

becomes large, but, since at these points $\|[H(\omega)]_A)]\|$ itself becomes large, thus it is likely that inequality (7.11) will be satisfied at the natural frequencies of the analytical model.

The above argument is similarly true for the case of joint identification for which equation (7.10) and inequality (7.11) can be written as:

[E] = contribution of the higher order elements in the r.h.s of equation (7.5)

$$= [\Delta H^{si}(\omega)]\ [AZ(o)]\ [H(\omega)]_A^{is}] \qquad (7.12)$$

and:

$$\|[\Delta H^{si}(\omega)][\Delta Z(\omega)][H(\omega)]_A^{is}]\| < \|[H(\omega)]_A^{si}][\Delta Z(\omega)][H(\omega)]_A^{is}]\| \qquad (7.13)$$

7.5 SOLUTION TECHNIQUES FOR EQUATION (7.5) & THE EFFECT OF VARIOUS PARAMETERS ON THE RESULTS

Similar to the approach used in section 5.4, since equation (7.5) is frequency-dependent, it can be solved with two different techniques, as follows:

solution technique 1- solving matrix equation (7.5) at each individual frequency over the frequency range of interest; or

solution technique 2- transforming equation (7.5) into a set of algebraic equations and then putting equations from different frequencies together and solving them simultaneously as a "least squares" problem.

7.6 CASE STUDIES

To study the performance of the solutions based on equation (7.5) and to examine their sensitivity to measurement noise, a series of case studies has been undertaken. In order to be able to compare the performance of FRF-based perturbation and direct techniques, i.e. equations (7.5) and **(5.5),** the test structures and the joint models have been chosen to be exactly the same as those in chapter 5 and can be seen in Fig. 5.1 and expressions (5.10) and (5.11). Briefly, the joint in structure X, i.e. real joint, has the following specifications:

$$L_{jx} = 100\%\ L_e\ ,\ E_{jx} = 1000\%\ E_e\ ,\ \rho_{jx} = 10\%\ \rho_e \qquad \mathbf{(7.14)}$$

where L_e, E_e, and ρ_e are the mechanical and geometrical properties of the base element shown in Fig. 3.2

7.6.1 CASE STUDIES USING SOLUTION TECHNIQUE 1

In this series of case studies, equation (7.5) will be solved as a matrix equation and at each individual frequency.

CASE STUDY 1

Fig. 7.1 shows typical results for the joint identified using equation (7.5) after 3 iterations at each frequency. The trial joint for this case study (and subsequent case studies unless otherwise stated) is the same as that in expressions (5.12) and (5.13) and has the following specifications:

$$L_{jt} = L_{jx} \quad , \quad E_{jt} = 50\%\ E_{jx} \, , \quad \rho_{jt} = 50\%\ \rho_{jx} \tag{7.15}$$

As is evident from Fig. 7.1, the results are satisfactory except for a few frequency points. Examining a typical FRF of the assembled structure, X, in Fig. 7.2 reveals that frequencies associated with poor results coincide with natural frequencies of structure X.

Having poor results at or near the natural frequencies of X, as explained in section 7.4, is due to the fact that at these frequencies $\|[\Delta H]\|$ exceeds the limit which is necessary for the first order perturbation assumption used in equation (7.5) to be valid.

Comparing the similar results in Fig. 5.3, achieved by using direct FRF-based method in chapter 5, with those in Fig. 7.1, it is evident that, as was expected, the results in Fig. 5.3 are better at the natural frequencies of X which is due to the direct nature of method used in chapter 5.

CASE STUDY 2

To examine the performance of equation (7.5) in the presence of measurement noise, “5% random noise” has been added to both real and imaginary parts of all FRFs involved in calculations.

Typical results of the analysis for this case are shown in Fig (7.3).

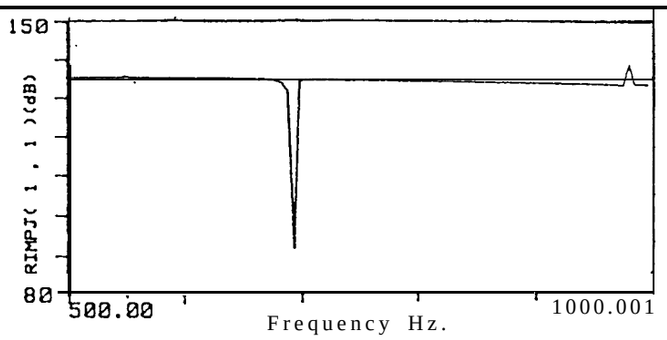

Fig 7.1 Typical result of identified joint impedance using solution technique 1

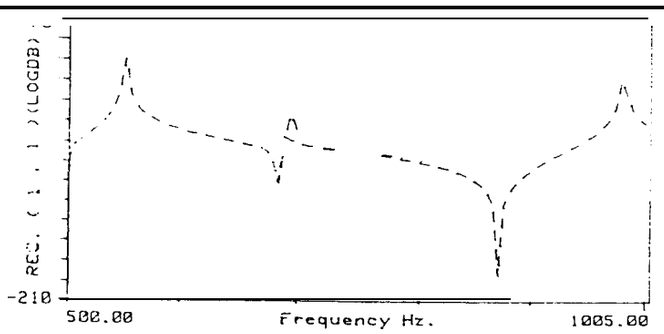

Fig 7.2 Typical FRF of structure X

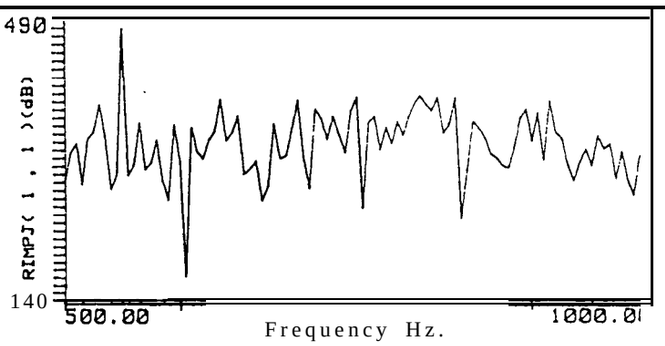

Fig. 7.3 Typical result of identified joint impedance with 5% noise using solution technique 1, ___ correct value

Examining Fig (7.3), it is evident that the results are very poor and thus that the method is very sensitive to noise. In addition to the reason for this high sensitivity to noise given in section 5.5.1 (i.e. the insignificant effect of joint on the structures response so that this

effect can be easily polluted by noise), the other factor responsible for the high sensitivity of equation (7.5) is the approximate nature of this equation.

Consider equation (7.12) as:

[E] = contribution of higher order elements in the r.h.s of equation (7.5)
$$= [\Delta H^{si}(\omega)]\,[\Delta Z(\omega)][H(\omega)]^{is}_{A}] \qquad (7.12)$$

If the noise effects dominate $[\Delta H(\omega)]^{is}$ in equation (7.12) (see section 5.5.1), then the matrix [E] in equation (7.12) changes dramatically and this induces an extra large error on the results. Comparing Fig. 7.3 with Fig. 5.4 (achieved using FRF-based direct analysis), it is evident that, due to noise effect on [E] explained above, the result in Fig. 7.3 is very much poorer than that in Fig. 5.4.

7.6.2 CASE STUDIES USING SOLUTION TECHNIQUE 2

In this section the application of solution technique 2 will be examined, i.e. transforming equation (7.5) to a set of linear algebraic equations by separating the joint mass and stiffness parameters in [AZ] and then combining the set of equations related to different frequencies together, solving the resulting over-determined set of algebraic equations using a least-squares method.

7.6.2.1 COMPUTATIONAL ASPECTS OF SOLUTION TECHNIQUE 2

Following the method used in section 5.5.2.1, considering matrix [AZ(o)] as:

$$[AZ(o)] = [AK] - [\Delta M]\omega^2 + i\,[AD] \qquad (7.16)$$

equation (7.5) can be transformed into a set of algebraic equations for each frequency ω, and having imposed a symmetry constraint on [AK],[AM] and [AD], one obtains:

$$[C(\omega)]_{(n_S x n_S) x 3/2(n_i(n_i+1))} \left\{ \begin{matrix} \{\Delta K\} \\ \{\Delta M\} \\ \{\Delta D\} \end{matrix} \right\}_{3/2(n_i(n_i+1))x1} = \{L(\omega)\}_{(n_S x n_S)x1} \qquad (7.17)$$

Further details about transforming equation (7.5) to equation (7.17) can be found in section 5.5.2.1.

Having combined equation (7.10) for each of nf frequency points together, let us set up the final over-determined set of equations as follows:

$$[P]_{(n_S x n_S x n_f) x 3/2(n_i(n_i+1))} \begin{Bmatrix} \{\Delta K\} \\ \{\Delta M\} \\ \{\Delta D\} \end{Bmatrix}_{3/2(n_i(n_i+1)) x\, 1} = \{q\}_{(n_S x n_S x n_f) x 1} \qquad (7.18)$$

Using the normal equation technique (explained in section 4.3) to solve the least-squares problem defined in equation (7.18), one obtains the following square set of equations:

$$\Big[\ [C(\omega_1)]^T[C(\omega_1)]+[C(\omega_2)]^T[C(\omega_2)]+....+[C(\omega_{nf})]^T[C(\omega_{nf})] \begin{Bmatrix} \{\Delta K\} \\ \{\Delta M\} \\ \{\Delta D\} \end{Bmatrix} =$$

$$\Big[\ [C(\omega_1)]^T\{\ L(\omega_1)\ \}+[C(\omega_2)]^T\{\ L(\omega_2)+....+[C(\omega_{nf})]^T\{\ L(\omega_{nf})\ \}\Big]$$

or

$$[S] \begin{Bmatrix} \{\Delta K\} \\ \{\Delta M\} \\ \{\Delta D\} \end{Bmatrix} = \{Q\} \qquad (7.19)$$

In order to balance matrix [C], the reference joint model based on a beam element model described in section 4.4.3, is used.

Having used equation (7.5) as the basic matrix equation to develop equations (7.17) and (7.18), the question is now "if the first-order approximation in equation (7.2) is valid for each individual frequency point used in developing equation (7.18), then would equation (7.18) always converge to a solution for sure?".

In order to be able to answer the above question, consider the convergence bound for equation (7.5) in equation (7.13) as:

$$\|[\Delta H^{si}(\omega)][\Delta Z(\omega)][H(\omega)]^{is}_{A}]\| < \|[H(\omega)]^{si}_{A}][\Delta Z(\omega)][H(\omega)]^{is}_{A}]\| \quad (7.13)$$

which, written in terms of equation (7.17) yields:

$$\| [C(\omega)]\begin{Bmatrix} \{\Delta K\} \\ \{\Delta M\} \\ \{\Delta D\} \end{Bmatrix} \| > \| [C_e(\omega)]\begin{Bmatrix} \{\Delta K\} \\ \{\Delta M\} \\ \{\Delta D\} \end{Bmatrix} \| \quad (7.20)$$

where [C,(O)] is produced by transforming the matrix of the contributions of the higher neglected terms in equation (7.12), [E], to a set of linear algebraic equations.

Now, consider the case where inequality (7.20) holds for each individual frequency point, i.e.

$$\| [C(\omega_1)]\begin{Bmatrix} \{\Delta K\} \\ \{\Delta M\} \\ \{\Delta D\} \end{Bmatrix} \| > \| [C_e(\omega_1)]\begin{Bmatrix} \{\Delta K\} \\ \{\Delta M\} \\ \{\Delta D\} \end{Bmatrix} \|$$

$$\| [C(\omega_2)]\begin{Bmatrix} \{\Delta K\} \\ \{\Delta M\} \\ \{\Delta D\} \end{Bmatrix} \| > \| [C_e(\omega_2)]\begin{Bmatrix} \{\Delta K\} \\ \{\Delta M\} \\ \{\Delta D\} \end{Bmatrix} \|$$

.....

$$\| [C(\omega_{nf})]\begin{Bmatrix} \{\Delta K\} \\ \{\Delta M\} \\ \{\Delta D\} \end{Bmatrix} \| > \| [C_e(\omega_{nf})]\begin{Bmatrix} \{\Delta K\} \\ \{\Delta M\} \\ \{\Delta D\} \end{Bmatrix} \| \quad (7.21)$$

But, having inequalities (7.21) satisfied does not necessarily mean that the following inequality, which is necessary for equation (7.18) to converge to a solution, is satisfied as well:

$$\| [C(\omega_1)]^T[C(\omega_1)]\begin{Bmatrix}\{\Delta K\}\\ \{\Delta M\}\\ \{\Delta D\}\end{Bmatrix} + ...+[C(\omega_{nf})]^T[C(\omega_{nf})]\begin{Bmatrix}\{\Delta K\}\\ \{\Delta M\}\\ \{\Delta D\}\end{Bmatrix} \| >$$

$$\| [C(\omega_1)]^T[C_e(\omega_1)]\begin{Bmatrix}\{\Delta K\}\\ \{\Delta M\}\\ \{\Delta D\}\end{Bmatrix} +....+[C(\omega_{nf})]^T[C_e(\omega_{nf})]\begin{Bmatrix}\{\Delta K\}\\ \{\Delta M\}\\ \{\Delta D\}\end{Bmatrix} \| \tag{7.22}$$

Thus, the answer to above question is: "using equation (7.5) to set up equation (7.18), although the first order approximation is valid at each individual frequency point, the resultant equation, i.e. equation (7.18), may not converge to any solution".

CASE STUDY 3

To illustrate the above-mentioned problem, two case studies have been undertaken based on the test structures in Fig. 5.1 and a joint model as in equation (7.14). The trial joint model for first case study is the same as that in equation (7.15) and is:

$$L_{jt} = L_{jx}\ ,\ E_{jt} = 50\%\ E_{jx}\ ,\ \rho_{jx} = 50\%\ \rho_{jx} \tag{7.15}$$

For the second case study, the trial joint has been chosen to be much closer to the joint model and its specifications are:

$$L_{jt} = L_{jx}\ ,\ E_{jt} = 90\%\ E_{jx}\ ,\ \rho_{jx} = 90\%\ \rho_{jx} \tag{7.23}$$

The frequency range of interest for both cases is 700 to 800 Hz calculated at 5 Hz increments so that n_f=20. It should be noted that according to Fig.7.1 the first-order approximation assumption is valid for equation (7.5), and consequently (7.17), in all frequency points within the range of 700-800 Hz. Thus, inequalities (7.20) and (7.21) are satisfied at each frequency point

Table 7.1 shows errors in typical identified joint parameters for two cases.

	Trans K Error %	Cross K Error %	Rotary K Error %	Trans M Error %	Cross M Error %	Rotary M Error %
1 st case	110	36	127	200	1200	480
2nd case	1.4	0.3	1.2	0.2	7.6	18

Table 7.1 Error values in the typical identified joint parameters for two cases in equations (7.15) &(7.23)

Examining the error values in Table 7.1 reveals that the results for the first case, i.e. where there is 50% difference between the real and the trial joint mass and stiffness matrices, are very poor while the results for second case, i.e. 10% difference between the two models mass and stiffness matrices, are very good. This means that in the first case, although the first-order approximation is valid at each individual frequency point, it is not valid for the resultant final equation (7.18) and so the calculation diverges. On the other hand, reducing the difference between two models in the second case, reduces the effect of the higher neglected terms in equation (7.5) (see equation (7.12)) so that inequality (7.22) **is** satisfied and calculation converges.

The other important result deduced from Table 7.1 is that, similar to the case studies in section 5.5.2.3, the error percentage related to rotary inertia is much larger than the other elements. This, once again, shows the insignificant effect of rotary inertia of the joint on the response of the structure.

7.7 CONCLUSIONS AND REMARKS.

From what has been presented in this chapter, the following conclusions can be drawn:

(a) - the only, and the very important, advantage of the FRF-based perturbation technique over the FRF-based direct method introduced in chapter 5, is that, in current technique, the measurement of the transfer FRFs between interface and slave coordinates is not required

(b) - drawbacks of the technique are:

(i)- a series of repetitive couplings are required to implement this technique;

(ii)- there is a limitation to the amount of error between the real joint and the trial joint which can be accommodated. Solving equation (7.5) as a matrix equation, the calculation diverges at natural frequencies of the structure for the noise-free

case. For a with-noise case, unless noise level is reasonably low, the calculation does not converge.

(iii)- (on the other hand), solving equation (7.23) as a least-squares problem and for the noise-free case, there is no guarantee that the calculations will converge unless the error between the real and the trial joints is small.

So, for cases where the measurement noise level is low, say about OS%, the application of equation (7.5) as a matrix equation is recommended.

CHAPTER (8)

INVERSE EIGEN-SENSITIVITY ANALYSIS METHOD (IEM) APPLIED TO JOINT IDENTIFICATION

8.1 INTRODUCTION:

In chapter 7, application of an FRF-based perturbation analysis to joint identification was investigated and it was found that, in spite of practical advantages associated with the method, it is not very efficient.

In this chapter, the modal-based version of the method of the chapter 7, i.e. the Inverse E&en-Sensitivity method (IEM), will be discussed and its applicability to joint identification problems will be investigated. Similar to the FRF-based perturbation method, the IEM technique for joint identification requires no measurement related to the interface coordinates of the assembled structure, i.e. the real structure, to be made.

Similar to other adaptive identification techniques, application of IEM requires an analytical model of the structure. In model updating practice, the required analytical model is generated by the finite element technique. In a joint identification analysis, on the other hand, the analytical model can be generated using one of the following methods:

method 1- generating the analytical model (A-C model) by coupling the constituent substructures of the assembled structure through a trial joint model, using experimentally-measured FRFs of the substructures; or

method 2- generating the analytical model by coupling the constituent substructures of the assembled structure through a trial joint model, using FE models of the substructures.

The study in this chapter is based on comparing the real structure, as an assembly, and its analytically-coupled model A-C, assumed to be generated using experimental FRFs of the substructures rather than their FE models, i.e method 1 above. Thus, the assumption that the mis-matched regions between the two models to be the interface coordinates can be strongly justified. On the other hand, using purely experimental data, some changes to the original IEM method used for model updating are necessary in order to consider the effect of the higher and lower truncated modes. These changes will be discussed in this chapter.

8.2 FORMULATION OF METHOD

8.2.1 UNDAMPED SYSTEM:

Consider [M J and $[K_0]$ as the mass and stiffness matrices of the A-C model and [M] and [K] as those of the assembled structure. The following relations hold:

$$[M] = [M_0] + [\Delta M] \qquad \text{and } [K] = [K_0] + [\Delta K] \tag{8.1}$$

where matrices [AM] and [AK] consist of mass and stiffness differences which, for joint identification applications, are concentrated at the interfaces of the assembled structure.

There are various ways of defining [AM] and [AK]. In a model updating problem these matrices are considered as being composed either of corrections in each individual element or of corrections in super or macro-elements of the FE model (each super-element consists of a combination of elements and covers a sub-domain of the structure).
In any case, one can define [AM] and [AK] as follows,

$$[\Delta M] = \sum_{d=1}^{n} \alpha_{md} [\Delta M]_d \qquad \text{and } [AK] = \sum_{d=1}^{n} \alpha_{kd} [\Delta K]_d$$

where, depending on the method, n is either the number of elements or the number of super-elements of the model and α_{md} and α_{kd} are the element's correction factors. Matrices $[\Delta M]_d$ and [AK], are of the same order as [AK], but except for the relevant coordinates to element d of the model, all other elements are zero. Taking derivatives of [K] and [M] in (8.1) with respect to α_{md} and α_{kd}, one obtains:

$$\frac{\partial M}{\partial \alpha_{md}} = [\Delta M]_d \qquad \text{and} \qquad \frac{\partial K}{\partial \alpha_{kd}} = [AK], \tag{8.2}$$

Thus, using the element or superelement-based definition of [AK] and [AM], the element's mass and stiffness matrices should be known in order to be able to calculate $\frac{\partial M}{\partial \alpha_{md}}$ and $\frac{\partial K}{\partial \alpha_{kd}}$. In the case of joint identification using experimental data only, there are two ways to define [AK] and [AM] at the interfaces, as explained in section 4.4.3, namely:

(a) - by considering $[\Delta K]_d$ and $[\Delta M]_d$, the mass and stiffness modifications to trial joint model at interfacing station "d", to be general symmetric matrices, as shown in equation (4.60). In this case each element is a variable parameter, and so if the number of interface coordinates at each junction is n_{id}, then the total number of variables of each matrix is equal to $n_{id}(n_{id}+1)/2$; or

(b) - by defining $[\Delta M]_d$ and $[\Delta K]_d$ using an assumed model for the joints. This model can be either FE-based or a lumped parameter model. As mentioned in section 3.5, for joint identification applications, one has to consider different correction factors for the consistent groups of degrees of freedom involved in the joint model (interfacing). For example, if one considers a beam element as the model of a joint between two beams, the correction factors for this joint model are as follow(see equation (4.58)):

$$[\Delta K]_i = \begin{bmatrix} [0] & [0] \\ [0] & \begin{bmatrix} a_1 & a_2 & -a_1 & a_2 \\ & 2a_3 & -a_2 & a_3 \\ & & a_1 & -a_2 \\ & & & 2a_3 \end{bmatrix}_{n_i \times n_i} \end{bmatrix}$$

leading to

$$[AK]_i = \alpha_1 \begin{bmatrix} [0] & [0] \\ [0] & \begin{bmatrix} a_1 & 0 & -a_1 & 0 \\ & 0 & 0 & 0 \\ & & a_1 & 0 \\ & & & 0 \end{bmatrix} \end{bmatrix} + \alpha_2 \begin{bmatrix} 0 & 0 \\ 0 & \begin{bmatrix} 0 & a_2 & 0 & a_2 \\ & 0 & -a_2 & 0 \\ & & 0 & -a_2 \\ & & & 0 \end{bmatrix} \end{bmatrix} + \alpha_3 \begin{bmatrix} [0] & [0] \\ [0] & \begin{bmatrix} 0 & 0 & 0 & 0 \\ & 2a_3 & 0 & a_3 \\ & & 0 & 0 \\ & & & 2a_3 \end{bmatrix} \end{bmatrix} \quad (8.3)$$

and similarly

$$[\Delta M]_i = \alpha_4 \begin{bmatrix} [0] & [0] \\ [0] & \begin{bmatrix} 156a_4 & 0 & 54a_4 & 0 \\ 0 & 0 & 0 & 0 \\ & & 156a_4 & 0 \\ & & & 0 \end{bmatrix} \end{bmatrix} + \alpha_5 \begin{bmatrix} [0] & [0] \\ [0] & \begin{bmatrix} 0 & 22a_5 & 0 & -13a_5 \\ 0 & 13a_5 & 0 & \\ & & 0 & -22a_5 \\ & & & 0 \end{bmatrix} \end{bmatrix}$$

$$+ \alpha_6 \begin{bmatrix} [0] & [0] \\ [0] & \begin{bmatrix} 0 & 0 & 0 & 0 \\ 4a_6 & 0 & -3a_6 & \\ 0 & 0 & & \\ & 4a_6 & & \end{bmatrix} \end{bmatrix} \qquad (8.4)$$

where a, to α_6 are modification factors for the mass and stiffness submatrices of the joint. Parameters a_i in equations (8.3) and (8.4) can be considered as unity but, from a balancing and condition of calculation point of view, it is better to use a prescribed reference joint model to define the parameters a_i (see section 4.4.3).

Thus, according to equations (8.3) and (8.4), corrections to the mass and stiffness matrices can be calculated using the six correction factors, α_i to α_6.

In either case (a) or (b), it follows from (8.2) that:

$$\frac{\partial[M]}{\partial m_{ij}} = [I_1] \qquad \frac{\partial[K]}{\partial k_{ij}} = [I_1] \qquad \text{for case (a)} \qquad (8.5)$$

and

$$\frac{\partial[M]}{\partial \alpha_i} = [I_2] \qquad \frac{\partial[K]}{\partial \alpha_i} = [I_2] \qquad \text{for case (b)} \qquad (8.6)$$

where $[I_1]$ is a matrix with 1 as its ij^{th} element and zero for all other elements and $[I_2]$ is a matrix with parameters a_i in specified stations depending on suffi (i) (see equations (8.3) and (8.4)). Since the general formulation is similar for both (a) and (b), the following discussions are based on the more general case of (a)

Considering the eigensolutions of [M] and [M J to be $(\{\phi\},\lambda)$ and $(\{\phi\}^0,\lambda^0)$ respectively, and using the Taylor series expansion of the eigenparameters, one can write :

$$\{\phi_h\} = \{\phi\}_r^0 + \sum_{i=1}^{n_i}\sum_{j=1}^{n_i}\frac{\partial\{\phi\}_r^0}{\partial m_{ij}}\Delta m_{ij} + \sum_{i=1}^{n_i}\sum_{j=1}^{n_i}\frac{\partial\{\phi\}_r^0}{\partial k_{ij}}\Delta k_{ij} \qquad (8.7)$$

where r is the mode subscript and n_i is the total number of interface coordinates in the joint identification problem. A similar equation can be written for the eigenvalues, as follows:

$$\lambda_r = \lambda_r^0 + \sum_{i=1}^{n_i}\sum_{j=1}^{n_i}\frac{\partial\lambda_r^0}{\partial m_{ij}}\Delta m_{ij} + \sum_{i=1}^{n_i}\sum_{j=1}^{n_i}\frac{\partial\lambda_r^0}{\partial k_{ij}}\Delta k_{ij} \qquad (8.8)$$

For equations (8.7) and (8.8) to be correct it is necessary that $\|\Delta K\|/\|K\|$ and $\|\Delta M\|/\|M\|$ should not be greater than a certain limit, otherwise the first order approximation of the Taylor series in (8.7) and (8.8) will not be met and convergence will not be achieved [28]. The matter of convergence of these equations will be further discussed later in this chapter.

Considering the limits of the summations in equations (8.7) and (8.8), it is seen that there are n_i^2 terms in each summation but, as mentioned before, considering the symmetry of [AK] and [AM] (which is a necessary assumption to preserve the self-adjoint of the structure), the number of terms in each summation reduces to $n_i(n_i+1)/2$. Using equations (8.7) and (8.8), and noting that in writing n_i the suffix "i" has been ignored, one can write:

$$\begin{Bmatrix} \{\phi\}_1 - \{\phi\}_1^0 \\ \{\phi\}_2 - \{\phi\}_2^0 \\ \vdots \\ (\lambda_1 - \lambda_1^0) \\ (\lambda_2 - \lambda_1^0) \\ \vdots \end{Bmatrix}_{m(L+1)x1} \cong$$

$$\begin{bmatrix} \{\frac{\partial\{\phi\}_1^0}{\partial k_{11}}\} \cdots \{\frac{\partial\{\phi\}_1^0}{\partial k_{nn}}\} & \{\frac{\partial\{\phi\}_1^0}{\partial m_{11}}\} \cdots \{\frac{\partial\{\phi\}_1^0}{\partial m_{nn}}\} \\ \{\frac{\partial\{\phi\}_m^0}{\partial k_{11}}\} \cdots \{\frac{\partial\{\phi\}_m^0}{\partial k_{nn}}\} & \{\frac{\partial\{\phi\}_m^0}{\partial m_{11}}\} \cdots \{\frac{\partial\{\phi\}_m^0}{\partial m_{nn}}\} \\ \frac{\partial\lambda_1^0}{\partial k_{11}} \cdots \frac{\partial\lambda_1^0}{\partial k_{nn}} & \frac{\partial\lambda_1^0}{\partial m_{11}} \cdots \frac{\partial\lambda_1^0}{\partial m_{nn}} \\ \frac{\partial\lambda_m^0}{\partial k_{11}} \cdots \frac{\partial\lambda_m^0}{\partial k_{nn}} & \frac{\partial\lambda_m^0}{\partial m_{11}} \cdots \frac{\partial\lambda_m^0}{\partial m_{nn}} \end{bmatrix}_{m(L+1)xn(n+1)} \cdot \begin{Bmatrix} Akll \\ Ak12 \\ \vdots \\ \Delta k_{nn} \\ Am11 \\ Am12 \\ \vdots \\ \Delta m_{nn} \end{Bmatrix}$$

or $\{\Delta E\} \simeq [S]\{\Delta p\}$ (8.9)

Where [S] is the so-called "modal sensitivity" matrix of the A-C model and m and L are the number of modes involved in the calculations and the number of coordinates which are considered in the calculation of differences in eigenvectors of each mode at the left hand side of (8.9), respectively. For example, for the joint identification case, it is possible that the vector on the l.h.s of equation (8.9) contains only the differences of modal vector elements related to slave coordinates and the differences vector on the r.h.s is due only to changes of mass and stiffness at the interface coordinates, i.e. changes in the slave coordinates modal parameters due to the joint at the interface coordinates. Equation. (8.9) is a set of algebraic equations which, depending on the values of L,m, and n, could be over- or under - determined. To be able to solve equation (8.9) one requires that:

$m(L+1) \geq n_i (n_i + 1)$

if L = n_i, i.e.the number of slave coordinates = the number of interface coordinates, then

$m \geq n_i$ (8.10)

For a small number of joints, satisfying (8.10) does not cause any problem but for a large number of joints, not only it is difficult to satisfy (8.10), but $n_i(n_i+1)$ will be a large value and the computation time will be considerable. To avoid this problem, one can assume a prescribed model for the joint (as explained in (8.3) and (8.4)) and thereby reduce the number of the correction factors to be determined.

Now, by choosing the correct number of coordinates and modes, one can solve (8.9) to find the differences in stiffness and mass which are responsible for the discrepancies in the modal models of the two systems which are believed to be due to joints. Apart from comparison between two cases of one structure to identify the joint characteristics, the method and concept can also be used for structural modification purposes i.e. to define the desired changes for the eigenvalues(s) and / or eigenvectors(s) and then, by solving (8.10), to find the necessary modifications to the structure.

It only remains to calculate the elements of matrix [S]. This can be done by taking partial derivatives of the following equations:

$[K - M \lambda_r] \{ \phi_r \} = 0$ (8.11)

$$\{ \phi_r \}^t [M] \{ \phi_r \} = 1$$

which leads to [24,43]:

$$\frac{\partial \lambda_r}{\partial \rho} = \{ \phi_r \}^t \left(\frac{\partial K}{\partial \rho} - \lambda_r \frac{\partial M}{\partial \rho} \right) \{ \phi_r \} \qquad (8.12)$$

and

$$\frac{\partial \{\phi_r\}}{\partial \rho} = \sum_{k=1}^{p} \zeta_{rk} \{\phi_k\} \qquad (8.13)$$

Where

$$\zeta_{rk} = \frac{\{ \phi_k \}^t \left(\frac{\partial K}{\partial \rho} - \lambda_r \frac{\partial M}{\partial \rho} \right) \{ \phi_r \}}{\lambda_r - \lambda_k} \qquad \text{for } r \neq k \qquad (8.14)$$

$$= -1/2 \left(\{ \phi_r \}^t \frac{\partial M}{\partial \rho} \{ \phi_r \} \right) \qquad r = k$$

The derivatives $\frac{\partial M}{\partial \rho}$ and $\frac{\partial K}{\partial \rho}$ can be easily determined using equations (8.5) and (8.6).

8.2.2 COMPENSATING FOR THE EFFECTS OF THE RIGID BODY & HIGHER MODES

In the experimental case, when only a few of the lower modes are identified and identification of rigid body modes is not easy, no problem arises in dealing with (8.12) but calculating expressions (8.13) and (8.14) will not be very accurate as they require the calculation of all eigenvalues and eigenvectors. Since $(\lambda_r - \lambda_k)$ appears in the denominator of (8.14), so for the first few modes where $\lambda_r << \lambda_m$ (where λ_m is the biggest measured eigenvalues) the omission of the higher modes in calculating (8.14) does not cause any problem but as r approaches m, the effects of these modes may become significant. The same is true for the effect of rigid body modes on the higher modes' sensitivity calculations, i.e., the higher λ_r is, the less significant the effects of the rigid body modes on the calculation become, but for lower modes, the effects of rigid body modes are significant

Compensating for the effect of the higher modes has been discussed for the FE updating problem in [43] and here the method will be modified for experimental applications and will also be extended for compensating for the effect of rigid body modes, as follows:

Consider equation (8.13) as:

$$\frac{\partial\{\phi_r\}}{\partial\rho} = \zeta_{rr}\{\phi_r\} + \{Z_r\} \tag{8.15}$$

where

$$\{Z_r\} = \sum_{j=1}^{n} \frac{\{\phi_j\}^t\{F_r\}}{\lambda_r - \lambda_j}\{\phi_j\}$$

or

$$\{Z_r\} \sum_{j=1}^{q} \frac{\{\phi_j\}^t\{F_r\}}{\lambda_r - \lambda_j}\{\phi_i\} \sum_{j=q+1}^{m} \frac{\{\phi_j\}^t\{F_r\}}{\lambda_r - \lambda_j}\{\phi_i\}$$

$$\sum_{j=m+1}^{n} \frac{\{\phi_j\}^t\{F_r\}}{\lambda_r - \lambda_j}\{\phi_j\} \tag{8.16}$$

where q is the number of rigid body modes or, more generally, the number of lower modes which have not been measured, and

$$\{F_r\} = \left(\frac{\partial K}{\partial\rho} - \lambda_r\frac{\partial M}{\partial\rho}\right)\{\phi_r\} \tag{8.17}$$

and $q < r \leq m$. If one assumes that $\lambda_q << \lambda_m << \lambda_{m+1}$ (which means assuming a large frequency gap between the measured and unmeasured modes, which is not always true) then for $j > m$ and $j \leq q$ one can write :

$$\begin{aligned} \lambda_r - \lambda_j &= -\lambda_j \qquad j > m \\ \lambda_r - \lambda_j &= \lambda_r \qquad j \leq q \end{aligned} \tag{8.18}$$

Substitution of (8.18) into (8.16) gives :

$$\{Z_r\} = \sum_{j=1}^{q} \frac{\{\phi_j\}^t\{F_r\}}{\lambda_r}\{\phi_j\} + \sum_{j=q+1}^{m} \frac{\{\phi_j\}^t\{F_r\}}{\lambda_r - \lambda_j}\{\phi_j\} + \sum_{j=m+1}^{p} \frac{\{\phi_j\}^t\{F_r\}}{-\lambda_j}\{\phi_j\} \quad \textbf{(8.19)}$$

Considering the nature of (F,) from (8.17),the first and third summations in (8.19) can be written as:

$$\sum_{j=1}^{q} \frac{\{\phi_j\}\{\phi_j\}^t}{\lambda_r})\{F_r\}$$

and

$$\sum_{j=m+1}^{p} \frac{\{\phi_i\}\{\phi_j\}^t}{-\lambda_j})\{F_r\} \quad (8.20)$$

Using equation (8.20), equation (8.19) can be rewritten as:

$$\{Z_r\} = \sum_{j=1}^{q} \frac{\{\phi_i\}\{\phi_i\}^t}{\lambda_r}\{F_r\} + \sum_{j=q+1}^{m} \frac{\{\phi_i\}^t\{F_r\}}{\lambda_r - \lambda_j}\{\phi_j\} +$$

$$\sum_{j=1}^{p} \frac{\{\phi_i\}\{\phi_j\}^t}{-\lambda})\{F_r\} - \sum_{j=1}^{m} \frac{\{\phi_j\}\{\phi_i\}^t}{-\lambda_j})\{F_r\} \quad (8.21)$$

or

$$\{Z_r\} = \sum_{j=1}^{q} \frac{\{\phi_i\}\{\phi_i\}^t}{\lambda_r}\{F_r\} + \sum_{j=q+1}^{m} \frac{\{\phi_j\}^t\{F_r\}}{\lambda_r - \lambda_j}\{\phi_j\} -$$

$$[K]^{-1}\{F_r\} - \sum_{j=1}^{m} \frac{\{\phi_j\}\{\phi_i\}^t}{-\lambda_j})\{F_r\} \quad (8.22)$$

Thus, in order to be able to compensate for the effect of the higher modes, it is necessary to have the flexibility matrix of the structure. Note that most eigen-solution routines use $[K]^{-1}$ so this matrix has already been calculated and does not consume any extra time. Since, when using only experimental data, the stiffness matrix is not available in a practical joint identification, the compensation technique described above needs to be

modified. Also, a method should be developed to compensate for the effect of rigid body modes in the first summation.

Following equation (8.20), and taking the modal expansion of the FRF matrix as :

$$[H] = \sum_{j=1}^{q} \frac{\{\phi_j\}\{\phi_j\}^t}{\lambda_j - \omega^2} + \sum_{j=q+1}^{m} \frac{\{\phi_j\}\{\phi_j\}^t}{\lambda_j - \omega^2} + \sum_{j=m+1}^{p} \frac{\{\phi_j\}\{\phi_j\}^t}{\lambda_j - \omega^2} \tag{8.23}$$

and considering $\lambda_q << \lambda_m << \lambda_{m+1}$, one has :

$$[H] = \sum_{j=1}^{q} \frac{\{\phi_j\}\{\phi_j\}^t}{-\omega^2} + \sum_{j=q+1}^{m} \frac{\{\phi_j\}\{\phi_j\}^t}{\lambda_j - \omega^2} + \sum_{j=m+1}^{p} \frac{\{\phi_j\}\{\phi_j\}^t}{\lambda_j} =$$

$$[R_M](-1/\omega^2) + \Sigma + [R_k] \tag{8.24}$$

where $[R_M]$ and $[R_k]$ are the so-called "residual matrices" which can be determined directly from the measured FRFs. Note that $[R_M]$ approximates the effect of rigid body modes (lower modes) by an inertia term while $[R_k]$ approximates the effect of the higher modes with a static deformation. Comparing equations (8.20) and (8.24) and using (8.19) one obtains:

$$\{Z_i\} = \sum_{j=q+1}^{m} \frac{\{\phi_j\}^t\{F_r\}}{\lambda_r - \lambda_j}\{\phi_j\} - [R_k]\{F_r\} + \frac{[R_M]}{\lambda_r}\{F_r\} \tag{8.25}$$

Equation (8.25) is a modified version of (8.19) and is suitable for experimental applications.

It should be noted that, in order to determine the [R] matrices in (8.25), it is not necessary to have the full FRF matrix of the A-C model. For example, assume that the variable ρ in equation (8.15) is k_{ij}. This means that $\frac{\partial K}{\partial k_{ij}}$ consists of a unit element in position ij and zero everywhere else. Calculating F_h in equation (8.17) yields:

$$\{F_h\} = \begin{Bmatrix} 0 \\ 0 \\ 0 \\ . \\ . \\ {}_h\phi_j \\ 0 \\ 0 \\ 0 \\ 0 \end{Bmatrix}$$

and calculating [R] F_h **gives:**

$$[R]\{F_h\} = \begin{Bmatrix} R_{1i} \\ R_{2i} \\ R_{3i} \\ \\ \\ \\ . \\ \\ R_{Li} \end{Bmatrix} {}_h\phi_j$$

As before, L is the number of coordinates used in the l.h.s of (8.9) (the slave coordinates). So, the number of elements of [R] which should be determined depends on the number of interface (modification) and slave coordinates.

If the stiffness matrix of the analytical model is singular in model updating, then, according to equation **(8.22),** the effect of the higher neglected modes cannot be compensated for. On the other hand, equation (8.25) is always applicable for the higher modes' contribution to the calculation and, thus, can be used in model updating applications with a singular **[K].**

8.2.3 FORMULATION OF THE METHOD FOR DAMPED SYSTEMS:

The extension of equation (8.9) to the case of a damped assembled structure will be discussed in this section. The structural damping mechanism will be considered for the damping model.

To extend the ideas in equations (8.5) and (8.6) to damped systems, equation (8.1) can be written as:

$$[M] = [M]_0 + [\Delta M] \quad \text{and} \quad [K] = [K_0 + [\Delta K] \quad [D = [D], + [AD] \tag{8.26}$$

and similarly for equation (8.5)

$$\frac{\partial M}{\partial m_{ij}} = [I_1] \qquad \frac{\partial K}{\partial k_{ij}} = [I_1] \qquad \frac{\partial D}{\partial d_{ij}} = [I_1] \tag{8.27}$$

where in equation (8.26) [D] represents the damping matrix. On the other hand, if a joint model is used to define $[\Delta M]_d$ and [AK],, as in equations (8.3) and (8.4), then $[\Delta D]_d$ can be defined as:

$$[\Delta D]_d = \sum_{i=1}^{g} \beta_i [\Delta K]_{di} \tag{8.28}$$

where "g" in equation (8.28) is designated as the number of sub-matrices which the stiffness matrix of interfacing station d has been decomposed to. For example, the stiffness matrix of a beam element type joint model in equation (8.3) has been decomposed into 3 submatrices, i.e. g=3 (also see section 4.4.3)

Using equations (8.3) and (8.28) for a beam element type joint model, one obtains:

$$[\Delta D]_i = \beta_1 \begin{bmatrix} [0] & [0] \\ [0] & \begin{bmatrix} a_1 & 0 & -a_1 & 0 \\ 0 & 0 & 0 & \\ & & a_1 & 0 \\ & & & 0 \end{bmatrix} \end{bmatrix} + \beta_2 \begin{bmatrix} [0] & [0] \\ [0] & \begin{bmatrix} 0 & a_2 & 0 & a_2 \\ 0 & -a_2 & 0 & \\ & 0 & -a_2 & \\ & & 0 & \end{bmatrix} \end{bmatrix} +$$

$$\beta_3 \begin{bmatrix} [0] & [0] \\ [0] & \begin{bmatrix} 0 & 0 & 0 & 0 \\ 2a_3 & 0 & a_3 & \\ & 0 & 0 & \\ & & 2a_3 & \end{bmatrix} \end{bmatrix} \tag{8.29}$$

There are two important points related to equation (8.28) as follows:

(a) - as equation (8.29) demonstrates, using the damping model in equation (8.28) does not imply that proportional damping has been considered for the joint; and

To extend the ideas in equations (8.5) and (8.6) to damped systems, equation (8.1) can be written as:

$$[M] = [M]_0 + [\Delta M] \quad \text{and} \quad [K] = [K]_0 + [\Delta K] \quad [D] = [D], + [AD] \tag{8.26}$$

and similarly for equation (8.5)

$$\frac{\partial M}{\partial m_{ij}} = [I_1] \qquad \frac{\partial K}{\partial k_{ij}} = [I_1] \qquad \frac{\partial D}{\partial d_{ij}} = [I_1] \tag{8.27}$$

where in equation (8.26) [D] represents the damping matrix. On the other hand, if a joint model is used to define $[\Delta M]_d$ and [AK],, as in equations (8.3) and (8.4), then $[\Delta D]_d$ can be defined as:

$$[\Delta D]_d = \sum_{i=1}^{g} \beta_i [\Delta K]_{di} \tag{8.28}$$

where "g" in equation (8.28) is designated as the number of sub-matrices which the stiffness matrix of interfacing station d has been decomposed to. For example, the stiffness matrix of a beam element type joint model in equation (8.3) has been decomposed into 3 submatrices, i.e. g=3 (also see section 4.4.3)

Using equations (8.3) and (8.28) for a beam element type joint model, one obtains:

$$[\Delta D]_i = \beta_1 \begin{bmatrix} [0] & [0] \\ [0] & \begin{bmatrix} a_1 & 0 & -a_1 & 0 \\ 0 & 0 & 0 & \\ & a_1 & 0 & \\ & & 0 & \end{bmatrix} \end{bmatrix} + \beta_2 \begin{bmatrix} [0] & [0] \\ [0] & \begin{bmatrix} 0 & a_2 & 0 & a_2 \\ 0 & -a_2 & 0 & \\ & 0 & -a_2 & \\ & & 0 & \end{bmatrix} \end{bmatrix} +$$

$$\beta_3 \begin{bmatrix} [0] & [0] \\ [0] & \begin{bmatrix} 0 & 0 & 0 & 0 \\ 2a_3 & 0 & a_3 & \\ & 0 & 0 & \\ & & 2a_3 & \end{bmatrix} \end{bmatrix} \tag{8.29}$$

There are two important points related to equation (8.28) as follows:

(a) - as equation (8.29) demonstrates, using the damping model in equation (8.28) does not imply that proportional damping has been considered for the joint; and

(b) - introducing damping to the analysis makes the sensitivity matrix [S] in equation (8.9) a complex matrix. However, using a damping model either in equation (8.27) or in equation (8.28), no extra effort is required to calculate the complex part of [S], i.e. the complex parts of elements like s_{ij} related to mass modifications are zero and those related to (complex) stiffness modification elements are exactly equal to their real part, or

$$[S] = [[S]_k , [S]_m] + i\,[[S]_k , [0]] \qquad (8.30)$$

The same remarks as were made for the undamped case also apply here when one is dealing with truncated higher modes.

8.2.4 CONCLUDING REMARKS:

(a) - A modified version of the sensitivity matrix analysis method has been developed which can be applied to purely experimental data. This not only seems to be very useful for identification of a joint's dynamic characteristics, but also seems promising for general experimental structural modification purposes.

(b) - Since the method is based on experimental data only, it does not need the development of an FE model and the dimension of the sensitivity matrix can be kept quite low as compared with the FE updating case. This is particularly true in structural modification applications where only localized modifications are required.

(c) - Compared with FRF-based identification methods, this method requires a very small amount of data storage.

(d) - The formulation has been modified so that the effects of neglected higher and lower modes could be accounted for. This, as will be shown in the case studies, will enable the analyst to use a selected number of modes.

8.3 CASE STUDIES

8.3.1 TEST STRUCTURES & JOINT MODELS

To study the performance of the IEM and its sensitivity to error, a number of case studies have been undertaken. The model X which simulates the real structure in all case studies, Fig. 8.1.(a), consists of two substructures coupled through a joint. Model A-C, or the "analytical" model, is generated using substructures similar to those of structure X plus a trial joint model, Fig. 8.1.(b). The FE models of the substructures are developed using a base element identical to that shown in Fig. 3.2.

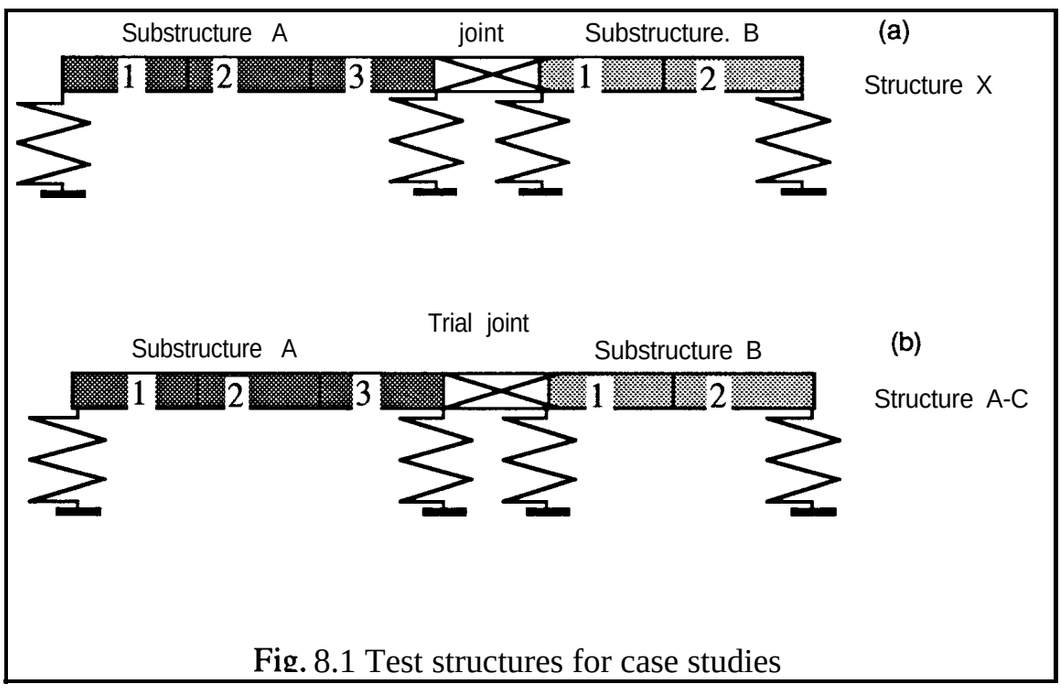

Fig. 8.1 Test structures for case studies

The substructures in Fig. 8.1 are represented by FE models of two beams with 3 and 2 elements so that the structure X and model A-C each have 14 degrees of freedom. In order to simulate a real test case from the rigid-body modes point of view, the substructures are supported on two soft springs. Note that in all case studies the rotational degrees of freedom related to the slave coordinates have been eliminated and, thus, $\{\Delta\phi\}$ in equation (8.9) includes only the differences between translational slave coordinates of the structure X and those of the model A-C. Considering the total number of degrees of freedom for each structure and the number of interface coordinates (which is 4), the number of translational slave coordinates will be 5, i.e. $\{\Delta\phi\}$ contains 5 elements for each mode.

The joint element of structure X has the following properties:

$$L_{jx} = 100\%\ Le\ ,\ E_{jx} = 1000\%\ Ee\ ,\ \rho_{jx} = 10\%\ \rho_e \qquad (8.31)$$

Thus, the joint element is 10 times stiffer and 10 times lighter than the base element (shown in Fig.3.2).

The specification in equation (8.3 1) yields the following mass and stiffness matrices for real joint model:

$$[M]_{jx} = \begin{bmatrix} .05 & .0021 & .01746 & -.00126 \\ & .00011 & .00126 & -.000087 \\ & & .05 & -.0021 \\ & & & .00011 \end{bmatrix}$$

$$[K]_{jx} = \begin{bmatrix} 6440000 & 966000 & -6440000 & 966000 \\ & 193200 & -966000 & 96600 \\ & & 6440000 & -966000 \\ & & & 193200 \end{bmatrix} \qquad (8.32)$$

All case studies are based on the application of a beam element model for the trial (and reference) joint and calculation of six modification factors, α_1 to α_6 in equations (8.3) and (8.4) and thereby updating the trial joint model.

8.3.2 COMPUTATIONAL ASPECTS OF SENSITIVITY ANALYSIS

Two points should be considered and dealt with during the sensitivity analysis calculations as follows:

(a) - modal vector scaling; and

(b) - balancing of the sensitivity matrix

These will now be examined.

(a)-Modal vectors scaling:

As has been discussed in section 8.2, the modal vectors used in the sensitivity analysis should be mass-normalized, i.e. they should satisfy the following relation:

$$\{\phi_r\}^t[M]\{\phi_r\} = 1 \qquad (8.33)$$

Depending on the particular eigen-solver used and the normalizing factor it uses during the solution of the eigenvalue problem, some of the eigenvectors may be determined with a 180^0 phase shift relative to their experimental counterpart. This does not violate relation (8.33) but affects both the sensitivity matrix and {AE} in equation (8.9). This effect on the sensitivity matrix is restricted to the eigenvector-related elements and the rows of the sensitivity matrix related to the phase-shifted modes will be multiplied by (-1). In cases where a truncated modal model is used in the calculation, residual terms representing the lower and higher modes in equation (8.25) will be affected in the same way, i.e., will be multiplied by (-1).

This error in the phase of some of the eigen-vectors, which alters the nature of equation (8.9), may lead to divergence in the calculations and should be identified and dealt with.

One other similar problem is the detection of related modes of the two models X and A-C. Sometimes, due to the complicated nature of the joint and significant differences between joint stiffness in different directions, it is difficult to pair the modes of the real structure with their counterpart in the analytical model, in which the complexity of joint is not properly considered. For example, it is quite possible that the first mode of the real structure is a torsional mode while that of the analytical model is a bending one. So, in order to be able to calculate the difference vector on the l.h.s of equation (8.9) correctly, it is essential that a form of correlation assessment must be used to pair the relevent modes of the real structure and the analytical model. The correlation assessment can be performed using MAC and/or COMAC values [44,45].

(b)-Balancing of the sensitivity matrix:

Table 8.1 shows some typical elements of the sensitivity matrix before any balancing. As is evident from this table, the sensitivity matrix contains elements with very different orders of magnitude and this can make the matrix ill-conditioned.

	trans.stiffness related	rotary stiffness related	translational mass related	rotary inertia related
a $\phi/\partial\rho$	4.5e- 11	-1.89e-8	.0558	-.354
$\partial\lambda/\partial\rho$	3.25e-6	.0025	-5043	-23457

Table 8.1 Typical elements of sensitivity matrix for lower modes

It is clear from Table 8.1 that the order of $s_m^{\lambda *}$ elements of [S] is much higher than the others. Examining equations (8.12) and (8.14), the reason for the large order of magnitude difference becomes clear, i.e. the multiplication of s_m^{λ} elements by λ in equation (8.12) and dividing s_m^{ϕ} and s_k^{ϕ} elements by λ in equation (8.14).
So, an unbalanced sensitivity matrix will look like:

$$\begin{Bmatrix} \{\Delta\phi\}_{mx1} \\ \{\Delta\lambda\}_m \end{Bmatrix} = \begin{bmatrix} [O(1e\text{-}10)]_{11} & [O(1)]_{12} \\ [O(1e\text{-}5)]_{21} & [O(1e4)]_{22} \end{bmatrix} \begin{Bmatrix} \{\Delta K\}_{nx1} \\ \{\Delta M\}_{1px1} \end{Bmatrix} \qquad (8.34)$$

Since equation (8.9) represents an over-determined set of equations, using a least-squares method for solving it, one has:

$$[S]^T[S] = \{S_1^{\phi}\}\{S_1^{\phi}\}^T + \ldots\ldots\ldots\ldots\ldots + \{S_1^{\lambda}\}\{S_1^{\lambda}\}^T + \ldots\ldots\ldots \qquad (8.35)$$
$$= \sum_{i=1}^{mxl} \{S_i^{\phi}\}\{S_i^{\phi}\}^T + \sum_{j=1}^{m} \{S_j^{\lambda}\}\{S_j^{\lambda}\}^T$$

where $\{S_i^{\phi}\}^T$ and $\{S_j^{\lambda}\}^T$ are the i^{th} and j^{th} rows of the sensitivity matrix related to the eigenvectors and eigenvalues, respectively. From equation (8.35) it is clear that $[S]^T[S]$ is dominated by the second summation and so is its rank. On the other hand, the rank of the second summation itself depends on the number of mass modification parameters, i.e. the rank of submatrix 22 in (8.34), and, thus, $[S]^T[S]$ is rank-deficient. So, it is not possible to obtain a full-rank sensitivity matrix without any balancing.

Using a reference joint model to define parameters a_i in equations (8.3) and (8.4) will automatically balance the order of the mass- and stiffness-related elements of the sensitivity matrix, [S], as explained in section 4.4.3. Also, in order to balance the relative order of the eigenvalue- and eigenvector-related elements, each row of the sensitivity matrix related to j^{th} eigenvalue should be divided by λ_j.

8.3.3 PERFORMANCE OF THE METHOD

Performance of the method for either complete or truncated modal models can be broadly categorized into the two following aspects:

(a) - performance with just a stiffness error;

---

* s_m^{λ} = element of sensitivity matrix representing $\partial\lambda/\partial\alpha_m$

(b) - performance with both mass and stiffness errors.

The reason for this classification is that with just a stiffness error introduced the identification calculation converges very rapidly and this is true even for large errors. On the other hand, when a mass error is involved in the calculations as well, convergence is poor and is restricted to relatively smaller error magnitudes. The following table, 8.2, better reveals this situation:

error %	$\|\Delta\phi\|_0$	$\|\Delta\lambda\|_0$	$\|\Delta\phi\|_R$	$\|\Delta\lambda\|_R$	convergence	κ
90% $[K]_j$& 0% $[M]_j$	.582	4.07E6	.006	33870	converges after 3 iterations	1E3
90% $[K]_j$ & 10% $[M]_j$	5523	3.92E6	.17	1.39E6	$[M]_j$ not P.D. 3rd iteration	1E5

Table 8.2. Results of calculation for with and without mass cases, modes 3-9 involved in calculations

As is evident from Table 8.2, there is no significant difference between $\|\Delta\lambda\|_0$ and $\|\Delta\phi\|_0$ for the two cases and the condition numbers are reasonable. It should be noted that for the case where mass error was involved modification factors were scaled after each iteration in order to prevent the mass matrix from becoming non-positive-definite.

Table 8.2 suggests that a two stage calculation process is potentially useful, i.e.

(i) - keep the mass error constant and iterate with m=constant for k and then, when the stiffness error is small enough;

(ii) - include m in the calculation and iterate until the desired results are achieved.

This method has been successfully applied to the second case in Table 8.2, i.e. 90% stiffness and 10% mass error, and results are shown in Figs. 8.2 and 8.3.

It is evident from Figs. 8.2 and 8.3 that the stiffness error has been reduced to less than 2% after 2 iterations and there is no significant change in the modal parameters' differences after the third iteration, using only stiffness in calculations. Once mass is included in the calculation and the stiffness error is small, the calculation converges to the correct values of m and k in one more iteration

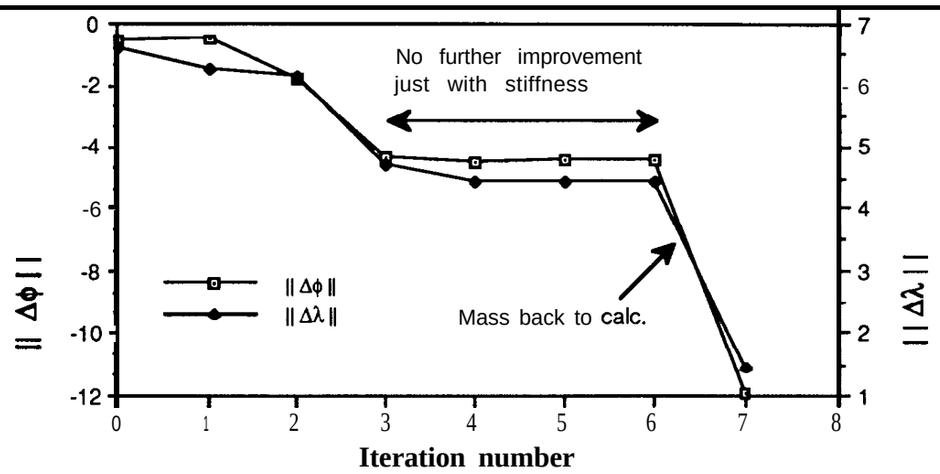

Fig. 8.2 Variation of norm of the eigen-parameters with iteration

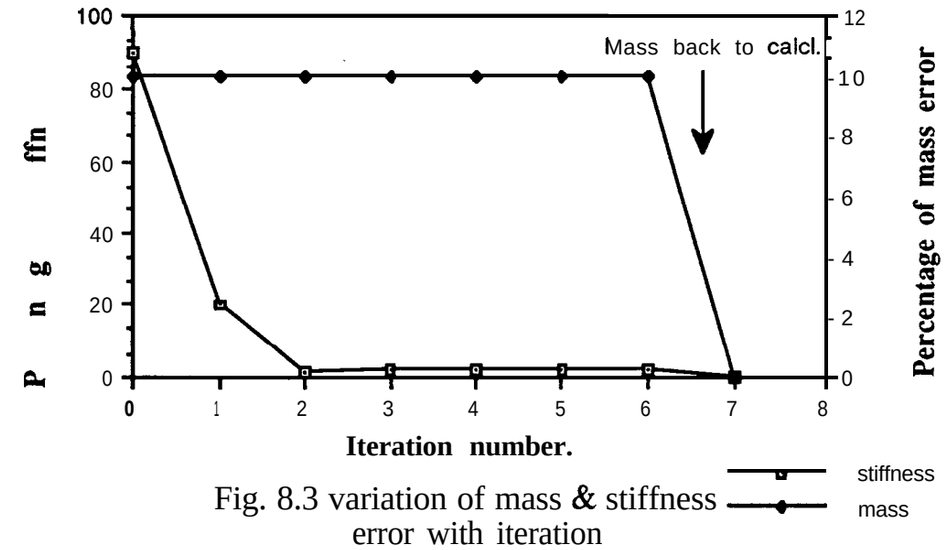

Fig. 8.3 variation of mass & stiffness error with iteration

It is worth mentioning here that for model updating applications, the IEM method converges to a solution even for large values of error in the both mass and stiffness matrices of analytical model. The reason for the deficiency in the joint identification case lies in the fact that each correction factor of an elemental mass or stiffness matrix in the updating case is divided into three modification factors for joint identification applications, as shown in equations (8.3) and (8.4). Decomposing the mass and stiffness matrices of an element (which is representing the joint) to submatrices and assigning a separate modification factor to each submatrix is inevitable in joint identification applications, (see chapter 3), and will have the following effects on the calculations:

(a) - an increase in the number of unknowns which affects condition of the calculations; and

(b) - an effect of some of the submatrices on the calculations which is so insignificant as to make the calculations diverge.

8.3.4 PERFORMANCE OF THE IEM METHOD WITH TRUNCATED MODAL MODEL

As mentioned before, the main objective of the present chapter is to study the applicability of the sensitivity-based joint identification method using experimental data. Since, when using experimental data, only a limited number of modes are available, study of the performance of the method with a truncated modal model comprises the major part of present chapter.

8.3.4.1 GENERAL CONSIDERATIONS

Consider a symmetric and positive-definite n-degree-of-freedom system. Writing the sensitivity equation (8.9) for this system, using the complete coordinate set and the modal model, one will obtain a unique set of solutions for the mass and stiffness corrections provided that the first order approximation is valid. In such a case, for each spatial parameter on the r.h.s of equation (8.9), one has:

$$\Delta k_i = a_{i1}\Delta\phi_{11} + a_{i2}\Delta\phi_{12} + \ldots\ldots\ldots + b_{i1}\Delta\lambda_1 + \ldots\ldots\ldots * \ldots\ldots b_{in}\,\mathrm{A\,h}, \tag{8.36}$$

where a_{ij} and b_{ij} are elements of the inverse of the sensitivity matrix. If some of the coordinates and/or modes are not present in the analysis, the related terms in equation (8.36) will be eliminated. This means that Δk_i will be under- or over-estimated. The magnitude of this mis-determination depends on the coordinates and/or modes which are eliminated.

It is clear that variations of each of the spatial parameters of the structure will affect some of the modes more than others. For example, if a beam is modified with a mass modification, Am, near to its mid-span, this modification will affect odd modes more than even ones and, of course, higher modes will be more affected. Now, if one neglects odd modes when calculating Am, its value cannot be correctly determined.

From the above discussion, it is concluded that in truncating the modal model one should try to include as many significant modes as possible (i.e. those modes significantly affected by the presence of the joint) in the calculation.

The question here is that "how can the significant modes be identified?". The answer to this question has been given in section 4.5.1, where the sensitivity of the modal parameters of a matrix to small perturbations has been discussed. Rewriting the equations derived in that section, one obtains:

$$|\Delta\lambda_r| \leq \frac{\|\{{}_l\phi\}_r^T\| \, \|[\Delta A]\| \, \|\{\phi\}_r\|}{|\{{}_l\phi\}_r^T\{\phi\}_r|} \tag{8.37}$$

and

$$\{\phi'\}_r - \{\phi\}_r = \sum_{s=1 \; s\neq r}^{N} \frac{\{\phi\}_s \{{}_l\phi\}_s^T [\Delta A]\{\phi\}_s}{\{{}_l\phi\}_s^T\{\phi\}_s(\lambda_r-\lambda_s)} \tag{8.38}$$

As equations (8.37) and (8.38) indicate, quantities $|\{{}_l\phi\}_r^T\{\phi\}_r|$ and $(\lambda_r-\lambda_s)$ can be used to assess the sensitivity of the eigenvalue and eigenvector respectively of mode r. If for mode r, a large $|\Delta\lambda_r|$ and/or $\{\phi'\}_r-\{\phi\}_r$ is associated with large $|\{{}_l\phi\}_r^T\{\phi\}_r|^{-1}$ and/or $(\lambda_r-\lambda_s)^{-1}$, then that mode is not a significant mode but an ill-conditioned* one and should not be considered in calculations.

It should be noted that sometimes using a significant mode as the fiit or last mode of a truncated set of modes make the calculation diverge. This is due to the fact that using a truncated modal model, elements of the sensitivity matrix related to eigenvectors are not calculated accurately and this inaccuracy is more marked for the first and last modes of the truncated set of modes. Now, if this first or last mode is a significant one (in the above-mentioned sense) then the effect of this inaccuracy will be more marked on the calculation. For example, in one of the case studies, reasonable results were obtained using modes 3 to 6 (out of the 12 modes) in the calculations while no convergence was achieved using modes 3 to 8! Examining $\|\Delta\phi\|$ for the two cases reveals that the contribution of modes 3 to 7 to $\|\Delta\phi\|$ is equal to 0.0137 while the contribution of mode 8

* As mentioned in section 4.5.1, Wilkinson proposes to consider $(|\{{}_l\phi\}_r^T(\phi\}_r|)^{-1}$ and $(\lambda_r-\lambda_s)^{-1}$ as condition numbers of modal parameters. This proposition is reasonable as large values for any of these quantities result in large value for $|\Delta\lambda_r|$ and/or $\{\phi'\}_r-\{\phi\}_r$, even when $\|[\Delta A]\|$ is small.

alone is 0.0307. This means that mode 8 is a significant mode and thus has a large effect on the calculations. On the other hand, mode 8 is the last of the truncated set of modes used in the calculations and, thus, it is very likely that the sensitivity elements related to mode 8 are not calculated precisely. In order to investigate the order of precision of the sensitivity matrix elements related to mode 8, typical exact and approximate sensitivity elements related to various modes are plotted in Fig. 8.4

As is evident from Fig. 8.4, exact and approximate sensitivity values show good agreement for all modes except mode 8 and this explains the reason for divergence of the calculations.

To demonstrate the performance of the method using a truncated modal model, a number of case studies have been carried out. The details of the models being used can be found in section 8.3.1.

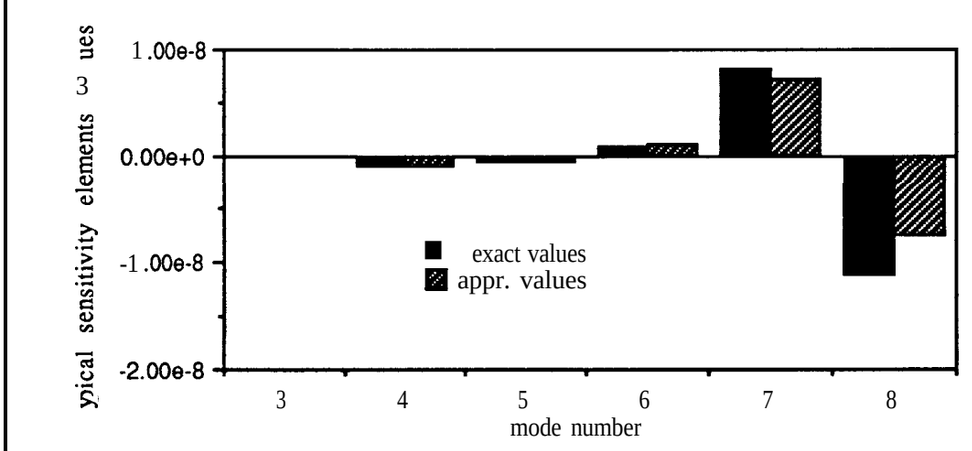

Fig. 8.4 Exact & approximate values of typical sensitivity matrix's elements

CASE STUDY 1

The test structures and joint model for this case study are shown in Fig 8.1. The trial joint model is similar to the real joint model with a 20% error in its mass and stiffness matrices. Two modes, 3 and 4, have been used in the calculations and so the sensitivity matrix is a 12x6 matrix (see 8.3.1). Note that mode 3 is the first elastic mode of the system. Table 8.3 shows the first seven eigenvalues of the real and trial structures.

	λ_1	λ_2	λ_3	λ_4	λ_5	λ_6	λ_7
real str.	531	839	27263	161320	606005	2.31E6	3.56E6
trial str	532	841	27129	161008	605727	2.3E6	3.57E6

Table 8.3 Typical eigenvalues of real and trial structures

To demonstrate the effect of the lower and higher truncated modes, Table 8.4 shows typical elements of the sensitivity matrix where each row shows the sensitivity elements related to a specified spatial parameter. For example, the sensitivity parameters in the first row relate to translational stiffness.

Table 8.4 shows the significant effect of the truncated modes. This effect is particularly marked for rigid body modes.

	Exact value E(S)	- rigid body & higher modes effect	Rigid body modes effect	Higher modes effect	+rigid body & higher modes effect
Transl. stiffness	1.1637E-6	3.792E-7 32% |E(S)|	9.253E-7 79% |E(S)|	1.581E-7 13.6% |E(S)|	1.146E-6 98% |E(S)|
Cross stiffness	-1.543E-5	-4.978E-6 32% |E(S)|	-1.229E-5 79.7% |E(S)|	-2.064E-6 13.4% |E(S)|	-1.52E-5 98.5% |E(S)|
Rotary stiffness	7.665E-5	2.44E-5 31.8% |E(S)|	6.122E-5 79.8% |E(S)|	1.013E-5 13.2% |E(S)|	7.549E-5 98.5% |E(S)|
Transl. mass	20.72	32 154% |E(S)|	-12.9 62.7% |E(S)|	-1.6 7.72% |E(S)|	20.697 99.9 %|E(S)|
Cross mass	3.242	2.23 68.8% |E(S)|	1.05 32.4% |E(S)|	.0775 2.4% |E(S)|	3.203 98.8% |E(S)|
Rotary inertia	-.235	.231 98.3% |E(S)|	-.554 235% |E(S)|	-.0969 41.2% |E(S)|	-.225 95.7% |E(S)|

Table 8.4. Typical elements of sensitivity matrix with and without rigid body and higher modes effect.(without balancing)

The results of the identification calculations are shown in Table 8.5. An important deduction which can be drawn from this and the following case studies is that very reasonable correction values are achieved for stiffness and translational mass in the first run. This implies that stiffness correction values may be reasonably calculated without iteration.

Iter. number	Transl K error %	Cross K error %	Rotary K error %	Transl M error %	Cross M error %	Rotary M error %	$\|\|\Delta\phi\|\|$	$\|\|\Delta\lambda\|\|$
Init. val.	20	20	20	20	20	20	.0032	339
1st run	0.6	1	1.6	5.4	53	534	.002	384
1	0.1	0.1	0.48	0.13	1	7	.0004	36
2	0.006	0.002	.0003	.038	2.3	10	2.6E-5	.216

Table 8.5 Mass and stiffness identification resultscalculations with 2 modes

To demonstrate the effect of increasing the number of modes involved in the calculations on the rate of convergence, Table 8.6 shows the results of this case study but here with modes 3 to 6 used in the calculations.

Iter. number	Transl K error %	Cross K error %	Rotary K error %	Transl M error %	Cross M error %	Rotary M error %	$\|\|\Delta\phi\|\|$	$\|\|\Delta\lambda\|\|$
Init. val.	20	20	20	20	20	20	.00377	3104
1st run	4.3	4.3	4.3	0.7	7	68	.0014	2824
1	0.055	0.066	0.078	0.096	0.26	5.3	4.3E-5	2.83
2	.055	0.066	.076	.0966	0.26	5.6	4.3E-5	2.83

Table 8.6 Mass and stiffness identification results calculations with 4 modes

Considering Tables 8.5 and 8.6 and comparing them with each other reveals the following points:

(a) - increasing the number of modes has no significant effect on the stiffness error reduction in the first run but has a remarkable effect on the mass error reduction, particularly for cross and rotary inertia terms;

(b) - although both Tables 8.5 and 8.6 show that after the first run the errors of stiffness and translational mass have been decreased significantly, the magnitudes of $\|\Delta\phi\|$ and $\|\Delta\lambda\|$ have not been reduced by the same proportion, due to an increase in the cross and rotary inertia errors. The ratio between error values in cross and rotary inertia on the one hand and $\|\Delta\phi\|$ and $\|\Delta\lambda\|$ on the other hand, once again illustrates the fact that cross and rotary inertia of the joint model in fig. 8.1 do not have a significant effect on the structure's response and, as will be shown shortly, their effect can easily be polluted by noise effects. For example, from Table 8.5, it is evident that after the first run, errors in the cross and rotary inertia terms have been increased by 165% and 1600% respectively

but, despite this increase, $\|\Delta\phi\|$ shows no increase and $\|\Delta\lambda\|$ increases only by 10%.

Apart from improving the rate of convergence, increasing the number of modes involved in the calculations allows for the identification of larger error in the joint mass and stiffness matrices. To illustrate this point, case study 1 has been repeated, this time with 6 modes involved in the calculation and 70% error in stiffness and 70% error in mass matrices and for this case the calculation converges after 4 iterations.

Generally speaking, increasing the number of modes involved in the calculations can improve the rate of convergence and allow for larger errors to be considered (although this is not always the case).

CASE STUDY 2

Everything in this case study is similar to case study 1 except that here only stiffness errors will be assumed.

Fig. 8.5 shows the calculation results for 80% error in the stiffness matrix and with two modes, 3 and 4, involved in the calculations.

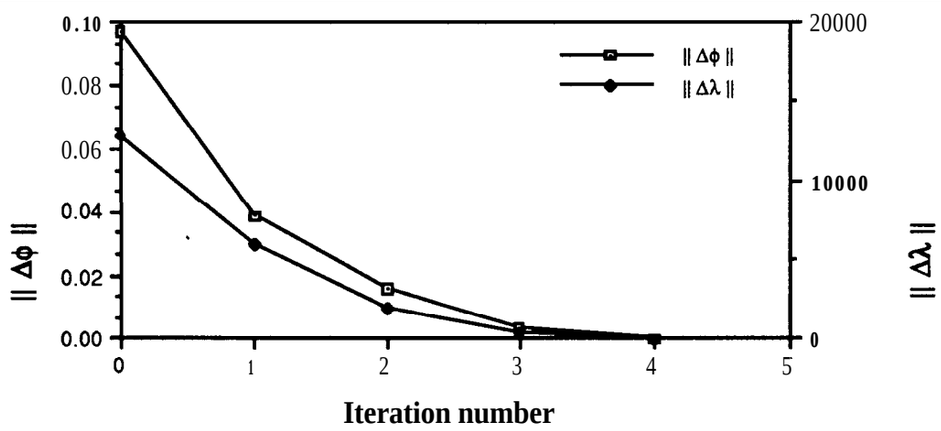

Fig. 8.5 Variation of differences of madal parameters with iteration

As is evident from Fig. 8.5, the calculation converges after 1 or 2 iterations. The same calculations with 50% error for stiffness matrix converge in the first run.

8.4 PERFORMANCE OF THE METHOD USING JUST EIGENVALUES

Sensitivity analysis using just eigenvalues in equation (8.9) seems to be very promising. This is due to the fact that the eigenvalue-related sensitivity elements can be calculated for each mode individually (equation (8.12)) and, thus, using a truncated set of modes does not affect the results. On the other hand, using eigenvalues only, more modes should be measured to prevent equation (8.10) becoming under-determined

Another advantage associated with the eigenvalues is that, at least for a reasonable number of lower modes, they can be measured with high accuracy while this is not the case for the eigenvectors (note that even for the first mode of a structure there could be a significant error in the eigenvector elements for points near to nodes). Although the measured eigenvalues are generally accurate, examination of equation (8.12) reveals that eigenvectors are involved in eigenvalue-related sensitivity element calculation and, thus, inaccurate eigenvectors can affect the accuracy of the sensitivity matrix.

To examine the performance of the method using just eigenvalues, the following case study has been carried out.

CASE STUDY 3

As before, the test structures and joint model for this case study are shown in Fig. 8.1

Table 8.7 shows the results of a case study with 20% error in joint mass and stiffness matrices, using modes 3 to 9 in the calculations. Here, 7 modes have been used for six unknowns (α_1 to α_1 in equations 8.3 and 8.4) which makes the order of the sensitivity matrix 7x6.

Iteration number	Transl K error %	Cross K error %	Rotary K error %	Transl M error %	Cross M error %	Rotary M error %	$\|\|\Delta\lambda\|\|$
Init. Val.	20	20	20	20	20	20	55086
2	7	7	7	6	1.3	94	5

Table 8.7 Mass and stiffness identification results using only eigenvalues, calculation with 7 modes

Table 8.7 indicates that after 2 iterations the stiffness and mass errors, apart from the error in the rotary inertia, have been reduced reasonably but the rotary inertia related error has been increased dramatically and $\|\Delta\lambda\|$ is virtually zero. This means that there is

another structure with slightly different mass and stiffness matrices and exactly the same eigenvalues. Note that for this case, further iteration has no effect on the results and this is the structure to which the calculations converge. The large error in rotary inertia again indicates that eigenvalues of the structure are not sensitive to this parameter.

The same calculation has been repeated using a complete modal model and this converges to the true joint mass and stiffness matrix after only one iteration.

So, generally speaking, the application of eigenvalues only is not recommended for a truncated modal model unless either a reasonably large number of modes are involved to make the calculation converge to the real joint, or an accurate mass matrix is not desired.

8.5 IMPORTANCE OF USING THE CORRECT JOINT MODEL

An important question which should be considered is: " how important is the application of the correct joint model from the connectivity point of view?" In other words, can we use a lumped parameter model for a joint which is FE -based in reality and, if we do so, does the calculation correct this mis-modelling? After carrying out many case studies the answer to this question is "NO". This was not unexpected since using a lumped parameter model for an FE-based model means 100% errors in cross elements of mass and stiffness matrices of the joint and in this case the calculation is very unlikely to converge.

So, when using the sensitivity method for joint identification, one must use engineering judgement about the nature of the joint and then choose the right joint model.

8.6 SENSITIVITY OF IEM TO. MEASUREMENT NOISE

As mentioned in section 6.6, measurement noise can induce typically 1% error in eigenvalues and 10% error in eigenvectors. Sensitivity of the method to measurement noise has been examined by carrying out a series of case studies. The error-adding mechanism adopted here is the same as that shown in equation (6.56), i.e.

$$\lambda_i = \lambda_i \pm (1/i) \times (e_1/100) \times RND \times \lambda_i$$
$$\phi_i = \phi_i \pm (e_2/100) \times RND \times \phi_i \qquad (8.39)$$

where e_1 and e_2 are 1 and 5 respectively, and RND is a random number generator such that 0 <RND< 1. The signs of noise-induced errors in equation (8.39) are also determined by a random function.

CASE STUDY 4

Using the test structures and joint model in Fig. 8.1 and with 20% error in the mass and stiffness matrices of the trial joint, Table 8.8 demonstrates the difference between the modal parameters with and without noise.

Mode No.	1	2	3	4	5	6	7
- Noise	-1.4	-1.6	134	312	278	3000	1200
+ Noise	-3	-1	20	243	309	7100	8600

Table 8.8 Differences of modal parameters with and without noise

8	9	10	11	12	13	14	$\|\|\Delta\phi\|\|$	$\|\|\Delta\lambda\|\|$
19723	51325	115075	1.24E6	189212	6.74E6	1.77E8	.0834	1.78E8
16000	72000	108000	1.2E6	70000	6.7E6	1.76E8	.4	1.8E8

Table 8.8 continued

Case study 1 has been repeated with noise added to the modal model and modes 3 to 9 involved. The results of this case are shown in Table 8.9 .

Iteration number	Transl K error %	Cross K error %	Rotary K error %	Transl M error %	Cross M error %	Rotary M error %	$\|\|\Delta\lambda\|\|,\|\|\Delta\phi\|\|$
Init. Val.	20	20	20	20	20	20	73730,. 1
10	29	33	37	40	203	773	1.5E5, .097

Table 8.9 Mass and stiffness identification results with 7 modes

From Table 8.9, it is evident that the calculation has not converged after 10 iterations and no improvement is achieved with further iteration. As was noticed in case studies in previous sections, the structure's response is insensitive to the joint's rotary and cross inertia variations and this, in turn, will cause the calculations to be sensitive to noise. For example, Table 8.9 illustrates that a small amount of noise added to the structure's modal parameters has resulted in a large amount of error in the identified rotary and cross inertia and this large error will affect the whole calculation.

The above argument suggests that the noise effect may be reduced by ignoring the mass modifications in the calculations altogether.

In what follows, the above idea will be examined.

CASE STUDY 5

Having repeated case study 4 with the mass removed from the calculations, Table 8.10 shows the results for this case.

Iteration number	Transl K error %	Cross K error %	Rotary K error %	Transl M error %	Cross M error %	Rotary M error %	$\|\|\Delta\lambda\|\|,\|\|\Delta\phi\|\|$
Init. Val.	20	20	20	20	20	20	73730,. 1
1	17	18	19	20	20	20	34282, .093

Table 8.10 Stiffness identification results without mass being involved, calculation with 7 modes

As is evident from Table 8.10, ignoring the mass, stiffness errors have been reduced slightly and $\|\Delta\lambda\|$ has been reduced remarkably.

So, when noise is present in the calculation, ignoring mass modification factors in the calculations proves to be useful.

CASE STUDY 6

Case study 3 is repeated here, i.e. using only eigenvalues in the calculations, with noise effect added to modal parameters. The results of this case study are shown in Table 8.11

Iteration number	Transl K error %	Cross K error %	Rotary K error %	Transl M error %	Cross M error %	Rotary M error %	$\|\|\Delta\lambda\|\|$
Init. Val.	20	20	20	20	20	20	73730
2	2	3	3	6.5	2.2	120	30252

Table 8.11 Mass and stiffness identification results with 7 modes

As Table 8.11 indicates, using just eigenvalues in the calculations, a great reduction in mass and stiffness error values have been achieved in just 2 iterations. This shows that identification is more sensitive to noise in eigenvectors than noise in eigenvalues.

Thus, generally speaking, using just eigenvalues in calculations gives better results, (which was expected as explained before), provided enough modes are used to prevent an under-determined set of equations.

8.7 CONCLUSIONS AND REMARKS.

Application of the inverse eigensensitivity method to the joint identification problem has been investigated in this chapter. The method has been modified to be applicable to the pure experimental data case. The following general conclusions can be drawn from the discussions throughout this chapter:

(a) - the method gives good results for the stiffness of the joint almost without any iteration required, but for the mass parameters this is not the case and a number of iterations are necessary to obtain a reasonable result for the mass;

(b) - for the joint model used in the case studies of this chapter, the structure's response turns out to be insensitive to the joint's cross and rotary inertia variations. This insensitivity leads to a large errors in the results when noise is present in the measured data;

(c) - when noise is involved in the data, the method fails to give reasonable results unless one of the following methods is used:

(i)- to ignore mass modifications in the calculation altogether; or

(ii)- to use just eigenvalues in the calculations. This option gives reasonable results Provided sufficient number of modes are available (measured); and

(d) - the major setback of the method for experimental applications is its iterative nature which makes repetitive couplings necessary. If couplings are performed using FRF models of the substructures, then there is a modal analysis necessary after each coupling. On the other hand, if a component mode synthesis technique is used for the coupling analysis, then one is faced with the difficulties in solving the eigenvalue problem as explained in chapter 2. Using FE models of substructures in the coupling analysis problem is not serious and the method can be used efficiently for this case.

CHAPTER 9

FRF-BASED DECOUPLING METHOD

9.1 INTRODUCTION:

Adaptive joint identification techniques were discussed in chapters 5 through 8. As mentioned in chapter 1, and observed in all chapters, an essential feature of any adaptive technique is that it needs an analytical model of the structure and, in most cases, this model must be generated by coupling the constituent substructures of the assembled structure through a trial joint model.

On the other hand, for all other adaptive joint identification techniques except the FRF-based direct identification method discussed in chapter 5, iteration is necessary to achieve the solution (see chapters 6 to 8). Thus, for almost all adaptive techniques, repeated coupling analyses are necessary which not only makes the identification calculations lengthy but also increases error levels in the results.

In the present chapter, an independent family of joint identification techniques called "structural decoupling techniques" by the author will be developed and their performance and sensitivity to measurement noise will be discussed. Since the method studied in this chapter is FRF-based, they exhibit all the advantages associated with FRF-based techniques described in section 5.1. Also, as will be seen, application of this new approach does not require any coupling analysis and, mathematically, is very simple to implement.

9.2 STRUCTURAL DECOUPLING METHODS

The basic idea of these methods is to extend the coupling formulation between two (or more) substructures, considering the joint explicitly as an intermediate substructure and

then solving the inverse problem, i.e, decoupling an assembled structure to its component and, using either experimental or analytical models of substructures, identifying the joint. This extension to the coupling formulation could be applied either to the FRF coupling or Component Mode Synthesis methods and, thus, decoupling methods can be categorized accordingly as follows:

(a) - modal-based decoupling method; and
(b) - FRF-based decoupling method

Investigation of the performance of modal-based decoupling method is the subject of the next chapter and we will concentrate here on the FRF-based decoupling method.

9.3 FRF-BASED DECOUPLING METHOD

As the name implies, this method is based on the use of the FRFs of the substructures and the coupled structure to extract the dynamic properties of the joints. Depending on the application cases and their feasibility, the following categories will be considered:

(a) - two elastic substructures decoupling;
(b) - one elastic substructure and ground decoupling.

It should be noted that the above-mentioned categories can be combined into a single general formulation, i.e, by considering case 2 as a special case of case 1. However, it will be shown later that this kind of general formulation is not suitable for experimental studies and from this aspect it is better to consider these two cases separately.

9.3.1 DECOUPLING OF AN ASSEMBLED STRUCTURE CONSISTING OF TWO ELASTIC SUBSTRUCTURES & JOINT ELEMENT

Consider two substructures A and B and the joint J as shown in Fig.2.1.

It is required to find the dynamic characteristics of joint J using FRFs of A and B and the coupled structure, C. Having Combined A and B to form a dummy structure, D, and recalling from chapter 2 the coupling equation relating FRFs of assembled structure, C, and dummy structure, D, and joint element, J, is :

CASE (1) slave coordinates only involved in $[H]_C$

$$[H]_c = [A] - [B]\,[[J]+[D]]^{-1}\,[C] \tag{9.1}$$

where

$$[A] = \begin{bmatrix} [H]_a^{ss} & [0] \\ [0] & [H]_b^{ss} \end{bmatrix} \qquad [B] = \begin{bmatrix} [H]_a^{si} & [0] \\ [0] & [H]_b^{si} \end{bmatrix} \qquad [C] = \begin{bmatrix} [H]_a^{is} & [0] \\ [0] & [H]_b^{is} \end{bmatrix}$$

$$[D] = \begin{bmatrix} [H]_a^{ii} & [0] \\ [0] & [H]_b^{ii} \end{bmatrix} \qquad [H]_j = [J] \tag{9.2}$$

where $[B]([J]+[D])^{-1}[C]$ is the effect of coupling and joint flexibility on the substructures' slave coordinates, transformed from the interface coordinates by matrices [B] and [C].

CASE (2) complete coordinate set of structure C involved in $[H]_c$

For this case:

$$[H]_c = \left[\bar{H}_d\right]\left[[\bar{H}]_d + [\bar{H}]_j - [\bar{H}]_j\,[\bar{I}]\,[\bar{H}]_d\right]^{-1}[\bar{H}]_j \tag{9.3}$$

or

$$[Z]_c = [\bar{Z}]_j + [\bar{Z}]_d - [\bar{I}]$$

where

$$[\bar{H}]_j = \begin{bmatrix} [I]_{sdxsd} & [0] \\ [0] & [H]_j \end{bmatrix} \qquad [\bar{H}]_d = \begin{bmatrix} [H]_d & [0] \\ [0] & [I]_{sjxsj} \end{bmatrix} \qquad [\bar{I}] = \begin{bmatrix} [I]_{sdxsd} & [0] \\ [0] & [I]_{sjxsj} \end{bmatrix} \tag{9.4}$$

and subscripts sd and sj designate the number of slave coordinates of structures D and J, respectively.

If there are no slave coordinates on structure J, then :

$$[\bar{H}]_d = [H]_d \qquad \text{and} \qquad [\bar{I}] = \begin{bmatrix} [I]_{sdxsd} & [0] \\ [0] & [0] \end{bmatrix} \tag{9.5}$$

For case (1), i.e. slave coordinates only involved in $[H]_c$, the joint FRF can be extracted from equation (9.1) as follows:

$$[J] = [\,[B]^+([A]-[H]_c)[C]^+\,]^{-1} - [D] \tag{9.6}$$

or

$$[\,[I]-([B]^+([A]-[H]_c)[C]^+)[D]\,][Z]_j = [\,[B]^+([A]-[H]_c)[C]^+\,] \tag{9.7}$$

The quantity $[A]-[H]_c$ in equation (9.7) represents the joint effect on slave coordinates and $[B]^+$ & $[C]^+$ transfer this effect to the interface coordinates.

A similar formula to (9.6) can be derived using impedances of the substructures. For this case, the definitions of matrices [A],[B],[C],.....[J] remain essentially as before but with impedances being used instead of receptances. Thus, one has:

$$[Z]_j = [\,[B]^+([A]-[Z]_c)[C]^+\,]^{-1} - [D] \tag{9.8}$$

Either (9.6) or (9.7) represent the essential formula for this method and define the receptance or impedance of the joint, respectively.

For case (2), i.e. all coordinates of C involved in $[H]_c$, the joint parameters are identified from equation (9.3) as:

$$[\bar{H}]_j = \left[\bar{H}_d\right]\left[\,[\bar{H}]_d - [H]_c + [H]_c\,[\bar{I}]\,[\bar{H}]_d\,\right]^{-1}\left[H_c\right] \tag{9.9}$$

or

$$[\bar{Z}]_j = [Z]_c - [\bar{Z}]_d + [\bar{I}] \tag{9.10}$$

Either one of equations (9.9) or (9.10) represent the essential formula for this part of this method.

9.3.1.1 REMARKS AND COMPARISON OF THE TWO METHODS BASED ON EQUATIONS (9.7) & (9.9):

Comparison of the two methods which are based on equations (9.7) and (9.9) (or (9.6) and (9.10)) yields the following observations

(a) - By using equation **(9.7)** , one does not have to measure the **FRFs** at the interface coordinates of the coupled structure C. Since this is always difficult, and in some cases impossible, this feature represents a considerable advantage for this method,

(b) - Application of equation (2.7) requires calculation of the pseudo-inverse of some matrices , i.e [B] and [C] in (9.6), unless $(s_a+s_b) = (i_a+i_b)$ which means that the number of slave coordinates of dummy structure D is equal to the number of interface coordinates. This assumption puts some constraints on the measurement.(Note that using the pseudo-inverse could be advantageous in an experimental analysis because it will serve to average the measurement errors and spread them over a greater number of data points.)

In performing these pseudo-inverses, it is necessary that $(s_a+s_b) > (i_a+i_b)$ and that neither s_a nor s_b be zero. Using equation (9.9) none of these problems exists and no considerations are required about choosing the correct number of coordinates. This is why both cases in section 9.2 can be handled by equation (9.9) but not by equation (9.7).

Thus, using equation (9.7) is generally better than using equation (9.9) and from an experimental point of view the most important advantage is that stated in (a).

Using equation (9.7), it is still sometimes very difficult to measure the interface coordinates' point **FRFs** on one of the substructures, and for such a case the method described below is proposed.

9.3.1.2 A METHOD TO DEAL WITH SUBSTRUCTURES WITH UNMEASURED INTERFACE COORDINATES

Reconsider equation (9.6) or (9.8) :

$$[J] = \left[[B]^{+}([A]-[H]_C)[C]^{+} \right]^{-1} - [D] \qquad (9.6)$$

$$[Z]_j = \left[[B]^{+}([A]-[Z]_C)[C]^{+} \right]^{-1} - [D] \qquad (9.8)$$

where for (9.6) :

$$[D] = \begin{bmatrix} [H]_a^{ii} & [\,] \\ [0] & [H]_b^{ii} \end{bmatrix} \tag{9.11}$$

and for (9.8)

$$[D] = \begin{bmatrix} [Z]_a^{ii} & [\,] \\ [0] & [Z]_b^{ii} \end{bmatrix} \tag{9.12}$$

In what follows, equation (9.6) will be used for the analysis but every conclusion is valid for (9.8) as well.

Equations (9.6) can be written as :

$$\begin{bmatrix} [J]_{aa}^{ii} & [J]_{ab}^{ii} \\ [J]_{ba}^{ii} & [J]_{bb}^{ii} \end{bmatrix} = \begin{bmatrix} [F]^{11} & [F]^{12} \\ [F]^{21} & [F]^{22} \end{bmatrix} - \begin{bmatrix} [H]_a^{ii} & [0] \\ [0] & [H]_b^{ii} \end{bmatrix} \tag{9.13}$$

where $[J]_{ab}^{ii}$ is the joint's transfer FRFs between the interface coordinates of the joint related to substructures A and B and

$$[F] = [\,[B]^{+}([A]-[H]_c)[C]^{+}\,]^{-1} \tag{9.14}$$

and from (9.13) :

$$[J]_{ab}^{ii} = [F]^{12} \quad \text{and} \quad [J]_{ba}^{ii} = [F]^{21} \tag{9.15}$$

This means that $[J]_{ab}^{ii}$ and $[J]_{ba}^{ii}$ could be easily determined without any need to measure the substructures point FRFs at the interface coordinates!

Using a prescribed joint model, e.g. an FE-based or lumped parameter model, it is a straight forward matter to calculate the complete joint model having $[J]_{ab}^{ii}$ and $[J]_{ba}^{ii}$. For a lumped parameter joint model, for example, a simple joint can be modeled as :

$$\begin{bmatrix} K_j & -K_j \\ -K_j & K_j \end{bmatrix}$$

while for n such joints (either rotational or translational) the model is:

$$\begin{bmatrix} K_1 & 0 & -K_1 & 0 \\ 0 & K_2 & 0 & -K_2 \\ -K_1 & 0 & K_1 & 0 \\ 0 & -K_2 & 0 & K_2 \end{bmatrix}$$

From this it is easily seen that, in equation (9.13), $[J]_{aa}^{ii} = -[J]_{ab}^{ii}$ and $[J]_{ab}^{ii}$ can be determined from (9.15) and thus that one has $[J]_{aa}^{ii}$ and $[J]_{bb}^{ii}$ in hand without measuring FRFs at the interface coordinates of either substructure.

For a more general type of joint model, considering (9.15), equation (9.13) could be written as :

$$\begin{bmatrix} [J]_{aa}^{ii} & [0] \\ [0] & [J]_{bb}^{ii} \end{bmatrix} = \begin{bmatrix} [F]^{11} & [0] \\ [0] & [F]^{22} \end{bmatrix} - \begin{bmatrix} [H]_a^{ii} & [0] \\ [0] & [H]_b^{ii} \end{bmatrix} \tag{9.16}$$

$$[J]_{aa}^{ii} = [F]^{11} - [H]_a^{ii} \tag{9.17}$$

$$[J]_{bb}^{ii} = [F]^{22} - [H]_b^{ii} \tag{9.18}$$

Usually, it is not a difficult task to measure the transfer FRFs between the interface coordinates of either A or B, i.e, the off-diagonal terms in $[H]_a^{ii}$ and $[H]_b^{ii}$, but the main difficulty lies in measuring the point FRFs of the interface coordinates. Let us assume that the point FRFs for B have been measured and thus that $[J]_{bb}$ can be calculated from (9.18).

If one assumes that $[H]_A^{ii}$ in equation (9.17) is an i x i matrix then there are i diagonal terms which have not been measured and also i unknowns related to the diagonal terms of $[J]_{aa}$. So, the system of equations (9.17) is an underdetermined set and there is no exact solution for it. One reasonable assumption is to consider the diagonal terms of $[J]_{aa}^{ii}$ as being equal to the diagonal terms of $[J]_{bb}^{ii}$. This can easily be justified if one considers an FE or simple lumped mass-spring-damper models for the joint.

Having $[J]^{ii}_{aa}$, one can easily calculate $[H]^{ii}_{A}$ and then assess these results by comparing them with the FRFs measured at adjacent points of the interface coordinates of A. If the results of this assessment are satisfactory, then the model found for J would be reliable and one could use it as well as $[H]^{ii}_{A}$ for further analysis.

9.3.2 DECOUPLING OF AN ASSEMBLED STRUCTURE CONSISTING OF ONE ELASTIC SUBSTRUCTURE

As its name implies, one of the substructures in this case is ground (relative to the other substructure), Fig.9.1.

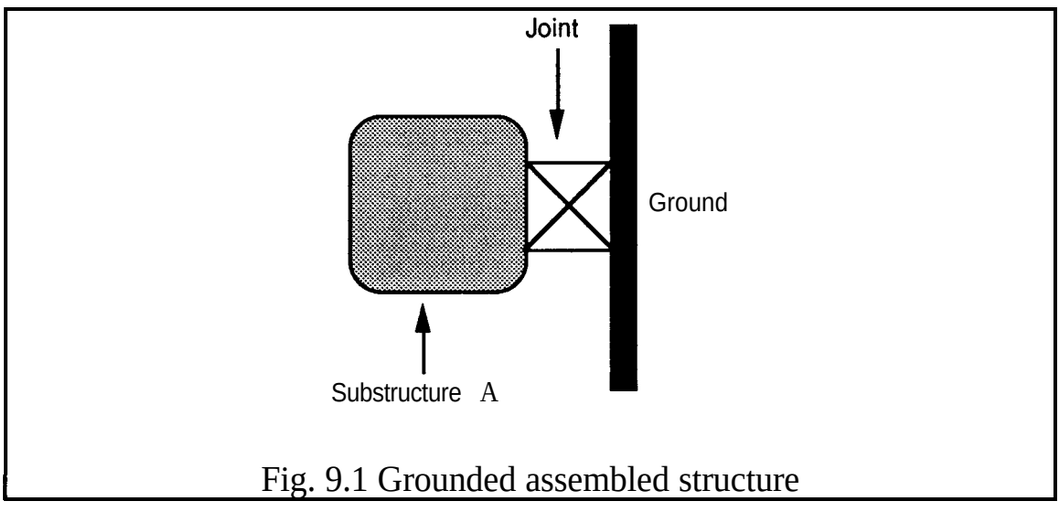

Fig. 9.1 Grounded assembled structure

For this case, the impedance model of the joint can be written as :

$$\begin{Bmatrix} \tilde{F}_{ja} \\ \tilde{F}_{jg} \end{Bmatrix} = \begin{bmatrix} [Z]^{gg}_{j} & [Z]^{ga}_{j} \\ [Z]^{ag}_{j} & [Z]^{aa}_{j} \end{bmatrix} \begin{Bmatrix} \tilde{x}_{ja} \\ \tilde{x}_{jg} \end{Bmatrix} \tag{9.19}$$

where g is a suffix for ground and notations "~" designates interface coordinates.

Since g is ground, $\{\tilde{x}\}_{jg} = 0 \qquad [Z]^{aa}_{j}\{\tilde{x}\}_{ja} = \{\tilde{F}\}_{ja}$ (9.20)

and, using a proper FRF model for substructure A along with the following compatibility and equilibrium equations we have:

$\{F\}_{a} = -\{F\}_{ja}$ and $\{\tilde{x}\}_{a} = \{\tilde{x}\}_{ja}$ (9.21)

From equations (9.20) and (9.21) it follows:

$$[H]_C = \left[[H]_a^{ss} - [H]_a^{si} \left([H]_a^{ii} + ([Z]_j^a)^{-1} \right)^{-1} [H]_a^{is} \right] \tag{9.22}$$

which can be solved for $[Z]_j^a$.

$$([Z]_j^a)^{-1} = \left[([H]_a^{si})^+ ([H]_a^{ss} - [H]_c) ([H]_a^{is})^+ \right]^{-1} - [H]_a^{ii} \tag{9.23}$$

or

$$[Z]_j^a = \left[I - [L] [H]_a^{ii} \right]^{-1} [L] \tag{9.24}$$

where

$$[L] = ([H]_a^{si})^+ ([H]_a^{ss} - [H]_c) ([H]_a^{is})^+$$

9.4 CONCLUDING REMARKS

From what has been said so far for frequency response decoupling methods, the following conclusions can be drawn :

(a) - neither of the methods discussed above uses a prescribed model for damping, i.e, hysteretic or viscous, and so the appropriate model should be selected after examining the identified joint's FRFs. This is a considerable advantage when identifying joints which reveal different damping mechanisms for different frequency ranges;

(b) - no prescribed model for the joint is considered. However, the nature of the joint, i.e, translational and rotational or just translational or....etc, depends on the interface coordinates used in coupling of the substructures;

(c) - these methods could be applied to non-linear structures using appropriately-measured FRFs;

(d) - the method proposed in 9.3.1.2 is a useful tool to deal with substructures where interface coordinates are difficult to measure.

9.5 CASE STUDIES

It was noted in the previous sections that either equation (9.7) or equation (9.9) can be used as the basic formula for a general decoupling analysis. Due to the practical advantages associated with using equation (9.7), explained in section 9.3.1.1, the performance and sensitivity of this equation will be investigated in this and subsequent sections

9.5.1 TEST STRUCTURES & JOINT MODELS

The assembled structure, C, and its constituent substructures are shown in Fig. 9.2.

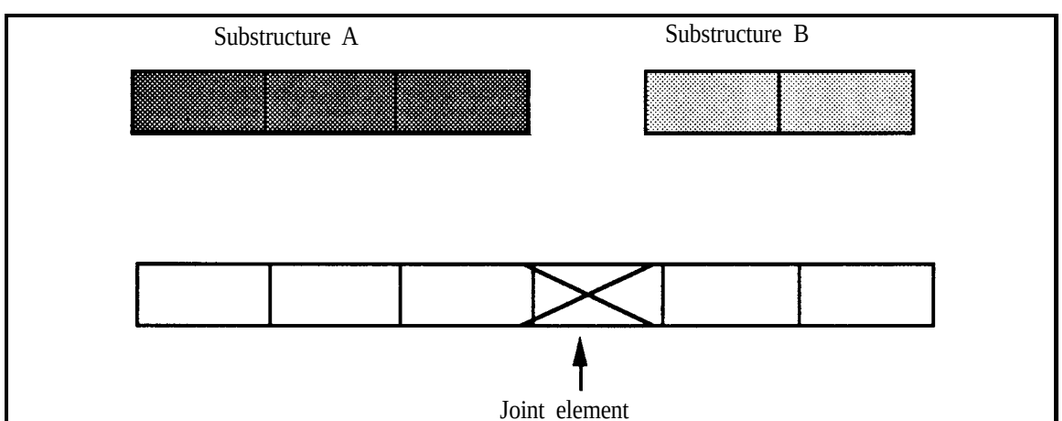

Fin. 9.2 Test structures used in all case studies

As is evident from Fig. 9.2, substructures A and B are FE-based beam models with 2 and 3 elements, respectively. These models are developed using a base element shown in Fig. 3.2 :

In order to simulate a practical case as much as possible, just the translational degrees of freedom of slave coordinates for both substructures and assembled structure are used in calculations in all case studies. It is clear that by not using rotational degrees of freedom in the calculations, one may lose valuable information about the joint's effect on the structure's response. In spite of this fact, since accurate evaluation of rotational degrees of freedom responses is very difficult, rotational parameters of the slave coordinates will be eliminated from the calculations.

The joint element of the assembled structure in Fig. 9.2 has the following specifications:

$$L_{jc} = L_e \ , \ E_{jc} = 1000\%E_e \quad \rho_{jc} = 10\%\rho_e \tag{9.25}$$

Thus, the joint element is 10 times stiffer and 10 times lighter than the base element in Fig. 3.2. The specifications in equation (9.25) yield the following mass and stiffness matrices for the joint element:

$$[M]_{jc} = \begin{bmatrix} .05 & .0021 & .01746 & -.00126 \\ & .0001 & .00126 & -.000087 \\ & & .05 & -.0021 \\ & & & .0001 \end{bmatrix}$$

$$[K]_{jc} = \begin{bmatrix} 6440000 & 966000 & -6440000 & 966000 \\ & 193200 & -966000 & 96600 \\ & & 6440000 & -966000 \\ & & & 193200 \end{bmatrix} \tag{9.26}$$

CASE STUDY 1

In this case study, equation (9.7) has been set up and solved for the test structures in Fig. 9.2. Typical results of the identified joint are shown in Fig. 9.3. It should be noted that since equation (9.7) is being solved at each individual frequency point, there is no need to decompose $[Z]_j$ in equation (9.7) into its constituent pararneters, i.e. mass, stiffness and (in damped case) damping. This is why the results in Fig. 9.3 are in terms of the elements Of joint impedance matrix $[Z]_j$.

As is evident from Fig. 9.3, the result is satisfactory. The condition number of the coefficient matrix on the l.h.s of equation (9.7) is shown in Fig. 9.4. As this figure indicates, the condition numbers of the coefficient matrix associated with resonance frequencies of the substructures and of the assembled structure are high, which means a greater possibility of high sensitivity to error at these frequencies.

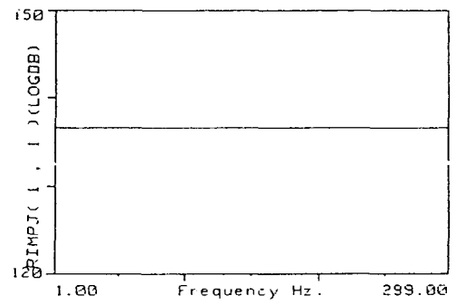

Fig. 9.3 Typical identified joint impedance without noise

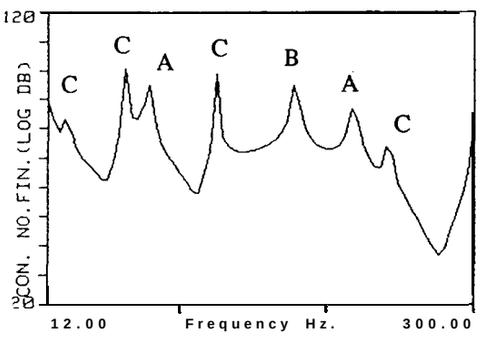

Fig. 9.4 Condition number of coefficient matrix on the l.h.s of equation (9.7)

To examine the effect of measurement noise on the results, 5% random noise has been introduced to both the real and imaginary parts of the FRFs of the substructures and of the coupled structure. Typical calculated joint impedance matrix elements, $z_j(1,1)$ and $z_j(1,2)$, are shown in Fig. 9.5. As is evident from this figure, the results are very poor and comparing calculated mean values of results with correct values, it becomes clear that computed results are at least 20 dB less than the correct values, which means 10 times under-estimated.

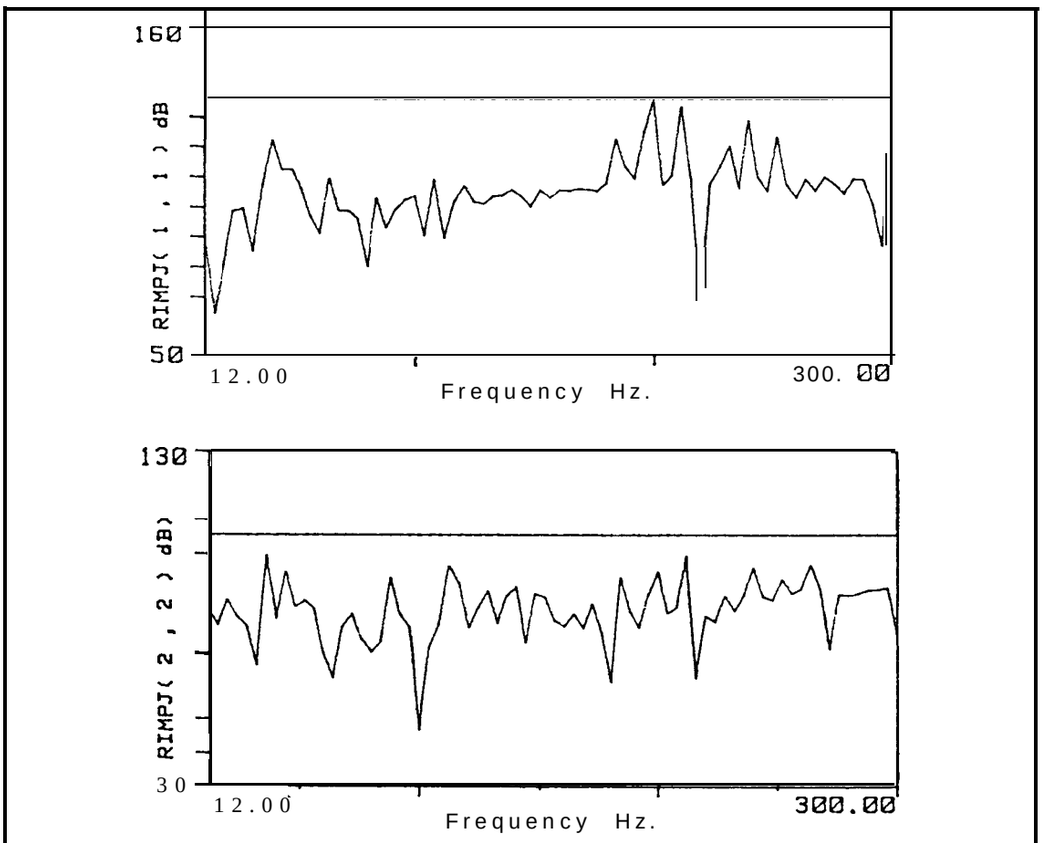

Fig. 9.5 Typical joint impedance matrix elements with 5% noise,
___ correct value

The above-mentioned results lead to the conclusion that the identification procedure is sensitive to noise. Investigation of the reason(s) for this high sensitivity and of methods for its reduction are the subjects of subsequent sections.

9.5.2 INVESTIGATION ON THE PARAMETERS CONTROLLING SENSITIVITY

In this section we will examine the nature of the identification problem sensitivity to noise and will try to identify the underlying controlling parameters.

As mentioned in section 4.2.2.2, the significance of the effect of a joint (each of its individual parameters) on the assembled structure's response plays a major role in the sensitivity of the identification procedure to measurement noise. In other words, a major reason for high sensitivity can be attributed to the insensitivity of the assembled structure's response to some of the joint parameters variations. The insensitivity of

assembled structure C in Fig. 2.1 to variation of the joint parameters in expression (9.26), for low and moderate frequency ranges, can be seen in Fig. 9.6. This figure shows the typical FRFs of the assembled structure, C, generated once with the joint model in expression (9.26) and the next time with a joint model 10 times stiffer and 10 times lighter than former joint model.

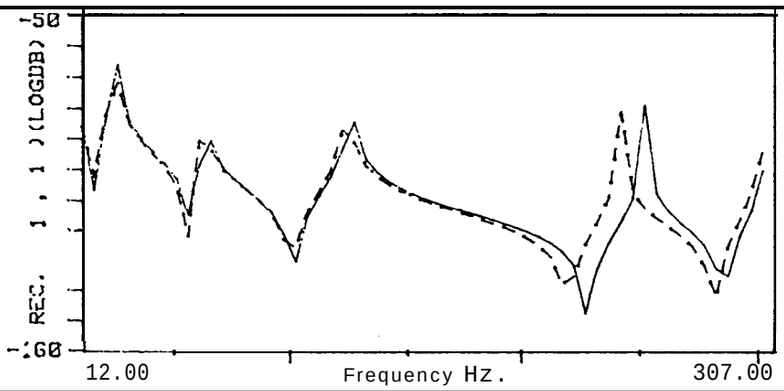

Fig. 9.6 Typical FRFs of two structures, --- joint model in (9.26)
___ 10 times stiffer joint

As a general rule, the stiffer the joint, the less sensitive is the assembled structure is to joint parameter variations.

CASE STUDY 2

Fig 9.7 shows the typical results of repeating case study 1 with just 5% random noise added to $[H]_c$. As can be seen from this figure, even without adding any noise to the FRFs of substructures, the results are very poor.

Recalling from section 4.2.2.2, and defining [E] as the noise-induced error matrix added to matrix $[H]_c$ ($\|[E]\| << \|[H]_c\|$), the matrix $[B]^+([A]-[H]_c)[C]^+$ in equation (9.7) can be written as:

$$[B]^+([A]-[H]_c-[E])[C]^+ = [B]^+([A]-[H]_c)[C]^+ + [B]^+[E][C]^+ \qquad (9.27)$$

where the first term on the r.h.s of equation (9.27) represents the correct effect of the joint on the assembled structure's response and the second term shows the noise effect. Now, as Fig. 9.7 indicates,

$$\|[B]+[E][C]+\| > \|[B]^+([A]-[H]_c)[C]^+\| \qquad (9.28)$$

i.e. the error effect has dominated the joint effect in the calculation.

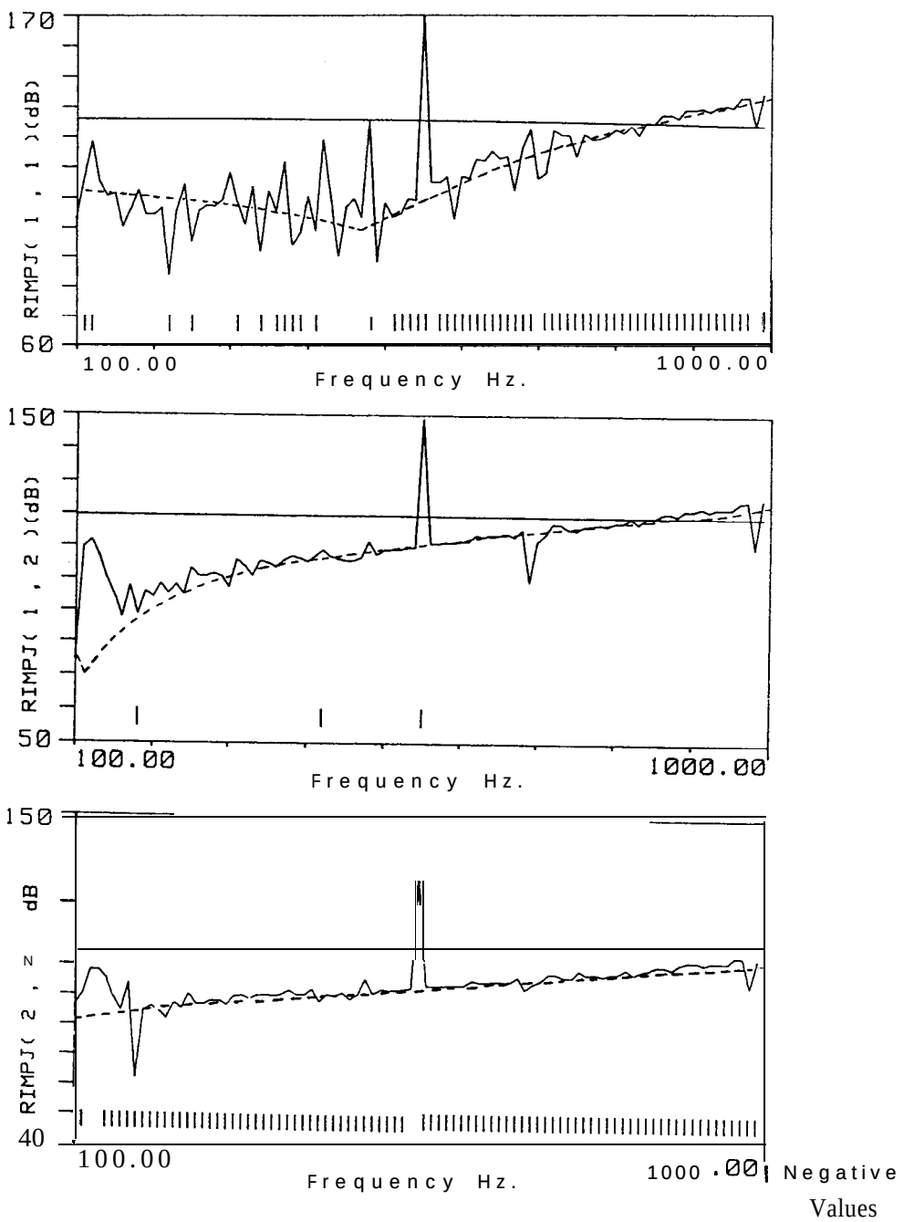

Fig. 9.7 Typical joint impedance matrix elements with 5% noise added only to FRFs of assembled structure, ___ correct value, - - - quadratic fitted curve

It is clear that the matter of the structure's sensitivity to joint parameter variations depends on many factors among which the interfacing configuration is one of the most important.

To illustrate the effect of the interfacing configuration, and other factors, on the structure's sensitivity and, consequently, on the results, the following case study has been carried out.

CASE STUDY 3

Fig. 9.9 shows the results of identifying the joint for an assembled structure with the interfacing configuration shown in Fig. 9.8 and with 5% random noise added to $[H]_c$

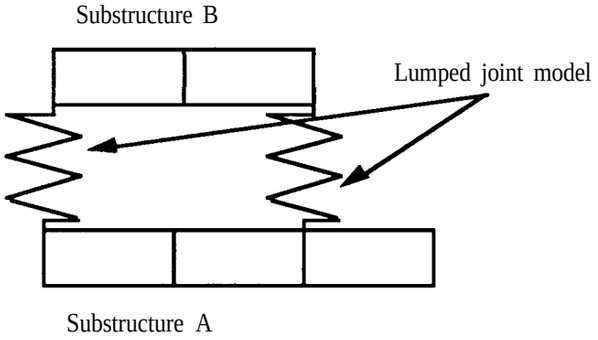

Fig. 9.8 Assembled structure C for case study 3

The constituent substructures of the assembled structure in Fig. 9.8 are the same as those in Fig. 9.2 but a lumped parameter joint model has been used in Fig. 9.8 and no rotational degrees of freedom are involved in the interfacing. The lumped parameter joint model in Fig. 9.8 has the following mass and stiffness matrices:

$$[M]_{jc} = \begin{bmatrix} .05 & 0 & 0 & 0 \\ & .0001 & 0 & 0 \\ & & .05 & .0001 \end{bmatrix}$$

$$[K]_{jc} = \begin{bmatrix} 6440000 & 0 & -6440000 & 0 \\ & 193200 & 0 & -193200 \\ & & 6440000 & 193200 \end{bmatrix} \qquad (9.29)$$

As expression (9.29) indicates, the joint model in Fig. 9.8 is a lumped parameter version of the (consistent) joint model in Fig. 9.2.

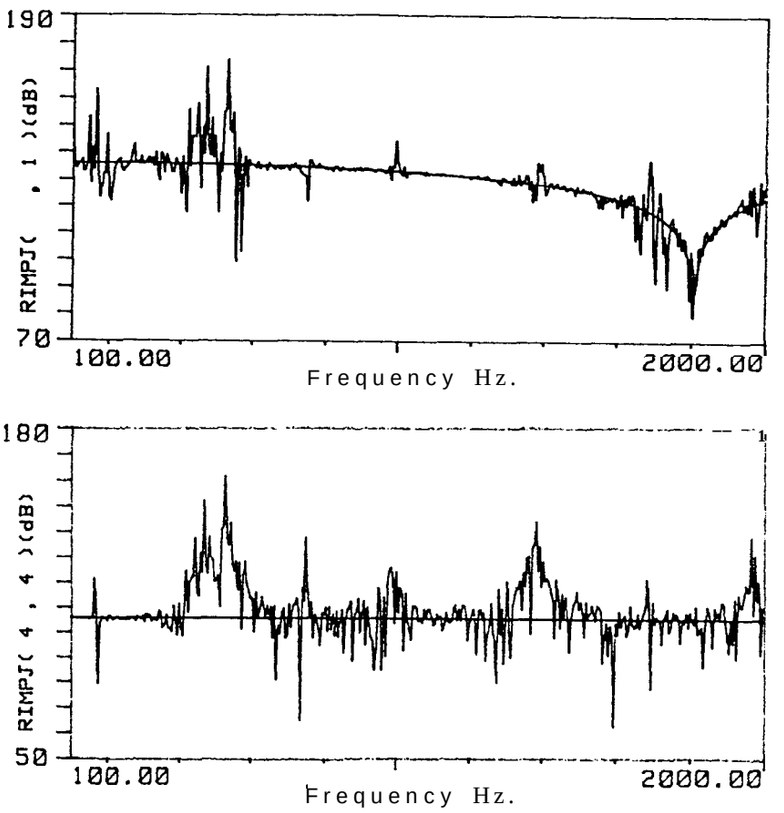

Fig. 9.9 Typical joint impedance matrix elements with 5% noise added to FRFs of assembled structure in Fig. 9.8

Examination of Fig. 9.9 reveals that the results are satisfactory. On the other hand, using the same interfacing configuration as in Fig. 9.2, i.e. with both translational and rotational degrees of freedom included, together with a lumped parameter joint in expression (9.29), again yields poor results.

The above observation indicates that, for the test structures of Fig. 9.2, the inclusion of rotational degrees of freedom in the interface coordinates deteriorates the result. This conclusion is in complete agreement with the conclusions drawn in chapters 5 to 8 (i.e. insignificant effect of the joint's rotational parameters on the assembled structure's response).

Further examination of the results in Fig. 9.7 reveals that, despite poor results in this figure, there is a clear trend in the identified joint impedances. Using a least-squares curve fitting technique, this trend can be well described as a quadratic function of the form:

$$Z_{ij} = k_{ij} - m_{ij}\omega^2 \qquad (9.30)$$

The fitted quadratic functions in Fig. 9.7 are shown by dashed lines. Note that the spikes on the identified impedance curves, are related to natural frequencies of the substructures and of the assembled structure (see Fig. 9.4).

The existence of the quadratic trend in the erroneous results in Fig. 9.7 indicates that the noise has not affected the quadratic nature of the joint impedance. So, the identification process identifies a joint element with an impedance of quadratic nature but, since the noise has affected the FRFs of the assembled structure and substructures, the calculations do not converge to the real joint but under-estimate it.

In the following sections, the methods of dealing with structures with insignificant joints will be investigated.

9.5.3 APPLICATION OF LS METHOD TO REDUCE THE NOISE EFFECT

Recalling from section 4.2.2.2 that, due to the fact that noise-induced errors dominate the matrix $[B]^{+}([A]-[H]_c)[C]^{+}$ in equation (9.7) (both sides of the equation) at each individual frequency point, it is not possible to reduce the noise effects on the calculation by combining equation (9.7) from different frequencies and using a least-squares (LS) solution. So, in contrast to the adaptive identification techniques, the LS method does not reduce the noise effect on the results.

9.5.4 APPLICATION OF SVD TECHNIQUE TO REDUCE THE NOISE EFFECT.

The SVD technique is usually used to invert an ill-conditioned matrix where a small amount of noise can affect the smallest singular values of the matrix.

In this section, the SVD is not used for inversion purposes (as it is not useful because of the dominant error effect), but rather to find the parameters which cause the dominant error effects in equation (9.7) and thus to eliminate them from the calculations. In this connection, we will first examine the noise effect on [A-H,] and, second, on $[H]_c$, as the main sources of error.

Fig. 9.10 demonstrates the ratio of the elements of the left singular vectors of matrix $[A\text{-}H_c]$ of case study 2, before and after adding noise to $[H]_c$, for f=200 Hz. Also, Table 9.1 demonstrates the singular values of [A-H,] with and without noise.

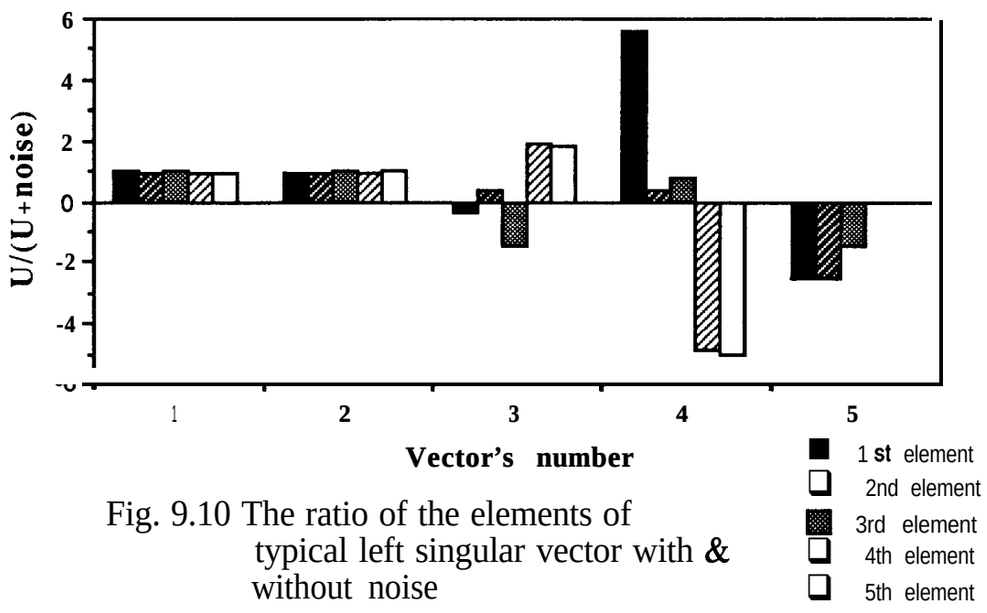

Fig. 9.10 The ratio of the elements of typical left singular vector with & without noise

	σ_1	σ_2	σ_3	σ_4	σ_5
- Noise	1.177E-5	3.7E-6	1.15E-9	1.13E-10	9.2E-22
+ Noise	1.177E-5	3.72E-6	4.16E-8	2.5E-8	4.11E-10

Table 9.1 Singular values of [A-H,] with and without noise

Although the data in Fig. 9.10 and Table 9.1 are typical, the variation of the elements of the right singular vectors and singular values shows the same pattern for the whole frequency range of interest, i.e. 100-1000 Hz. Also, since only translational slave coordinates are involved in $[H]_c$ and in [A-H,], both matrices are of order of 5x5.

Examining Fig. 9.10 and Table 9.1, two conclusions can be deduced as follows:

(a) - except for the two first column vectors of [U] and [V], the other columns are affected by noise dramatically; and

(b) - the 3rd, 4th and 5th singular values are very small compared with the 2nd one.

To determine the physical implications of the two above deductions, extend the method introduced in [31] for the case of coupling analysis and define $[\Delta]=[A-H_c]$ as the matrix of the difference of FRFs of the assembled structure, C, and the dummy structure, D, at their slave coordinates. Then using the SVD of [A], one obtains:

$$[A] = [A\text{-}H,] = [U][\Sigma][V]^H = [\delta][V]^H \Longrightarrow [\delta] = [A][V] = [U][\Sigma] \qquad (9.31)$$

As is evident from equation (9.31), the columns of $[\delta]$ are equal to columns of [U] multiplied by the appropriate σ. Also, columns of [A] can be represented by linear combinations of the columns of $[\delta]$. Now, saying that i^{th} singular value of [A-H,] is very small means that:

$$\|[\Delta]\{V\}_i\| \text{ is very small} \quad \Longrightarrow \quad \|[A-H_c]\{V\}_i\| \text{ is very small} \qquad (9.32)$$

Expression (9.32) means that, for every small singular value, there is a certain pattern of the slave coordinates' response differences which has very insignificant contribution to [A-H,], i.e. to the slave coordinates' FRFs difference matrix, and consequently to the calculations. This insignificant contribution can easily be dominated by the noise effects.

With the above physical explanation in mind, it is clear that the two above deductions about the singular parameters of [A-H,], are cause and effect, i.e. the small singular values related to the 3rd, 4th and 5th singular vectors are the cause of the dramatic noise effect on their related singular vectors.

Therefore in order to prevent the insignificant difference patterns occuring, when noise is present, the appropriate singular values are set to be zero.

To investigate the effect of noise on $[H]_c$, this matrix's singular parameters have been calculated for the frequency range of interest.

Examining the singular values of $[H]_c$ reveals that, except at the natural frequencies of the assembled structure, these parameters are not affected dramatically by noise. On the other hand, exploring the left and right singular vectors of $[H]_c$ shows that the noise effect on these vectors is significant for the two following cases:

(a) - for cases where two adjacent singular values are close (see section 4.51); and

(b) - for the 4th right and left singular vectors.

The first case above has been thoroughly discussed in section 4.5.1. For the second case, closer examination shows that:

$$\|\{V\}_4\| << \|\{V\}_i\| \quad i= 1 \text{ to } 5 \ \& \ i \neq 4 \quad \Rightarrow \text{from equ. (9.31)} \ \|[H_c]\{V\}_i\| = \text{very small} \tag{9.33}$$

Expression (9.33), again, means that the contribution of a certain pattern of deflection of the slave coordinates of the assembled structure to $[H]_c$ is insignificant. Note that in this case, in contrast to expression (9.32) for [A-H,], small $\|\{V\}_4\|$ is not associated with small σ_4.

So, from the above discussions on the quality of the noise effects on the singular parameters of $[H]_c$ and [A-H,], it becomes clear that proper selection of singular parameters of these matrices can improve the results of the identification.

CASE STUDY 4

The test structures and joint model for this case study are the same as those for case study 2, shown in Fig. 9.2 and equation (9.25). In order to reduce the noise effect on [A-H,], this matrix has been regenerated using only the first two singular vectors and singular values. Also, $[H]_c$ has been regenerated using averaged [U], and $[V]_c$ and either one or two first singular values and singular vectors, i.e. if $\sigma_1/\sigma_2 < 2$ then use only σ_1 and if $\sigma_1/\sigma_2 > 2$ use σ_1 and σ_2 in regeneration of $[H]_c$ (see section 4.5.1).

A typical result for the identified joint can be seen in Fig. 9.11. It is evident from this figure that the results are much better than those in Fig. 9.7. Note that the calculated mean values in Fig. 9.11, shown by dotted lines, give a reasonable approximation to the correct impedances.

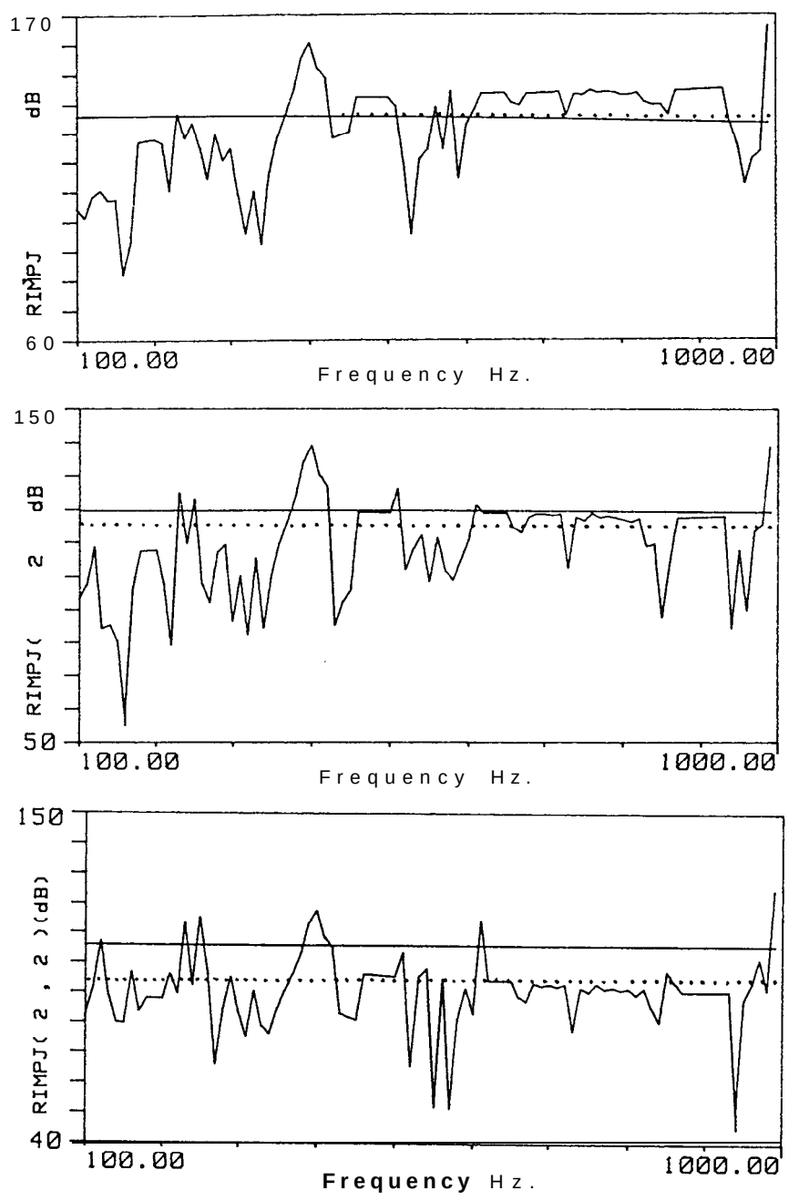

Fig. 9.11 Typical joint impedance matrix element with 5% noise with SVD technique applied to reduce noise effect

Finally, numerical case studies show that increasing the number of slave coordinates involved in the calculation improves the results. This improvement was expected because more slave coordinates means more points are involved in the calculation of matrix [A-H], and since, depending on their position in the structure, responses of different points are differently affected by the joint, one has more estimates of the joint in the calculation. This deduction is particularly true if the added slave coordinates are close to an interfacing position. On the other hand, excessive number of slave coordinates may

increase the error level in the calculations. For example, selecting a point which is a nodal point (or near to a nodal point) for one or more modes in the frequency range of interest as a slave coordinate can introduce a huge amount of measurement error to the calculations. Thus, selection of the number of slave coordinates and selection of their location on the substructures and assembled structure is a delicate matter.

9.6 CONCLUSIONS & REMARKS

From the results achieved in the foregoing sections and the subsequent discussions, the following conclusions can be drawn for the FRF-based decoupling method:

(a) - the method is sensitive to measurement noise. This sensitivity, which depends on the interfacing configuration, is due to insignificant joint effect on the structure's response. So, reduction of measurement noise is crucial. At a preliminary stage of analysis this reduction of noise can be achieved by proper selection of the slave coordinates and by post-processing of measured FRFs, using modal analysis. If the post-processing is used, one should be very careful when using regenerated FRFs, as even very slight differences between original and regenerated FRFs can affect the results of the computed joint remarkably ;

(b) - the following factors improve the result:

(i)-increasing the number of slave coordinates and properly selecting them. The most useful slave coordinates are those which are most affected by the joint In other words, the most useful slave coordinates are those which do not cause any insignificant difference pattern in [A-H], (see expression 9.32); and

(ii)- application of SVD technique to identify insignificant difference patterns and eliminate them from calculations;

(c) - in cases where the effect of errors is dominant, the application of a LS technique is not useful.

CHAPTER 10

MODAL-BASED DECOUPLING METHOD

10.1 INTRODUCTION

The FRF-based decoupling technique was discussed in chapter 9. As was noted in that chapter, provided that the noise effect is not dominant, the FRF-based decoupling method is very efficient. In the present chapter, the performance and sensitivity of a modal-based version of the decoupling method will be investigated.

The basic idea in modal-based decoupling method is the same as in the FRF version, i.e. to extend the coupling formulation between two (or more) substructures, considering the joint explicitly as an intermediate substructure and then solving the inverse problem, i.e, decoupling an assembled structure to its components and, using either experimental or analytical models of substructures, identifying the joint

10.2 FORMULATION OF MODAL-BASED DECOUPLING METHOD

Consider the assembled structure, C, shown in Fig. 9.1. This assembled structure consists of two substructures A and B and a joint element J.

Recalling the coupling equation from chapter 2 and assuming that substructures A and B constitute a dummy structure D, the modal-based coupling equation can be written (see equation (2.3 1)):

$$-\lambda_{cr}\begin{Bmatrix}\{p_{ar}^{c}\}\\ \{p_{br}^{c}\}\end{Bmatrix}+\left[\begin{bmatrix}[\lambda_{ak}] & 0\\ 0 & [\lambda_{bk}]\end{bmatrix}+\begin{bmatrix}[\phi_{aki}] & 0\\ 0 & [\phi_{bki}]\end{bmatrix}^{T}\left[[H_j]+[R_{di}]\right]^{-1}\begin{bmatrix}[\phi_{aki}] & 0\\ 0 & [\phi_{bki}]\end{bmatrix}\right]\begin{Bmatrix}\{p_{ar}^{c}\}\\ \{p_{br}^{c}\}\end{Bmatrix}=0 \tag{10.1}$$

where notations i, s and k are designated as interface and slave coordinates and kept modes, respectively, and,

$$[R]_{di}=\begin{bmatrix}[\phi_{ae}][\omega_{ae}^{2}]^{-1}[\phi_{ae}]^{T} & 0\\ 0 & [\phi_{be}]\,[\omega_{be}^{2}]\,[\phi_{be}]^{T}\end{bmatrix} \tag{10.2}$$

As was described in chapter 2, $[R_{di}]$ represents the residual contribution of the eliminated higher modes to the flexibility of substructures A and B at their interface coordinates. Thus, $[R_{di}]$ can be interpreted physically as a dummy spring or, generally speaking, as an elastic medium which connects the interface coordinates of two substructures to each other. Also, the joint which is a real elastic medium is present at the interface coordinates of the substructures and connects the substructures to each other and as is evident from equation (10.1) the flexibility matrices of these dummy and real elastic media are in series and combine to constitute the total elastic element acting between the interface coordinates of the substructures.

In order to be able to calculate $[H_j]$ from equation (10. 1), this equation should be solved as an inverse eigenvalue problem. The solution procedure starts from calculation of $\begin{Bmatrix}\{p_{ar}^{c}\}\\ \{p_{br}^{c}\}\end{Bmatrix}$ using expansion equation (2.21) as follows:

$$\begin{Bmatrix}\{\phi_{ars}^{c}\}\\ \{\phi_{brs}^{c}\}\end{Bmatrix}=\begin{bmatrix}[\phi_{aks}] & 0\\ 0 & [\phi_{bks}]\end{bmatrix}\begin{Bmatrix}\{p_{ar}^{c}\}\\ \{p_{br}^{c}\}\end{Bmatrix} \tag{10.3}$$

where $\{\phi_{ars}^{c}\}$ and $\{\phi_{brs}^{c}\}$ are subvectors of structure C's r^{th} eigenvector, containing the slave coordinates related elements. Also, $[\phi_{aks}]$ and $[\phi_{bks}]$ are eigen-matrices of substructures A and B, respectively, containing slave coordinates related elements of the kept modes.

Calculation of $\begin{Bmatrix} \{p_{ar}^c\} \\ \{p_{br}^c\} \end{Bmatrix}$ from equation (10.3) requires measurement of the rth eigenvector of the assembled structure C as well as a sufficient number of modal parameters of substructures A and B. It should be noted that only the slave coordinate eigenvector parameters of structure C are required and thus no interface coordinates need to be measured on structure C (which may be difficult to measure in practice.) Having calculated $\begin{Bmatrix} \{p_{ar}^c\} \\ \{p_{br}^c\} \end{Bmatrix}$ and putting it in equation (10. 1), this can be rewritten as:

$$\left[\begin{bmatrix} [\phi_{aki}] & 0 \\ 0 & [\phi_{bki}] \end{bmatrix}^T [A] \begin{bmatrix} [\phi_{aki}] & 0 \\ 0 & [\phi_{bki}] \end{bmatrix}\right]\begin{Bmatrix} \{p_{akr}^c\} \\ \{p_{bkr}^c\} \end{Bmatrix} = \lambda_{cr}\begin{Bmatrix} \{p_{ar}^c\} \\ \{p_{br}^c\} \end{Bmatrix} - \begin{bmatrix} [\lambda_{ak}] & 0 \\ 0 & [\lambda_{bk}] \end{bmatrix}\begin{Bmatrix} \{p_{ar}^c\} \\ \{p_{br}^c\} \end{Bmatrix} \tag{10.4}$$

where

$$[A] = [\,[H_j] + [R_{di}]\,]^{-1} \tag{10.5}$$

Matrix [A] contains the unknown parameters of the joint which are to be found Equation (10.5) can be converted into a set of algebraic equations with the elements of [A] as unknowns. If ni is the number of interface coordinates, then $[H_j]$ will be $n_i x n_i$ and the total number of unknowns, taking symmetry into the consideration, will be $n_i.x(n_i+1)/2$ while the number of equations is $(m_a$ + mb) where m_a and mb are the numbers of measured modes of substructures A and B, respectively. Now, if it is desired to identify the joint from equation (10.4) using only one measured mode, the following inequalities must be satisfied:

for equation (10.3) $(ma + m_b) \leq n_{cs} = (n_{as} + n_{bs})$ (10.6)

for equation (10.4) $n_i.x(n_i+1)/2 \leq (ma + m_b)$ (10.7)

where n_{as}, nbs and n_{cs} are the numbers of measured slave coordinates of substructures A and B and assembled structure C, respectively.

Inequalities (10.6) and (10.7) simply mean that in order to be able to identify the joint using a single measured mode of the assembled structure C, the number of measured

slave coordinates of the substructures must at least be equal to the number of unknowns in the joint impedance matrix.

In contrast to the FRF-based decoupling method where solving the governing equation for each individual frequency yields good results due to the approximate nature of equation (10.3), in which the contribution of higher modes has been ignored and coordinate set is incomplete, i.e. part of information related to the joint effect is missed (see equation (2.21)), solving equation (10.4) for only one mode does not yield a satisfactory result. In order to achieve a satisfactory result it is necessary to incorporate more modes of the assembled structure in the calculations, i.e. equation (10.4) for different modes of the assembled structure must be combined to set up an over-determined set of algebraic equations and, to be able to combine equations for different r, it is necessary to separate the mass and stiffness parameters in $[H_j]$, which is not possible. The only way of separating the mass and stiffness parameters of $[H_j]$ is to ignore the higher modes' residual matrix $[R_{di}]$ in equation (10.1), or (10.4). Then, using $[Z_j] = [H_j]^{-1}$ in equation (10.4), it will be an easy task to separate the mass and stiffness parameters.

The other, more suitable, way of solving equation (10.1) is to write it as follows:

$$\begin{bmatrix} [\phi_{aki}] & 0 \\ 0 & [\phi_{bki}] \end{bmatrix}^T [Z_j] \left[\begin{bmatrix} [\phi_{aki}] & 0 \\ 0 & [\phi_{bki}] \end{bmatrix} - [R_{di}] \begin{bmatrix} [\phi_{aki}] & 0 \\ 0 & [\phi_{bki}] \end{bmatrix}^{T+} [Ah] \right] \{p_{xr}\} =$$

$$\begin{bmatrix} [\phi_{aki}] & 0 \\ 0 & [\phi_{bki}] \end{bmatrix}^T \begin{bmatrix} [\phi_{aki}] & 0 \\ 0 & [\phi_{bki}] \end{bmatrix}^{T+} [\Delta\lambda] \{p_{xr}\} \qquad (10.8)$$

where

$$[\Delta\lambda] = [\lambda_{xr}] - \begin{bmatrix} [\lambda_{ak}] & 0 \\ 0 & [\lambda_{bk}] \end{bmatrix} \qquad (10.9)$$

Using equation (10.9), no approximation is introduced to equation (10.1) but, on the other hand, in order to be able to calculate $\begin{bmatrix} [\phi_{aki}] & 0 \\ 0 & [\phi_{bki}] \end{bmatrix}^{T+}$, it is necessary to satisfy inequality (10.7) for each mode. Also, inequality (10.6) must be satisfied as well.

10.3 CASE STUDIES

In order to study the performance of the modal-based decoupling method, a series of case studies have been undertaken. Test structures used in all case studies are shown in Fig. 10.1. Substructure A is an 8-element FE model of a cantilever beam and substructure B is also an FE model of a cantilever beam with 7 elements.

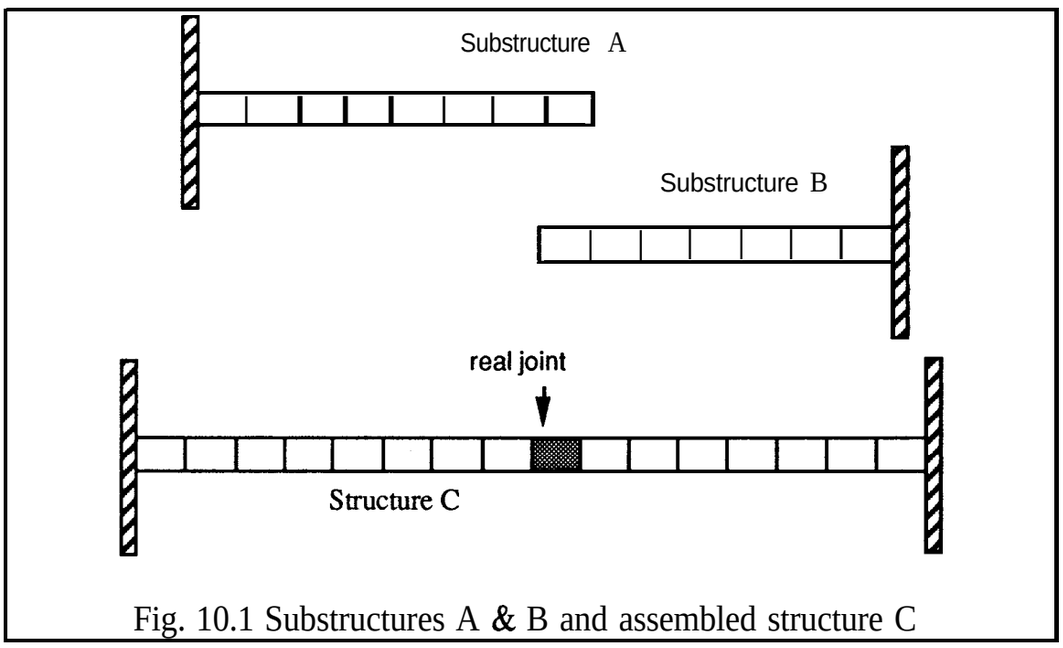

Fig. 10.1 Substructures A & B and assembled structure C

The specifications of the base element used to generate the substructures models are the same as those in Fig. 3.2 of chapter 3. Also, the specifications of the joint model used to generate the assembled structure are the same as those in equation (6.43) of the same chapter, which yields following joint mass and stiffness matrices:

$$[M]_{jx} = \begin{bmatrix} .05 & .0021 & .01746 & -.00126 \\ & .00011 & .00126 & -.000087 \\ & & .05 & -.0021 \\ & & & .00011 \end{bmatrix}$$

$$[K]_{jx} = \begin{bmatrix} 3220000 & 483000 & -3220000 & 483000 \\ & 96600 & -483000 & 48300 \\ & & & \\ & & 3220000 & -483000 \end{bmatrix} \qquad (10.10)$$

Since, as mentioned before, only the translational slave coordinates of substructures **A** and B and structure C are used in the calculations, there are 13 coordinates in the eigenvector of structure C on the r.h.s of the equation (10.3)

In contrast to the FRF-based decoupling method, solving equation (10.9) even for a single mode requires one to transform the matrix equation (10.8) into a set of algebraic equations, as follows:

$$[\ C(\lambda_r)\ ]_{(ma+mb)x(n_ix(n_i+1))} \begin{Bmatrix} \{K\} \\ \{M\} \end{Bmatrix}_{n_ix(n_i+1)} = \{\ L(\omega_i)\ \}_{(ma+mb)x1} \tag{10.11}$$

Thus, the introduction of a reference joint model is necessary, in order to balance the coefficient matrix **[C].** The reference joint model used in the subsequent case studies is the same as that in equation (4.60) of chapter 4, i.e. a 20-parameter reference model as follows:

$$[K]_j = \begin{bmatrix} \alpha_1 a_1 & \alpha_2 a_2 & \alpha_3 a_3 & \alpha_4 a_4 \\ & \alpha_5 a_5 & \alpha_6 a_6 & \alpha_7 a_7 \\ & & \alpha_8 a_8 & \alpha_9 a_9 \\ & & & \alpha_{10} a_{10} \end{bmatrix}$$

$$[M]_j = \begin{bmatrix} \alpha_{11} a_{11} & \alpha_{12} a_{12} & \alpha_{13} a_{13} & \alpha_{14} a_{14} \\ & \alpha_{15} a_{15} & \alpha_{16} a_{16} & \alpha_{17} a_{17} \\ & & \alpha_{18} a_{18} & \alpha_{19} a_{19} \\ & & & \alpha_{20} a_{20} \end{bmatrix} \tag{10.12}$$

Note that $[M_j]$ and $[K_j]$ have been used in equation (10.12), and not $[\Delta M_j]$ and $[\Delta K_j]$, as the decoupling technique identifies the joint parameters directly and not modifications to them (as in the adaptive techniques). Also, since there is no trial joint model defined in the decoupling method, the parameters a_i can be defined using an arbitrary reference joint model.

CASE STUDY 1

Equation (10.8) is solved in this case study, using the first 7 modes and the first 6 modes of substructures A and B respectively. Thus the transformation matrix on the r.h.s of equation (10.3) is a 13x13 matrix. Further, the matrix $[C(\lambda_r)]$ on the l.h.s of equation (10.11) is a 13x20 matrix, for each mode of assembled structure, r.

Expression (10.13) shows the identified joint mass and stiffness matrices, using 5 modes of the assembled structure in the calculations.

$$[K]_j = \begin{bmatrix} 294257(90\%) & 22013(95\%) & -265246 & 47779 \\ & & -25105 & 415 \\ & & & \\ & 8816(90\%) & 293275 & -45206 \end{bmatrix}$$

and

$$[M]_j = \begin{bmatrix} .0074(85\%) & .00015(93\%) & .003 & -.00019 \\ & 1.7E\text{-}5(85\%) & .0001 & -1.2E\text{-}6 \\ & & .0074 & -.00032 \\ & & & 2.94E\text{-}5 \end{bmatrix} \qquad (10.13)$$

Error values in brackets in expression (10.13) indicate the poor quality of the result. In spite of this, the proportionality between various elements of the stiffness and mass matrices is reasonably well preserved.

CASE STUDY 2

Case study 1 is repeated, this time using the complete set of slave coordinates of the assembled structure in the calculations, i.e. rotational slave coordinates are involved as well. Under these circumstances, the transformation matrix on the r.h.s of equation (10.3) is 26x26 which means that the first 13 modes of substructures A and B are involved in the calculations. Furthermore, the coefficient matrix [C] in equation (10.11) is a 26x20 matrix for each mode of assembled structure.

Expression (6.14) shows the result of this case.

$$[K]_j = \begin{bmatrix} 2.6E6(18\%) & 600000(24\%) & -2.44E6 & 83015 \\ & & -4377 & 18 & -42639 \\ & & & & \\ & & 277725(186\%) & 3.72E6 & -26497 \end{bmatrix}$$

and

$$[M]_j = \begin{bmatrix} & .0005(354\%) & .0018 & .00012 \\ & & .093 & -.0015 \\ .064(18\%) & .0042(98\%) & .021 & -1.24E\text{-}5 \end{bmatrix} \qquad (10.14)$$

Comparing results in expression (10.14) with those in expression (10.13), it is seen that the stiffness results are slightly better in expression (10.14).

Generally speaking, the results achieved from modal-based decoupling method are not satisfactory. It was explained in section 6.5.2 that achieving a satisfactory result from equation (10.8) depends mainly on the accuracy of the expansion of the assembled structure's modes in equation (10.3). The accuracy of this expansion, in turn, depends on the how close the mode to be expanded, i.e. $\{\phi_{rs}^{c}\}$ is to the range space of the transformation matrix, i.e.

$$\begin{bmatrix} [\phi_{aks}] & 0 \\ 0 & [\phi_{bks}] \end{bmatrix}$$

Since the base vectors of the transformation matrix's range space -i.e. the columns of the transformation matrix- lie in the subspaces of the space which $\{\phi_{rs}^{c}\}$ belongs to (i.e columns of transformation matrix belong to smaller space of substructures modal matrices), thus it is very unlikely that one obtains a reasonably accurate expansion from equation (10.3).

10.4 REMARKS AND CONCLUSIONS

In this chapter, a new modal-based decoupling method is proposed for joint identification and its performance has been examined.

Although the method is very simple and easy to implement, due to the inaccurate expansion in equation (10.3) caused by ignoring the higher modes of substructures in the expansion, achieving good results is very case-dependent and in general unlikely.

As the component mode synthesis method is a well-established technique which is used for coupling purposes efficiently [19], the deficiency of the modal-based decoupling method is a good example of a case where the direct problem can be solved efficiently while the inverse problem cannot

CHAPTER 11

EXPERIMENTAL CASE STUDY

11.1 INTRODUCTION

Various joint identification techniques have been thoroughly discussed in chapters 5 to 10 and the advantages and shortcomings associated with each technique were also investigated.

In this chapter, the applicability of a typical joint identification technique to a practical problem will be examined.

11.2 STATEMENT OF THE PROBLEM

As a practical engineering case, it is desired to identify the dynamic characteristics of the soft medium which isolates a blade from its stator support ring, Fig. 11.1. The blade itself is made from a special steel alloy and is very stiff while the soft medium, which will be called the isolator from here on, is also made from steel but is much softer than the blade and support ring.

The configuration of the assembled structure, Fig.1 1.1, is such that it would not allow any access to the interface coordinates and, thus, it is not possible to measure the transfer FRFs, H_x^{si}. Considering the fact that these FRFs are not required in the FRF-based decoupling technique, and other practical advantages associated with the FRF-based decoupling method, this technique is chosen to be used in this analysis.

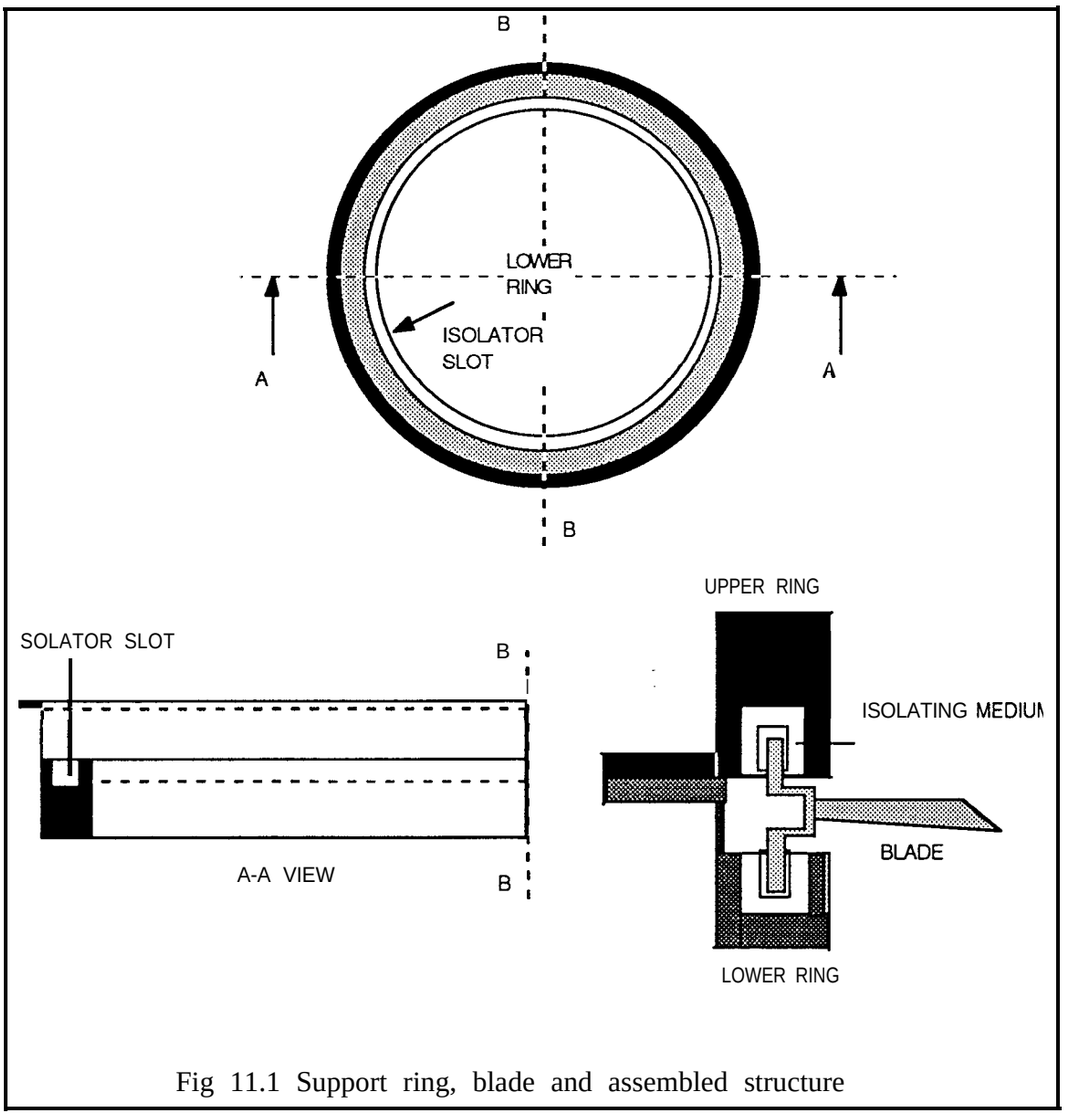

Fig 11.1 Support ring, blade and assembled structure

The two substructures are the blade and its support ring for which the slave and interface coordinates should be measured. Due to the skewed nature of the blade and also due to very difficult access to the support ring interface coordinates, it is very difficult to make accurate FRF measurements on these substructures. On the other hand, the nature of the joint and its dynamic characteristics which are going to be identified are independent of the substructures configuration and their mechanical properties, provided that the interfacing configuration and conditions are maintained.

Considering the above argument, it was decided to substitute the support ring by a clamp and the skewed blade with a straight one. These “equivalent” clamp and blade are shown in Fig. 11.2.a

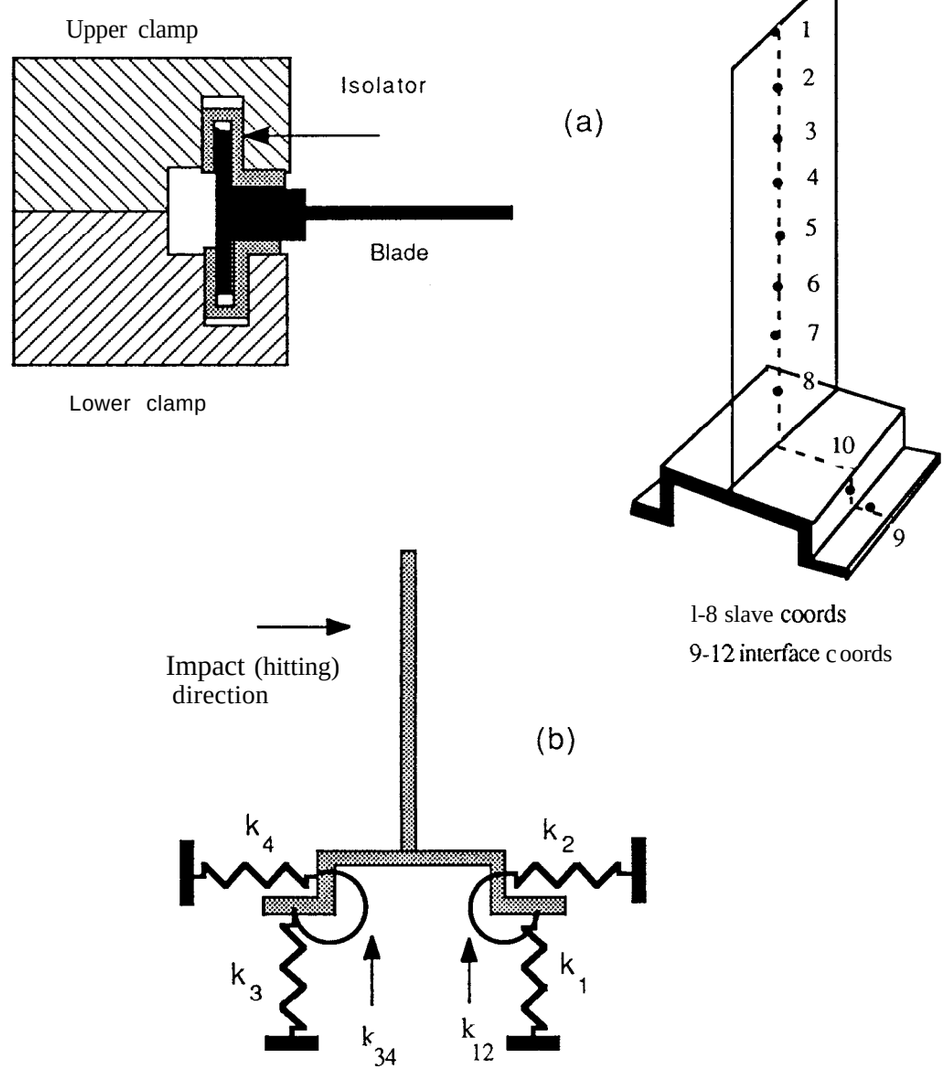

Fig. 11.2 (a)-The substitutional blade & clamped structures & the slave and interface coordinates' position, (b)- joint model & hitting direction

The clamp and blade, especially the blade root, were designed in such a way that the interfacing configuration of the equivalent assembled structure closely resembles those of the real assembled structure.

The reason for choosing a clamped configuration for the equivalent assembled structure, i.e. using the clamp instead of the support ring, is that the sensitivity of the calculations to noise is relatively low for clamped configurations, due to the fact that the effect of a soft joint in the root of a clamped structure has a significant effect on the assembled structure's response.

11.3 JOINT MODEL AND MEASUREMENT POINTS SELECTION

The basic identification formula for this case study is (see section 9.3):

$$[Z]_j^a = \left[I - [L]\,[H]_a^{ii} \right]^{-1} [L] \qquad (11.1)$$

where

$$[L] = ([H]_a^{si})^{+} ([H]_a^{ss} - [H]_c) ([H]_a^{is})^{+}$$

with notations “a” and "c" designating the blade substructure and assembled structure, respectively.

The slave coordinates which are measured on the blade substructure and clamped assembled structure must be consistent with each other and with the interfacing configuration. Also, the joint model should be selected in such a way that it represents the connectivity and configurational features of the real joint. It should be noted that there is no need to consider a prescribed joint model when solving equation (11.1) and the only reason for defining such a joint model is to clarify the sort of the model which is consistent with the slave coordinates and the interfacing configuration considered. The joint model and measurement points on the substructures and the assembled structure are shown in Fig. 11.2.b.

As is evident from this figure, there are 8 slave and 4 interface coordinates considered on the blade which are selected on the geometrical symmetry axis of the blade. So, the interfacing configuration and the slave coordinates selected are consistent, provided no torsional mode is involved in the slave coordinates’ FRFs in the frequency range of interest, O-3200 Hz. Now, since the slave coordinates are selected on the geometrical symmetry axis, it seems that one can assume that there will be no effect from torsional modes in the measured FRFs. On the other hand, if, due to production imperfections, the mass symmetry axis is not coincident with the geometrical one and/or measurements are not perfect, then it is very likely that there will be some contributions of torsional modes in the FRFs.

To minimize any torsional mode effects, measurements have been carried out with the maximum possible accuracy which can be achieved by a hammer test and repeated several times. Also, performing FE analysis of the blade for the free-free and clamped configurations, it has been established that there is a torsional mode in frequency range of

interest for both configurations. Table 11.1 shows the natural frequencies of the blade for the two configurations, obtained from the FE analysis and experimental measurement. The mode shapes of the blade achieved from the FE analysis can be seen in appendix A.

Natural frequency	1st (bending)		2nd (bending)		3rd(torsional)	
	Substr.	Ass. Str	Substr.	Ass. Str.	Substr.	Ass. Str.
FE prediction	815	222	1976	1440	2102	1910
Measured	888	220	2076	1436	2228	1964

Table 11.1 Measured and predicted natural frequencies of substructure & assembled structure in frequency range of interest.

Although having the effects of this torsional mode in the FRFs is a problem, examining some typical measured FRFs in Fig. 11.3 shows that, as expected, the effect of the torsional mode is very small and localized. This effect can either be eliminated from the FRFs by modal analysis or the results achieved around and at the torsional mode's frequency can be ignored in identification.

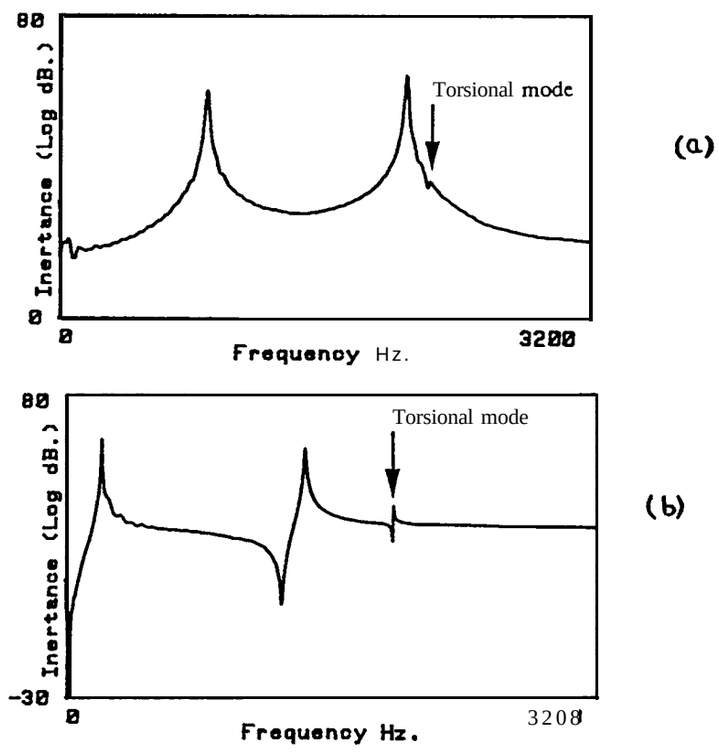

Fig 11.3 Typical FRFs of substructure & assembled structure, (a) substructure (b) assembled structure.

it is evident from equation (11.1) that the necessary and sufficient condition for this matrix equation to be solved is that:

$$n_i \leq n_s \tag{11.2}$$

where n_s=8 and n_i=4 are the number of the slave and interface coordinates, respectively. The reasons for choosing n_s to be twice that of n_i are:

(a) - as mentioned in chapter 9, increasing the number of the slave coordinates generally increases the information of the joint effect in the calculations and, thus, a better estimation of the joint properties is expected, when noise is present in the calculation;

(b) - as will be shown later, the identification process will be repeated several times using different groups of the slave coordinates in the calculations. This not only offers a way of taking a large number of samples and, thus, obtaining a reliable statistical average but, can also act as a consistency check to see whether there is any underlying trend in the different results. If there is no consistency between the results achieved using different groups of the slave coordinates, then one can conclude that what is identified is controlled only by noise; and

(c) - examining mode shapes of the blade in both free-free and clamped configurations in appendixA shows that, inevitably, some of the slave coordinates are near the nodal points of some of the bending modes. Now, performing the identification using different groups of the slave coordinates can minimize the effect of such slave coordinates.

It should be noted that increasing the number of the slave coordinates beyond a limit may result in ill-conditioned matrices in equation (11.1).

11.4 VALIDATING THE MEASURED DATA

In order to examine the accuracy of the measured data, the blade is considered to be coupled to ground, the analysis performed using its measured FRFs, and some typical results of the coupled structure FRFs are compared with the clamped blade FRFs in Fig. 11.4.

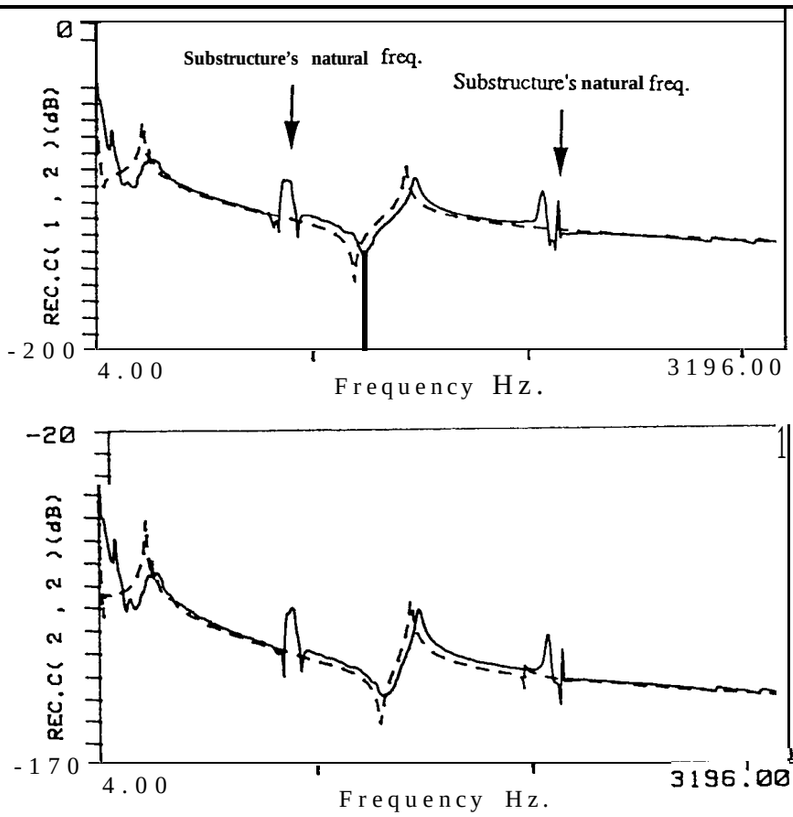

Fig. 11.4 Typical measured and regenerated FRFs,---- Measured FRFs
_____ Regenerated FRFs

It is evident from this figure that there is good agreement between the generated and measured FRFs. The exceptions are regions close to the natural frequencies of the assembled structure and these are believed to be due to the joint effect. It should be noted that with regenerated FRF we mean the FRF generated by coupling (i.e predicted), throughout this chapter.

11.5 DISCUSSION OF THE RESULTS

Fig. 11.5 shows some typical identified joint impedance matrix's elements, using all of the 8 slave coordinates and a raw measured FRFs in the calculations.

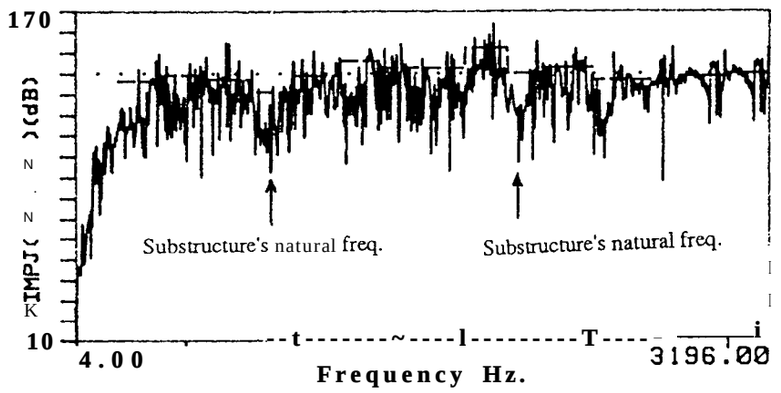

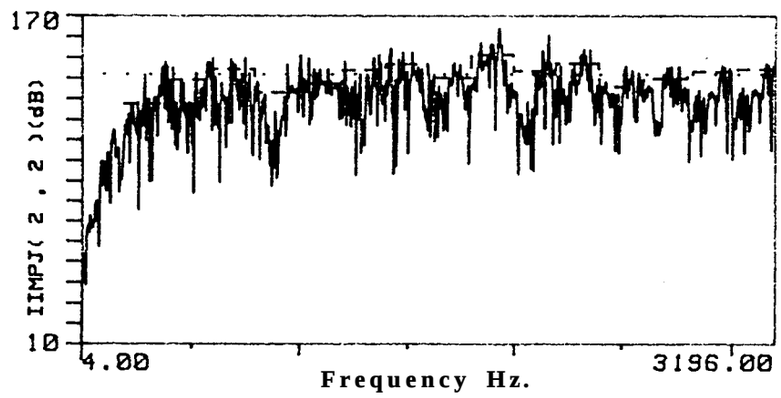

$$[\bar{Z}_J]_R = \begin{bmatrix} 1.6E6 & 3.1E6 & 0 & 0 \\ & 1E7 & 0 & 0 \\ & & 2.1E6 & 4.9E6 \\ & & & 1.7E7 \end{bmatrix} \qquad [\bar{Z}_J]_I = \begin{bmatrix} 1.8E6 & 5.4E6 & 0 & 0 \\ & 1.2E7 & 0 & 0 \\ & & 2E6 & 4.3E6 \\ & & & 1.5E7 \end{bmatrix}$$

Fig. 11.5 Typical Identified joint impedances using row data, _____ Moving averages, ... Total average

As can be seen from this figure, the results are very noisy especially at frequencies near to the natural frequencies of the substructure (also see Fig. 9.4). Using statistical analysis based on moving averages, the mean value of each z(i,j) has been calculated for 15 averaging spans starting from 200 Hz, i.e. each span covers 200 Hz, as well as the total average over whole frequency range, i.e. 200-3200 Hz, using each span's mean value. The details of the statistical method used can be seen in appendix B. Also, the total mean joint impedance is given in Fig. 11.5.

In order to reduce the noise effect on the calculations, it was decided to perform modal analysis on the substructure's FRFs. Two points are considered in this connection as follows:

(a) - modal analysis is not performed on the assembled structure FRFs because these data contain the effect of joint and using modal analysis can alter this effect, especially the damping effect; and

(b) - the blade itself is a fairly lightly-damped structure (mild steel) and performing a very accurate modal analysis on its measured data may improve the results.

The coupling test for validating the data, described in section 11.4, is used here again, this time using processed FRFs of the substructure in the coupling analysis. Typical regenerated FRFs along with measured ones can be seen in Fig. 11.6. As is evident from these figures, the two curves are reasonably close which indicates the validity of the processed data. It should be noted that two different levels of processed data have been used in Fig. 11.6 and later on in identification. The first level of processing is just to smooth the measured FRFs individually and to eliminate any random noise effects. The second level of processing is to rationalize all measured FRFs, in order to minimize systematic error and inconsistency. The reason for using two levels of processed data is to examine the effect of analyst interaction on the identified joint.

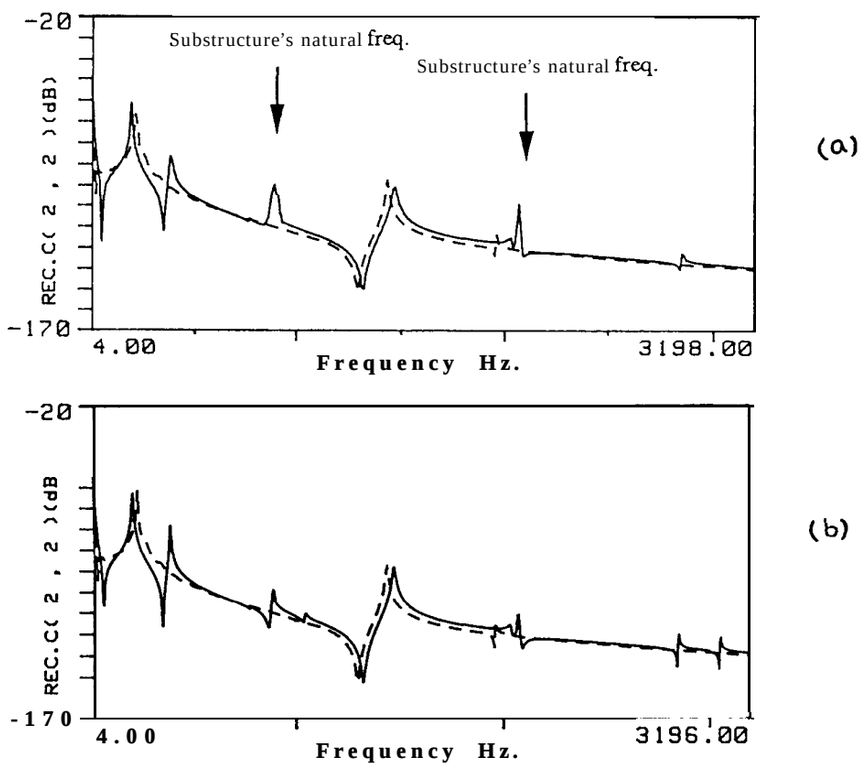

Fig. 11.6 Typical measured & regenerated FRFs using processed data,
(a) only smoothed, (b) rationalized, --- Measured data, _____ Regenerated data

Having performed the modal analysis, typical results of identified joint impedances can be seen in Fig. 11.7. Comparing the mean impedance matrices in Fig. 11.7 with those in Fig. 11.5 it can be seen that the real parts of these matrices are more or less correlated and consistent but this is not the case for imaginary parts.

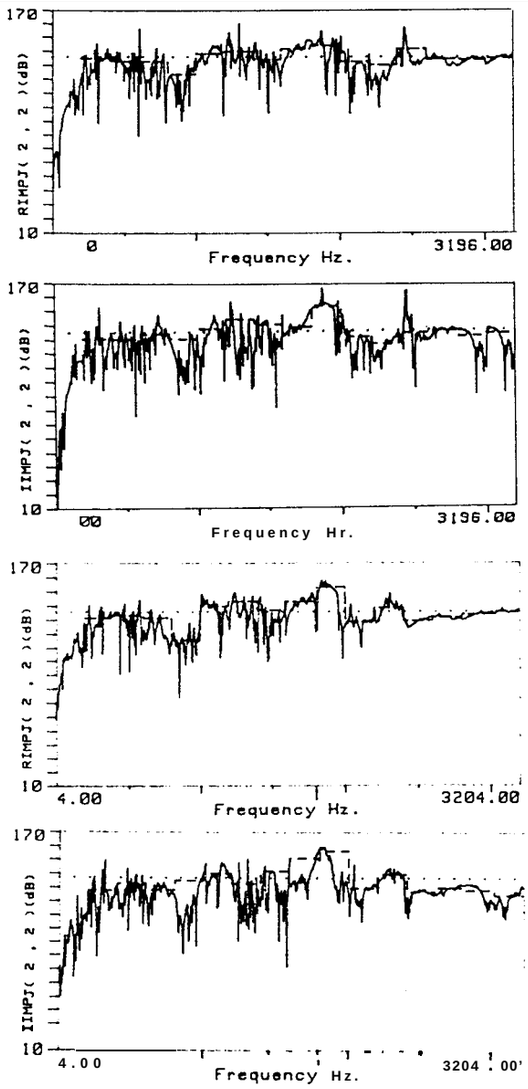

$$[\bar{Z}_J]_R = \begin{bmatrix} 1.7E6 & 3.97E6 & 0 & 0 \\ & 6.5E6 & 0 & 0 \\ & & 1.1E6 & 3.3E6 \\ & & & 1.2E7 \end{bmatrix}$$

$$[\bar{Z}_J]_I = \begin{bmatrix} 1.3E6 & 2.2E6 & 0 & 0 \\ & 5.8E6 & 0 & 0 \\ & & 1.4E6 & 1.5E6 \\ & & & 7.3E6 \end{bmatrix}$$

(a)

$$[\bar{Z}_J]_R = \begin{bmatrix} 1.2E6 & 3.3E6 & 0 & 0 \\ & 6.3E6 & 0 & 0 \\ & & 1.3E6 & 2.4E6 \\ & & & 1E7 \end{bmatrix}$$

$$[\bar{Z}_J]_I = \begin{bmatrix} 1.4E6 & 2.8E6 & 0 & 0 \\ & 7.2E6 & 0 & 0 \\ & & 1.5E6 & 2.3E6 \\ & & & 7.7E6 \end{bmatrix}$$

(b)

Fig. 11.7 Typical identified joint using two level of processed data, (a) smoothed data, (b) rationalized data, _____Moving average, ... Total averag

As was mentioned in section 11.3, the main reason for measuring redundant slave coordinates is to be able to repeat the identification process using different groups of slave coordinates. Some typical results of these attempts are shown in Fig. 11.8. Comparing the identified joints in Fig. 11.8 with those in Figs. 11.5 and 11.7, a reasonable degree of consistency between the various results can be deduced.

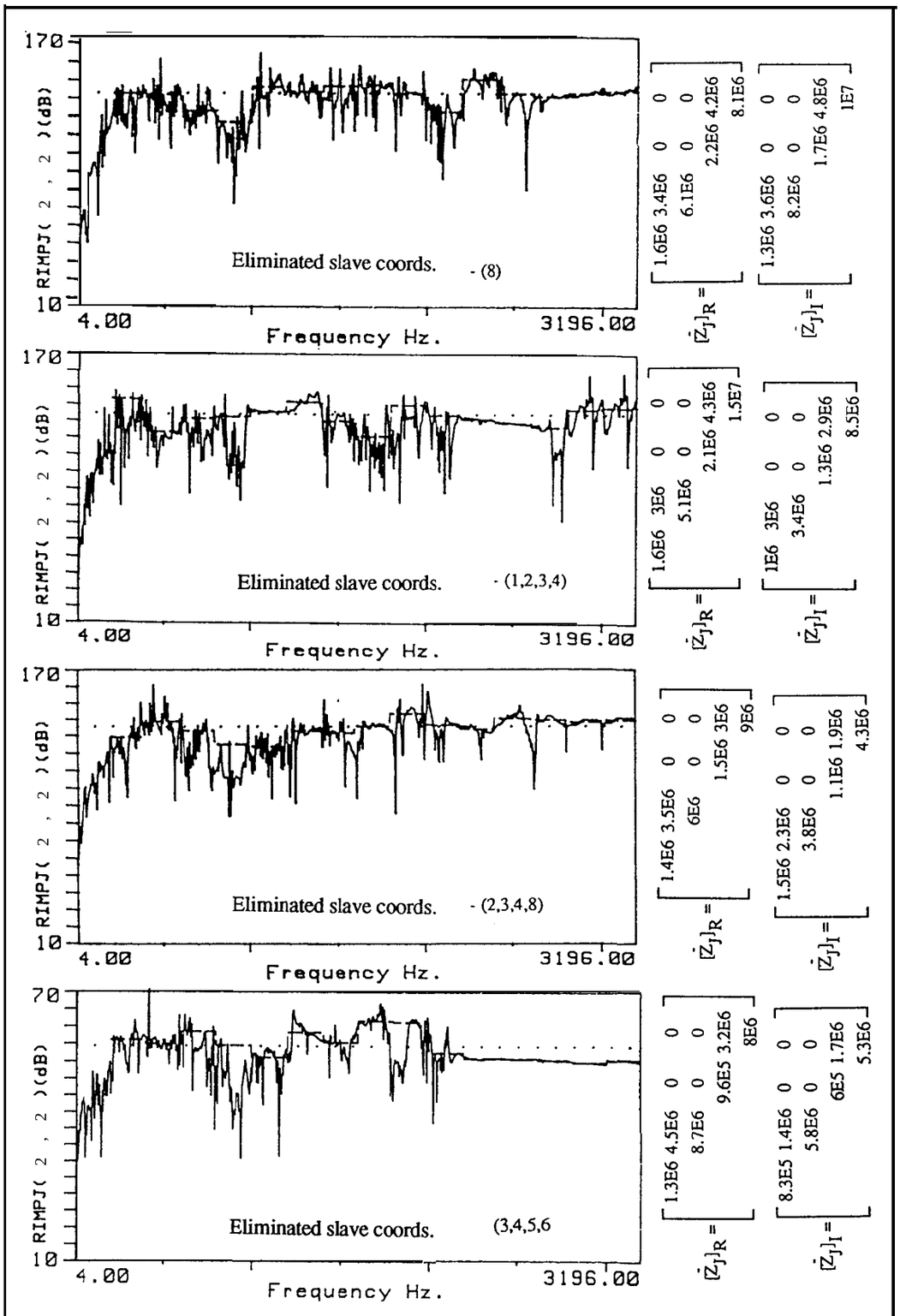

Fig. 11.8 Typical identified joint impedances using different groups of slave coordinates in the calculations

This consistency, which is especially notable for some of the joint impedances like z(2,2), is both qualitative and quantitative. Qualitatively, all identified joint impedances (i.e. joint contributions) first increase with frequency until they reach their maximum values and then start to decrease, as frequency increases further. The frequency spans over which joint impedances increase, remain constant and decrease are almost the same for all identified joints and are O-1000 Hz, 1000-2000 Hz and 2000 Hz and onward, respectively.

The quantitative consistency is reflected in the following points:

(a) - consistency in the magnitude of identified values; and

(b) - for all results, the impedance values identified for the springs 1 and 3, i.e. z(l,l) and z(3,3) (see Fig. 11.2.b), are much smaller than those identified for springs 2 and 4. Considering the joint model and the impact direction in Fig. 11.2.b and the mode shapes of free-free blade in appendix A, the reason for relatively lower values identified for the springs 1 and 3 becomes clear. According to the free-free blades' mode shapes in appendix A, the root of the blade remains rigid in the frequency range of interest which means that the root constitutes a much stiffer structure than the blade aerofoil . Considering this rigidity of the blade's root, impact direction and joint model the relatively insignificant contribution of springs 1 and 3 to the blade's response can be deduced.

As was mentioned in section 11.3, the existence of consistency in the different sets of results is very important and proves that it is not measurement noise which controls the identified joint.

Having established consistency in the results, the next step will be to calculate a statistical average of all sets of results from different identification attempts. This has been carried out by combining the all results and calculating the statistical average for each span of 200 Hz. Then, using these average values, the following averages have been calculated:

(a) - average over the whole frequency range, O-3200 Hz

(b) - averages over three frequency spans, i.e. 0- 1200, 1200-2200, 2200-3200

Typical results of these averages are shown in Fig. 11.9. The total average and averages over three frequency spans are shown in expressions (11.3) and (11.4)

$$[\bar{Z}_J] = \begin{bmatrix} 2.2E6 & 3.7E6 & 0 & 0 \\ & 6.9E6 & 0 & 0 \\ & & 1.6E6 & 3.7E6 \\ & & & 1.1E7 \end{bmatrix} \qquad (11.3)$$

$$[\bar{Z}_J] = \begin{bmatrix} 7.5E5 & 1.9E6 & 0 & 0 \\ & 5.7E6 & 0 & 0 \\ & & 6.4E5 & 1.5E6 \\ & & & 4.1E6 \end{bmatrix} \quad \text{O-1200 Hz}$$

$$[\bar{Z}_J] = \begin{bmatrix} 4.6E6 & 5.9E6 & 0 & 0 \\ & 8.6E6 & 0 & 0 \\ & & 2.4E6 & 4.4E6 \\ & & & 1.3E7 \end{bmatrix} \quad \text{1200-2200 Hz}$$

$$[\bar{Z}_J] = \begin{bmatrix} 1.2E6 & 3.3E6 & 0 & 0 \\ & 6.3E6 & 0 & 0 \\ & & 1.7E6 & 5.1E6 \\ & & & 1.6E7 \end{bmatrix} \quad \text{2200-3200 Hz} \qquad (11.4)$$

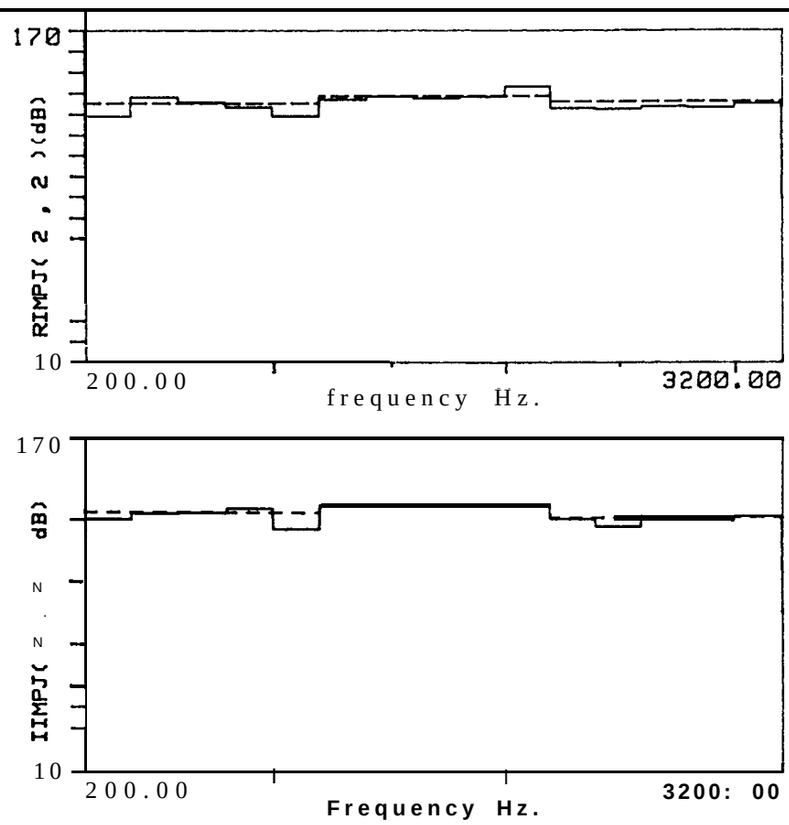

Fig. 11.9 Typical results of statistical calculation performed on whole set of identified joints _ Moving Average, -- Total Averages over 3 frequency spans

Defining a confidence criterion as $(\sigma_{ij} / E(z_{ij}))$ [46], where σ_{ij} is standard deviation of element ij of joint mean impedance matrix and $E(z_{ij})$ is the mean value of element ij, and calculating this value for each element ij of $[\bar{Z}_J]$ and for each span relating to Fig. 11.9, shows that confidence criterion changes between 2% to 10% for different elements and, for the different spans of each element ij.

11.6 VALIDATING THE IDENTIFIED JOINT

In this section the identified joint will be used in the coupling of the blade to ground, as was done in section 11.4, and the results will be compared with measured FRFs of the clamped blade. If the identified joint is a reasonable representation of the real joint, then the coupling results should show better match with measured data than those achieved in Fig. 11.4.

Fig 11.10 shows typical regenerated FRFs using the joint model in expression (11.3), i.e. the average impedance over the whole frequency range. As can be seen from this figure, the match between measured FRFs and the regenerated ones is good up to about 800 Hz. It is also notable from this figure that the first regenerated natural frequency is much closer to the 1 st measured natural frequency than is the case in Fig. 11.4 but this is not the case for second natural frequency.

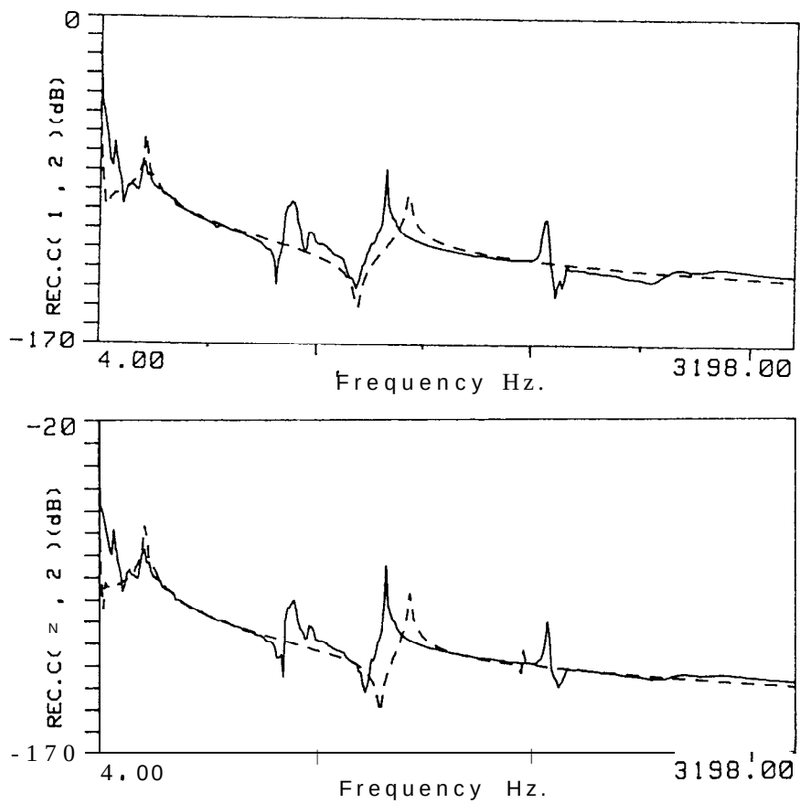

Fig. 11 .10 Typical regenerated FRFs using total average joint impedance in exp. (11.3)

Having used only the diagonal terms of the mean impedance matrix in expression (11.3), typical results of regenerated FRFs are shown in Fig. 11. 11. Comparing the results in Fig. 11.11 with those in Fig. 11.10, it is evident that the match between regenerated curves and measured ones is much better in former case than the latter, at least up to about 1000 Hz. The reason for this better match in Fig. 11.11 lies in the fact that, examining the blade moda shapes in appendix A, it is seen that the root of the blade is much stiffer than the blade's aerofoil and remains rigid in the lower and moderate frequency ranges which, in turn means that for these frequency ranges the cross stiffness k_{12} and k_{34} in Fig. 11.2.b have very small contribution to the response and can be considered as zero.

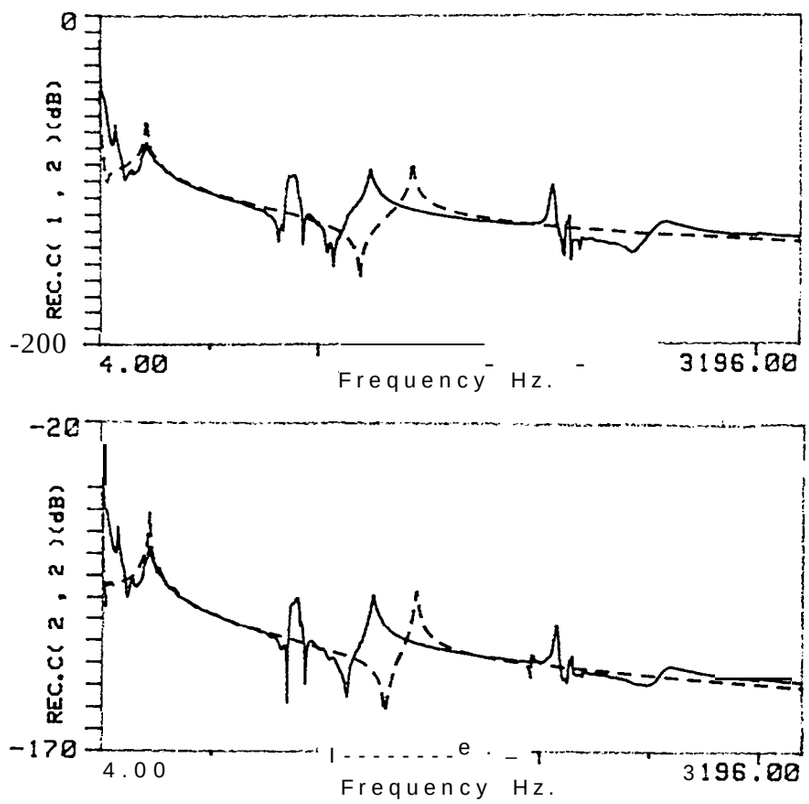

Fig. 11.11 Typical regenerated FRFs using the diagonal elements of the total average impedance matrix in exp. (11.3)

Fig. 11.12 demonstrates typical regenerated FRFs using three spans impedance averages in expression (11.4). As is evident from these figures, the match between the two curves in each is satisfactory except for the very high frequency range. There are some spikes on the regenerated curves which correspond to the joint impedance change frequencies in expression (11.4), in which the structure's characteristics change discontinuously. Comparing the results in Fig. 11.12 with those in Fig. 11.4, it is concluded that a better match is achieved by incorporating the joint in the coupling and, especially, the differences in the 1st and 2nd natural frequencies have become smaller

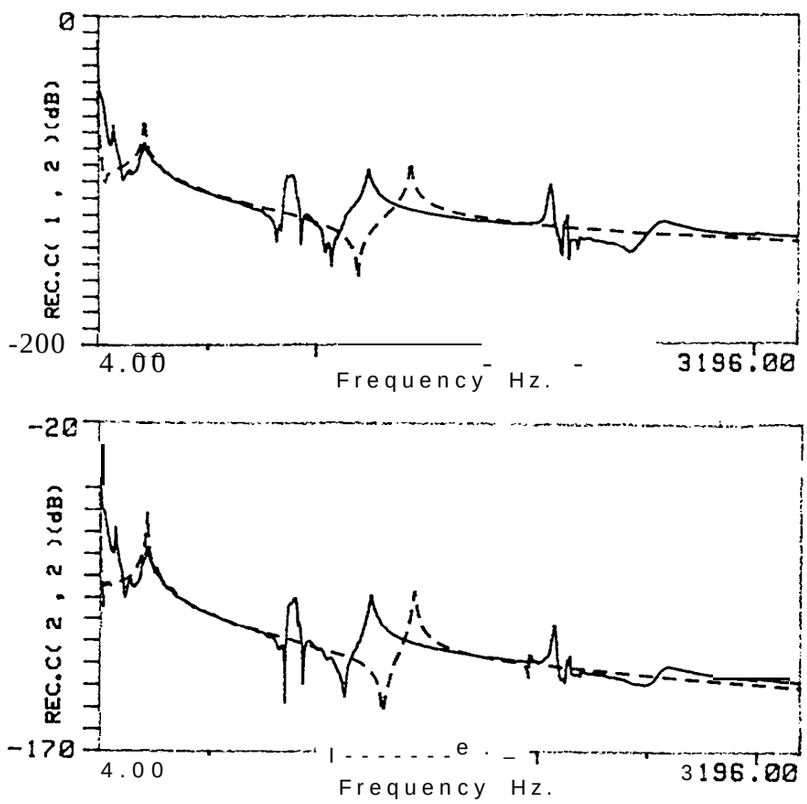

Fig. 11.11 Typical regenerated FRFs using the diagonal elements of the total average impedance matrix in exp. (11.3)

Fig. 11.12 demonstrates typical regenerated FRFs using three spans impedance averages in expression (11.4). As is evident from these figures, the match between the two curves in each is satisfactory except for the very high frequency range. There are some spikes on the regenerated curves which correspond to the joint impedance change frequencies in expression (11.4), in which the structure's characteristics change discontinuously. Comparing the results in Fig. 11.12 with those in Fig. 11.4, it is concluded that a better match is achieved by incorporating the joint in the coupling and, especially, the differences in the 1st and 2nd natural frequencies have become smaller

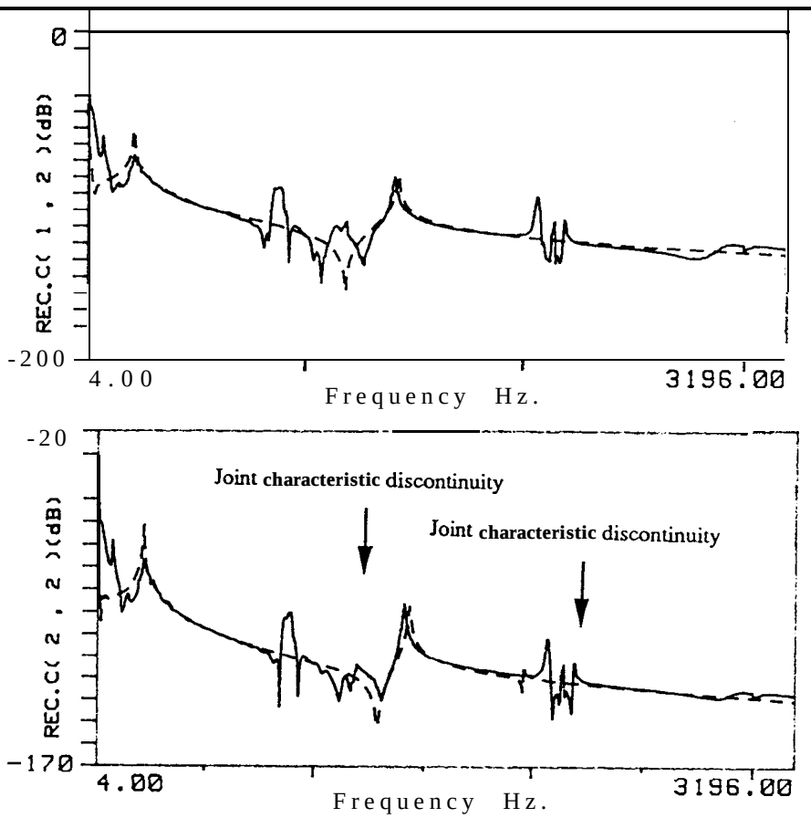

Fig. 11.12 Typical regenerated FRFs using the three spans average valu in exp.(11.4)

In order to prevent discontinuities in the structure's response, it was decided to use the middle span joint impedance average value in expression (11.4), i.e. the average value over the range 1200-2200 Hz, for the whole frequency range. Typical results of this case are shown in Fig. 11.13.

In order to examine the sensitivity of the assembled structure's response predictions to variations in the identified joint parameters, the coupling process has been repeated using the middle span average multiplied by different factors. Some typical results of these couplings are given in Fig. 11.14. Also, Fig. 11.15 and Table 11.2 demonstrate the variation of the 1st and 2nd natural frequencies with the middle-span average impedance variation.

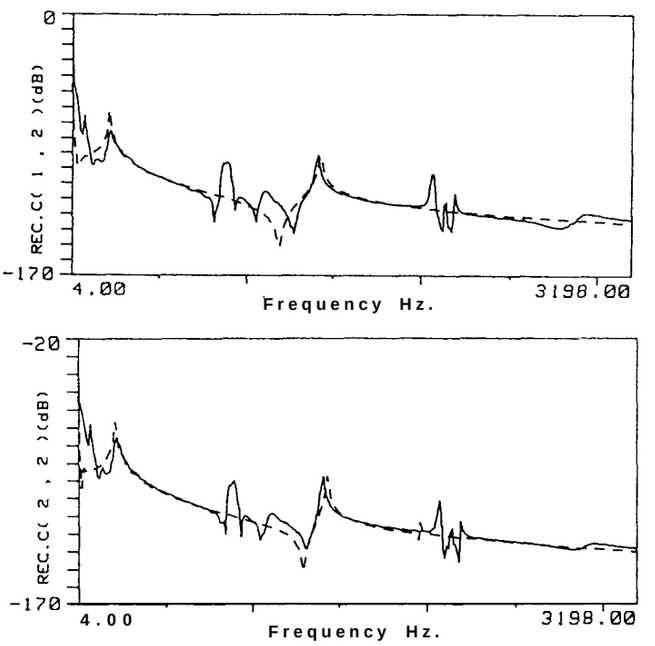

Fig. 11 .13 Typical regenerated FRFs using the middle span average impedance in exp. (11.4) over whole frequency range

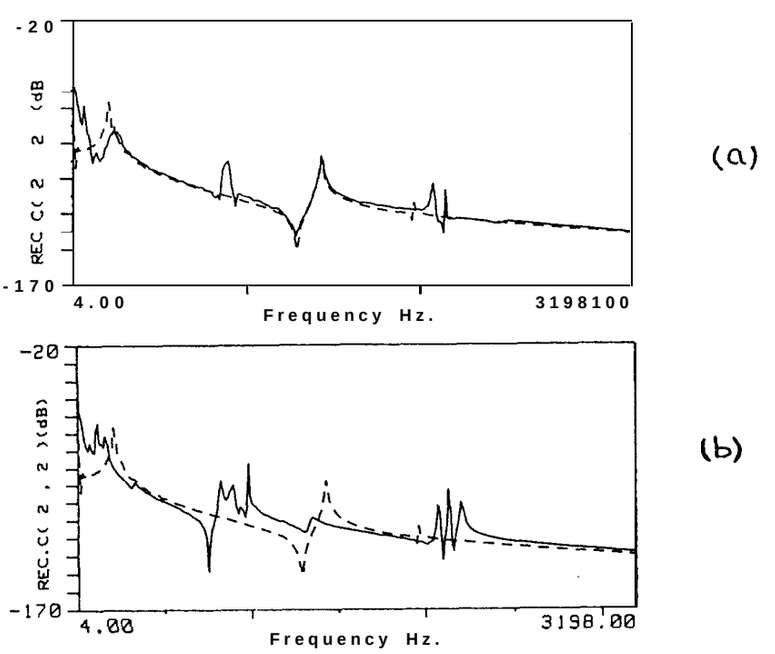

Fig. 11.14 Typical regenerated FRFs using different multiplications of middle span's average impedanc (a) 10 times stiffer, (b) 10 times softe

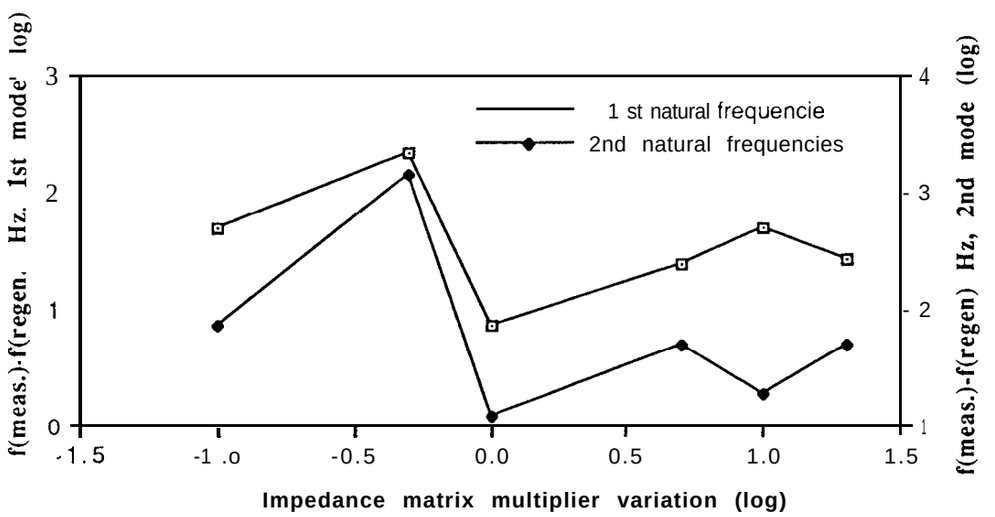

Fig. 11.15 Variation of the differences in natural frequencies of measured & regenerated FRFs with mean impedance multiplier

	$[\bar{z}]_i/10$	$[\bar{z}]_i/5$	$[\bar{z}]_i$	$[\bar{z}]_i x5$	$[\bar{z}]_i x10$	$[\bar{z}]_i x\infty$
Δf_1(Hz)	48	13	-7	-24	-48	-26
Δf_2(Hz)	71	298	12	48	-19	-48

Table 11.2 Variation of the differences in natural frequencies of measured & regenerted FRFs with mean impedance multiplier, $f_{measured} - f_{regenerated}$

As is evident from Fig. 11.15 and Table 11.2, the identified joint yields the closest match between regenerated and measured natural frequencies. Also, examining Figs. 11.14 and 11.15 one can conclude that the assembled structure's response is sensitive to the identified joint variation and, thus, one can claim that the identified joint in expression (11.4) is a reasonable representation of the joint under investigation.

11.7 CONCLUDING REMARKS

Application of the FRF-based decoupling technique, as a typical joint identification procedure, to a practical joint identification problem has been examined in this chapter. The most important deductions and practical implications are highlighted below:

(a) - although using processed FRFs in an identification calculation yields smoother results, it seems that one can achieve almost the same results using raw data in the calculation;

(b) - by performing modal analysis on measured FRFs, one should be very careful not to change the original measured data. In any case, modal analysis of the FRFs of the assembled structure is not recommended as these FRFs contain the joint effects which can be easily altered; and

(c) - having FRFs for a couple of redundant slave coordinates is very valuable in order to check the consistency in the identified joint using different groups of slave coordinates in the identification process.

CHAPTER 12

CONCLUSIONS

12.1 GENERAL CONCLUSIONS:

The main object of this work has been to develop a unified approach to the identification of a linear model of structural joints. The work was mainly based on the assumption that a joint identification technique must be applicable to both mixed analytical/experimental ("hybrid") data and pure experimental data. In this connection, special attention has been given to measurement noise effects on the results and to ways of reducing these effects.

As the joint identification problem is a special case of the more general identification problem, it was appropriate to discuss important and relevant topics of the general identification problem such as overlaps of joint identification and model updating problems. Further, the computational aspects of the identification problem in general, and the joint identification problem in particular, have been discussed in detail, in which crucial questions concerning the existence and uniqueness of the solution have been addressed.

Although remarks and conclusions have been given in each of the preceding chapters, it is appropriate now to provide a general summary of each of these conclusions and important findings so that the various parts of the work which constitute new developments are highlighted.

12.1.1 EFFECT OF JOINT(S) ON DYNAMIC COUPLING ANALYSIS

Joint(s) effect is not routinely considered in structural dynamic coupling analysis. In a few cases where joint(s) effect is considered [8], its mass and stiffness matrices have been directly added to those of FE models of substructures, i.e. spatial coupling. It has

been shown in chapter 2 that including joint effect in coupling process leads to a quadratic eigenvalue problem of a nonsymmetric matrix, using a free interface component mode synthesis technique.

Also, equations have been developed which enables the joint to be incorporated directly in the coupling process.

12.1.2 CLASSIFICATION OF IDENTIFICATION TECHNIQUES

After spending some time studying different identification (and model updating) techniques, the author realized that there is a lack of an acceptable classification of identification techniques. For example, 'when can a method be called direct'? or 'when is a method perturbation-based'?

Based on the mathematical nature of the procedure which is used to formulate an identification technique (and not its computational limitations), the author has proposed a classification for identification techniques explained in chapters 1 and 6. According to this classification, an identification technique is direct if, using complete measured data, no approximations are involved in its formulation and, consequently, no iterations are necessary in its implementation. On the other hand, for perturbation-based techniques, approximations and, consequently, iterations are inevitable, even if a complete set of measured data are used. So, no computational aspects are considered in above criteria.

In addition to classification according to the mathematical nature of the derivation, identification techniques are further classified according to the type of the data being used in the analysis.

Based on the above classification criteria, the author succeeded in predicting the existence of a modal-based direct method and to formulate it, as explained in chapter 6.

In addition to adaptive identification techniques which are applicable to joint identification problems, a new family of methods which are particularly developed for joint identification was introduced in the classification, as decoupling techniques.

12.1.3 A NEW MODAL-BASED DIRECT IDENTIFICATION TECHNIQUE

A new modal-based identification technique has been developed and described in chapter **6.** The method was first formulated based on a component mode synthesis approach and, later on, it was realized that it is related to the eigendynamic constraint method. As a matter of fact, the new method can be considered as a modified eigendynamic constraint technique.

It has been shown in section **6** that, although the new method is a direct method according to author's classification, one still has to solve the governing equations iteratively, due to incompleteness of the measured data. Also, for the same reason, i.e. data incompleteness, there are limits on $\|\Delta\phi\|$ and $\|\Delta\lambda\|$ for which the calculation will converge to a solution.

12.1.4 COMPUTATIONAL ASPECTS OF IDENTIFICATION PROBLEM

Generally speaking, the structural identification problem is an ill-posed problem. This is basically due to the fact that, in practice, the identification problem is a process of extracting a large amount of data from an incomplete and, thus, relatively smaller available set of data. The poor formulation of the identification problem reveals itself in computational inconsistencies and difficulties which, in turn, result in approximations imposed on calculations.

In addition to the poor formulation, there are other parameters contributing to computational difficulties such as, a poor analytical model and inappropriately balanced matrices.

Due to the smaller number of unknowns involved in a joint identification problem, it is possible to prevent poor formulation for them, using certain identification techniques such as FRF-based decoupling or FRF-based direct techniques. Having said that, the ill-conditioning problem still exists for the joint identification process, and in order to prevent ill-conditioning, balancing techniques have been proposed in chapter 4.

One of the popular methods of artificially increasing the amount of available data in an adaptive identification problem is to preserve the connectivity pattern of the analytical FE model. It was shown in chapter 4 that by preserving the connectivity pattern of the analytical model, one will identify the closest possible model (in a least-squares sense) to the real structure but it is impossible to identify the real structure exactly.

12.1.5 MODEL UPDATING & JOINT IDENTIFICATION IN PRACTICE

It was shown in chapter 3 that for a complex structure, it is virtually impossible either to update its analytical model ignoring its joint(s), or to identify its joints and update its analytical model simultaneously within a single model updating process.

The author believes that the only practical approach to the updating problem of a complex structure is to update separate substructures without any joints (or with obviously rigid joints) and then to assemble them together making sure that the only source of difference(s) between the analytical model and the real structure come(s) from the joints. Naturally, the next step will be to identify the joints and incorporate them into the analytical model.

12.1.6 CHOOSING THE APPROPRIATE MODEL FOR A TRIAL JOINT WHEN USING ADAPTIVE IDENTIFICATION TECHNIQUES

One of the common characteristics of adaptive joint identification techniques is that they require the construction of the so-called analytically coupled structure, A-C. This requirement, in turn, makes the selection of a trial joint model inevitable and proper selection of a trial joint can have an important effect on the results.

The first step in selecting a trial joint model is to decide on its configurational features, i.e. the number of degrees of freedom involved in the trial joint model and their type. It is clear that both the number of trial joint degrees of freedom and their type are dictated by the configurational characteristics of the interface coordinates of constituent substructures of the assembled structure.

So, the first step in selecting a proper trial joint model is to decide on the quality and quantity of the interface coordinates. For example, with beam substructures, the question is whether tension or torsion must be included in the coupling, and consequently in the joint model, or not. Thus, as long as the configurational features of the trial joint are concerned, the proper selection of this element is case-and analyst-dependent, although not too difficult.

Once the proper configurational model is derived for the trial joint, the next question is: whether it is possible to group different elements of the trial joint mass and stiffness matrices in some sub-matrices, according to their consistency? This grouping can be done using either an FE model pattern, or a lumped parameter pattern for the trial joint, as

discussed in chapter 3. Having grouped the unknowns, the number of unknowns which must be identified reduces dramatically and, as explained in chapter 4, this is an advantage from a computational point of view.

12.1.7 SENSITIVE NATURE OF THE IDENTIFICATION PROBLEM

It has been shown throughout this thesis that the identification problem is sensitive to noise. As thoroughly explained in chapter 4, the sensitivity of the identification procedure is inherent and is due mainly to insensitivity of structure's response to variations in some of the structure's components.

Based on the above explanation, in spite of the larger number of unknowns involved in a model updating problem, the joint identification problem can be more sensitive to noise than a model updating problem. Note that, although the number of unknowns is typically larger for the updating problem, the chance that variations in the whole mass and/or stiffness matrices of an element having insignificant effects on structure's response is much less than possibility of insignificant effect due to variation in the individual components of that elements mass and/or stiffness matrices. For example, considering a beam element as a part of an analytical model, that model's response is likely to be much more sensitive to variations of elemental mass matrix as a whole rather than the variations of individual components in the elemental mass matrix, say, rotary inertia. (Note that in modelling a joint, it is necessary to split the elemental mass and stiffness matrices into consistent sub-matrices, as explained in chapter 3.)

It has been observed in chapters 5 through 9 that the insignificant effect of joint rotary inertia on a structure's response was responsible for a high sensitivity of the identification process.

Through a discussion of the concept of ill-conditioning of a matrix in chapter 4, it has been shown in chapter 9 that the insensitivity of the response of the structure to variation in some of its components reveals itself in computations by causing small or very close singular values for relevant matrices involved in calculations.

12.1.8 GUIDE-LINES FOR PROPER JOINT IDENTIFICATION METHOD SELECTION

The matter of selection of a suitable joint identification technique is very case-dependent and depends mainly on the type and amount of data available. Thus, it is difficult to give a

general guide-line which covers every joint identification problem. Questions like whether a reliable FE model of the substructures are available or, how much the cost of this identification is going to be must first be answered before selecting a suitable technique.

Based on the advantages and disadvantages of the various joint identification techniques shown in Fig. 12.1, the method selection flow-chart of Fig. 12.2 is proposed.

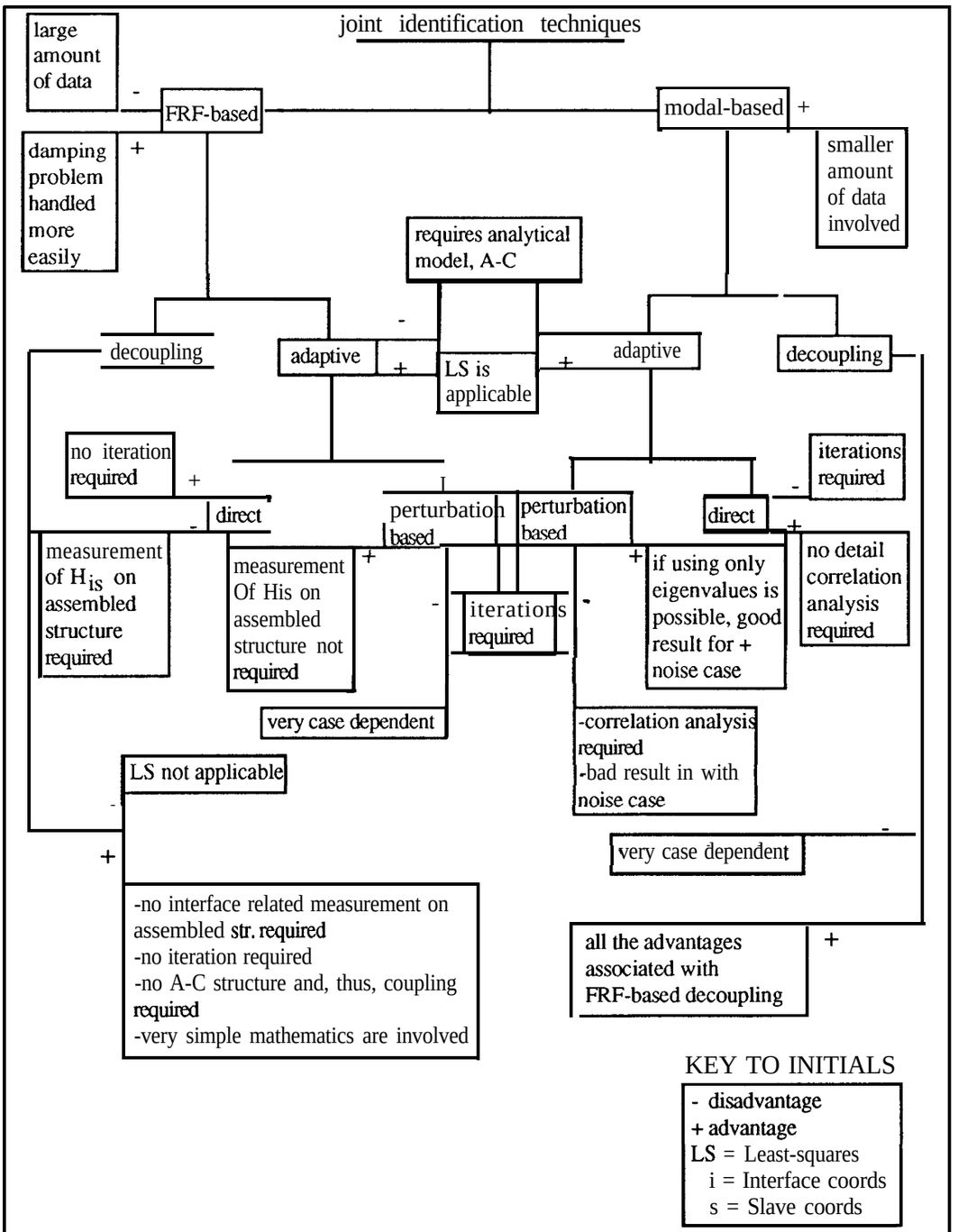

Fig. 12.1 The table of advantages & disadvantages of joint identification techniques

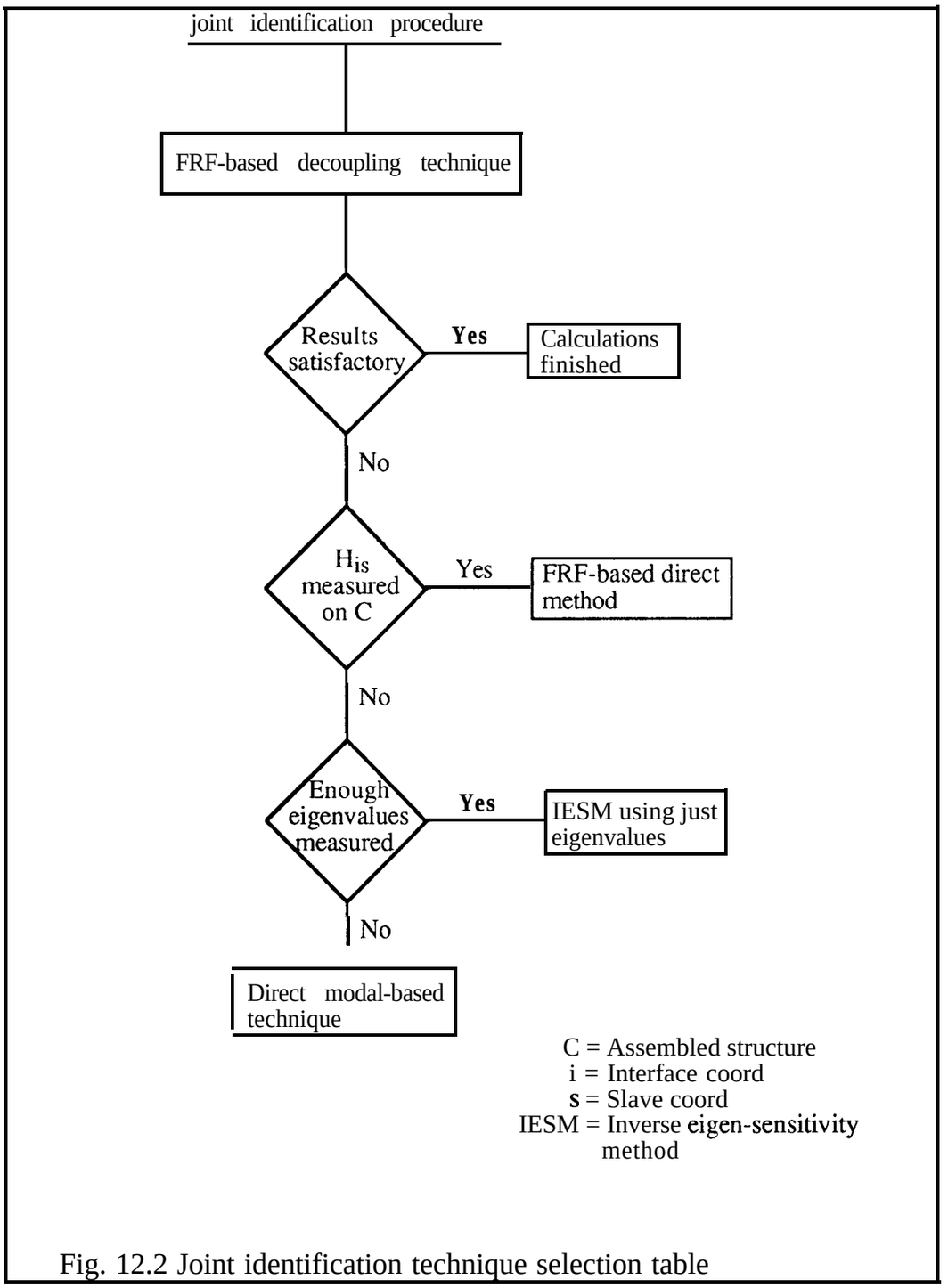

Fig. 12.2 Joint identification technique selection table

12.2 CONTRIBUTIONS OF THE PRESENT RESEARCH

To Newton is attributed the saying “If I have seen a little farther than others it is because I have stood on the shoulders of giants” [47]. Although the author does not compare himself with Newton, nevertheless, the fact remains that any contribution I have made is based on a massive amount of previous work, done by other researchers and scientists.

Bearing above-mentioned fact in mind, it is appropriate at this stage to present a brief review of the contributions of the research described in the thesis, as follows:

classification of identification techniques in general and the joint identification techniques in particular;

discussion of the range of applications and overlaps of joint identification and model updating methods;

investigation of the effect of joint(s) on structural dynamic coupling;

discussion of the uniqueness and existence of the solution of an identification problem and the effect of preserving the connectivity pattern of the analytical model in the solution;

illustrating the essence of the least-squares formulation in an identification problem;

discussion of the usefulness limit of the least-squares solution when dealing with noisy data;

extensive investigation of the sensitivity of the identification problem to measurement noise and its connection with singular parameters of the matrices involved in calculations;

discussion of the concept of ill-conditioning of a matrix and development of a new criterion for a matrix’s sensitivity assessment;

extensive discussion of the possibilities and limitations of various joint identification techniques;

development of a new model updating and joint identification technique;

modification of some of the existing identification techniques to be applicable to the joint identification problem; and

extensive research on the sensitivity analysis of various joint identification techniques and the methods of reducing noise effect on results.

12.3 SUGGESTIONS FOR FURTHER WORK

It seems that further research is required in following areas:

investigation on the joint effect on the structural dynamics coupling;

The effect of a joint on the structural dynamics coupling analysis was examined in chapter 2. It was shown there that introduction of a joint into the coupling process will cause some complications. Some numerical case studies are necessary in order to assess the performance of solution techniques proposed in chapter 2 and to examine the effects of various simplifying assumptions, e.g. ignoring joint's mass, on results.

examination of mis-modelling effects on the identified joint, using a hybrid approach for joint identification;

As the application of FE models of substructures can facilitate the joint identification process for complex structures, it is necessary to examine the effect of mis-modelling of the FE model on the predicted result.

investigation on the performance of the new model updating technique on real structure; and

identification of isolating medium of chapter 11 using the genuine blade and supporting ring;

Due to the simplification made on the real blade and support ring problem in chapter 11, it was possiblesible to use a relatively simple joint model in the identification process. Now, considering a genuine skewed blade and ring a more complicated model should be tested for the joint, although the procedure is exactly the same as that used in chapter 11

REFERENCES

1- **Maloney, Shelton, Underhill,** *"Structural Dynamic Properties of Tactical Missile Joints"*, General Dynamics Report No. CR-6-384-945-001, 1970

2- **Ewins D.J., Silva J.M., Maleci G.,** *"Vibration Analysis of a Helicopter Plus an Externally-Attached Structure", Shock* and Vib. Bul., 1970

3- **Mead D.J.,** *"Prediction of the Structural Damping of a Vibrating Stiffened Plate"*, AGARD Conference Proc. No. 277

4- **Levina E.M.,** *"Calculation of Contact Deformation in Slideways", Machines and Tooling"*, Vol. 36 pp 8-17, 1965

5 **Botkin M.E., Lubkin J.L.,** *"Welded Joints Stiffness Obtained Using Solid Finite Element"*, A.S.M.E Paper 75-det-3

6- **Yuan J.X., Wu S.M.,** *"Identification of the Joint Structural Parameters of Machine Tool by DDS and FEM"*, Trans. A.S.M.E J.Eng. for Ind., Vol.107, Feb. 1985.

7- **Wang J., Sas p.,** *"A Method for Identifying Parameters of Mechanical Joints"*, Trans. A.S.M.E, J. Applied Mechanics, Vol. 57, June 90

8- **Huckelbridge A.A., Lawrence C.,** *"Identification of Structural Interface Characteristics Using Component Mode Synthesis"*, J. Vib. Acoustics, Stress and Reliability in Design, Vol. 111, April 89

9- **Carneiro H.S., Arruda R.F.,** *"Updating Mechanical Joint Properties Based on Experimentaly Determined Modal Parameters"*, IMAC 8, 1990

10- **Chung K.R.,** *Identification and Dynamic Reanalysis of Vibrating Structures by Modal Analysis,* Dept of Mech. Eng., Korea Advanced Institute of Science and Tech., 1987.

11- **Tsai J.S., Chou Y.F.,** *"The Identification of Dynamic Characteristics of a single Bolt Joint"*, J. Sound and Vib., 125(3), pp 487-502, 1988

12- **Lee C.W., Hong S.W.,** *"Estimation of Joint Structural Parameters from Measured and Computed Frequency Responses",* IMAC 8, 1990

13- **Wang J.H., Liou C.M.,** *"Experimental substructure Synthesis With special Consideration of Joints Effect",* IJAEMA 5(1): 13-24, Jan 89

14- **Hong S.W., Lee C.W.,** *" Identification of Linearized Joint structural Parameters by Combined Use of Measured and Computed Frequency Responses",* Mechanical systems and signal Processing, Vol. 5, No.4, 1991

15- **Mohammad K., Tomlinson G.R,** *"Estimating Physical Parameters of Nonlinear Structures",* 15th Int. Seminar on Modal Analysis, 1990

16- **Potter R., Richardson M.,** *"Mass, Stiffness and Damping Matrices from Measured Modal Parameters",* Int. Instr.-Autom. Con., New york City, 1974

17- **Ewins D.J.,** *Modal Testing Theory and Practice,* Research Studies Press, 1984

18- **Larsson P.O.,** *"Methods Using FRF for The Analysis of Assembled Mechanical Structures",* Research Report 88-02C, ABB Corporate Research, Jan. 1988

19- **Urgueira A.P.V,** *Dynamic Analysis of Coupled Structures Using Experimental Data,* Ph.D Thesis, Dynamic Section, Imperial College, 1989

20- **Craig R.R. , Chang,** *"Substructure Coupling for Dynamic Analysis and Testing",* Nasa Contract Report CR-278 1, Feb. 1977

21- Przemieniecki J.S., *Theory of Matrix Structural Analysis,* McGraw-Hill, 1968

22- **Newland** D.E., *An Introduction to Mechanical Vibration Analysis and Computation,* Longman, 1989

23- **Meirovitch L.,** *Computational Methods in Structural Dynamics,* Sijthhoff & Noordhoff, 1980

24- **Zehang Q., Lallement G.,** *"A Complete Procedure for the Adjustment of a Mathematical Model From Identified Complex Modes"*, IMAC 5, April 1987.

25- **Brandon J.A.,** *Strategies for Structural Dynamic Modification,* Research Studies Press, 1990, pp 97- 109

26- **Sidhu J., Ewins D.J.,** *"Correlation of Finite Element and Modal Test Studies of a Practical Structure",* IMAC 2, 1984

27- **Lin R.M., Ewins D.J.,** *"Model Updating Using FRFs"*, 15th International Seminar on Modal Analysis, Lueven, 1990

28- **To W.M.,** *Sensitivity Analysis of Mechanical Structure Using Experimental Data,* Ph.D Thesis, Dynamics Section, pp 101-106, 1990

29- **Lawson C.L., Hanson R.J.,** *Solving Least Squares Problems,* Printice-Hall, 1974, pp 194- 198

30- **Gladwell G.M.L,** *Inverse Problems in Vibration,* Martinus Nijhoff Publisher, 1986

31- **Leuridan J., Grangier,** *"Coupling of Structures Using Measured FRFs by Means of SVD-Based Data Reduction Technique",* IMAC 8, 1990

32- **Ben-Israel, Greville,** *Generalized Inverses Theory and Applications,* Wiley, *1974*

33- **Golub, Van Loan,** *Matrix Computations,* North Oxford Academic Publishing Co., 1983

34- **Stewart,** *Introduction to Matrix Computations,* Academic Press Inc., 1973

35- **Wilkinson J.H.,** *The Algebraic Eigenvalue Problem,* **Oxford** University Press, 1963, pp 62-109

36- **Rubin S.,** *"Improved Component-Mode Representation for Structural Dynamic Analysis",* AIAA Journal, Vol. 13, No. 8, August 1975.

37- **Kidder R.L.,** *"Reduction of Structural Frequency Equations",* AIAA 1 1(3), p892, 1973

38- **Lieven N.A. J, Ewins D.J,** *"Expansion of Modal Data for Correlation"*, IMAC 8, 1990

39- Lin **R.M**, *"Identification of the Dynamic Characteristics of Nonlinear structures"*, Ph.D Thesis, Dynamic Section, Imperial College, 1990

40- **Ibrahim S.R, Starinids C., Fissete E., and Brunner O.,** *" A Direct Two Response Approach for Updating Analytical Dynamic Models of Structures with Emphasis on Uniqueness"*, IMAC 7, 1989

41- **Fissete E. and Ibrahim S.R,** *"Error Location and Updating of Analytical Dynamic Models Using a Force Balance Method"*, IMAC 6, 1988 p 1063

42- **Luber W., Lotze A.,** *"Application of Sensitivity Methods for Error Localization in Finite Element Systems"*, IMAC 8, 1990

43- **Lim K.B., Junkins J.L.,** *"Re-examination of Eigenvector Derivatives"*, J. Guidance, Vol. 10, No. 6, Nov. 1987

44- **Aliemeng R.J., Brown D.L.,** *"A Correlation Coefficient for Modal Testing"*, IMAC 1, 1983

45- **Lieven N.A.J., Ewins D.J.,** *"Spatial Correlation of Mode Shapes, The Coordinate Modal Assurance Criterion (COMAC)"*, IMAC 6, 1988

46- **Newland D.E,** *An Introduction to Random Vibrations and Spectral Analysis*, Longman, 1987

47- **Bell E.T,** *Men of Mathematics*, Vol. 1, Penguin Books, 1953

APPENDIX A

MODE SHAPES OF THE BLADE STRUCTURE

As indicated in chapter 11, the mode shapes of the blade for the free-free and clamped configurations are presented in this appendix. These mode shapes have been derived from a FE analysis using ANSYS and play a major role in determining the consistency between the slave coordinates, interface coordinates and joint model selected. In what follows, the first three mode shapes of the blade for (a) the free-free configuration and (b) the clamped configuration will be demonstrated.

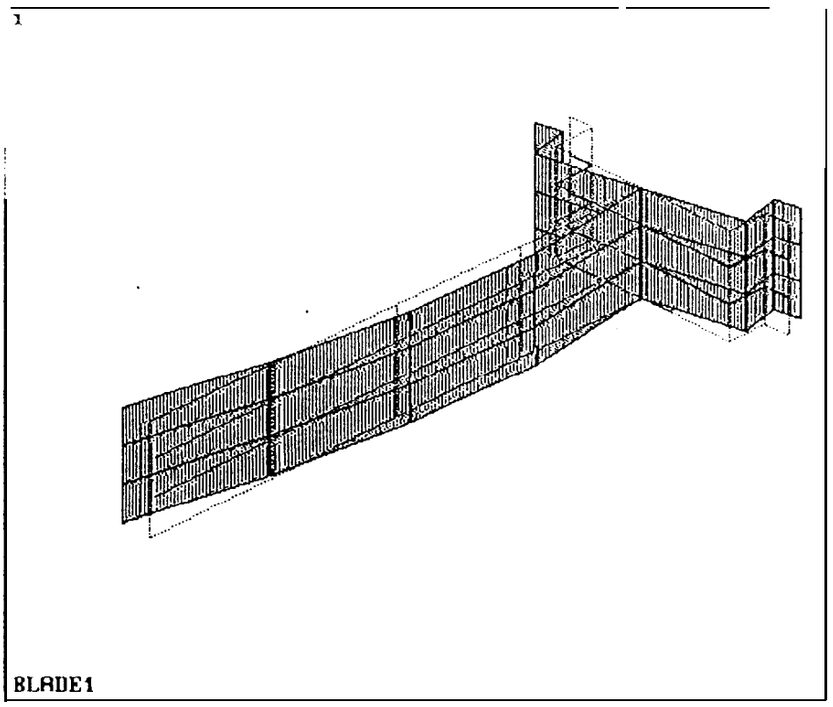
1
ANSYS 4.4
UNIV VERSION
SEP 23 1991
11:18:24
POST1 DISPL.
STEP=1
ITER=7
FREQ=815.212
DMX =6.518
DSCA=0 86 1E-03
XV =1
YV =1
ZV =1
DIST=0.082814
YF =0.0125
ZF =0.0485
BLADE1

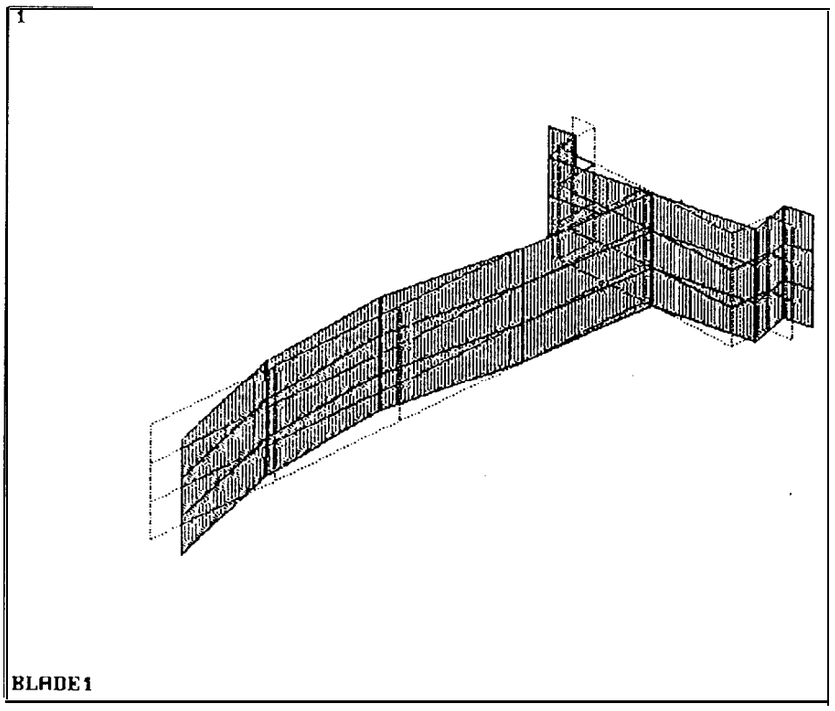
1
ANSYS 4.4
UNIV VERSION
SEP 23 1881
11::25:26
POST1 DISPL.
STEP=1
ITER=8
FREQ=1976
DMX =6.931
DSCA=0.861E-03
XV =1
YV =1
ZV =1
DIST=0.082614
YF =0.0125
ZF =0.0485
BLADE1

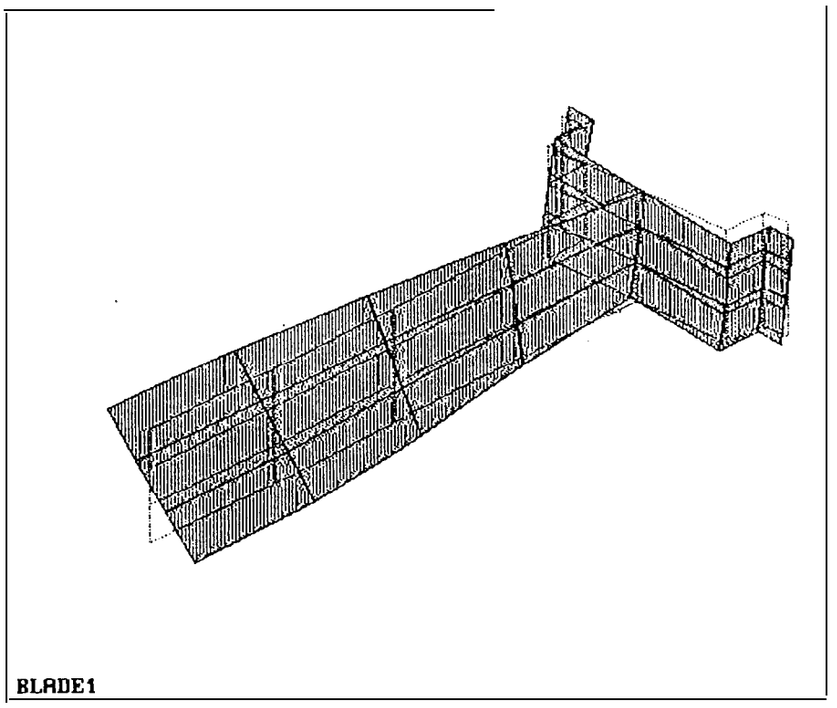
ANSYS 4.4
UNIU VERSION
SEP 23 1881
11:27:50
POST1 DISPL.
STEP=1
ITER=8
FREQ=2102
DMX =9.678
DSCA=0.861E-03
XV =1
YV =1
ZV =1
DIST=0.082814
YF =0.0125
ZF =0.0485
BLADE1

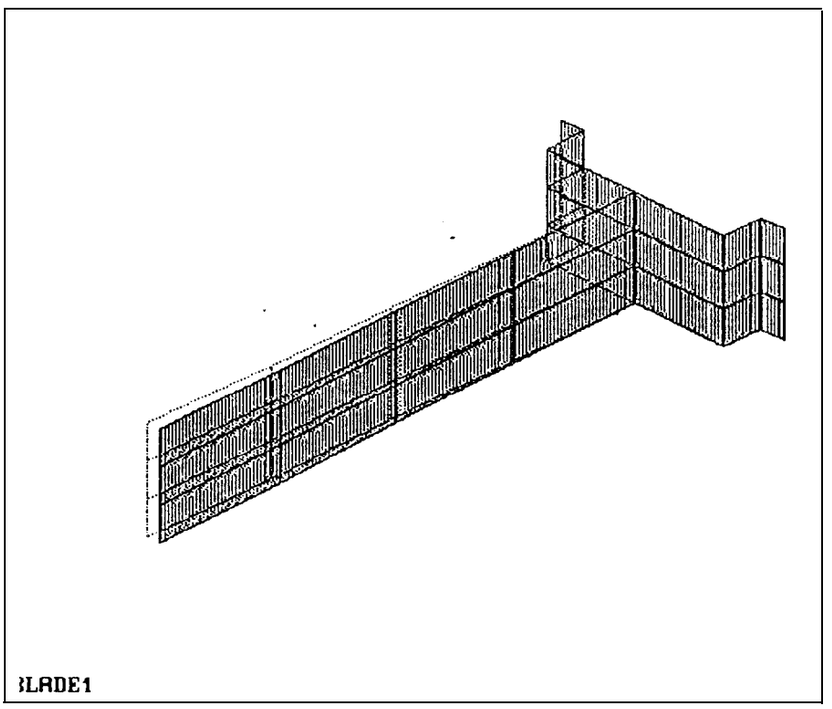
ANSYS 4.4
UNIU VERSION
SEP 23 1881
11:50:38
POST1 DISPL.
STEP=1
ITER=1
FREQ=222.764
DMX =8.018
DSCA=0.328E-03
XV =1
YV =1
ZV =1
DIST=0.082814
YF =0.0125
ZF =0.0485
BLADE1

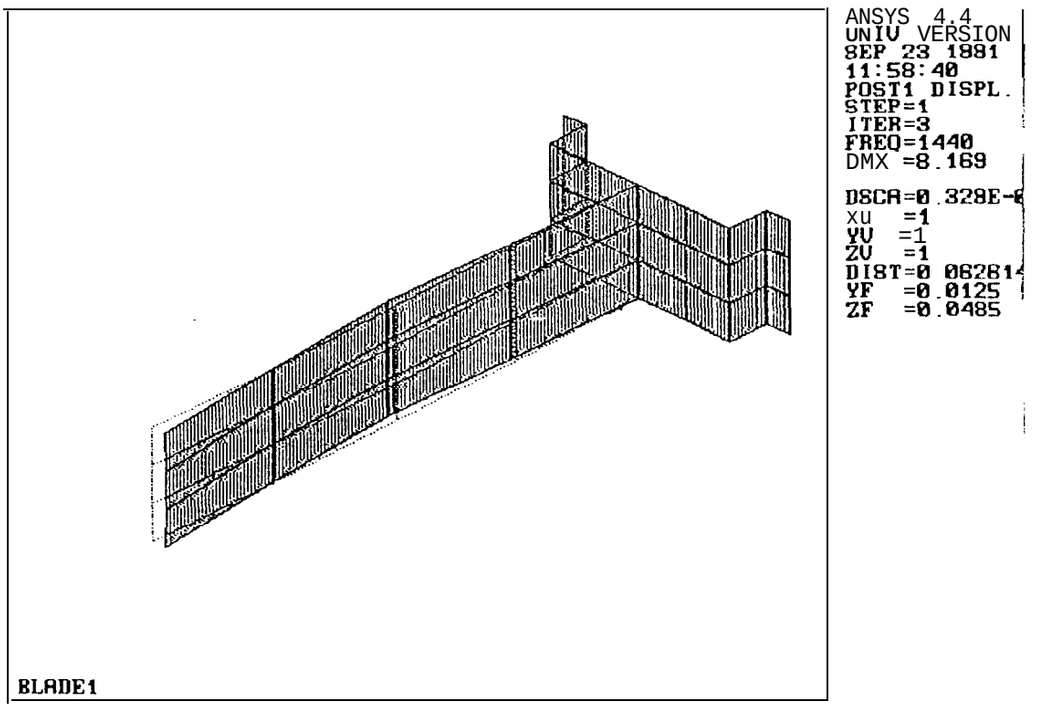
ANSYS 4.4
UNIV VERSION
SEP 23 1981
11:58:40
POST1 DISPL.
STEP=1
ITER=3
FREQ=1440
DMX =8.169
DSCA=0.328E-
XU =1
YU =1
ZU =1
DIST=0 06281
YF =0.0125
ZF =0.0485
BLADE1

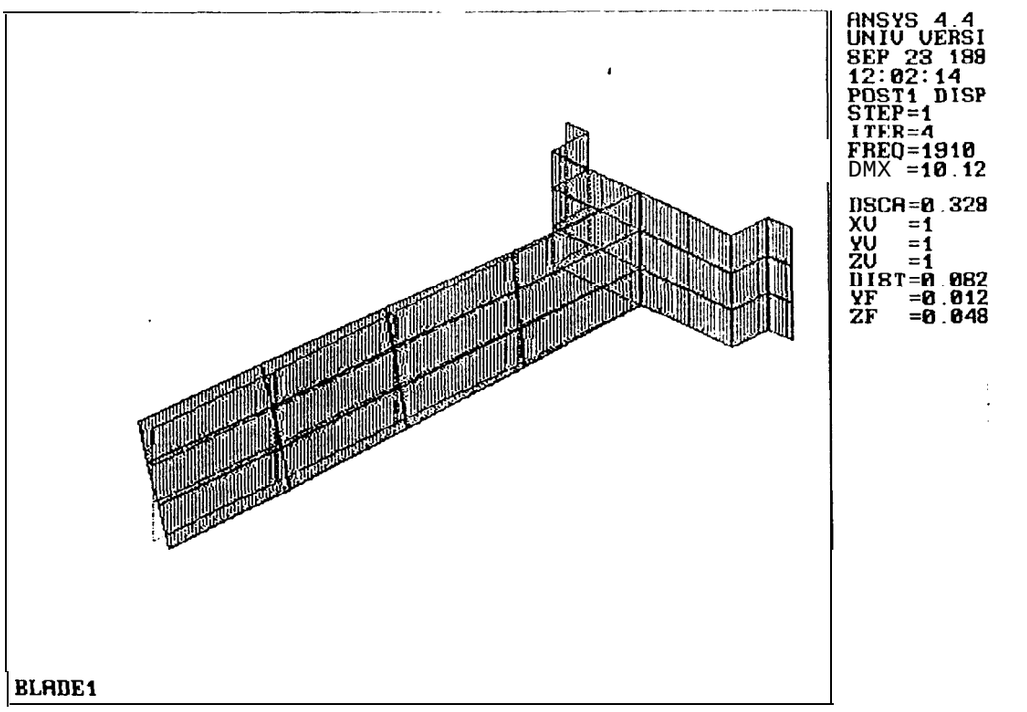
ANSYS 4.4
UNIV VERSI
SEP 23 198
12:02:14
POST1 DISP
STEP=1
ITER=4
FREQ=1910
DMX =10.12
DSCA=0.328
XU =1
YU =1
ZU =1
DIST=0.082
YF =0.012
ZF =0.048
BLADE1

APPENDIX B

STATISTICAL METHOD USED FOR DATA ANALYSIS

In the present appendix the statistical method used to analyse noisy data in chapter 11 will be explained. The explanation for the statistical terms used here can be found in [38].

The method is shown in the following flow chart.

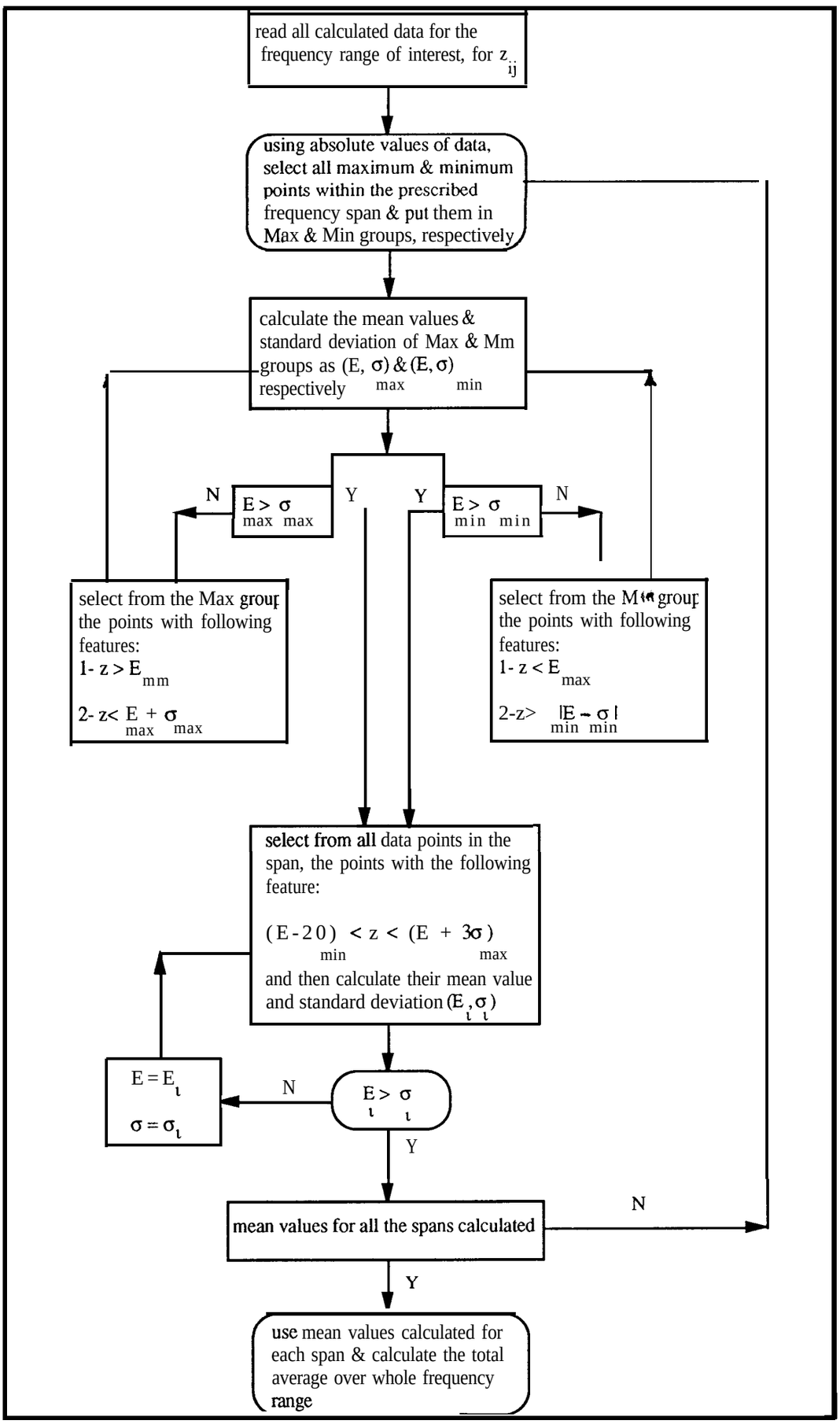
read all calculated data for the frequency range of interest, for z_{ij}
using absolute values of data, select all maximum & minimum points within the prescribed frequency span & put them in Max & Min groups, respectively
calculate the mean values & standard deviation of Max & Mm groups as $(E, \sigma)_{max}$ & $(E, \sigma)_{min}$ respectively
N
$E > \sigma$ max max
Y
Y
$E > \sigma$ min min
N
select from the Max group the points with following features:
1- $z > E_{mm}$
2- $z < E_{max} + \sigma_{max}$
select from the Mm group the points with following features:
1- $z < E_{max}$
2- $z > |E_{min} - \sigma_{min}|$
select from all data points in the span, the points with the following feature:
$(E_{min} - 20) < z < (E_{max} + 3\sigma)$
and then calculate their mean value and standard deviation (E_i, σ_i)
$E = E_i$
$\sigma = \sigma_i$
N
$E > \sigma$ i i
Y
mean values for all the spans calculated
N
Y
use mean values calculated for each span & calculate the total average over whole frequency range